

ION INSERTION IN
TUNGSTEN TRIOXIDE ELECTRODES

Thesis submitted for the degree of
Doctor of Philosophy
at the University of Leicester

by

Sally Elizabeth Garner BSc (Leicester)

Department of Chemistry

University of Leicester

October 1997

UMI Number: U531852

All rights reserved

INFORMATION TO ALL USERS

The quality of this reproduction is dependent upon the quality of the copy submitted.

In the unlikely event that the author did not send a complete manuscript and there are missing pages, these will be noted. Also, if material had to be removed, a note will indicate the deletion.



UMI U531852

Published by ProQuest LLC 2013. Copyright in the Dissertation held by the Author.
Microform Edition © ProQuest LLC.

All rights reserved. This work is protected against
unauthorized copying under Title 17, United States Code.



ProQuest LLC
789 East Eisenhower Parkway
P.O. Box 1346
Ann Arbor, MI 48106-1346

To my parents
with much love

ION INSERTION IN TUNGSTEN TRIOXIDE ELECTRODES

Sally Elizabeth Garner

ABSTRACT

The role of ion insertion into the electrochromic metal oxide WO_3 has been studied using a combination of electrochemical, gravimetric and spectroscopic techniques. The electrochemical quartz crystal microbalance (EQCM) was used to investigate the effect of electrolyte composition by studying the identity of the cations and anions involved and the concentration of the electrolyte used. It was found that the effect of electrolyte concentration and choice of anion did not affect film reduction and re-oxidation. The two cations studied, Li^+ and Na^+ , however cause marked differences in film redox behaviour.

The effect of film history was studied using a combination of EQCM and spectrophotometry. The initial cycle at a slow scan rate (5 mV s^{-1}) showed responses different to those of subsequent cycles. Results indicated that at completion of the first cycle there is both injected charge and mass remaining in the WO_3 film. This effect has been termed the "break-in" effect and has been seen for all experiments initially cycled at this slow scan rate, irrespective of anion or cation, or the electrolyte concentration. It is possible to correlate current (or charge), mass change and absorbance data together in a novel way, to give information regarding electrons, ions and solvent and electron and ion distribution (via the extinction coefficient, ϵ). Also, the effect of long term cycling ($>10,000$ cycles) has been investigated with respect to cation insertion. This shows that Li^+ insertion yields stable WO_3 films after many cycles, whereas Na^+ insertion does not.

The effect of experimental time scale also has been studied using cyclic voltammetry and chronoamperometry, together with the EQCM. Again, the "break-in" effect was recorded using chronoamperometry, indicating that the effect is not only seen for cyclic voltammetric experiments. Under all experimental conditions used, there is a second, neutral species being inserted and extracted alongside cations.

ACKNOWLEDGEMENTS

Firstly, I would like to thank my supervisor Prof. Rob Hillman and my second supervisor Dr Andy Abbott for all their advice, help and suggestions during the duration of this PhD. I would also like to thank Dr Richard Batchelor and Dr Mark Burdis of the Surfaces and Coatings group at Pilkington Glass in Lathom for coating my samples and answering any questions that I put to them.

I would like to thank my parents for their years of support, especially during this last year. I would not have been able to do this without their help and will be forever grateful to them.

I also want to say a big thank-you to Nick who has been tremendously supportive throughout the last two years, especially whilst I have been writing up. I really don't think that I would have been able to see the light at the end of the tunnel without his help. Without his laser printer, things would have probably been a little more difficult at the bitter end!

I must thank everybody who has been in the lab over the last 4 years, from third year project students (especially Huw) to overseas visitors (such as Silvana). I also want to thank Dave and Paul, both of whom are now abroad but they are two people who helped me enormously during my PhD. Without Dave's help at the beginning I would never have been able to figure out the EQCM and Paul provided many good ideas for me before he left this "warm" climate and went back to Oz! Huge thanks have to go to Lou who got the EQCM up and running again (and made it better than ever!), and who has been invaluable over the last few weeks. Thanks alot Lou; you were right, it is a relief to get it all finished!!! Now onto the folks in the lab; many thanks to Lorraine, who I have known since being a third year project student and together we have seen both the bad and the good times. Thanks also go to Helen, Sarah, Mark B, Little Rob, Lee and Mark H. There are probably many more people to whom thanks must go. Without any of these people the last few years would not have been as much fun!

*There are no such things as applied sciences,
only applications of science*

(Louis Pasteur, 1822-1895)

CONTENTS

1. INTRODUCTION	1
1.1 Electrochromism	1
1.1.1 Introduction	1
1.1.2 Present technology	1
1.1.2.1 Cathode ray tubes	1
1.1.2.2 Liquid crystal display	2
1.1.2.3 Light emitting diodes	2
1.1.3 Electrochromic Terminology	2
1.1.3.1 Primary and secondary electrochromism	2
1.1.3.2 Colour	3
1.1.3.3 Response time	4
1.1.3.4 Cycle life	4
1.1.3.5 Insertion coefficient	4
1.1.4 Types of electrochromes	5
1.1.5 Metal oxides	6
1.1.5.1 Structure of metal oxides	6
1.1.5.1.1 Perovskite-like structures	6
1.1.5.1.2 Rutile structures	7
1.1.5.1.3 Layer and block structures	8
1.2. Electrochromic devices	8
1.2.1 Introduction	8
1.2.2 “Smart windows”	9
1.2.3 Design of ECDs	9
1.2.3.1 Reflective devices	10
1.2.3.2 Transmissive devices	11
1.2.3.3 Electrolytes	11
1.3 Tungsten Trioxide	12
1.3.1 Introduction	12
1.3.2 Structure	13
1.3.3 Colouration	14
1.3.4 Preparation of WO ₃ films	17
1.3.4.1 Evaporation	17
1.3.4.2 Sputtering	18
1.3.4.3 Other techniques	18
1.3.5 Properties of WO ₃ films	19
1.3.5.1 Optical properties	19
1.3.5.2 Ion insertion	20
1.3.5.3 Stress	22
1.3.5.4 Electrochemical properties	22
1.3.5.5 Influence of water	23
1.3.5.6 Ageing	23
1.3.5.7 Other properties	23
1.3.6 Devices	24
1.3.6.1 Liquid electrolytes	24
1.3.6.2 Solid electrolytes	25
1.3.6.3 Counter electrodes	26

1.4 Summary	26
<i>References</i>	28
2. THEORY	37
2.1 Introduction	37
2.2 Electrochemical techniques	37
2.2.1 Introduction	37
2.2.2 Cyclic voltammetry	37
2.2.1 Chronoamperometry	39
2.3 The quartz crystal microbalance	43
2.3.1 Introduction	43
2.3.2 Quartz crystals	44
2.3.3 Relationship between mass and frequency	46
2.3.4 Effect of crystal in contact with solution	47
2.3.5 Other effects	48
2.4 Interpretation of EQCM data	49
2.4.1 Introduction	49
2.4.2 Mass change versus charge relationship	49
2.4.3 Analysis of EQCM and electrochemical data	53
2.5 Other techniques	54
2.5.1 Introduction	54
2.5.2 Crystal impedance	54
2.5.3 Spectroelectrochemistry	55
<i>References</i>	58
3. EXPERIMENTAL	60
3.1 Introduction	60
3.2 Equipment	60
3.2.1 The three electrode cell	60
3.2.2 The electrochemical quartz crystal microbalance	61
3.2.3 Spectrophotometric experiments	63
3.3 Materials	64
3.3.1 Electrodes and cells	64
3.3.2 Chemicals	65
3.3.3 WO ₃ films	65
3.4 Experimental Procedure	66
3.4.1 Chemicals/glassware	66
3.4.2 Procedure for EQCM data collection	67
3.4.3 Procedure for collection of spectrophotometric data	69
<i>References</i>	70
4. EFFECT OF ELECTROLYTE COMPOSITION	71
4.1 Introduction	71
4.2 Electrochemistry of WO ₃	71
4.2.1 General features	71
4.2.2 The electrochemical quartz crystal microbalance	73
4.2.3 Relationship between mass and charge	75

4.2.4 Interpretation of $\Delta M_T F/Q_T$ values	76
4.3 Effect of changing the cation	77
4.3.1 Introduction	77
4.3.2 Comparison of Li^+ and Na^+ insertion into WO_3 films using cyclic voltammetric data	77
4.3.3 Mass changes versus potential responses	81
4.3.4 Variations from the $\Delta M_T F/Q_T$ data	89
4.4 Effect of changing anion	92
4.4.1 Introduction	92
4.4.2 Current responses recorded for ion insertion into WO_3 using 0.1M LiClO_4 /propylene carbonate and 0.1M LiCF_3SO_3 /propylene carbonate	93
4.4.3 Mass responses	95
4.4.4 Correlation of mass and charge responses	99
4.5 Effect of changing electrolyte concentration	106
4.5.1 Introduction	102
4.5.2 Cyclic voltammetric responses for differing activities of LiClO_4 /propylene carbonate	106
4.5.3 Normalised mass responses	109
4.5.3.1 Normalised mass changes versus charge responses for different electrolyte activities of LiClO_4	113
4.5.4 Explanation of non-ideal $\Delta M_T F/Q_T$ values	115
4.5.5 Influence of increasing concentration of LiClO_4	116
4.6 Summary	117
<i>References</i>	122
5. THE EFFECT OF ELECTRODE HISTORY	125
5.1 Introduction	125
5.2 Electrochemistry of WO_3	125
5.2.1 Electrochemical features	125
5.2.2 The “break-in” effect	126
5.2.3 Effect of potential scan rate	127
5.2.4 Cation insertion into WO_3	128
5.3 Electrochemical quartz crystal microbalance studies of WO_3	128
5.3.1 Quartz crystal microbalance experiments	128
5.3.2 Analysis of electrochemical quartz crystal microbalance data	130
5.3.3 Insertion of neutral species	133
5.3.4 Separation of overall mass changes into charged and neutral species	133
5.3.5 Ion insertion into WO_3 films	133
5.4 Spectroscopy of WO_3 films	137
5.4.1 Spectroscopic experiments	137
5.4.2 The “break-in” effect	138
5.4.3 EQCM and spectroscopic data	141
5.5 Effects of long term cycling	147
5.5.1 Introduction	147
5.5.2 Li^+ insertion	147
5.5.3 Na^+ insertion	152

5.6 Summary	155
<i>References</i>	157
6. EFFECTS OF EXPERIMENTAL TIME SCALE ON ION INSERTION INTO WO ₃ FILMS	160
6.1 Introduction	160
6.2 General electrochemical interpretation	160
6.2.1 Introduction	160
6.2.2 Chronoamperometry	160
6.2.3 <i>x</i> values	167
6.2.4 Diffusion coefficients	168
6.2.5 Cyclic voltammetric experiments	169
6.3 EQCM measurements	171
6.3.1 Introduction	171
6.3.2 EQCM data	171
6.3.3 Mass change versus charge measurements	173
6.3.4 Three-dimensional data analysis	178
6.3.5 The “break-in” effect	182
6.3.6 Mass responses from cyclic voltammetric data shown with respect to time	188
6.4 Effect of cation composition	192
6.4.1 Introduction	192
6.4.2 Chronoamperometric experiments	192
6.4.3 The “break-in” effect	200
6.4.4 Cyclic voltammetric data	205
6.5 Summary	209
<i>References</i>	212
7. CONCLUSIONS	213

CHAPTER 1 : INTRODUCTION

1.1 ELECTROCHROMISM

1.1.1 Introduction

In 1961, a paper was published by Platt^[1] in which a new term was used to describe the fact that absorption and emission spectra of certain dyes could be influenced upon the application of a strong electric field: this new word was electrochromism. Whereas thermochromism and photochromism describe colour changes produced by heat or light respectively, electrochromism describes the property of a system or material to change colour reversibly when a potential is applied^[2].

Electrochromic materials can be divided generally into two different classes; inorganic and organic. Organic systems include bipyridilium systems and electroactive conducting polymers (eg, polybithiophene, polyterthiophene, polypyrrole and polyaniline). Examples of inorganic systems are phthalocyanine compounds, Prussian blue and metal oxides. Since the colour contrast seen when electrochromic materials are used is so distinct, a logical application is for displays.

1.1.2 Present technology^[3]

Present display devices in use are cathode ray tubes, liquid crystal displays and light emitting diodes.

1.1.2.1. Cathode ray tubes

Cathode ray tubes (CRTs) produce sharp, clear rapidly changing images of a composite nature in television sets that have a fast response time. A disadvantage of CRTs is that they require both a high vacuum and also a high energy electron source (which

consumes a large amount of power). The cost of manufacture of these devices is kept small due to the large-scale manufacture of the CRTs, although the screen pigments for television sets are made from expensive rare-earth compounds.

1.1.2.2 Liquid crystal displays

Compared to CRTs, liquid crystal displays (LCDs) consume little power and have a low manufacturing cost. The images produced are sharp and clear but most displays are monochromatic, as colour LCDs are both rare and expensive.

1.1.2.3 Light emitting diodes

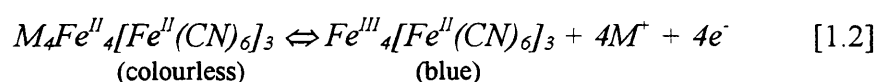
Light emitting diodes (LEDs) are devices comprising a p,n junction between two semi-conductors. Conducting organic polymers have been recently reported as being used as LEDs, although they are usually inorganic.

1.1.3 Electrochromic Terminology

The terminology used in electrochromism is described in detail in reference ^[3], this section outlines the terms used by the electrochromic community.

1.1.3.1 Primary and secondary electrochromism

If both the working and counter electrode are electrochromic materials, then it is obvious that for use in an ECD they must complement each other. Secondary electrochromes complement the primary electrochrome with one colouring on ion insertion and the other colouring when ions are extracted. The secondary electrochrome however does not need to colour at all. An example of this is tungsten trioxide (WO₃) and Prussian blue (PB)^[4]. Equations [1.1] and [1.2] show the electrochromic reactions of both materials



In equation [1.1], WO_3 becomes coloured upon reduction, whereas PB is coloured when oxidation occurs [1.2]. WO_3 is labelled the primary electrochrome and PB acts as a secondary electrochrome. The secondary electrochrome can be one of many materials to complement WO_3 , these include IrO_2 , Nb_2O_5 or V_2O_5 .

1.1.3.2 Colour

Table 1.1 shows how visible light is split up into the recognisable colours from violet (420nm) to red (700nm). White light is light that consists of all the visible wavelengths, and in white light the perceived colour of the material studied is the complementary colour of the light which it absorbs (ie, the complementary colour of red is green, of blue is orange and of yellow is violet).

Table 1.1 : Table showing how white light is split up into six general colours. Data taken from ref^[5]

Colour	frequency / $\times 10^{14}\text{Hz}$	wavelength / nm	wavenumber / cm^{-1}
Red	4.3	700	1.43
Orange	4.8	620	1.61
Yellow	5.2	580	1.72
Green	5.7	530	1.89
Blue	6.4	470	2.13
Violet	7.1	420	2.38

A single wavelength of absorption is seen when only single-ion or single-atom photon absorption occurs. The excitation of an electron between energy levels transforms the photon energy into internal electronic energy. In molecules, the energy levels which are involved are actually broadened by both vibrational and rotational energy and upon light absorption there is a transition between two areas of energy levels which gives rise to an absorption band. The average transition corresponds to the maximum absorption which is roughly in the centre of the band.

The molecule is termed a chromophore, and the colour resulting from absorption (when produced electrochemically) is an electrochromophore (or electrochrome).

The absorption spectrum of a chromophore depicts the relative intensity (number of photons) which are absorbed at each wavelength. A spectrophotometer records the absorption spectrum and plots absorbance (Abs) or its inverse, transmittance (T), against wavelength (λ) or wavenumber (λ^{-1}). The Beer-Lambert law relates absorbance (which is the log of the ratio of the intensities) to concentration of the chromophore and optical pathlength through the sample studied.

1.1.3.3 Response time

The term response time (τ) refers to the amount of time it takes an ECD to colour from its bleached state or bleach from its coloured state. For most devices, these values are usually a few seconds^[3], and for ECDs generally τ is slower than for CRTs or LCDs. This is usually because of the need for diffusion, be it the electrochrome diffusing to the electrode or the diffusion of a charged species through the electrode film. For electrochromic mirrors or windows, then a τ value of a few minutes (for windows) or seconds (for mirrors) is acceptable, but for ECDs to be used as optical switches, then very fast τ values are needed.

1.1.3.4 Cycle life

The cycle life of an ECD is the measure of the number of colouring/bleaching cycles possible before the device fails. Failure may result from chemical side reactions or physical changes within the ECD. For an ECD to be reliable, then a long cycle life is of great importance.

1.1.3.5 Insertion coefficient

The insertion coefficient x is found to be dependent on the charge passed in an electrochromic system. For metal oxides of the general formula C_xAB_n , the amount of x inserted into the system can determine the colour of the metal bronze^[3].

1.1.4 Types of electrochromes

Chang *et al*^[6] published a paper in which electrochromes were classified into four different types. All the electrochromic systems were based upon an electrochemical redox reaction and are labelled type I, II, III or IV

Type I electrochromes are defined as being species which undergo simple redox reactions, where ions or molecules in solution are either reduced or oxidised, at the cathode or anode respectively, to produce a coloured absorbing species. Examples of these are the polytungstate anion^[6] or the methyl viologen dication^[3].

Type II electrochromes are species which undergo a simple redox reaction, but they are combined with an independent chemical reaction. It is this chemical reaction which controls the rate of reversal of the coloured electrochrome back to its bleached state. An example of this is the polytungstate anion and hydrogen peroxide^[6].

A type III electrochrome is one where there is a redox reaction combined with a chemical reaction, resulting in formation of an insoluble coloured species. It is only upon the onset of an electrochemical reaction that the colour is bleached. An example of this is heptyl viologen^[3].

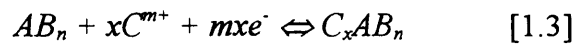
The final type of electrochrome (type IV) is where there is a redox reaction in which a solid film deposited upon an electrode is reduced. Upon reduction or oxidation of this solid film an intense colour change is produced and formation of the colour is confined to the solid film.

Two separate diffusion processes occur in the solid film. There is ion diffusion from the electrolyte/solid interface and also electron diffusion from the electrode/electrochrome interface. It will be the slowest diffusion coefficient in the electrochrome that will be observable and this is called the chemical diffusion coefficient^[3]. This type of electrochrome

is most commonly used for ECDs and examples of these are prussian blue and metal oxides^[3].

1.1.5 Metal oxides

The general mechanism for ion insertion into a metal oxide was given by Dautremont-Smith^[2]



where AB_n and C_xAB_n have different imaginary parts of their refractive index, m is a small integer (either positive or negative), x is non-integral (usually $0 < x < 1$) and n is close to integral. If the metal oxides have a reduced coloured state, then they are “cathodically colouring”, whereas, if they have an oxidised coloured state then they are “anodically colouring”. Dautremont-Smith published two comprehensive reviews of both anodically^[7] and cathodically colouring^[2] metal oxides. Examples of anodically colouring metal oxides are iridium, nickel, cobalt and rhodium oxides, and cathodically colouring metal oxides are vanadium, niobium, titanium, molybdenum and tungsten oxides.

1.1.5.1. Structure of metal oxides

Metal oxides can be split into four main groups with respect to their bulk crystalline structures^[8]. They are perovskite-like, rutile-like and layer and block structures.

1.1.5.1.1 Perovskite-like structures

Perovskite structures have the general formula ABX_3 and are named after the mineral perovskite $CaTiO_3$. The general structure is shown in Figure 1.1 and it can be seen that Ti occupies the corners of the cell, Ca is at the centre and O are at the mid points of its edges^[9].

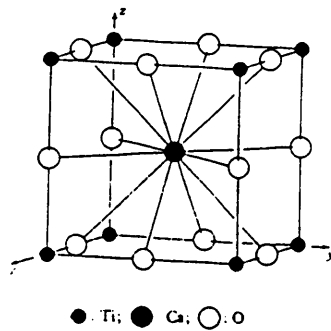


Figure 1.1 : The perovskite structure as seen for CaTiO_3 . Taken from ref^[9].

1.1.5.1.2 Rutile structures

Rutile and rutile-like structures are found amongst a group of materials which can exhibit either cathodic or anodic electrochromism. The structure is considered as being built from almost octahedral MeO_6 units which form infinite edge-sharing chains. The chains are arranged in such a way that they form an equal number of vacant tunnels^[8]. Many rutile and rutile-like structures take the formula MeO_2 , examples of which are TiO_2 , MnO_2 , VO_2 , IrO_2 , RuO_2 and RhO_2 ^[8]. Figure 1.2 shows a general structure for rutile^[9].

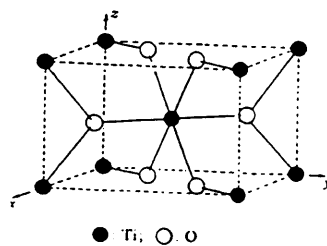


Figure 1.2 : The rutile structure for TiO_2 . Structure taken from ref^[9]

1.1.5.1.3 Layer and block structures

These structures are partially defined and their structural properties are not as well explored as those described above. Examples of layer and block structure are hydrated NiO_x , V_2O_5 and Nb_2O_5 ^[8].

1.2. ELECTROCHROMIC DEVICES

1.2.1 Introduction

Electrochromic devices (ECDs) have to compete with both CRTs and LCDs commercially, although they have advantages over both systems^[3]. ECDs use little power to produce images and, once the images are formed, they continue with little or no extra input of power. This effect is termed the “memory effect”^[10]. Another advantage is that an ECD has no limitation (in principle) to the size of the device, and either a large electrode or a number of smaller electrodes can be used^[3]. There is a disadvantage though, that if a large area is used, then there may be the formation of patchy areas which is due to uneven current distribution across the electrode surface^[3].

Another disadvantage with ECDs is that under certain conditions, external lighting may be needed to produce a visible image and there is also the possible problem of storage and construction of these devices.

With optical data storage, pixels can be either “on” or “off” when coloured and bleached which can then interrupt (or not) a light or laser beam. However, fast response times (sub-nanosecond) are needed and as of yet, there are no ECDs of this speed.

Electrochromic mirrors in cars are considered a useful application of ECDs^[11]. Electrochromic sunglasses which can be darkened at will have been produced, and from

this, windows which can be coloured electrochemically to reduce light entering a room have been studied.

1.2.2 “Smart windows”

In 1984 papers were published by both Rauh *et al*^[12] and Svensson and Granqvist^[13] regarding materials for electrochromic windows. Svensson and Granqvist^[13] noted that if the beginning of high reflectance occurs at a wavelength of $\approx 0.7 \mu\text{m}$ then window coatings can be used to decrease the inflow of the infra-red solar radiation. This will reduce the need for air-conditioning in warm climates. On the other hand, if the start of high reflectance is at a wavelength of $\approx 3 \mu\text{m}$, then these windows will provide a low thermal emittance and therefore improve thermal isolation needed in colder climates. Therefore, by constructing suitable electrochromic devices, “smart windows” can be produced^[14].

1.2.3 Design of ECDs

ECDs are generally made up of a sandwich structure of thin layers, the number of layers is dependent upon the use of the ECD. Electrochromic systems can be employed in one of two ways; reflective or transmissive devices. Figure 1.3 shows a general diagram of both modes.

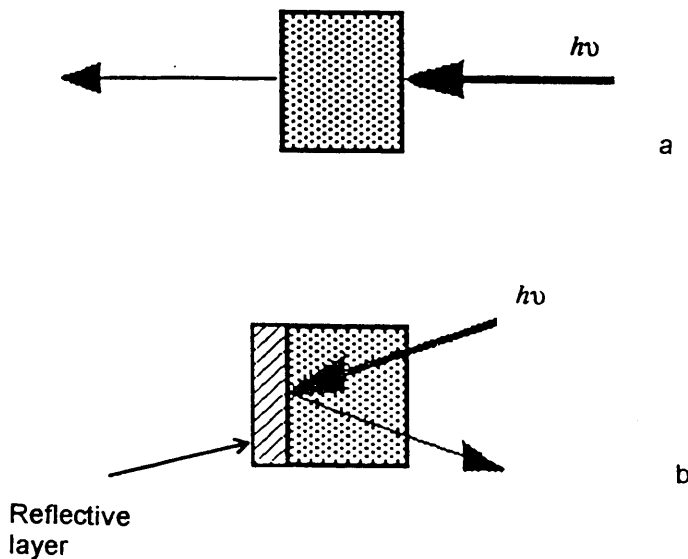


Figure 1.3 : General diagram showing both types of ECD. Figure 1.3a shows an ECD in the transmissive mode. Figure 1.3b shows an ECD in the reflective mode.

1.2.3.1 Reflective devices

Figure 1.4 shows a schematic diagram of a reflective ECD. The front panel is a solid support, for example glass, which has a thin transparent, conductive film on the side which is in solution. This film is usually indium-tin-oxide (ITO). This front panel is termed an optically transparent electrode (OTE) and acts as a conductor of the electrons needed for the electron transfer to occur in the electrochromic material. The primary electrochromic layer is then deposited onto the OTE which will minimise contact resistances.

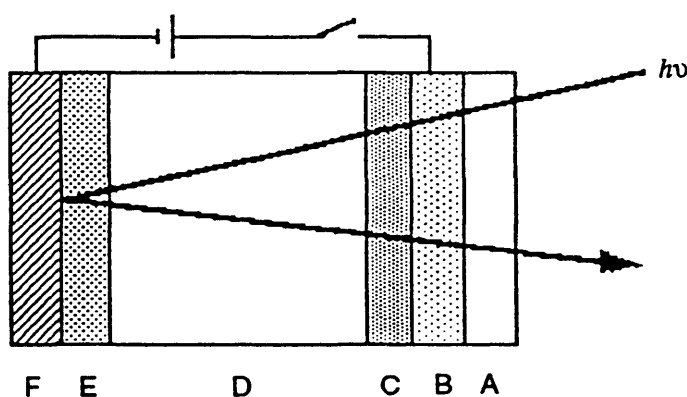


Figure 1.4 : General schematic showing an ECD constructed to act as a reflective device. Labels are as follows; A : glass support or window, B : optically transparent electrode, C : solid primary electrochromic layer, D : ionically conductive electrolyte, E : solid secondary electrochromic layer, F : reflective counter electrode.

ECDs which are reflective use a reflective material such as polished platinum or a rhodium alloy, in front of which both the primary and secondary electrochromes are placed. The counter electrode and reflector are usually combined and potential is applied between the front OTE and the rear electrode/reflector. ECDs where a separate reflector is placed in front of the secondary electrochromic layer have also been constructed^[15] in which the counter electrode does not need to be electrochromic.

1.2.3.2 Transmissive devices

Figure 1.5 shows a transmissive cell for use as an ECD. Again, as for the reflective device, the primary electrode is deposited onto an OTE. The major difference between the two devices is that the transmissive cell also has a secondary electrochrome deposited onto an OTE. All layers have to be fully transparent in the visible region of the spectrum. The intensity change seen from a transmissive device is only half that of a reflective ECD. This is because light is passing through the primary electrochrome twice in a reflective ECD (both before and after reflection), but only once through a transmissive ECD.

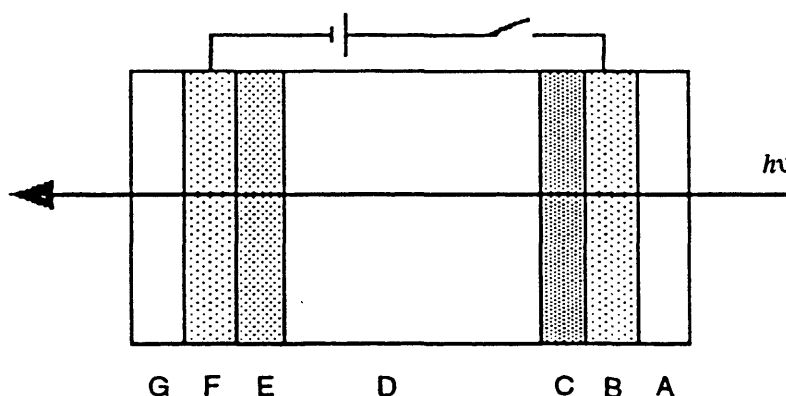


Figure 1.5 : General schematic showing an ECD constructed to act as a transmissive device. Labels are as follows; A : glass support or window, B : optically transparent electrode, C : solid primary electrochromic layer, D : ionically conductive electrolyte, E : solid secondary electrochromic layer, F : optically transparent electrode, G : glass substrate.

1.2.3.2 Electrolytes

An important consideration in ECD construction is the type of electrolyte to be used. Electrolytes can be divided into either liquid or solid electrolytes.

For liquid electrolytes to be used, then ionic charge carriers are needed in the area between the primary and secondary electrochromes. An unreactive salt which will ionise acceptably in the solvent chosen, and which is stable to photolysis is ideal for a liquid

electrolyte. The most commonly used solvents for liquid electrolytes are propylene carbonate or dimethylformamide. Perchlorates, such as LiClO_4 , are commonly used as the salt for these electrolytes^[3].

One major factor to be considered in the use of a liquid electrolyte in an ECD is that device needs to be sealed securely. Initially, liquid electrolytes were developed for small devices such as wrist watches, where high contrast (even when viewed at a large angle of incidence) and excellent viewing properties were reported^[16].

Solid electrolytes can be split into two different categories; organic and inorganic. Organic electrolytes are often either polymer electrolytes or polyelectrolytes^[3]. Polymer electrolytes are macromolecular species, examples of which are poly(ethylene oxide) or poly(propylene glycol). In these polymers, dissolved salts, such as LiClO_4 or HCF_3SO_3 are found and have been used extensively with electrochromic materials such as WO_3 ^[17]. Polyelectrolytes are defined as being polymers which contain ion-labile groups, for example poly(2-acrylamido-2-methylpropanesulphonic acid) (poly-AMPS) which has proton molecules along its backbone which act as donor molecules^[18].

Inorganic solid electrolytes are considered to be superior to organic electrolytes since they are more stable to photolytic degradation^[3]. An example of this type is hydrogen uranyl phosphate^[19].

1.3 TUNGSTEN TRIOXIDE

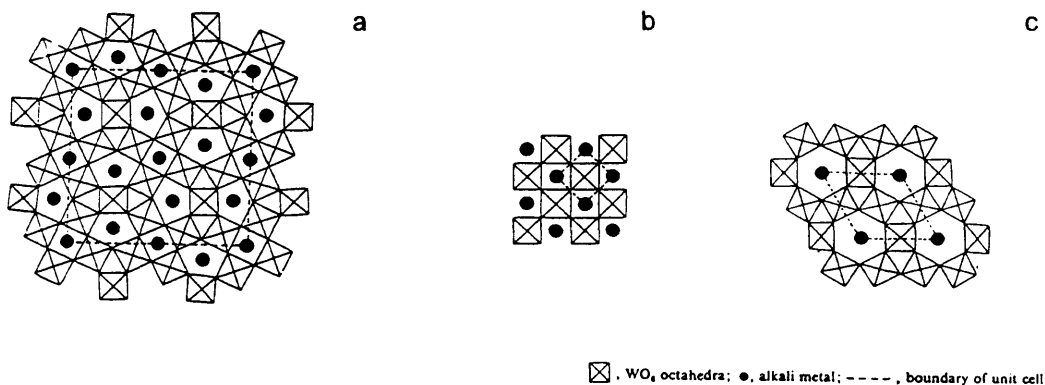
1.3.1 Introduction

The electrochromic properties of amorphous tungsten trioxide (WO_3) were first discussed by Deb^[20] who investigated both optical and electrical properties. There have been many reviews written since about WO_3 , including those by Granqvist^{[16][21]} and Faughnan and Crandall^[22]. The ease with which cations such as H^+ and Li^+ can be inserted

into WO_3 films has led to the suggestion that this electrochromic metal oxide could be used in ECDs^[23].

1.3.2 Structure

The structure of WO_3 is based upon corner sharing WO_6 octahedra and is termed perovskite, as discussed in Section 1.1.5.1. Figure 1.1 showed the perovskite structure for the metal oxide CaTiO_3 . WO_3 is said to have the distorted perovskite-like structure which is referred to as the rhenium oxide (ReO_3) structure. Deviations from the ideal perovskite structure can be seen when W atoms are displaced and also when there is rotation of the O octahedra seen. These distortions are temperature dependent and pure WO_3 crystals go through the structural transformations of tetragonal \rightarrow orthorhombic \rightarrow monoclinic \rightarrow triclinic \rightarrow monoclinic as the temperature is lowered from 900°C to -189°C ^[24]. Cation insertion into WO_3 films has been reported to produce tungsten bronzes with different structures, depending on which cation is inserted. At low to intermediate x values for Li_xWO_3 and Na_xWO_3 bronzes and intermediate x values for K_xWO_3 , the structure is tetragonal. Hexagonal phases are seen upon insertion of a small amount of large cations, for example in K_xWO_3 , Cs_xWO_3 or In_xWO_3 ^[25]. Figure 1.6 shows the general structures for tetragonal, cubic and hexagonal structures of the tungsten bronzes, together with the relationship between crystal structure and ion insertion.



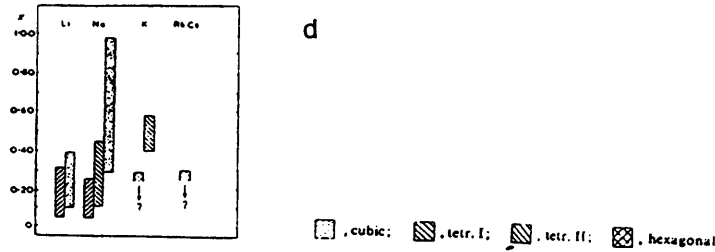
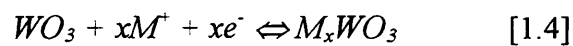


Figure 1.6 : The general structures of the tungsten bronzes are shown. Figure 1.6a represents the tetragonal structure, 1.6b shows the cubic structure and 1.6c gives the hexagonal structure. Figure 1.6d shows the relationship between crystal structure and ion insertion. Figures taken from ref^[25].

1.3.3 Colouration

Colouration of WO_3 films arises from the transition of W^{VI} to W^V , with electron transfer between the two states causing colouration. Equation [1.4] shows the general equation for ion insertion into WO_3 .



where M^+ represents a singly charged cation such as H^+ or Li^+ , and x is the insertion coefficient, discussed in Section 1.1.3.5.

Figure 1.7 shows the corresponding energy level diagram for the perovskite structure of MeO_3 . The atomic s , p and d orbitals for the metal are shown, along with the $2s$ and $2p$ levels of oxygen. For ReO_3 and WO_3 then the energy levels of interest are $6s$, $6p$ and $5d$. The $5d$ level is split up into e_g and t_{2g} levels. This occurs because the e_g orbitals point directly to the electronegative O and the t_{2g} orbitals point away from O and therefore the t_{2g} orbitals are of lower energy than e_g . The $O2p$ level is also split up into $2p_\sigma$, which

point directly at the electropositive Me and $2p_{\pi}$ which point into empty space. Therefore, as for the Me $5d$ levels, the $2p_{\pi}$ orbitals are at a lower energy.

Since the number of states available for electron occupancy is fixed for each band, then WO_3 which has 24 electrons, occupies the s and p levels and the Fermi energy is found to lie in the gap between the t_{2g} and p_{π} bands which makes the bandgap wide enough to make WO_3 transparent^[25]. However, in comparison, ReO_3 has 25 electrons and so occupies the lower part of the t_{2g} level and the material is not transparent.

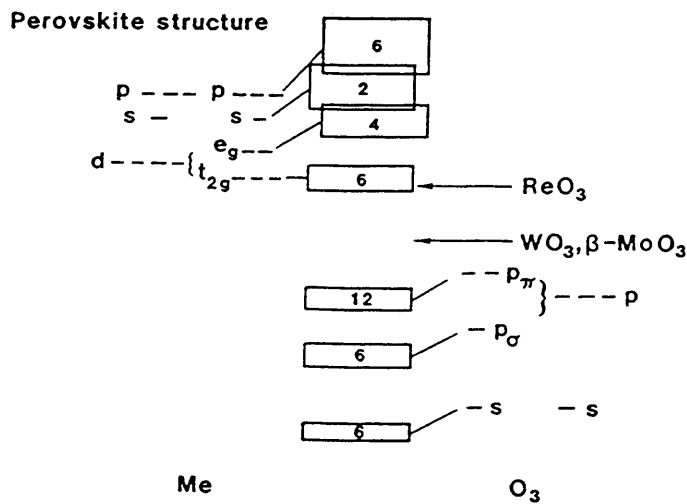


Figure 1.7 : Energy level diagrams for perovskite-like metal oxides. Arrows indicate position of Fermi levels. Band structure diagrams for WO_3 , $\beta\text{-MoO}_3$ and ReO_3 are shown. Data taken from ref^[26].

When ions and electrons are inserted into the metal oxides, then the Fermi level is moved upwards. For WO_3 , excess electrons enter the t_{2g} band and the material then becomes either absorbing or reflecting (depending on whether electrons are occupying localised or extended states). Upon extraction of electrons, the material again becomes transparent. When electrons are inserted into ReO_3 , then the Fermi level moves upwards but remains well inside the t_{2g} band and the material is not electrochromic.

WO_3 has a band gap of ≈ 3.5 eV and is considered to be virtually an insulator^[11]. Before colouration, WO_3 is pale yellow, with all W atoms of valency +6. When a tungsten

bronze is formed, then some W^{VI} ions are transformed into W^V and a mixed valency compound where both states exist is formed. Figure 1.8 shows a diagram of the valence and conduction band of WO_3 and the tungsten bronze. It can be seen in Figure 1.7 that the $5d$ electrons of W^V lie below the empty conduction band. When these electrons are promoted into the conduction band the photon energy is $\approx 1.4\text{eV}$ which corresponds to the electron transfer from $W^V \rightarrow W^{VI}$. This process causes an optical absorption band at the red end of the spectrum^[11].

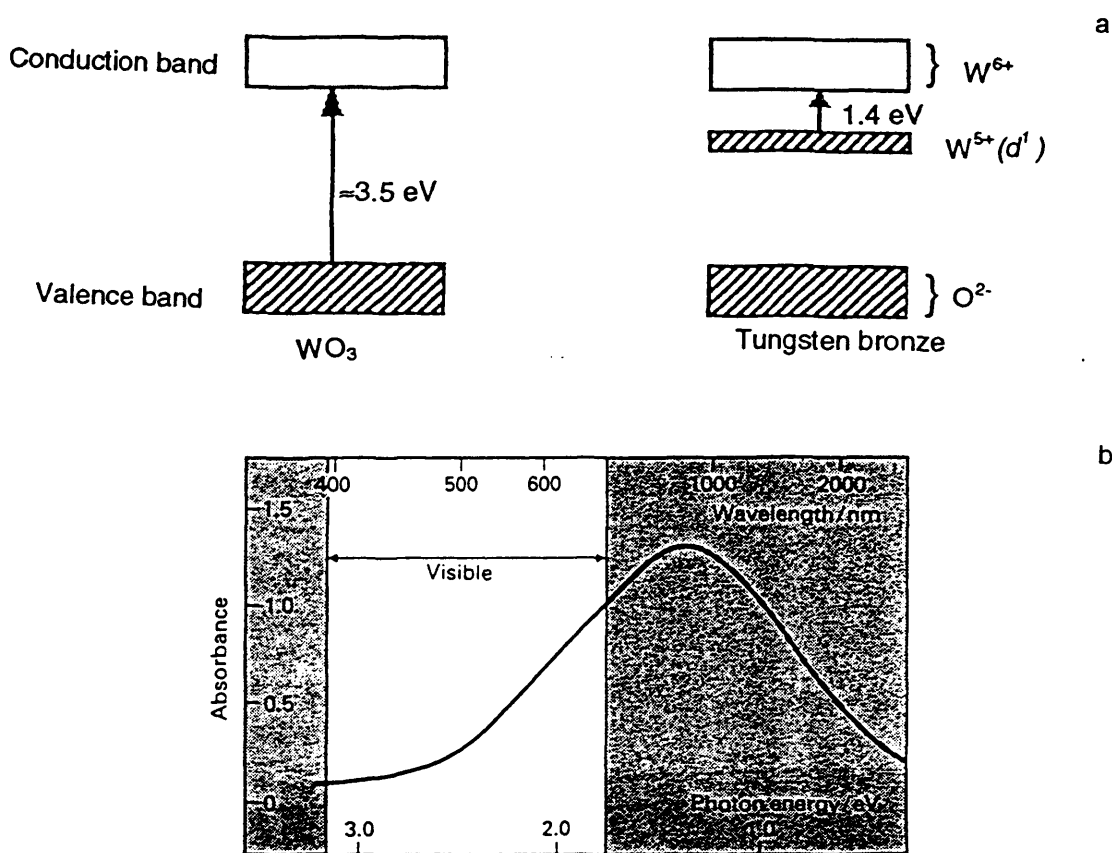
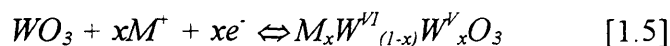


Figure 1.8 : Figure 1.8a shows a general diagram showing the conduction and valence band for WO_3 and tungsten bronze. Intermediate band seen in tungsten bronze schematic indicates the position of the $5d$ electron of W^V . Figure 1.8b shows the absorption spectrum of the tungsten bronzes of the composition $H_{0.17}WO_3$. Figure 1.8a adapted from ref^[11]. Data for Figure 1.8b taken from ref^[11].

Therefore the ion insertion mechanism can be written more accurately as



There have been many theories put forward regarding the nature of colouration of WO_3 films. Deb^[20] suggested the formation of F-centres where the electrochromic effect is caused by the injection of electrons which are then trapped at oxygen vacancies where F-centres are formed. Gabrusenoks *et al*^[27] suggest that electrons injected during colouration are localised in the W $5d$ orbitals, and then propose that the optical absorption seen for ion insertion is due to the intervalence charge transfer transition between W^{V} and W^{VI} . The intervalence charge transfer transition (ICTT) was first discussed by Faughnan and Crandall^[22].

Another theory for colouration of WO_3 films is that of polarons. Kuzmin and Purans^[28] used X-ray absorption spectroscopy to establish that due to structural changes seen when WO_3 films are coloured, small-radius polarons are formed. This effect is accompanied with a strong lattice deformation around the W ions that have trapped electrons and that their electronic structure is rearranged upon forming W^{V} .

1.3.4 Preparation of WO_3 films

Thin films of WO_3 can be prepared using a number of different techniques. The two most common techniques are evaporation and sputtering although there are many others which are also discussed.

1.3.4.1 Evaporation^[29-35]

Evaporation is a convenient and widely used technique. Whilst in a foil boat, the bulk material is heated within a vacuum chamber and the film sublimes onto the substrate to be coated^[3]. If the film is annealed, then the amorphous film will become crystalline, a fact which is important when depositing WO_3 , as amorphous and crystalline films give slightly different results^[16]. Following evaporation, to minimise annealing effects, the substrate may

be placed on a cooled holder, as crystallisation occurs at $\approx 400^{\circ}\text{C}$. Granqvist^[16] states that the films should be regarded as being micro-crystalline rather than amorphous.

1.3.4.2 Sputtering^[36-40]

Sputtering is another widely used technique. There are two types of sputtering; RF or DC-magnetron. WO_3 films are produced when a target of tungsten or tungsten oxide is bombarded with reactive oxygen molecules^[3]. These reactive molecules arise from the mixture of O_2/N_2 or O_2/Ar gases at low temperatures. The substrates on which the WO_3 film is to be deposited are cooled with water. This prevents thermal annealing together with the chance that the deposited film may be evaporated. The sputter parameters (deposition rate, gas mixture, temperature) can be adjusted to produce WO_3 films which exhibit good electrochromic properties^[36].

1.3.4.3 Other techniques

Vapour deposition can be either chemical (CVD)^[40-42], in which the pyrolysis of $\text{W}(\text{CO})_6$ at 400°C produces the WO_3 film, or photochemical (PVD)^[43], in which a low pressure mercury lamp is used as the light source for the pyrolysis and the deposition temperature is lowered to $\approx 200^{\circ}\text{C}$.

Anodisation has also been used to deposit WO_3 films. Delichere *et al*^[44-45] potentiostatically polarised tungsten plates in 1N H_2SO_4 at potentials between 0 and 70 V to produce WO_3 films.

Another technique is the use of the sol-gel technique to produce WO_3 films^[46-47]. Agnihotry^[47] has reported that, to produce an electrochromic film using sol-gel processing costs less money than by producing films by the usual vacuum methods. Sol-gel can produce films which can be deposited over large areas. These two factors should lower the cost of producing the ECD.

1.3.5 Properties of WO₃ films

Many different properties of WO₃ films and tungsten bronzes have been studied since it was first discovered. This section deals with those properties which have been studied in some detail.

1.3.5.1 Optical properties

As equation [1.5] shows, when an cation is inserted into WO₃, a tungsten bronze $M_xW^{VI}_{(1-x)}W^{V}_xO_3$, is formed. Depending on the amount of M⁺ inserted, the bronze may show a variety of colours. Figure 1.9 shows the various x values together with their corresponding colours for Na⁺ insertion into WO₃.

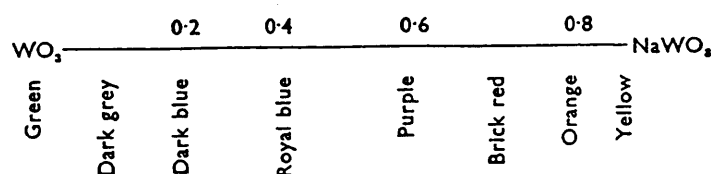


Figure 1.9 : Schematic diagram showing the colour change for increasing x values for the sodium tungsten bronzes. Data taken from ref^[24].

Baucke *et al*^[48], studied the tungsten bronze H_xWO_3 at the visible-near IR range of the spectrum. The absorption band seen at 9,000 - 10,000 cm⁻¹ was assigned to the transition between W^V and W^{VI}. Spectroscopy has been used to study ion insertion into WO₃, where the ions studied are Li⁺, H⁺, Na⁺ and Ag⁺^{[42][49-58]}. Temmink *et al*^[59] used electron spectroscopy for chemical analysis (ESCA) to study hydrogen tungsten bronzes and saw that the change in electronic structure from W^{VI} to W^V was seen by chemical shifts in the 4*f* doublet. They concluded that the extinction coefficient (ϵ) for each wavelength is proportional to the amount of W^V present up to a certain injected charge value.

Raman spectroscopy has been studied by various authors^{[27][33][38][60-62]}. Gabrusenoks *et al*^[27], reported that Raman shows the presence of terminal W-O-W bonds in amorphous WO₃ films, whilst Ohtsuka *et al*^[61] suggested that the decrease of the Raman band at 960 cm⁻¹ (the terminal W^{VI}=O bond) shows the terminal bond reacting with water in the film to produce W^V-OH.

Deb used UV-visible spectrophotometry to study WO₃ films at various temperatures^[20]. He determined that the band gap for WO₃ is 3.25 eV. He found that as WO₃ goes from the amorphous to the crystalline state then the optical absorption gap decreases in energy. Studies in the UV region of the spectrum has also been carried out by other workers^{[45][50]}. Shen *et al* used a combination of UV-visible and chronoamperometric techniques to determine *x* values for tungsten bronzes M_xWO₃^[63].

Other spectroscopic techniques used to study WO₃ films include ellipsometry^{[55][64-65]}, ac impedance^{[51][56]}, x-ray diffraction^[41], FTIR^{[33][58][66-67]}, XANES, XFAS^{[27][68]}, SIMS^[69], XPS^{[31][70-71]} and ESR^[26]. Nanba *et al*^[38] used a combination of Raman and x-ray radial distribution analysis to find that amorphous WO₃ films consisted of three-, four- and six-membered rings of WO₆ octahedra, almost identical to hexagonal WO₃ crystals. Badilescu *et al* used spectroscopy to study Li⁺ insertion into WO₃ films prepared by different methods^[72]. They showed that the formation of lithium tungstate is independent of the method of preparation.

1.3.5.2 Ion insertion

Insertion of cations into WO₃ films has been studied using a variety of techniques. The change in optical density has been studied upon Li⁺ insertion into a WO₃ film which suggests that under certain conditions, a large irreversible amount of Li⁺ is seen which is attributed to the presence of oxygen within the film^[73-74]. Zhong *et al*^[75] showed that insertion of Li⁺ into the WO₃ film is dependent upon film preparation, whereas Pyun and

Bae showed that chemical diffusion of Li^+ increases as Li^+ content in the tungsten bronze is increased^[76]. Xu and Chen determined the chemical diffusion coefficient of Li^+ using a overvoltage decay method and concluded that the chemical diffusion coefficient is large in nearly pure WO_3 films, but decreases as the Li^+ content increases^[77]. Bohnke *et al* saw an increase in electrical conductivity during Li^+ insertion, followed by a decrease upon extraction^[78].

Kamimori *et al* studied Li^+ insertion into WO_3 using a variety of techniques and concluded that the diffusion coefficient was strongly dependent upon the water content in the electrolyte^[79]. Zhang and co workers reported that the rate of colouration for the Li_xWO_3 bronze is limited by decreasing electromotive force, whereas bleaching is limited by either diffusion impedance or by the space charge^[80]. Mohapatra^[81] also noted that the colouring/bleaching kinetics are dominated by two separate effects; colouration is dominated by charge transport across the WO_3 -electrolyte interface, whereas bleaching is dominated by space charge limited current flow.

Proton insertion has also been studied^[82] and diffusion coefficients calculated for H^+ ^[83]. Nishimura *et al*^[84] demonstrated that by studying WO_3 films in D_2O then the bronze D_xWO_3 is formed. Reichman and Bard studied H^+ insertion using a variety of electrochemical techniques and different WO_3 films. They concluded that kinetic behaviour is dependent upon the amount of water present in the film and the porosity of the WO_3 film under investigation^[32].

The mechanism of ion insertion into WO_3 films has been investigated by various authors. Hashimoto and Matsuoka used XPS and found that a state below the Fermi level is seen in tungsten bronzes studied^[31]. When the amount of Li^+ injected increases then this level is found to increase proportionally. They concluded that the electron occupies the

bottom of the unoccupied colouration band (seen in Figure 1.8) after colouration and an intraband transition from the occupied colouration band to another empty state is the reason that colouration is seen. XPS was also used by other groups to investigate tungsten bronzes and it was found that there is simultaneous injection of electrons and cations into the WO_3 film upon colouration^[70-71]. Goldner *et al* found evidence that free electrons played a dominant role in the electrochromic properties of crystalline WO_3 films^[85].

1.3.5.3 Stress

Stress within WO_3 films has been studied by various groups. Kaneda and Suzuki^[36], found that stress, density and film structure is dependent on sputtering conditions. This suggestion was also suggested by Hugon and co workers^[35] and Haghiri-Gosnet *et al*^[86]. Fang *et al*^[87] used both Ar and Xe gases when depositing sputtered films and found that film stress is dependent on the defect content of the films, such as voids, the columnar film structure and entrapped impurities of gas. They concluded that the stresses generated in sputtered thin films can be successfully controlled via Ar or Xe ion energy.

1.3.5.4 Electrochemical properties

Combined electrochemical and gravimetric properties have been studied by several workers^[88-94] who investigated ion intercalation into WO_3 films using the quartz crystal microbalance. Zhang *et al*^[34] and Dini *et al*^[30] used a galvanostatic intermittent titration technique (GITT) to study diffusion coefficients of various ions entering and leaving the WO_3 film. Kamimori used a variety of methods, including chronoamperometry, to establish that the diffusion coefficient is dependent on the water content in the WO_3 film^[79], and Zhang concluded that the diffusion coefficient is dependent on the preparation of the film^[34]. Crandall and Crandall used electrical measurements to calculate diffusion coefficients^[95].

Green and Travlos^[96] studied the electrical properties of Na_xWO_3 and concluded that with increasing x there is a decrease in activation energy for these sodium tungsten

bronzes. A relatively new technique; probe beam deflection has also been used in combination with cyclic voltammetry to study charge transfer reactions together with ion diffusion and/or migration in WO_3 ^[97].

1.3.5.5 Influence of water

It has been found that the presence of water in a WO_3 film aids colouration. Bohnke and co-workers^[29] suggested that no more than 10% water (by weight) can be added to a propylene carbonate solution (the limit of miscibility for these two solvents) and suggest that simultaneous H^+ and Li^+ ion insertion occurs. The introduction of water to the deposition process was investigated by Shigesato *et al*^[33]. They found that carrier density was increased for ITO films and that there was an increase in $\text{W}=\text{O}$ bonds seen by Raman spectroscopy. Water penetration of the amorphous WO_3 film, studied by Shiyanovskaya lead to a decrease in electrochromic efficiency due to the formation of $\text{WO}_3 \cdot n(\text{H}_2\text{O})$ ^[62]. Inaba *et al* reported that the addition of water to LiClO_4 /organic solvent gave no change in the mass of intercalated ions although the bleaching rate was increased^[93].

1.3.5.6 Ageing

Ageing effects of WO_3 films have been studied by various workers^{[68][98-100]}. All workers found that tungsten bronzes could be successfully coloured and bleached for many thousands of cycles. Work carried out by Nagai *et al*^[101] showed that there are two types of active sites available for accepting Li^+ into WO_3 . Sun and Holloway^[102] found that oxygen backfilling during evaporation of the WO_3 film exhibit longer lifetimes and improved corrosion resistance.

1.3.5.7 Other properties

The kinetics of WO_3 films have been widely studied. Electrochemical techniques have been used to study kinetics by Sunseri *et al*^[103] and Bohnke *et al*^[104] concluded that colouration is limited by ionic diffusion of the inserted cation into the host matrix.

Vuillemin and Bohnke^[105] also noted that for amorphous WO₃, the kinetics of colouration, studied using absorption data from spectrophotometric techniques are slower than the electrochemical reaction studied by observing the charge passed during colouration.

Other properties of WO₃ which have been investigated are thermochemistry^[106], thermodynamics^[107] and photochemistry^[108]. This wide range of properties which have been studied shows the versatile nature of WO₃ thin films.

1.3.6 Devices

WO₃ devices can be used for both transmissive and reflective electrochromic devices. As already discussed in Section 1.2.3.2 the type of electrolyte used is of major importance in ECD design.

1.3.6.1 Liquid electrolytes

When WO₃ was first proposed as a suitable electrochromic thin film to act as the working electrode in an ECD, aqueous H₂SO₄ was initially used as the electrolyte. Randin^[109] showed that dissolution of the WO₃ film was seen to occur using H₂SO₄ and that WO₃ was more stable in non-aqueous solvents. Work carried out by Petit and Plichon^[110] showed that proton insertion into WO₃ films using a binary mixture of H₃PO₄/H₂O gave stable films when continuously cycled. They concluded that supercooled phosphoric acid (SCPA) improves film stability. Ando *et al*^[111] showed that using LiClO₄ as the salt to provide Li⁺ in propylene carbonate leads to films with a good cycle life, suitable for uses in ECDs. The use of LiClO₄/propylene carbonate as the electrolyte in an ECD has been studied by Rocco *et al*^[111], who used a polypyrrole counter electrode. Decker *et al*^[112] compared WO₃ and NiO_x in LiClO₄/propylene carbonate.

In an ECD, sealing of the device must also be considered and care must be taken that the liquid electrolyte does not leak out of the device. This leads to the conclusion that

for reliable ECDs, liquid electrolytes are not thought to be suitable. For the type of study chosen, a liquid electrolyte is a convenient option as they are easy to manipulate and a liquid media is required for the method of study.

1.3.6.2 Solid electrolytes

As previously mentioned, solid electrolytes can be separated into two categories; solid inorganic bulk-type ion conductors and solid inorganic thin film ion conductors.

The majority of work so far carried out has focused on inorganic bulk-type electrolytes as proton conductors. Mohapatra and co-workers used phosphotungstic acid and zirconium phosphate as possible proton donors for WO_3 films when produced as cold pressed pellets^[113]. However, both electrolytes were found to be susceptible to variations of the water content and reacted with the WO_3 films. A further candidate for a solid proton-containing electrolyte was reported by Howe *et al*^[19]. Hydrogen uranyl phosphate tetrahydrate (HUP) is known to have a high proton conductivity and the possibility of using HUP as a solid electrolyte was explored.

Inorganic thin film ion conductors are commonly known as “Deb devices”. Here there is a sandwich which consists of a water containing dielectric which has to be porous. Water incorporation occurs spontaneously on exposure to humid air and when a potential of approx 1.3V is applied then water can be decomposed into H^+ and OH^- . This results in H^+ being inserted into the WO_3 film^[16]. Lusic *et al*^[114] used $\text{SiO}_2 \cdot z\text{H}_2\text{O}$ as the electrolyte. Baucke, Bange and Gambke^[15] published a comprehensive study on all reflecting electrochromic devices where other solid electrolytes suggested for use are ZrO_2 , HfO_2 , Ta_2O_5 , MgF_2 and CaF_2 . These type of devices can be produced in either transmissive or reflective mode and some work has been carried out using Li^+ conducting films such as LiWO_4 ^[115-116].

The third type of electrolyte considered for ECD design is the polymer electrolyte. Proton containing polymers have been studied by Giglia and Haacke^[18] and Ho, Rukavina and Greenberg^[4], who both studied many types of proton conducting polymers and found that poly-2-acrylamido-2-methylpropanesulphonic acid (poly-AMPS) is a suitable solid proton containing polymer electrolyte to be used in ECDs. Using a WO₃ working electrode and a PB counter electrode configuration has given rise to solid electrolytes containing lithium salts such as LiClO₄, LiBF₄ or LiCF₃SO₃ with polymers such as poly(ethylene oxide) (PEO)^[17], oxymethylene polyoxyethylene^[117] or co polymers^[118-119].

1.3.6.3 Counter electrodes

Aside from prussian blue as a counter electrode to WO₃, work has also been done on a copolymer of polyaniline and nitrilic rubber^[120] and nickel oxide^[121]. Another possible counter electrode is to use an iron-graphite mixture as the potential of the counter electrode has an effect on the colouring and bleaching characteristics of the device^[122].

1.4 SUMMARY

The area of electrochromic device development and construction appears to be a suitable area of research for many electrochemists. The versatile nature of WO₃ indicates that it is a suitable material for a working electrode for many devices. The colouration of WO₃ by simultaneous insertion of cations and electrons demands more research into the complex insertion/expulsion mechanism. Combined electrochemical and gravimetric experiments using the electrochemical quartz crystal microbalance (EQCM) appears a likely route for further research because it is possible to study the amount of ion (in the case of WO₃, the cation) which is entering and leaving the WO₃ film to form the tungsten bronze. Any changes from the expected responses will lead to investigation of the possibility of another species entering the film parallel to ions.

The third type of electrolyte considered for ECD design is the polymer electrolyte. Proton containing polymers have been studied by Giglia and Haacke^[18] and Ho, Rukavina and Greenberg^[4], who both studied many types of proton conducting polymers and found that poly-2-acrylamido-2-methylpropanesulphonic acid (poly-AMPS) is a suitable solid proton containing polymer electrolyte to be used in ECDs. Using a WO₃ working electrode and a PB counter electrode configuration has given rise to solid electrolytes containing lithium salts such as LiClO₄, LiBF₄ or LiCF₃SO₃ with polymers such as poly(ethylene oxide) (PEO)^[17], oxymethylene polyoxyethylene^[117] or co polymers^[118-119].

1.3.6.3 Counter electrodes

Aside from prussian blue as a counter electrode to WO₃, work has also been done on a copolymer of polyaniline and nitrilic rubber^[120] and nickel oxide^[121]. Another possible counter electrode is to use an iron-graphite mixture as the potential of the counter electrode has an effect on the colouring and bleaching characteristics of the device^[122].

1.4 SUMMARY

The area of electrochromic device development and construction appears to be a suitable area of research for many electrochemists. The versatile nature of WO₃ indicates that it is a suitable material for a working electrode for many devices. The colouration of WO₃ by simultaneous insertion of cations and electrons demands more research into the complex insertion/expulsion mechanism. Combined electrochemical and gravimetric experiments using the electrochemical quartz crystal microbalance (EQCM) appears a likely route for further research because it is possible to study the amount of ion (in the case of WO₃, the cation) which is entering and leaving the WO₃ film to form the tungsten bronze. Any changes from the expected responses will lead to investigation of the possibility of another species entering the film parallel to ions.

To study ion insertion into WO_3 films, a direct method of measurement is required. It is not possible to use electrochemical or spectroscopic methods alone, so the electrochemical quartz crystal microbalance (EQCM) is used to study ion movement. In this study, the role of electrolyte composition is studied by studying different cations, anions and the effect of electrolyte concentration using the EQCM. The effect of film history can also be investigated using the EQCM, with the effect of the initial cycle at slow scan rates investigated both by the EQCM and the spectrophotometer. The effect of ion insertion on WO_3 films when cycled for many thousands of cycles can also be studied using the EQCM. The final effect to be studied is that of experimental time scale. This effect can be studied by using the EQCM in combination with cyclic voltammetric and chronoamperometric techniques.

REFERENCES

1. J. R. Platt, *Journal of Chemical Physics*, 34, 1, (1961), 862.
2. W. C. Dautremont-Smith, *Displays - Technology and Applications*, 3, (1982), 3.
3. P. M. S. Monk, R. J. Mortimer, and D. R. Rosseinsky, Electrochromism, Fundamentals and Applications, VCH Publishers, Weinheim, 1995.
4. K.-C. Ho, T. G. Rukavina, and C. B. Greenberg, *Journal of the Electrochemical Society*, 141, 8, (1994), 2061.
5. P. W. Atkins, Physical Chemistry, 4th Edition, Oxford University Press, 1990.
6. I. F. Chang, B. L. Gilbert, and T. I. Sun, *Journal of the Electrochemical Society*, 122, 7, (1975), 955.
7. W. C. Dautremont-Smith, *Displays - Technology and Applications*, 3, 2, (1982), 67.
8. C. G. Granqvist, *Applied Physics A-Solids and Surfaces*, 57, 1, (1993), 3.
9. R. C. Evans, An Introduction to Crystal Chemistry, Cambridge University Press, 1966.
10. J. Silver, *New Scientist*, (1989), 48.
11. F. G. K. Baucke and J. A. Duffy, *Chemistry in Britain*, July, (1985), 643.
12. R. D. Rauh, S. F. Cogan, and M. A. Parker, *Proceedings of the Society of Photo-Optical Instrumentation Engineers*, 502, (1984), 38.
13. J. E. S. M. Svensson and C. G. Granqvist, *Proceedings of the Society of Photo-Optical Instrumentation Engineers*, 502, (1984), 30.
14. C. G. Granqvist, *Solid State Ionics*, 53, 6, (1992), 479.
15. F. G. Baucke, K. Bange, and T. Gambke, *Displays - Technology and Applications*, 9, 4, (1988), 179.

16. C. G. Granqvist, *Physics of Thin Films*, 17, (1993), 301.
17. N. Oyama, T. Ohsaka, M. Menda, and H. Ohno, *Denki Kagaku*, 57, 12, (1989), 1172.
18. R. D. Giglia and G. Haacke, *Proceedings of the SID*, 23, 1, (1982), 41.
19. A. T. Howe, S. H. Sheffield, P. E. Childs, and M. G. Shilton, *Thin Solid Films*, 67, (1980), 365.
20. S. K. Deb, *Philosophical Magazine*, 27, (1973), 801.
21. C. G. Granqvist, Handbook of Inorganic Electrochromic Materials, Elsevier Science B.V., Amsterdam, 1995.
22. B. W. Faughnan and R. S. Crandall, in "Display Devices" (J. I. Pankove, ed.), Springer-Verlag, Berlin, 1980.
23. E. Ando, K. Kawakami, K. Matsuhira, and Y. Masuda, *Displays-Technology and Applications*, 6, 1, (1985), 3.
24. E. Salje and K. Viswanathan, *Acta Crystallographer*, 31, (1975), 356.
25. P. G. Dickens and M. S. Whittingham, *Quarterly Review Chemical Society*, 22, (1968), 30.
26. C. G. Granqvist, *Solar Energy Materials and Solar Cells*, 32, 4, (1994), 369.
27. J. V. Gabrusenoks, P. D. Cikmach, A. R. Lasis, J. J. Kleperis, and G. M. Ramans, *Solid State Ionics*, 14, 1, (1984), 25.
28. A. Kuzmin and J. Purans, *Journal of Physics-Condensed Matter*, 5, 15, (1993), 2333.
29. O. Bohnke, C. Bohnke, G. Robert, and B. Carquille, *Solid State Ionics*, 6, 2, (1982), 121.
30. D. Dini, F. Decker, and E. Masetti, *Journal of Applied Electrochemistry*, 26, 6, (1996), 647.

31. S. Hashimoto and H. Matsuoka, *Journal of Applied Physics*, 69, 2, (1991), 933.
32. B. Reichman and A. J. Bard, *Journal of the Electrochemical Society*, 126, 4, (1979), 583.
33. Y. Shigesato, Y. Hayashi, A. Masui, and T. Haranou, *Japanese Journal of Applied Physics Part 1-Regular Papers Short Notes & Review Papers*, 30, 4, (1991), 814.
34. J. G. Zhang, C. E. Tracy, D. K. Benson, and S. K. Deb, *Journal of Materials Research*, 8, 10, (1993), 2649.
35. M. C. Hugon, F. Varniere, B. Agius, M. Froment, and C. Arena, *Applied Surface Science*, 38, (1989), 269.
36. K. Kaneda and S. Suzuki, *Japanese Journal of Applied Physics*, 30, 8, (1991), 1841.
37. M. Kitao, S. Yamada, S. Yoshida, H. Akram, and K. Urabe, *Solar Energy Materials and Solar Cells*, 25, 3-4, (1992), 241.
38. T. Nanba, T. Takahashi, J. Takada, A. Osaka, Y. Miura, I. Yasui, A. Kishimoto, and T. Kudo, *Journal of Non-Crystalline Solids*, 178, (1994), 233.
39. M. Rubin, *Journal of Vacuum Science & Technology A-Vacuum Surfaces and Films*, 10, 4 Pt2, (1992), 1905.
40. D. Davazoglou and A. Donnadieu, *Journal of Non-Crystalline Solids*, 169, 1-2, (1994), 64.
41. T. Maruyama and S. Arai, *Journal of the Electrochemical Society*, 141, 4, (1994), 1021.
42. Y. Villachon-Renard, G. Leveque, N. Abdellaoui, and A. Donnadieu, *Thin Solid Films*, 203, (1991), 33.
43. T. Maruyama and T. Kanagawa, *Journal of the Electrochemical Society*, 141, 9, (1994), 2435.

44. P. Delichere, P. Falaras, M. Froment, A. Hugot le Goff, and B. Agius, *Thin Solid Films*, 161, JUL, (1988), 35.
45. P. Delichere, P. Falaras, and A. Hugot le Goff, *Thin Solid Films*, 161, JUL, (1988), 47.
46. M. I. Yanovskaya, I. E. Obvintseva, V. G. Kessler, B. S. Galyamov, S. I. Kucheiko, R. R. Shifrina, and N. Y. Turova, *Solid State Communications*, 124, (1990), 155.
47. S. A. Agnihotry, *Bulletin of Electrochemistry*, 12, 11-12, (1996), 707.
48. F. G. Baucke, J. A. Duffy, and R. I. Smith, *Thin Solid Films*, 186, (1990), 47.
49. W. C. Dautremont-Smith, M. Green, and K. S. Kang, *Electrochimica acta*, 22, (1977), 751.
50. M. Green and A. Travlos, *Philosophical Magazine B-Structural Electronic Optical and Magnetic Properties*, 51, 5, (1985), 501.
51. J. P. Randin and R. Viennet, *Journal of the Electrochemical Society*, 129, 10, (1982), 2349.
52. M. Green and Z. Hussain, *Journal of Applied Physics*, 74, 5, (1993), 3451.
53. A. Hjelm, C. G. Granqvist, and J. M. Wills, *Physical Review B-Condensed Matter*, 54, 4, (1996), 2436.
54. A. Donnadieu, D. Davazoglou, and A. Abdellaoui, *Thin Solid Films*, 164, OCT, (1988), 333.
55. D. J. Beckstead, G. M. Pepin, and J. L. Ord, *Journal of the Electrochemical Society*, 136, 2, (1989), 362.
56. C. Bohnke and O. Bohnke, *Journal of Applied Electrochemistry*, 18, 5, (1988), 715.

57. R. B. Goldner, D. H. Mendelsohn, J. Alexander, W. R. Henderson, D. Fitzpatrick, T. E. Haas, H. H. Sample, R. D. Rauh, M. A. Parker, and T. L. Rose, *Applied Physics Letters*, 43, 12, (1983), 1093.
58. M. A. Habib and S. P. Maheswari, *Journal of the Electrochemical Society*, 138, 7, (1991), 2029.
59. A. Temmink, O. Anderson, K. Bange, H. Hantsche, and X. Yu, *Thin Solid Films*, 192, 2, (1990), 211.
60. M. F. Daniel, B. Desbat, J. C. Lassegues, B. Gerand, and M. Figlarz, *Journal of Solid State Chemistry*, 67, 2, (1987), 235.
61. T. Ohtsuka, N. Goto, N. Sato, and K. Kunimatsu, *Ber. Bunsenges. Phys. Chem*, 91, (1987), 313.
62. I. V. Shiyankovskaya, *Journal of Non-Crystalline Solids*, 187, (1995), 420.
63. P. K. Shen, K. Y. Chen, and A. C. C. Tseung, *Journal of the Electrochemical Society*, 141, 7, (1994), 1758.
64. D. H. Mendelsohn and R. B. Goldner, *Journal of the Electrochemical Society*, 131, 4, (1984), 857.
65. T. Ohtsuka, N. Goto, and N. Sato, *Journal of Electroanalytical Chemistry and Interfacial Electrochemistry*, 287, (1990), 249.
66. M. S. Burdis, J. R. Siddle, and S. Taylor, *Pilkington group research, private communication*
67. P. K. Shen, K. Y. Chen, and A. C. C. Tseung, *Journal of the Chemical Society-Faraday Transactions*, 90, 20, (1994), 3089.
68. A. Kuzmin and J. Purans, *Journal of Physics, Condensed Matter*, 5, , (1993), 9423.
69. N. Yoshiike, Y. Mizuno, and S. Kondo, *Journal of the Electrochemical Society*, 131, 11, (1984), 2634.

70. P. Gerard, A. Deneuve, G. Hollinger, and T. M. Duc, *Journal of Applied Physics*, 48, 10, (1977), 4252.
71. H. N. Hersh, W. E. Kramer, and J. H. McGee, *Applied Physics Letters*, 27, 12, (1975), 646.
72. S. A. Badilescu, P.V., N. Minh-Ha, G. Bader, F. E. Girouard, and V.-V. Truong, *Thin Solid Films*, 250, (1994), 47.
73. M. S. Burdis and J. R. Siddle, *Thin Solid Films*, 237, (1994), 320.
74. R. A. Batchelor, M. S. Burdis, and J. R. Siddle, *Journal of the Electrochemical Society*, 143, 3, (1996), 1050.
75. Q. Zhong, J. R. Dahn, and K. Colbow, *Journal of the Electrochemical Society*, 139, 9, (1992), 2406.
76. S. I. Pyun and J. S. Bae, *Journal of Alloys and Compounds*, 245, (1996), L1.
77. G. B. Xu and L. Q. Chen, *Solid State Ionics*, 28, SEP, (1988), 1726.
78. O. Bohnke, A. Gire, and J. G. Theobald, *Thin Solid Films*, 247, 1, (1994), 51.
79. T. Kamimori, J. Nagai, and M. Mizuhashi, *Proceedings of the Society of Photo-Optical Instrumentation Engineers*, 428, (1983), 51.
80. J. G. Zhang, D. K. Benson, C. E. Tracy, and S. K. Deb, *Journal of Materials Research*, 8, 10, (1993), 2657.
81. S. K. Mohapatra, *Journal of the Electrochemical Society*, 125, 2, (1978), 284.
82. M. Denesuk, J. P. Cronin, S. R. Kennedy, and D. R. Uhlmann, *Journal of the Electrochemical Society*, 144, 3, (1997), 888.
83. B. Reichman, A. J. Bard, and D. Laser, *Journal of the Electrochemical Society*, 127, 3, (1980), 647.
84. T. Nishimura, K. Taira, and S. Kurita, *Applied Physics Letters*, 36, 7, (1980), 585.

85. R. B. Goldner, P. Norton, K. Wong, G. Foley, E. L. Goldner, G. Seward, and R. Chapman, *Applied Physics Letters*, 47, 5, (1985), 536.
86. A. M. Haghiri-Gosnet, F. R. Ladan, C. Mayeux, H. Launois, and M. C. Joncour, *Journal of Vacuum Science and Technology A*, 7, 4, (1989), 2663.
87. C. C. Fang, F. Jones, R. R. Kola, G. K. Celler, and V. Prasad, *Journal of Vacuum Science and Technology B*, 11, 6, (1993), 2947.
88. S. J. Babinec, *Solar Energy Materials and Solar Cells*, 25, 3-4, (1992), 269.
89. O. Bohnke, B. Vuillemin, C. Gabrielli, M. Keddam, and H. Perrot, *Electrochimica Acta*, 40, 17, (1995), 2765.
90. O. Bohnke, B. Vuillemin, C. Gabrielli, M. Keddam, H. Perrot, H. Takenouti, and R. Torresi, *Electrochimica acta*, 40, 17, (1995), 2755.
91. C. Gabrielli, M. Keddam, H. Perrot, and R. Torresi, *Journal of Electroanalytical Chemistry*, 378, 1-2, (1994), 85.
92. H. Inaba, M. Iwaku, T. Tatsuma, and N. Oyama, *Denki Kagaku*, 61, 7, (1993), 783.
93. H. Inaba, M. Iwaku, T. Tatsuma, and N. Oyama, *Journal of Electroanalytical Chemistry*, 387, 1-2, (1995), 71.
94. S. I. C. De Torresi, A. Gorenstein, R. M. Torresi, and M. V. Vazquez, *Journal of Electroanalytical Chemistry and Interfacial Electrochemistry*, 318, 1-2, (1991), 131.
95. R. S. Crandall and B. W. Faughnan, *Applied Physics Letters*, 26, 3, (1975), 120.
96. M. Green and A. Travlos, *Philosophical Magazine B-Structural Electronic Optical and Magnetic Properties*, 51, 5, (1985), 521.
97. R. Kotz, C. Babero, and O. Haas, *Journal of Electroanalytical Chemistry and Interfacial Electrochemistry*, 296, (1990), 37.

98. C. Bohnke and M. Rezrazi, *Materials Science and Engineering B-Solid State Materials For Advanced Technology*, 10, 4, (1991), 313.
99. J. L. Paul and J. C. Lassegues, *Journal of Solid State Chemistry*, 106, 2, (1993), 357.
100. H. Akram, H. Tatsuoka, M. Kitao, and S. Yamada, *Journal of Applied Physics*, 62, 5, (1987), 2039.
101. J. Nagai, T. Kamimori, and M. Mizuhashi, *Proceedings of the Society of Photo-Optical Instrumentation Engineers*, 502, (1984), 59.
102. S. S. Sun and P. H. Holloway, *Journal of Vacuum Science & Technology A-Vacuum Surfaces and Films*, 2, 2, (1984), 336.
103. C. Sunseri, F. Di Quarto, and A. Di Paola, *Journal of Applied Electrochemistry*, 10, (1980), 669.
104. O. Bohnke and M. Rezrazi, *Materials Science and Engineering B-Solid State Materials For Advanced Technology*, 13, 4, (1992), 323.
105. B. Vuillemin and O. Bohnke, *Solid State Ionics*, 68, 3-4, (1994), 257.
106. C. Bechinger, D. Ebner, S. Herminghaus, and P. Leiderer, *Solid State Communications*, 89, 3, (1994), 205.
107. O. Bohnke and B. Vuillemin, *Materials Science and Engineering B-Solid State Materials For Advanced Technology*, 13, 3, (1992), 243.
108. P. G. Dickens and S. A. Kay, *Solid State Ionics*, 8, (1983), 291.
109. J. P. Randin, *Journal of Electronic Materials*, 7, 1, (1978), 47.
110. M. A. Petit and V. Plichon, *Journal of the Electrochemical Society*, 143, 9, (1996), 2789.
111. A. M. Rocco, M. A. De Paoli, A. Zanelli, and M. Mastragostino, *Electrochimica Acta*, 41, 18, (1996), 2805.

112. F. Decker, R. Pileggi, S. Passerini, and B. Scrosati, *Journal of the Electrochemical Society*, 138, 11, (1991), 3182.
113. S. K. Mohapatra, G. D. Boyd, F. G. Storz, and S. Wagner, *Journal of the Electrochemical Society*, 126, 5, (1979), 805.
114. A. R. Lusic, J. J. Kleperis, A. A. Brishka, and E. V. Pentyush, *Solid State Ionics*, 13, 4, (1984), 319.
115. T. Yoshimura, M. Watanabe, Y. Koike, K. Kiyota, and M. Tanaka, *Japanese Journal of Applied Physics*, 22, 1, (1983), 157.
116. T. Yoshimura, M. Watanabe, Y. Koike, K. Kiyota, and M. Tanaka, *Japanese Journal of Applied Physics*, 22, 1, (1983), 152.
117. M. A. Habib and S. P. Maheswari, *Journal of the Electrochemical Society*, 139, 8, (1992), 2155.
118. Y. M. Li, Y. Aikawa, A. Kishimoto, and T. Kudo, *Electrochimica Acta*, 39, 6, (1994), 807.
119. H. Inaba, M. Iwaku, K. Nakase, H. Yasukawa, I. Seo, and N. Oyama, *Electrochimica Acta*, 40, 2, (1995), 227.
120. E. L. Tassi and M. A. Depaoli, *Electrochimica Acta*, 39, 16, (1994), 2481.
121. S. Passerini, B. Scrosati, V. Hermann, C. Holmblad, and T. Bartlett, *Journal of the Electrochemical Society*, 141, 4, (1994), 1025.
122. K. Yamanaka, *Japanese Journal of Applied Physics*, 21, 6, (1982), 926.

CHAPTER 2 : THEORY

2.1 INTRODUCTION

This chapter summarises theory for selected techniques applied in the two general approaches employed in this study, electrochemistry and the electrochemical quartz crystal microbalance.

2.2 ELECTROCHEMICAL TECHNIQUES

2.2.1 Introduction

This section describes the two standard electrochemical techniques used, namely cyclic voltammetry and chronoamperometry. The basic concepts behind both techniques, along with the equations used are given. More detailed explanations of both the theory and equations are discussed in the literature^[1].

2.2.2 Cyclic Voltammetry

In cyclic voltammetry, a potential is linearly swept between two limits at a constant scan rate (ν) and the current is measured as a function of the potential. This is seen in Figure 2.1 where the current versus potential response seen in Figure 2.1b, is for



with the potential scanned positively (anodic voltage) initially. As the potential is swept, the current increases in accordance to the Butler-Volmer equation [2.2.8], and at a certain point, mass transport becomes rate limiting and the current decreases in a diffusion controlled manner.

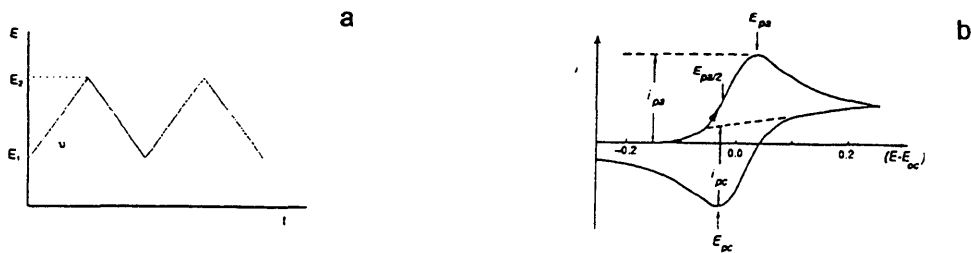


Figure 2.1 : Figure 2.1a shows potential versus time profile for a cyclic voltammetric experiment. Slope ν gives scan rate of experiment. Figure 2.1b shows potential versus current response for a reversible cyclic voltammetric experiment $O + e^- \rightleftharpoons R$. E_{pc} and E_{pa} represent potential of cathodic and anodic peak respectively. i_{pc} and i_{pa} represent corresponding current for E_{pc} and E_{pa} . E_{OC} represents open-circuit potential and E gives the potential of the electrode. Figure 2.1b taken from ref^[1].

On reversal of the scan, there is a high concentration of the product, R , near the electrode, which is subsequently reduced back to O . This reduction of R leads to the formation of the current peak on the cathodic scan. If the reaction is electrochemically reversible, then the two peaks are separated by $59/n$ mV, where n is the number of electrons involved in the overall electrochemical reaction. The midpoint of the two peaks are then defined as E_0 when α equals $1/2$. As $\alpha \approx 1/2$ almost always, then E_0 is a good approximation. The peak heights of the cyclic voltammogram are proportional to the square root of the scan rate as defined by the Randles-Sevcik equation

$$I_p = 0.4463nF \left(\left(\frac{nF}{RT} \right) D\nu \right)^{1/2} c^\infty \quad [2.2.2]$$

where I_p , is the peak current density ($A \text{ cm}^{-2}$). n is the number of electrons, F the Faraday constant ($C \text{ mol}^{-1}$), D the diffusion coefficient ($\text{cm}^2 \text{ s}^{-1}$), ν is the scan rate ($V \text{ s}^{-1}$) and c^∞ is the concentration of species being studied (mol cm^{-3}). Therefore a plot of I_p versus $\nu^{1/2}$ should give the diffusion coefficient for the species studied if the reaction is totally reversible.

For a surface process such as adsorption, where only the adsorbed forms of O and R are electroactive, then a symmetric cyclic voltammogram is obtained. The symmetric peak

arises due to the fact that only O on the surface at the beginning of a sweep can be reduced, ie the amount of reactant is fixed. The peak height I_p is now proportional to the scan rate :

$$I_p = \left(\frac{n^2 F^2 \Gamma^2}{4RT} \right) \nu \quad [2.2.3]$$

where Γ is defined as the surface coverage of the electrode (mol cm^{-2}) and Q the charge passed (C)

$$\Gamma = \left| \frac{Q}{nF} \right| \quad [2.2.4]$$

2.2.3 Chronoamperometry^[1]

Chronoamperometry is the term given to the electrochemical technique where the potential of the working electrode is stepped from a region where there are no electrochemical reactions occurring to a potential at which a reaction is occurring. The current-time, or charge-time response is measured.

If reaction [2.2.1]



is considered, where the two species are in equilibrium then the working electrode's potential (E) which is controlled is defined by the Nernst equation as

$$E = E^0 + \frac{RT}{nF} \ln \left(\frac{a_o}{a_R} \right) \quad [2.2.5]$$

where E^0 (V) is the standard electrode potential of the O/R couple with respect to the standard hydrogen electrode (SHE) which is defined as being zero, n is the number of electrons involved in the reaction, F is the Faraday constant (C mol^{-1}) and a is the activity (mol cm^{-3}).

When there is no net current flowing, there will be no overall chemical change in the cell and there is a dynamic equilibrium at the working electrode's surface (ie, O is being reduced, R is being oxidised and both processes are of equal rate), therefore

$$-I_f = I_b = I_0 \quad [2.2.6]$$

where I_f , I_b and I_0 are the partial forward, partial backward and exchange current densities respectively.

The magnitude of the current flowing at any potential will also be dependent upon the kinetics of electron transfer. I_f and I_b are each only dependent on a rate constant (k) and the concentration of the electroactive species at the electrode surface, therefore

$$I = I_f + I_b = -nFk_f c_O^s + nFk_b c_R^s \quad [2.2.7]$$

k_f and k_b are found to vary exponentially with respect to the applied electrode potential. The value η , (overpotential), is defined as the difference between E and E_0 . One can show that

$$I = I_0 \left[\exp\left(\frac{\alpha_A nF}{RT} \eta\right) - \exp\left(-\frac{\alpha_C nF}{RT} \eta\right) \right] \quad [2.2.8]$$

where α_A and α_C are defined as the transfer coefficients for the anodic and cathodic scans respectively. This is the Butler-Volmer equation. For a simple electron transfer $\alpha_C + \alpha_A = 1$ (which means that one transfer coefficient can be eliminated from any equation). The Butler-Volmer equation shows how measured net current density varies with exchange current density, overpotential and the transfer coefficients. In a case where a positive overpotential is applied, the anodic current density is given by

$$\log|I| = \log I_0 + \frac{\alpha_A nF}{2.3RT} \eta \quad [2.2.9a]$$

similarly where a high negative overpotential is applied, the cathodic current density is

$$\log|-I| = \log I_0 - \frac{\alpha_c nF}{2.3RT} \eta \quad [2.2.9b]$$

[2.2.9a] and [2.2.9b] are known as Tafel equations. A plot of $\log|I|$ versus η will give both the transfer coefficient (α) and I_0 .

If the potential of the working electrode is stepped to progressively higher overpotentials, the reaction will proceed faster and faster. At some point, the mass transport of R from the bulk solution to the electrode surface will become rate limiting and the surface concentration of R will decrease to zero: R is now consumed faster than it is supplied. Fick's first law shows how the current is proportional to the concentration gradient at the electrode surface.

$$I = nFD_R \left(\frac{dc_R}{dx} \right)_{x=0} \quad [2.2.10]$$

Where D_R is the diffusion coefficient ($\text{cm}^2 \text{s}^{-1}$) of species R and x is the distance from the electrode surface (cm).

Fick's second law, describes the change in concentration of R with respect to time, as a result of diffusion

$$\frac{\partial c_R}{\partial t} = D_R \frac{\partial^2 c_R}{\partial x^2} \quad [2.2.11]$$

for the given boundary conditions. For chronoamperometry, these conditions are

$$\begin{aligned} t = 0 \quad c_R^x &= c_R^{bulk} \quad \text{for all } x \\ t > 0 \quad c_R^s &= 0 \quad \text{and } c_R^x = c_R^{bulk} \quad x = \infty \end{aligned}$$

The solution of [2.2.11] leads to the Cottrell equation

$$i = nFAc_R^{bulk} \left(\frac{D_R}{\pi t} \right)^{1/2} \quad [2.2.12]$$

It can be seen that the current falls as $t^{1/2}$ and a plot of i versus $t^{1/2}$ should be linear and D_R can be calculated from the gradient of the plot.

For the experiments carried out where the diffusion coefficient of the cation was to be investigated, the concentration of Li^+ at the WO_3 surface was required. The concentration of WO_3 on the electrode was calculated using

$$c = \frac{\rho}{MW_{\text{wo}_3}} = \frac{5.5}{232} \quad [2.2.13]$$

where c is the concentration (moles cm^{-3}), ρ the density of WO_3 (5.5 g cm^{-3}) and MW_{WO_3} the molecular weight of WO_3 (232 g mol^{-1})^[2]. Since

$$\Gamma = cL \quad [2.2.14]$$

where c is defined above and L is the thickness of the film (cm), the concentration of Li^+ is $0.0237 \text{ mol cm}^{-3}$ for both WO_3 film thicknesses. Then the surface coverage of the WO_3 film is found to be $640 \text{ nmoles cm}^{-2}$ for a 2700\AA thick film and $569 \text{ nmoles cm}^{-2}$ for a 2400\AA thick film as used here.

If the plot of i versus $t^{1/2}$ is departs from linearity at long times, then finite diffusion must be accounted for. The Cottrell equation [2.2.12], can be modified to account for this:

$$i = nFAc_R^{\text{bulk}} \left(\frac{D_R}{\pi t} \right)^{1/2} \left[1 - \sum_{n=1}^{\infty} \exp \left(-\frac{n^2 D t_*}{L^2} \right) \right] \quad [2.2.15]$$

At the time t_* when i_{obs} is equal to $1/2 i_{\text{Cottrell}}$, then Equation [2.2.15] becomes

$$\left[1 - \exp \left(-\frac{D t_*}{L^2} \right) \right] = 1/2 \quad [2.2.16]$$

which leads to

$$t_* = \ln 2 \left(\frac{L^2}{D} \right) \quad [2.2.17]$$

This measurement of t_* can be used as a check on the gradient-derived value of D .

Figure 2.2 shows the potential-time and current-time profiles for a chronoamperometric experiment. The sharp peak which arises on the current-time response is due to the charging of the electrochemical double layer. This is dependent upon the cell configuration, but may last for a few hundred microseconds.

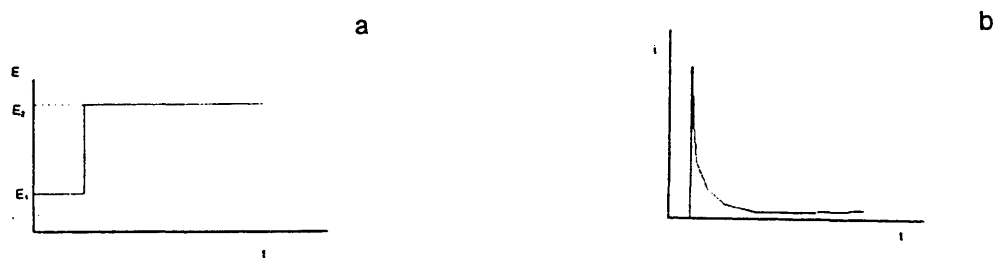


Figure 2.2 : Potential-time profile (Figure 2.2a) and current-time profile (Figure 2.2b) for a single chronoamperometric experiment.

2.3 THE QUARTZ CRYSTAL MICROBALANCE^[3]

2.3.1 Introduction

The piezoelectric nature of quartz was first noted in 1880, when Jacques and Pierre Curie observed that the application of pressure on a piece of quartz produced a small potential difference^[3-4]. They also noted that the application of a potential across quartz produced a corresponding deformation. Sauerbrey^[5] in 1952, demonstrated that it was possible that the changes in resonant frequency (f) measured for an oscillating quartz crystal could be used as a sensitive measurement of a rigidly attached mass (m). He defined a relationship between Δf and Δm .

In 1985, Bruckenstein and Shay^[6] published findings which detailed the use of one side of a quartz crystal oscillator, in contact with an electrolyte as the working electrode in a three electrode electrochemical cell, for *in situ* electrogravimetry. The electrochemical quartz crystal microbalance (EQCM) has since been a useful and highly sensitive technique

for monitoring *in situ* electrode mass changes. The device sensitivity is in the nanogram range dependent on the base frequency f_0 . The EQCM has been used to study many processes, including monolayer and multilayer deposition/dissolution, electroless deposition and corrosion processes at electrodes.

2.3.2 Quartz Crystals

A piezoelectric quartz crystal is produced from a precisely cut slab from a natural or synthetic single quartz crystal. Figure 2.3 shows the assignment of the x, y and z axes to a quartz crystal. When electrodes are fixed to a quartz crystal, and a potential is applied, the quartz crystal will vibrate at the frequency of the exciting potential.

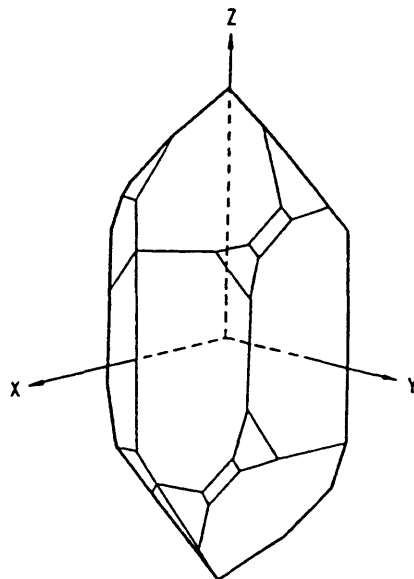


Figure 2.3 : Figure showing the assignment of axes to a quartz crystal. Figure taken from ref^[4].

For the use in an EQCM, the most sensitive vibration to the addition or removal of mass for a quartz crystal is the high frequency thickness-shear mode. Figure 2.4 shows the fundamental of vibration for the thickness-shear mode. In order for a quartz crystal to oscillate in the thickness-shear mode, the quartz plate must be cut in a specific orientation

with respect to the crystal axes shown in Figure 2.3. The most common cut is the “AT-” cut, which is cut at $35^{\circ}15'$, shown in Figure 2.5.

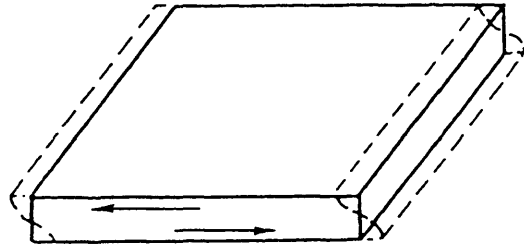


Figure 2.4 : Figure showing thickness-shear mode of vibration for a quartz crystal. Figure taken from ref^[4].

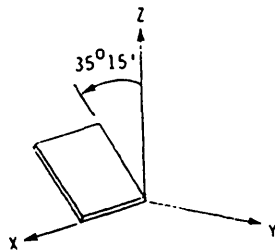


Figure 2.5 : Figure showing the AT-cut quartz crystal. Figure taken from ref^[4].

A small change in the orientation of the quartz plate with respect to the axes generally does not alter the resonance. However, the effect of both temperature and stress to the frequency are found to be very sensitive to orientation. For a standard “AT-” crystal, it is found to be insensitive to temperature change in a region around room temperature.

Two other crystal cuts have been used in EQCM experiments. These are the “BT-” cut (which has a frequency stress response opposite to “AT-”), and “SC-” (stress compensated) where the quartz crystal plate has been doubly rotated in the y-axis. The “BT-” cut crystal is shown in Figure 2.6. “BT-” cut quartz crystals can be used for a comparison to the standard “AT-” cut for the investigation of internal stress^[7].

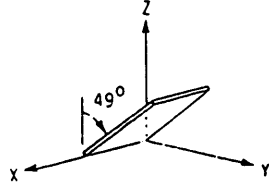


Figure 2.6 : Figure showing “BT-” cut quartz crystal plate. Figures taken from ref^[4].

2.3.3 Relationship between mass and frequency^[5]

For a piece of quartz of thickness t (cm), a standing wave can be set up inside the crystal. Using the wave equation $v = f\lambda$;

$$f_0 = \frac{V_{tr}}{2t} = \frac{N}{t} \quad [2.3.1]$$

where f_0 is the fundamental frequency (Hz), V_{tr} the transversal wave velocity normal to the plane of the plate (cm s^{-1}) and N is the frequency constant for the “AT-” cut crystal ($1.670 \times 10^5 \text{ cm}^2$)^[5]. The thickness t can be related to its mass by

$$t = \frac{M}{d_q A} \quad [2.3.2]$$

where d_q is the density of quartz (2.65 g cm^{-3}), A the area of the quartz crystal undergoing oscillation (between the two electrodes on opposite faces) (cm^2) and M is the mass of the oscillating quartz (g). Combination of [2.3.1] and [2.3.2] gives

$$f_0 = \frac{d_q N}{m} \quad [2.3.3]$$

where $m = M/A$ (g cm^{-2}). Therefore, it can be shown that the mass between the electrodes only affects the frequency.

If a rigid, uniform mass (ΔM) is then attached to one of the electrodes (of area A)

and $\Delta m = \Delta M/A$, then

$$f_0 + \Delta f = \frac{d_q N}{m + \Delta m} \quad [2.3.4]$$

Δf , the change in frequency caused by the rigid, uniform mass can be written as

$$\Delta f = - \left\{ \frac{f_0^2}{d_q N} \right\} \left\{ \frac{\Delta m}{\left[1 + \frac{\Delta m}{m} \right]} \right\} \quad [2.3.5]$$

the values for d_q (2.65 g cm^{-3}) and N ($1.670 \times 10^5 \text{ cm}$) can be substituted into [2.3.5], and if $m \gg \Delta m$, the change in frequency of an oscillating quartz crystal upon the addition of a small mass Δm can be given as

$$\Delta f = - 2.26 \times 10^{-6} f_0^2 \Delta m \quad [2.3.6]$$

where Δf is given in Hz and Δm in g cm^{-2} . This equation is called the Sauerbrey equation.

For a 10 MHz "AT-" quartz crystal, the Sauerbrey equation can be written as

$$\Delta m = - 4.426 \times 10^{-9} \Delta f \quad [2.3.7]$$

and for a gold coated quartz crystal of area 0.25 cm^2 , a mass change of 1.1 ng cm^{-2} will cause a 1 Hz frequency change.

2.3.4 Effect of crystal in contact with solution^[6]

When an oscillating quartz crystal is immersed in a liquid, an oscillating liquid boundary layer is set up next to the crystal surface. The thickness of this layer can be given approximately by

$$L = \left(\frac{\nu}{f_L} \right)^{1/2} \quad [2.3.8]$$

where L is the thickness of the boundary layer (cm), ν the kinematic viscosity of the liquid ($\text{cm}^2 \text{s}^{-1}$) and f_L is the frequency of oscillation of the crystal in the liquid (Hz). The effective additional liquid mass per unit area Δm_L attached to each face of the quartz crystal in contact with the liquid is

$$\Delta m_L = d_L \left(\frac{\nu}{f_L} \right)^{1/2} = \left(\frac{\eta_L d_L}{f_L} \right)^{1/2} \quad [2.3.9]$$

where d_L is the density of the liquid (g cm^{-3}) and η_L is the viscosity of the liquid.

If $f_L \cong f$, then by substituting [2.3.9] into [2.3.6], we get

$$f = - 2.26 \times 10^{-6} n f^{3/2} (\eta_L d_L)^{1/2} \quad [2.3.10]$$

where $n = 1$ or 2 , depending on whether one or both sides of the crystal are in contact with the solution. Therefore, if a thin, rigid film is deposited onto the electrode from the solution, then the overall frequency change will simply be a summation of the frequency changes from the attached film and the liquid (ie, [2.3.10] + [2.3.6]).

2.3.5 Other effects

It is known that there are variables which can affect the resonant frequency of a crystal which will then complicate the data interpretation. Such variables include the surface roughness of the crystal, changing the structure of the double layer^{[5][8-9]} and the radial distribution of mass on the electrode^{[5][10]}. Bruckenstein and Shay showed that the height of a column of liquid above the quartz crystal has negligible effect upon the crystal frequency and that the resonant frequency varies as the square root of solution viscosity^[6].

As mentioned in Section 2.3.2, other quartz crystal cuts can be used in EQCM experiments^[7]. Since "BT-" cut quartz crystals have a frequency stress response opposite to the commonly used "AT-" cut, then the combination of the recorded responses from both

“AT-” and “BT-” crystals should give a stress-free frequency change by the use of simultaneous equations. The “SC-” cut crystals do not respond to stress but only the areal mass density changes and so are of use when temperature effects induce stress in an overlayer.

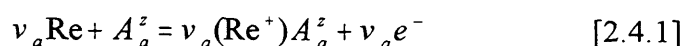
2.4 INTERPRETATION OF EQCM DATA

2.4.1 Introduction

The EQCM makes use of the fact that one electrode of the QCM in contact with a liquid, is also the working electrode for a three electrode electrochemical cell. The changes in frequency can be monitored at the working electrode surface for an electrochemically driven process. The Sauerbrey equation [2.3.6] shows that the frequency response of a quartz crystal will give the change in mass for a rigid film. For an electrochemical reaction, the charge passed will give the number of electrons consumed in the reaction. By combining electrochemical data (charge (Q) and current (i)) with EQCM data (Δm), information can be retrieved regarding the mobile species involved in the electrochemical process studied.

2.4.2 Mass changes versus charge relationship^[11]

Hillman *et al*^[11] considered the half reaction for a system with redox sites (“ Re ”) undergoing a single electron oxidation in a single electrolyte solution



where $(C_c^z)_{v_c} (A_a^z)_{v_a}$ defines the single, unsymmetrical and electroinactive electrolyte and $v_i = |z_i|$. If there were multiple electrolytes present, then the half reaction would also include a weighted sum of analogues of [2.4.1] for the various anions (A) present. The weighting

would be dependent upon the selectivity coefficients of the various anions. Reactions and expressions for cations could also be written. Equation [2.4.1] shows only electronic changes and the resulting net ionic changes which are demanded by electroneutrality.

The net total mass change (ΔM) at the interface can be expressed as

$$\Delta M = \sum m_k \Delta \Gamma_k = \sum m_n \Delta \Gamma_n + \sum m_i \Delta \Gamma_i \quad [2.4.2]$$

where m_k is the molar mass of species k (which is a “sensitivity factor” for detection by mass of transfer of species $k^{[10]}$) and $\Delta \Gamma_k$ is the change of molar population of k within the film. $m_k \Gamma_k$ corresponds to the individual mass changes across the film-solution interface and is made up of two separate components; neutral molecular changes ($m_n \Gamma_n$) and ion population changes ($m_i \Gamma_i$). Neutral species transfer are determined by their activity gradient, whereas the charged species will depend upon any potential gradient which may enhance (or impede) transfer.

The net charge (Q) which is passed can be expressed as

$$Q = \int i dt = - \sum z_i F \Delta \Gamma_i \quad [2.4.3]$$

where $z_i F$ can be described as the charge carried by species i and $\Delta \Gamma_i$ is the surface coverage. The charge can be measured as an integral of the external current circuit and is defined as negative when film reduction occurs (and positive for film oxidation).

By combining electrochemical and EQCM data, it is possible to extract the term

$$\frac{\Delta M_T F}{Q_T} = \left(\frac{\sum m_n \Delta \Gamma_n + \sum m_i \Delta \Gamma_i}{\sum m_i \Delta \Gamma_i} \right) = \frac{\Delta m}{\Gamma} \quad [2.4.4]$$

which gives the mass change per mole of redox sites or “molar mass” (g mol^{-1}), and is of use when investigating the overall electrochemical process, as the “end to end” values ($\Delta M_T F / Q_T$) can be easily obtained from mass change versus charge plots.

However, the EQCM gives only overall mass changes and it is not possible to separate out the component ΔM values. It may be that there is more than one species entering and leaving the system. We then use an algebraic tool, and define the quantity Φ from [2.4.3] and [2.4.4]

$$\Phi_j = \Delta M + Q \left(\frac{m_j}{z_j F} \right) = \sum m_n \Delta \Gamma_n + \sum \left(\frac{m_i - m_j z_i}{z_j} \right) \Delta \Gamma_i \quad [2.4.5]$$

for a particular species j which is the ion taking part in the half reaction described above. Where m_j is the mass of the ion (g), z_j the charge of the ion, F the Faraday constant (C mol⁻¹) and ΔM and Q the EQCM and electrochemical variables respectively. The term ΔM refers to the total mass measured, $Q(m_j/(z_j F))$ refers to the ion j contribution and Φ_j relates to any neutral species contribution. Therefore, it is possible to select the species for investigation, and by substituting in the various values (ΔM and Q are obtained from the experiment, m_j and z_j from the chosen species) establish whether there are any other species being transferred in to the film. If only the species j is being inserted, then the value for the ions will equal that of the overall mass and Φ_j will equal zero. However, if $\Phi_j \neq 0$, then there is the implication that there is a second species entering the film. This second species may be the opposite ion to the one initially investigated and so it is possible to substitute the values of m_j and z_j for this species. There is also the possibility that a neutral species (eg solvent) may be entering the film. Thus Φ is a useful aid for the investigation of the mass changes seen from the EQCM experiment.

For both cyclic voltammetric and chronoamperometric experiments, it is possible to calculate the amount of cation (x) entering and leaving the WO₃ film upon reduction and oxidation using

$$x = \frac{QM}{FdlA} \quad [2.4.6]$$

where Q is the injected charge (C), M is the molecular weight of WO_3 (232 g mole^{-1}), F is the Faraday constant (C mol^{-1}), d is the density of WO_3 (5.5 g cm^{-3}), l is defined as the thickness of the film (cm) and A is the electrode area (cm^2)^[2].

For EQCM experiments obtained using cyclic voltammetry, the maximum and minimum charge passed during each cycle is substituted into Equation [2.4.6] to give x values. For chronoamperometric experiments, the total amount of charge passed at the end of the potential step and also at the end of the experiment is substituted into Equation [2.4.6] in order to calculate x .

The effect of concentration on an experiment can also be investigated using the EQCM^[12]. At low concentrations, there is very little salt entering the film during the electrochemical reaction and so we have a permselective condition. The ΔM_{perm} values obtained from the EQCM experiment at these low concentrations, should reflect contributions from ion (ΔM_{ion}) and solvent (ΔM_{solv}) transfer only.

$$\Delta M_{perm} = \Delta M_{solv} + \Delta M_{ion} \quad [2.4.7]$$

As the concentration is increased, the condition becomes nonpermselective and salt enters the film during the reaction. Therefore, a third term (ΔM_{salt}) must be included in Equation [2.4.7] to account for the salt insertion. This gives

$$\Delta M_{nonperm} = \Delta M_{solv} + \Delta M_{salt} + \Delta M_{ion} \quad [2.4.8]$$

therefore, if varying concentrations for the same electrolyte are used, it is possible to investigate the role which salt plays in the electrochemical reaction.

2.4.3 Analysis of EQCM and electrochemical data^[12]

As the previous section has shown, the combination of EQCM and electrochemical data can be used to obtain information regarding the movement of species both into and out of the film. Plots of current versus potential or charge versus potential from the cyclic voltammetry can give information regarding changes in equilibrium film populations. A plot of mass change versus potential from the EQCM experiment will establish whether global equilibrium is achieved for all species (electrons, neutrals and ions) if the plot is symmetrical.

However, if all the plots mentioned above do not trace, then a plot of mass change versus charge will give information about the mobile species. If the plot shows no hysteresis and the $\Delta M_{TF}/Q_T$ values equal the expected value for single ion insertion/expulsion, then there is only the single ion moving during the electrochemical experiment. However, if the plot shows hysteresis and the $\Delta M_{TF}/Q_T$ values calculated do not equal the single ion value (ie, are larger or smaller than expected on the basis of Faraday's law), then this is evidence of more than one species moving in and out of the film. There may be the case however, that the plot shows very little hysteresis but the $\Delta M_{TF}/Q_T$ values are larger than expected. Now there is more than one species moving in and out of the film, but they are moving at comparable rates.

In conjunction with the mass change versus charge plots, it is possible to also plot $\Delta\Phi$ versus charge. As Φ is used as a method for separating the various species (charged and neutral) then the gradient measured from a plot of $\Delta\Phi$ versus charge can also give information about the movement of species. If there is only a single charged species moving, then the $\Delta\Phi_{TF}/Q_T$ value should be equal to zero. If this is not the case, then it is possible to calculate the amount of neutral species involvement in the electrochemical process by using Equation [2.4.9]

$$\left[\left(\frac{\Delta\Phi_T F}{Q_T} \right) / MW_{PC} \right] = A \quad [2.4.9]$$

where $\Delta\Phi_T F/Q_T$ is calculated value from $\Delta\Phi$ versus charge plots (g mol^{-1}), MW_{PC} is the molecular weight of propylene carbonate (104 g mol^{-1}), and the answer, A is given in the number of moles of propylene carbonate per mole of C^+/e^- where C^+ is the cation being studied.

2.5 OTHER TECHNIQUES

2.5.1 Introduction

This section describes other techniques which can be used in conjunction with the EQCM. They can be used as a diagnostic tool for the investigation of the quartz crystal (crystal impedance) and also as a measure of the film optical properties (spectroelectrochemistry).

2.5.2 Crystal impedance

This section covers the role of crystal impedance in EQCM experiments. The Sauerbrey equation [2.3.6] indicates that for a rigidly coupled mass upon a quartz crystal, there will be a linear relationship between the changes in resonant frequency (Δf) and the changes in the electrode-film mass (Δm). If the film is not rigidly attached to the crystal surface, then the frequency response is determined by the viscoelastic characteristics of the system. The role of crystal impedance is to measure the entire resonant curve of the quartz crystal, rather than the centre frequency of the crystal as monitored by the EQCM. Therefore, it has become a requirement for the crystal impedance to be measured both before and after film deposition to check film rigidity. If the deposited film shows non-rigid

characteristics then there will be under-estimation of the mass changes recorded as the Sauerbrey equation fails^[13].

It is possible to use the Δf measurement for an uncoated and coated quartz crystal (obtained from the crystal impedance measurements) to calculate the number of moles per unit area of WO_3 using

$$\Gamma_{\text{WO}_3} = \left(\frac{\Delta f_{\text{WO}_3} \times 1.1}{A} \right) / M_{\text{WO}_3} \quad [2.5.1]$$

where 1.1 is the conversion factor for frequency to mass ($1\text{Hz} \rightarrow 1.1 \text{ ng electrode area}^{-1}$), A is the area of the electrode and M_{WO_3} is the molecular weight of WO_3 (232 g mol^{-1}). Γ_{WO_3} is given in nmol cm^{-2} of WO_3 .

By taking the charge density passed (Q) from the EQCM experiment, the number of moles cm^{-2} of electrons can be calculated using

$$\Gamma_e = \left(\frac{Q}{F} \right) \quad [2.5.2]$$

where F is the Faraday constant and Γ_e is measured in nmol cm^{-2} .

Combining [2.5.1] and [2.5.2], gives the insertion coefficient (x) or ratio of cation to WO_3 units being inserted into the film by

$$x = \frac{\Gamma_e}{\Gamma_{\text{WO}_3}} \quad [2.5.3]$$

2.5.3 Spectroelectrochemistry^[14]

Although spectroscopy is the most obvious means of analysis of electrochromic systems and has been employed frequently elsewhere, it was not the main focus of this study. The main use for spectroelectrochemistry in this study is as a complement to the EQCM experiments. The Beer Lambert law, which is generally associated with spectroscopy can be linked via a “conversion factor” to electrochemical equations

For electrochemical reactions, the conversion factor linking charge (Q), to the number of moles (N) is the Faraday constant

$$N = \frac{Q}{F} \quad [2.5.4]$$

For films of surface coverage Γ , N can be normalised with respect to the electrode area ($A(\text{cm}^2)$)

$$\Gamma = \frac{N}{A} = \frac{Q}{FA} \quad [2.5.5]$$

In spectroscopy, the Beer Lambert law, can be expressed as the log of the ratio of the incident and transmitted intensities (I_0 and I), and can also relate absorbance (Abs) to the concentration of chromophore species (c (mol cm^{-3})) and the pathlength (L (cm))

$$Abs = \log\left(\frac{I_0}{I}\right) = \varepsilon cL = \varepsilon \Gamma \quad [2.5.6]$$

It is possible to combine [2.5.5] and [2.5.6] to give

$$Abs = \left(\frac{\varepsilon}{FA}\right)Q \quad [2.5.7]$$

ε can be determined by plotting Abs (spectroscopy) against Q (electrochemistry). The molar absorption coefficient will vary with wavelength (as Abs varies with respect to wavelength) as ε is defined as the parameter quantifying the strength of the optical absorbance at each wavelength. The values of both $\varepsilon(\lambda)$ and ε_{max} (the value of ε at wavelength λ , and maximum value respectively), will in general depend upon the solvent or the solid matrix in which the chromophores are dispersed.

For the purposes of comparing WO_3 coated quartz crystals of different film thicknesses, we elect to “normalise” data (current, charge or mass changes) with respect to coverage. Normalisation can be carried out using

$$Y^* = \frac{Y}{\Gamma} \quad [2.5.8]$$

where Y^* is the normalised value (i , Q , ΔM), Y the value to be changed, and Γ the film thickness (\AA). Comparison of normalised data (Y^*) allows (electro)chemical effects to be separated from film thickness effects when comparing different films.

REFERENCES

1. Southampton Electrochemistry Group, Instrumental Methods in Electrochemistry, 2nd Edition, Ellis Horwood Limited, 1990.
2. O. Bohnke, B. Vuillemin, C. Gabrielli, M. Keddad, H. Perrot, H. Takenouti, and R. Torresi, *Electrochimica Acta*, 40, 17, (1995), 2755.
3. S. Bruckenstein and A. R. Hillman, in Surface Imaging and Visualisation (A. T. Hubbard, ed.), Chapter 9, CRC Press, Boca Raton London, 1995.
4. C. Lu and A. W. Czanderna, Applications of Piezoelectric Quartz Crystal Microbalances, Elsevier Science, Amsterdam, 1984.
5. G. Sauerbrey, *Zeitschrift für Physik*, 155, , (1959), 206.
6. S. Bruckenstein and M. P. Shay, *Electrochimica Acta*, 30, 10, (1985), 1295.
7. G. T. Cheek and W. E. O'Grady, *Journal of Electroanalytical Chemistry*, 368, (1994), 133.
8. R. Schumacher, G. Borges, and K. K. Kanazawa, *Surface Science*, 163, 1, (1985), L621.
9. R. Schumacher, A. Muller, and W. Stockel, *Journal of Electroanalytical Chemistry and Interfacial Electrochemistry*, 219, 1-2, (1987), 311.
10. D. M. Ullevig, J. F. Evans, and M. G. Albrecht, *Analytical Chemistry*, 54, 13, (1982), 2341.
11. A. R. Hillman, M. J. Swann, and S. Bruckenstein, *Journal of Physical Chemistry*, 95, (1991), 3271.
12. A. R. Hillman, M. J. Swann, and S. Bruckenstein, *Journal of Electroanalytical Chemistry and Interfacial Electrochemistry*, 291, (1990), 147.

13. H. L. Bandey, M. Gonsalves, A. R. Hillman, A. Glidle, and S. Bruckenstein, *Journal of Electroanalytical Chemistry*, 410, (1996), 219.
14. P. M. S. Monk, R. J. Mortimer, and D. R. Rosseinsky, Electrochromism, Fundamentals and Applications, VCH Publishers, Weinheim, 1995.

CHAPTER 3 : EXPERIMENTAL

3.1 INTRODUCTION

This chapter describes the experimental set-up for the EQCM and spectrophotometric experiments carried out to investigate ion insertion into WO₃ films. The equipment used will be described initially, followed by the materials used, collection of the data and the experimental procedures.

3.2 EQUIPMENT

3.2.1 The three electrode cell^[1]

For the experiments carried out in this investigation, a three electrode cell was used. A three electrode cell, comprises a working electrode (WE), a counter electrode (CE) and a reference electrode (RE) all exposed to the electrolyte. The working electrode is the electrode at which the electrochemical reaction of interest occurs. It may take a variety of forms, from a piece of foil to a single crystal of either semi conductor or metal. Working electrodes should not react chemically with the solvent nor components of the solution. To measure the potential at which electrochemical reactions are occurring, the potential difference (E) between the working electrode and the reference electrode is controlled. The reference electrode's role is to provide a fixed potential which does not vary during the experiment. There are many different reference electrodes used in electrochemical experiments. The one used here was the saturated calomel electrode (SCE). All potentials are quoted with respect to the SCE, unless otherwise stated.

The third electrode, which completes the three-electrode cell, is the counter electrode. When an electrochemical reaction occurs at the working electrode, there is passage of charge at the electrolyte-working electrode interface which disturbs the

electrolyte composition. If a current were to pass through the reference electrode, inaccurate potential measurements would be taken since the reference electrode would no longer be at equilibrium. Therefore we desire that no current will flow through the reference electrode. The purpose of the counter electrode is to supply the current needed by the working electrode without limiting the measured responses. In some experiments, the counter electrode reaction can be considered as the reverse of working electrode reaction, so that the composition of the electrolyte is unaltered. As seen in Section 1.1.3.1, Prussian Blue can be used as the counter electrode for a WO_3 working electrode^[2].

3.2.2 The electrochemical quartz crystal microbalance

The EQCM instrumentation has been described elsewhere^[3] in the literature. Some modifications to the original set-up have been carried out. The potentiostat is now a computer controlled AUTOLAB (EcoChemie PGSTAT20) which records both the current-potential response and also the frequency-voltage response. Figure 3.1 shows a schematic set-up of the EQCM used for these experiments. The EQCM cell and crystal oscillating circuit are isolated in a Faraday cage and supported on a purpose built brick pillar to eliminate any vibrations caused by equipment around the experiment.

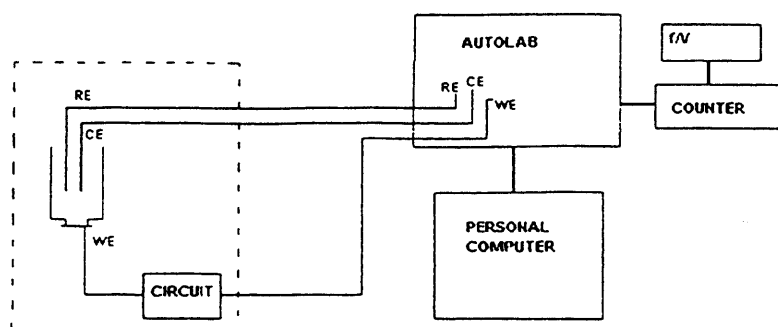


Figure 3.1 : Schematic set-up of the EQCM circuit used for experiments. Dotted line represents the Faraday Cage surrounding electrochemical cell and oscillating circuit. Circuit denotes circuit board containing quartz crystal oscillating mechanism and reference crystal.

The EQCM cell used for these experiments is a modification on a three electrode cell. The working electrode is a 10 MHz gold coated “AT-” cut quartz crystal, onto which a WO_3 film has been deposited. The WO_3 coated quartz crystal is then glued onto the base of a cell. The counter and reference electrodes are supported using a quick-fit lid. Figure 3.2 shows the EQCM cell and lid used together with the quartz crystal used as the working electrode.

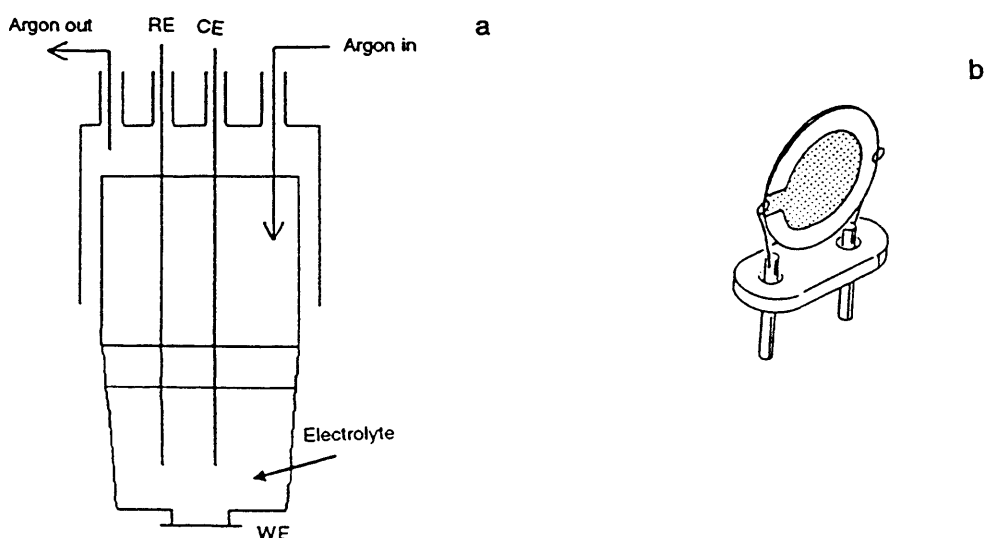


Figure 3.2 : Figure 3.2a shows EQCM cell and lid used for experiments. Figure 3.2b shows the working electrode (the quartz crystal). Figure 3.2b taken from ref^[4]

3.2.3 Spectrophotometric experiments

The spectrophotometer used in the experiments was a Perkin Elmer Lambda 19 spectrophotometer capable of working in the ultra violet, visible and near infra red range. The program used to run experiments was stored on a personal computer linked to the spectrophotometer. Potentiostatic control was achieved from an Oxford Electrodes potentiostat. Figure 3.3 shows the equipment arrangement for the spectrophotometer. The cell used to measure the absorbance of the WO_3 films during reduction and oxidation was placed inside the spectrophotometer and is shown in Figure 3.4. The cell was made of Teflon™ and both the counter and working electrodes were sealed onto the cell using vacuum grease.

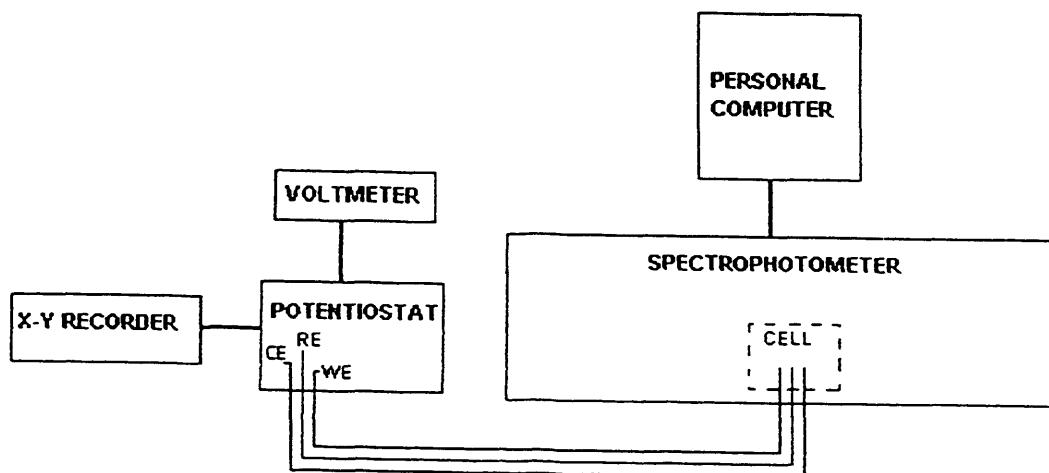


Figure 3.3 : Schematic showing arrangement for spectrophotometric experiments. Dotted line indicates position of spectrophotometer cell.

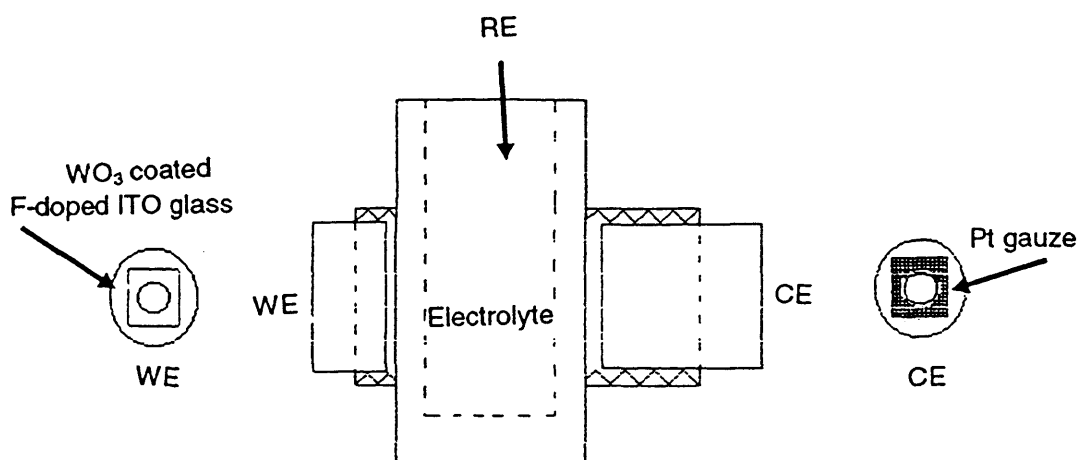


Figure 3.4 : Diagram showing spectrophotometer cell used. Arrows indicate position of reference, counter and working electrodes with respect to cell.

3.3 MATERIALS

3.3.1 Electrodes and cells

As mentioned in the previous section, a three electrode set-up was used for both EQCM and spectrophotometric experiments. For both types of experiments the reference electrode was a home-made saturated calomel electrode (SCE), made to the design in Sawyer and Roberts^[5]. The potential of the SCE was checked against an commercial SCE before use. The counter electrode for the EQCM experiments was a platinum gauze with a surface area larger than the chosen working electrode. A platinum gauze was also used for the spectrophotometric experiments, but as can be seen in Figure 3.4, a hole, the size of the quartz window, had to be cut out of the centre to allow the beam to pass through. The working electrodes were either 10 MHz unpolished gold coated quartz crystals bought from ICM of Oklahoma City, or F-doped indium tin oxide (F-ITO) glass supplied by Pilkington Glass. Both the quartz crystals and glass were then coated with a WO₃ film.

3.3.2 Chemicals

The chemicals used for the investigation of ion insertion into WO_3 films are detailed in Table 3.1. Any water used for cleaning equipment used, was firstly run through a Permutt Houseman Model 3C resin chamber, and then was deionised using a Milli-Q plus water purification system.

Table 3.1 : Table showing chemicals used for experiments carried out to investigate ion insertion into WO_3 .

Chemical	Supplier	Purity
LiClO_4	Fluka	>99%
NaClO_4	BDH	AnalaR (>99%)
LiCF_3SO_3	Aldrich	97%
Propylene carbonate	Aldrich (stored under N_2)	99.7%

3.3.3 WO_3 films

As mentioned in the Introduction, there are many methods of deposition for WO_3 films. The method used by the Surfaces and Coatings Group of Pilkington Glass is d.c. magnetron sputtering. This is where a d.c. electric field is used to generate a plasma which is held in place by a magnetic field within the sputterer. The WO_3 films were sputtered from a W metal target in an atmosphere of Ar and O_2 . Twenty five 10 MHz "AT-" cut unpolished gold quartz crystals were coated at any one time, to ensure that films within each batch were of the same thickness. The two batches of quartz crystals used for the ion insertion experiments had calculated thicknesses of 2700Å and 2400Å using DekTek, a surface profilometer^[6]. This difference meant that if any experiments were carried out on crystals of two different thicknesses and then compared, then a normalisation of the experimental data had to be carried out before the comparisons could take place as mentioned in the Theory chapter (section 2.5.3). The F-ITO glass used for the spectrophotometric experiments was coated at the same time as the quartz crystals so as to ensure that both substrates were coated with the same thickness of WO_3 film. This

therefore meant that a comparison between EQCM and spectrophotometric data could be undertaken.

Pilkington Glass carried out x-ray diffraction studies on the samples before delivery, and found that there was no structure which could be associated with polycrystalline WO_3 . Therefore, the WO_3 films studied here were amorphous^[6].

Initially, polished gold quartz crystals were also coated with WO_3 , but after the films had been cycled for a few cycles (<10), the WO_3 and gold peeled away from the quartz. This therefore meant that the polished gold crystals could not be used for the EQCM studies.

As mentioned in the Theory Chapter, the EQCM will give an underestimation of the Sauerbrey equation if the film studied is non-rigid^[7]. To ensure that the WO_3 coated quartz crystals were rigid, crystal impedance data was collected. It was seen that when the WO_3 film was cycled at 5 mV s^{-1} for two cycles in $0.1\text{M LiClO}_4/\text{propylene carbonate}$, the admittance did not alter significantly. This suggests that the WO_3 films are rigid, and therefore there is no concern regarding the validity of the EQCM results.

3.4 EXPERIMENTAL PROCEDURE

3.4.1 Chemicals/glassware

All solutions used in the EQCM and spectrophotometric experiments were prepared freshly prior to each experiment. The propylene carbonate used was extracted from a 1 litre Winchester using a 25 ml syringe, with a steady flow of nitrogen (passed through silicone oil) flowing over the top. The seal on the top of the Winchester was not removed, therefore ensuring that only a minimal amount of water could contaminate the solvent. Before each experiment was carried out, the solution was degassed thoroughly for approximately 20 minutes using argon.

The glassware used for all the experiments was thoroughly cleaned in an ultrasonic bath (containing a dilute solution of Decon 90) for approximately 30 minutes. The glassware was then rinsed using deionised water and oven dried before being used. The Teflon™ cell used in the spectrophotometer was also cleaned as described above.

The quartz crystals used were attached onto the EQCM cell by using Dow Corning Silicone Adhesive Sealant (RTV 3145). The quartz crystals were glued onto the cell ~24 hours before an experiment to ensure that the sealant was completely dry. The reference electrode (SCE) was rinsed in deionised water and thoroughly dried before being placed into the EQCM cell. The counter electrode (platinum gauze) was either flamed in a Bunsen burner (until the gauze glowed white) or dipped in a mixture of concentrated H₂SO₄/HNO₃ and then thoroughly rinsed using deionised water before being dried. It was not possible to flame the gauze if the electrode had been sealed inside a glass tube, and so dipping in H₂SO₄/HNO₃ was the alternative method of cleaning.

The WO₃ coated F-ITO glass was attached onto the Teflon™ cell using Dow Corning Silicone Coating (RTV 3140). As for the quartz crystals, the glass was adhered ≈24 hours before an experiment. The holders onto which the working and counter electrodes were glued, were fastened into the Teflon™ base using vacuum grease, to ensure that there were no leakages.

3.4.2 Procedure for EQCM data collection

Data collection for the EQCM experiments was carried out using two pre-written programmes on the AUTOLAB. For cyclic voltammetry experiments, the chosen programme was *LSV and CV including second signal*. Procedures were established for experiments at varying scan rates at the beginning of the experimental, so as to ensure that time and potential intervals were reproduced for any experiment. Table 3.2 below shows

the experimental parameters used for the combined cyclic voltammetry and EQCM experiments.

Table 3.2 : Table showing experimental parameters used throughout EQCM cyclic voltammetry experiments.

Experiment name	Scan rate / $V s^{-1}$	Step interval / V	Time interval / s
WO3-1	0.100	0.004	0.004
WO3-2	0.050	0.002	0.049
WO3-3	0.020	0.002	0.099
WO3-4	0.010	0.002	0.244
WO3-5	0.005	0.003	0.610

The display during each experiment showed both the current versus potential response and also the frequency versus potential response. Since $\Delta f \propto \Delta m$, then it could be easily noted if there was a frequency (and hence mass) increase or decrease during the experiment. Five cycles between the potential limits of $-1.0V \rightarrow +1.0V$ were recorded, with the starting potential set to 0V for each experiment. At the termination of the experiment, each cycle was recorded separately as *.OSC files onto disc and then transferred to a spreadsheet programme.

For the chronoamperometric experiments, the programme chosen was *Amp./Coul. And pot including second signal*. At the end of each experiment, the data was collected as a single *.OSX file and again transferred to a spreadsheet programme.

For both the cyclic voltammetry and chronoamperometric experiments, the Δf value was noted prior to the beginning of the experiments. This ensured that the correct frequency/voltage (f/V) range could be selected so that there is no saturation of the signal during the experiment (which would lead to incorrect data). Also, the gain setting on the f/V unit was noted as this is used for calculation of the mass changes.

3.4.3 Procedure for collection of spectrophotometric data

As mentioned in Section 3.2.3., the spectrophotometer was linked to a personal computer and this was used for data acquisition. For the experiments where a single wavelength was chosen to be monitored for a specific amount of time during a cyclic voltammetric experiment (fixed wavelength), the programme used was called *TDRIVE*. The wavelength to be studied was entered into the programme, as was the duration of measurement and wavelength interval. For the experiments using WO_3 films, the wavelength interval was 1.00nm, and the time was set at 1000 seconds, therefore, a complete cycle scanned at 5 mV s^{-1} could be recorded during this time. The data collected was then converted into ASCII text which could be read in to a suitable spreadsheet programme.

REFERENCES

1. Southampton Electrochemistry Group, Instrumental Methods in Electrochemistry, 2nd Edition, Ellis Horwood Limited, Chichester, England, 1990.
2. S. Bruckenstein and M. P. Shay, *Electrochimica Acta*, 30, 10, (1985), 1295.
3. K.-C. Ho, T. G. Rukavina, and C. B. Greenberg, *Journal of the Electrochemical Society*, 141, 8, (1994), 2061.
4. C. Lu and A. W. Czanderna, Applications of Piezoelectric Quartz Crystal Microbalances, Elsevier Science, Amsterdam, 1984.
5. J. L. Roberts and D. T. Sawyer, Experimental Electrochemistry for Chemists, Wiley-Interscience, 1974.
6. R. A. Batchelor and M. J. Burdis, *personal communication*, 1995-1997.
7. H. L. Bandey, M. Gonsalves, A. R. Hillman, A. Glidle, and S. Bruckenstein, *Journal of Electroanalytical Chemistry*, 410, (1996), 219.

CHAPTER 4 : EFFECT OF ELECTROLYTE COMPOSITION

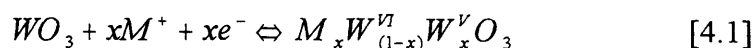
4.1 INTRODUCTION

This chapter will look at the basic electrochemical features seen during ion insertion into WO_3 as a function of the composition of the electrolyte. The influence of the nature of both cations and anions are investigated using electrochemical and quartz crystal microbalance techniques. The effect of electrolyte concentration is also studied using these techniques.

4.2 ELECTROCHEMISTRY OF WO_3

4.2.1 General features

A cyclic voltammogram showing Li^+ insertion into a WO_3 film is shown in Figure 4.1. The mechanism for the reduction of the WO_3 film to form a tungsten bronze is generally understood to be



where M is usually Li^+ , Na^+ or H^+ .

The WO_3 film (the working electrode) is scanned between the potential limits +1.0V and -1.0V (versus SCE), with the starting potential set at 0.0V. It can be seen that as the cycle begins, current is flowing almost immediately which indicates that reduction of the WO_3 film is occurring ($W^{VI} + e^- \Leftrightarrow W^V$). When the scan is reversed at -1.0V, a negative current is still recorded for a short period, which indicates that the WO_3 film is still being reduced. It is only 0.198V after scan reversal at -0.802 (± 0.002)V that the current becomes positive and oxidation of the film begins. Measurements of the optical changes during

cycling have shown that the colouration process is optically reversible^[1], and independent of the cation chosen^[2-4].

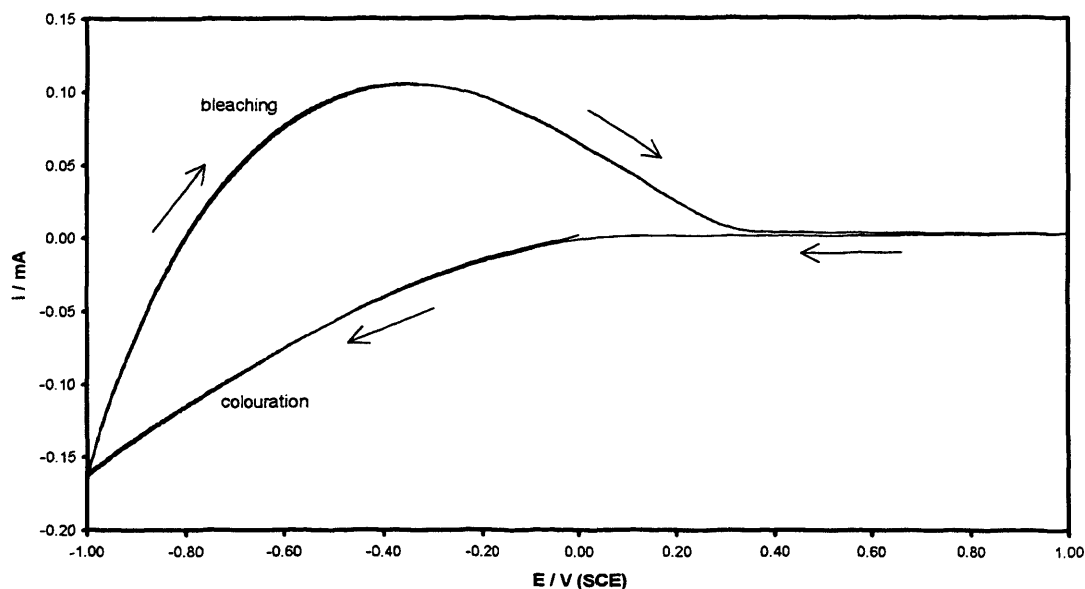


Figure 4.1 : Cyclic voltammograms showing Li^+ insertion into a 2700\AA thick WO_3 film. Electrolyte : $0.1\text{M LiClO}_4/\text{propylene carbonate}$. Total number of cycles recorded : 5. Scan rate 20 mV s^{-1} . All five scans are penwidth reproducible. $\Gamma \cong 640\text{nmoles cm}^{-2}$.

It can be seen that the cyclic voltammograms obtained show a smooth curve, which indicates that there are no phase changes occurring during ion insertion^[5-6]. The maximum current passed on the reverse scan indicates the oxidation of W^{V} species (which cause colouration) back to W^{VI} ^[7]. Much work has been carried out on the insertion of H^+ into the WO_3 lattice^[8-12], but decomposition of the film in acidic media has been shown to be a considerable drawback for the use of WO_3 in electrochromic display devices^[13]. H^+ is not considered a suitable cation for this study, since film longevity is important for electrochromic display devices.

4.2.2 The electrochemical quartz crystal microbalance

The electrochemical quartz crystal microbalance (EQCM) utilises the fact that quartz is a chemically inert piezoelectric material^[14-15]. The gold coated quartz crystals are coated on one side with WO_3 by d.c. magnetron sputtering^[16]. One side of the crystal is then in contact with the electrolyte chosen for study, and measurement of the ions entering/leaving the WO_3 can be monitored by recording changes in mass.

Figure 4.2 shows the mass versus potential response for Li^+ insertion from 0.1M LiClO_4 /propylene carbonate into WO_3 . The initial mass increase is defined as the zero for mass changes and charge measurements. As reduction occurs, the film mass begins to increase, and it subsequently decreases on oxidation. Where zero charge indicates a fully oxidised film and values decrease upon reduction and increase as oxidation occurs.

It can be seen that there is very little mass change until -0.200V when the mass begins to increase, which indicates insertion of ions into the WO_3 film. At reversal of the scan (-1.0V), since reduction of the WO_3 film is still occurring, the mass continues to increase, and reaches a maximum at -0.762 (± 0.005)V. This potential is slightly more positive than the one measured for the start of bleaching and has been seen for various concentrations and scan rates. After the maximum mass has been reached, the mass begins to decrease as Li^+ is expelled from the WO_3 film (bleaching). After +0.20V, there appears to be very little mass change, which indicates that bleaching of the Li_xWO_3 bronze has occurred. The mass is not seen to increase again until the beginning of the next scan, when colouration of the WO_3 film begins again.

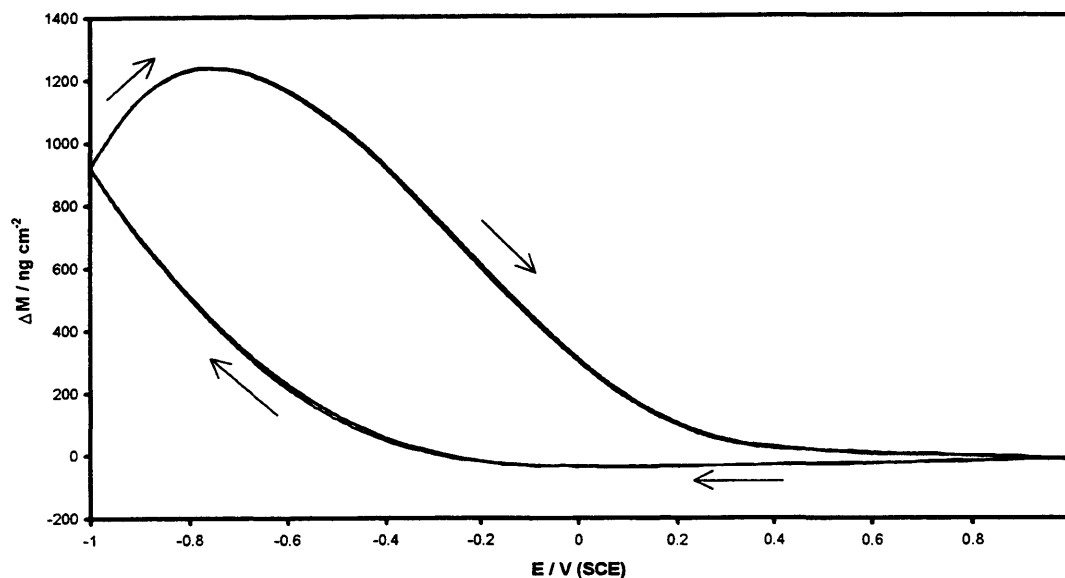


Figure 4.2. : Mass changes versus potential response for a voltammetric experiment on a 2700Å thick WO₃ film. Electrolyte : 0.1M LiClO₄/propylene carbonate. Total number of cycles recorded : 5. Scan rate : 20 mV s⁻¹. All five scans are penwidth reproducible. $\Gamma \cong 640\text{nmoles cm}^{-2}$.

The charge passed during ion insertion/expulsion can be calculated using

$$Q = \int i dt \quad [4.2]$$

and the corresponding charge versus potential response for Li⁺ insertion from 0.1M LiClO₄/propylene carbonate electrolyte into WO₃ is shown in Figure 4.3. It should be noted that the charge values are given in mC cm⁻², not mC. This is because the integration of current carried out also includes the area of the electrode. The zero point for the charge values have been defined above.

As with the mass data, it can be seen that the charge begins to change at the start of the scan, and a steady decrease in charge is seen. The charge continues to decrease after reversal of the scan, but this is expected as reduction of the film is still occurring. The minimum charge is seen at -0.802 (±0.001)V, which is at the same the potential where the beginning of oxidation is recorded. This is expected, as the charge values are an integral of the recorded current. The charge begins to increase steadily as bleaching of the tungsten

bronze occurs and at positive potentials very little charge is recorded. As with the mass versus potential plot, the charge does not appear to change dramatically again until the next scan begins.

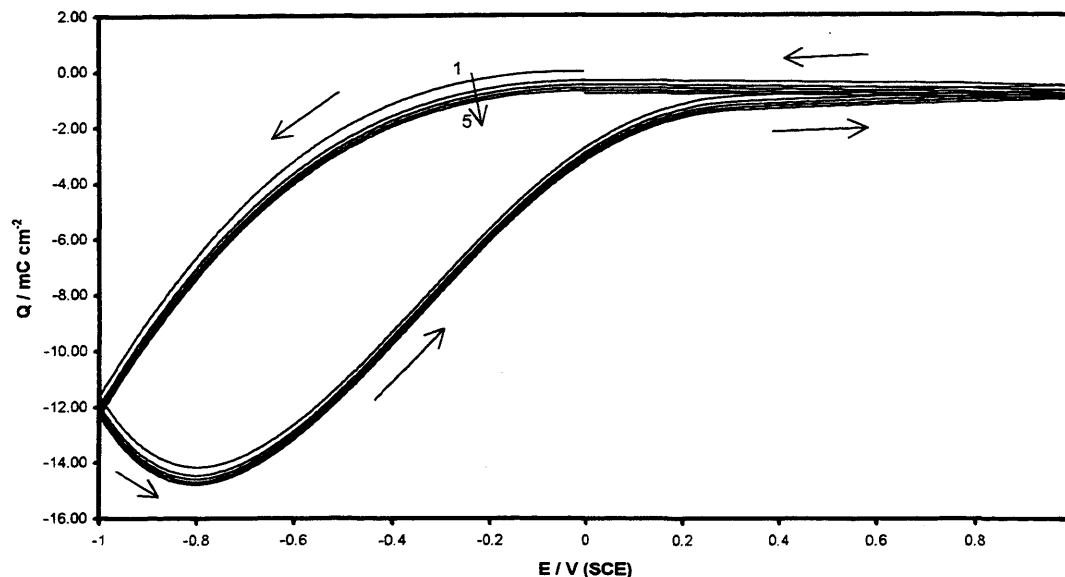


Figure 4.3. :Charge versus potential response for a voltammetric experiment on a 2700Å thick WO_3 film. Electrolyte : 0.1M LiClO_4 /propylene carbonate. Total number of cycles recorded : 5 (marked on plot). Scan rate : 20 mV s^{-1} . $\Gamma \cong 640 \text{ nmol cm}^{-2}$.

4.2.3 Relationship between mass and charge

It is possible to plot the overall mass changes (ΔM) seen for ion insertion/expulsion against the charge (Q) calculated during the cycle. This type of plot can give information regarding the species transfer into and out of the WO_3 film.

The “end to end” values of the mass changes and the charge data can be obtained and manipulated to extract information regarding the species both entering and leaving the WO_3 film. As charge is defined as the integral of the current [4.2], it is possible to obtain the number of redox sites changed (Γ) using the relationship

$$\Gamma = \frac{Q}{FA} \quad [4.3]$$

which is expressed in mol cm⁻². F is the Faraday (C mol⁻¹), Q is the charge passed (C) and A the electrode area (cm²). The overall mass changes are given by ΔM_T . By dividing ΔM_T by Q_T (the total charge passed) and multiplying by F , the mass change per mole of redox sites changed can be found using the equation

$$\frac{\Delta M_T F}{Q_T} = \frac{\Delta m}{\Gamma} \quad [4.4]$$

4.2.4 Interpretation of $\Delta M_T F/Q_T$ values^[17-18]

The mass data obtained from the EQCM experiment only gives information regarding the overall mass changes seen during the experiment. Therefore, it is difficult to tell whether the mass changes seen for ion insertion into WO₃ involve just one species (the cation) or other species such as anions or neutrals (eg, solvent). Φ is an algebraic tool used to deconvolute the overall mass changes seen, by using the equation below.

$$\Phi_{ion} = \Delta M + Q \left(\frac{m_{ion}}{z_{ion} F} \right) \quad [4.5]$$

neutrals *total mass* *ions*
 change

where ΔM is the mass change per unit area, Q is the charge density (in the case of insertion into WO₃, Q is negative) and m_{ion} and z_{ion} are the mass and charge number of the ion chosen for study, respectively. If it is deduced that there is only a single ion (of mass m and charge number z) entering/leaving the WO₃ film, then the expression for the charged species in the above equation will be of an equal and opposite sign to the overall ΔM value and hence $\Phi = 0$. However, if the Φ value calculated does not equal zero then there must be another species entering/leaving the WO₃ film. It is possible to calculate Φ for both cations and anions, to give an overall picture of the insertion of species into WO₃.

4.3 EFFECT OF CHANGING THE CATION

4.3.1 Introduction

As already mentioned, insertion of H^+ into WO_3 using an acid solution as the electrolyte causes degradation of the film. This effect has been seen not only on SnO_2 -coated glass substrates^[13] but when preliminary studies were carried out here using the gold coated quartz crystals used for the EQCM experiments, with H_2SO_4 (aq) as the electrolyte, the WO_3 film was found to degrade upon cycling. Although work has been carried out elsewhere using polymer gel electrolytes^{[8][12][19-22]} as the electrolyte for H^+ , this medium is not suitable for EQCM experiments, as a liquid medium is required for EQCM study. For the purpose of display devices, the most common cation studied is Li^+ , as many studies have shown that it inserts into WO_3 easily. For this study, $NaClO_4$ has been chosen to compare with $LiClO_4$, as sodium is a group I metal, with a larger ionic radius, which may give information about the WO_3 lattice, and has also been used previously in ion insertion studies of WO_3 . The solvent used for both electrolytes is propylene carbonate.

4.3.2 Comparison of lithium and sodium insertion into WO_3 films using voltammetric data

Figure 4.4 shows two cyclic voltammograms as a function of varying electrolyte. The electrolytes chosen for these experiments were 0.1M $LiClO_4$ /propylene carbonate and 0.1M $NaClO_4$ /propylene carbonate. It can be seen that there are smaller currents recorded during the cycle in the $NaClO_4$ /propylene carbonate electrolyte compared to using $LiClO_4$ /propylene carbonate as the electrolyte ($\approx 6.7\%$ difference between Na^+ and Li^+). It has been reported by other authors, that the intercalation kinetics for Na^+ are slower than for Li^+ , and Na^+ is seen to have a slower rate of diffusion^[23]. The slower diffusion of Na^+ is therefore thought to be responsible for a build up of the cation, which leads to a Na_xWO_3 bronze being formed with a lower colouration efficiency compared to Li_xWO_3 bronzes^[24].

This would explain the difference in cyclic voltammograms, as the smaller Li^+ is able to fully insert into the WO_3 film at the scan rate chosen (10 mV s^{-1}), and also be expelled during the bleaching half cycle. It appears that Na^+ is also inserted into WO_3 , but as the kinetics for Na^+ are slower, then complete cation insertion may not be occurring at this scan rate.

The size of the two cations would indicate that Li^+ (0.6\AA) would be preferentially inserted into the WO_3 film than Na^+ (0.95\AA)^[25]. This would lead to differences in the two experiments, with larger values of x calculated for $\text{LiClO}_4/\text{propylene carbonate}$ than for $\text{NaClO}_4/\text{propylene carbonate}$ and larger mass changes being seen in the EQCM experiments.

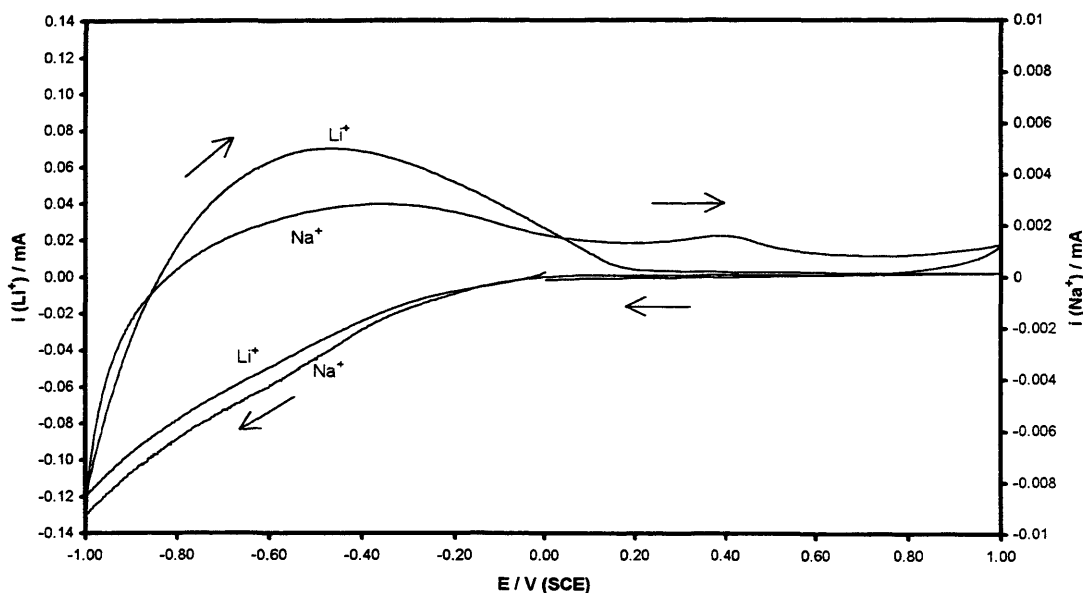


Figure 4.4 : Cyclic voltammograms showing the effect of using two different electrolytes to study cation insertion into 2700\AA thick WO_3 films. Electrolytes : $0.1\text{M LiClO}_4/\text{propylene carbonate}$ and $0.1\text{M NaClO}_4/\text{propylene carbonate}$ (marked on plot). Total number of cycles recorded : 5 (1st cycle from each experiment shown for ease of comparison). Scan rate 10 mV s^{-1} . $\Gamma \cong 640\text{nmoles cm}^{-2}$.

As the scan is reversed and bleaching occurs, it appears that not all the sodium cations that have entered during colouration leave the WO_3 film, as the current does not return to zero, as seen for Li^+ . The cyclic voltammogram for Na^+ insertion indicates that some sodium cations remain in the film after the completion of the cycle. For various

concentrations of NaClO_4 used and at different scan rates ($5 - 100 \text{ mV s}^{-1}$), this type of cyclic voltammogram is always seen.

As charge is defined as the integral of the current passed, then it is possible to plot the charge versus potential responses for the different ion insertion into WO_3 as a function of electrolyte. Figure 4.5 shows the charge versus potential response for ion insertion into WO_3 using $0.1\text{M LiClO}_4/\text{propylene carbonate}$ and $0.1\text{M NaClO}_4/\text{propylene carbonate}$ as the electrolytes.

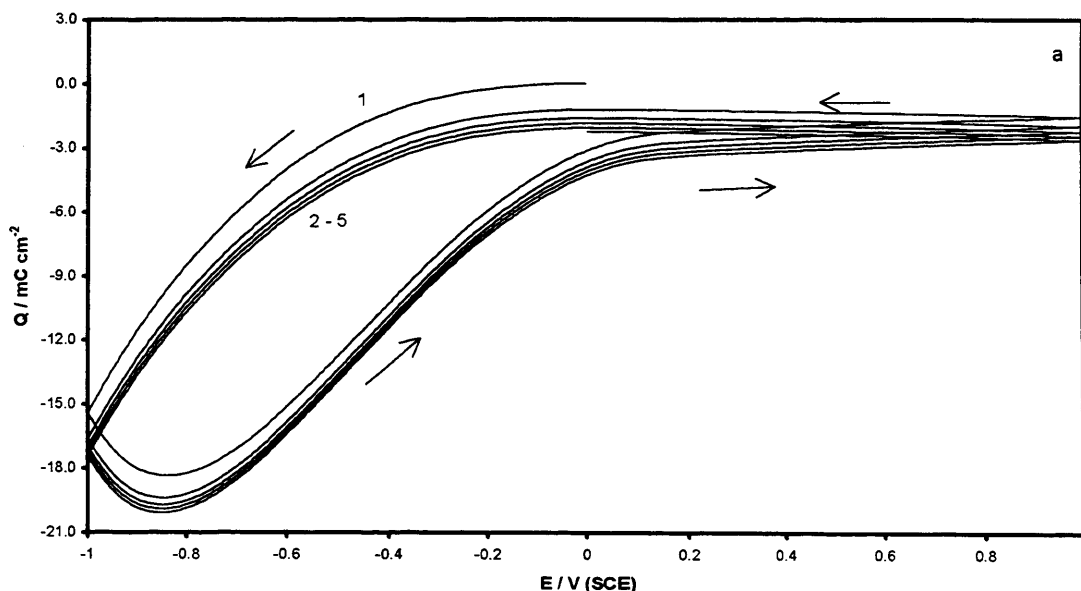
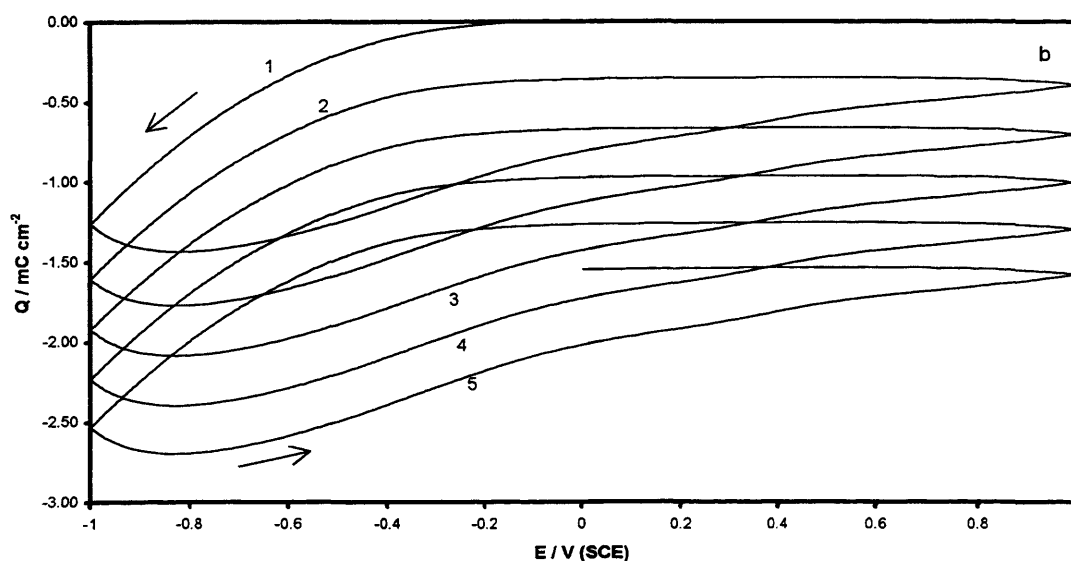


Figure 4.5 :Charge versus potential response for a voltammetric experiment showing the effect of using two different electrolytes to study cation insertion into 2700\AA thick WO_3 films. Electrolytes : $0.1\text{M LiClO}_4/\text{propylene carbonate}$ (4.5a) and $0.1\text{M NaClO}_4/\text{propylene carbonate}$ (4.5b) Total number of cycles recorded : 5 (marked on plot). Scan rate : 10 mV s^{-1} . $\Gamma \cong 640\text{nmoles cm}^{-2}$.



On the first scan measured using 0.1M LiClO₄/propylene carbonate as the electrolyte, it can be seen that there is less charge being passed, compared with the following scans ($\approx 5\%$ difference between the first and second cycle), but this not found to be of great importance. It is seen that in 0.1M LiClO₄/propylene carbonate, the charge versus potential response is very reproducible. This indicates that there is almost the same amount of charge entering and leaving WO₃ during each cycle. However, when the charge versus potential response using 0.1M NaClO₄/propylene carbonate as the electrolyte, is studied, there appears to be a constant decrease in charge passed during the recording of the five cycles. This indicates an accumulation of ionic charge in the WO₃ film when cycled in a Na⁺ electrolyte.

Both plots show that the minimum charge seen occurs as oxidation begins, as expected. This is rather less marked in 0.1M NaClO₄/propylene carbonate compared to LiClO₄/propylene carbonate. As Figure 4.4 shows, the current response for 0.1M NaClO₄/propylene carbonate is less than in 0.1M LiClO₄/propylene carbonate and subsequently the charge responses are also smaller.

4.3.3 Mass changes versus potential responses

As previously mentioned in Section 4.2.2, the EQCM data obtained can give information about the charged species entering and leaving the WO_3 film. Mass versus potential responses for the cyclic voltammetric experiments described in Section 4.3.2 are detailed below.

Representation of the mass changes versus potential response for the cyclic voltammogram experiment outlined in Section 4.3.2 are shown in Figure 4.6. As for the charge versus potential response, it can be seen that a reproducible response is obtained in 0.1M LiClO_4 /propylene carbonate. The mass begins to increase at -0.20V which indicates insertion of ions into the WO_3 film and continues to increase after scan reversal. The potential at which the maximum mass value is recorded is at -0.828 (± 0.007)V and, very small mass changes are seen after +0.20V when complete bleaching is proposed to have occurred.

For ion insertion using 0.1M NaClO_4 /propylene carbonate as the electrolyte, it can be seen that the mass changes are smaller than for Li^+ ($\approx 19\%$ smaller when WO_3 is cycled in 0.1M NaClO_4 /propylene carbonate, compared to when WO_3 is cycled in 0.1M LiClO_4 /propylene carbonate) and it appears, that there is a gradual increase in mass seen during each cycle. This mass is not recovered at the end of each cycle, which indicates that Na^+ remains in the film and that complete oxidation of the WO_3 film does not occur (see above). The maximum mass values are recorded at -0.839 (± 0.003)V for Na^+ insertion, which is at a slightly more negative potential than for Li^+ insertion. Again, as for Li^+ , after +0.200V, there are only very small mass changes seen, which indicates that the Na^+ is not leaving the film at these potentials.

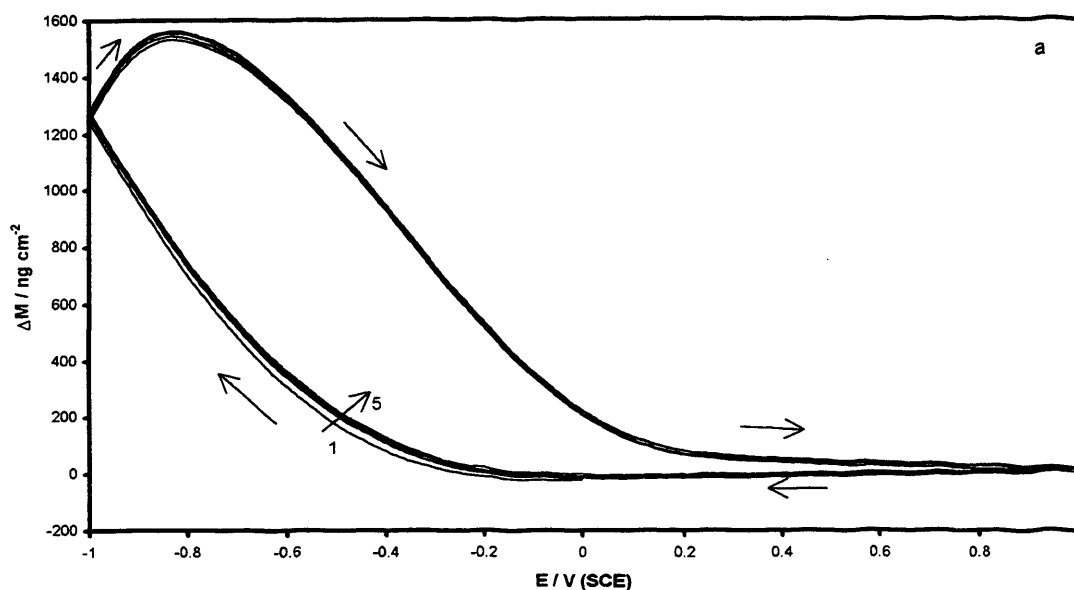
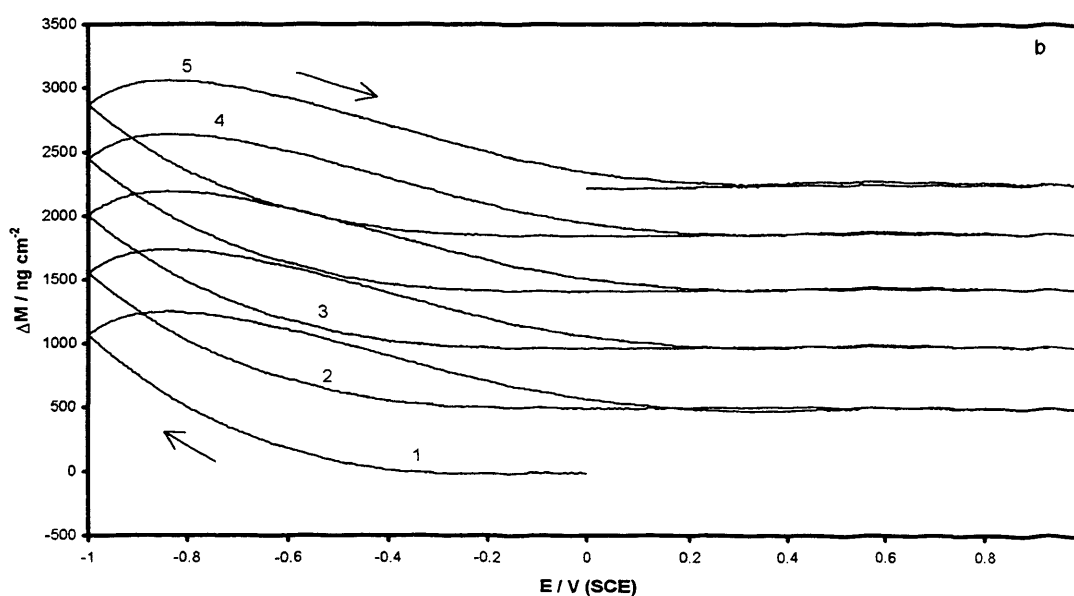


Figure 4.6 :Mass changes versus potential response for a voltammetric experiment showing the effect of using two different electrolytes to study cation insertion into a 2700Å thick WO_3 film. Electrolytes : 0.1M LiClO_4 /propylene carbonate (4.6a) and 0.1M NaClO_4 /propylene carbonate (4.6b) Total number of cycles recorded : 5 (marked on plot). Scan rate : 10 mV s^{-1} . $\Gamma \cong 640 \text{ nmol cm}^{-2}$.



As previously mentioned, it is possible to plot the mass changes against the charge data acquired from the experiments and calculate the $\Delta M_{\text{T}}F/Q_{\text{T}}$ ratio to obtain information

regarding the species entering and leaving the film. Figure 4.7 shows the mass versus charge plots for the EQCM data that has been discussed already in this chapter.

FTIR work carried out by MacFarlane *et al*^[26] on LiCF_3SO_3 and NaCF_3SO_3 in a copolymer (called 3-PEG5000) show that there are differences between the two solutions. A band attributed to “free” ions is found to be more intense in NaCF_3SO_3 than in LiCF_3SO_3 . They estimate that the “free” ion band is almost twice as large in NaCF_3SO_3 than in LiCF_3SO_3 . This suggest that there are a greater number of “free” ions present in the solution containing Na than in the corresponding Li solutions. This is a surprising result due to the fact that it is expected that Li^+ would enter into the strongest ether-oxygen solvation. When FTIR experiments are carried out in NaCF_3SO_3 /propylene carbonate then it is seen that at low concentrations the “free” ion dominates, whereas at higher concentrations, there is domination of monodentate pairs.

The plot for Li^+ insertion shows that there are two definite slopes, one for reduction and the other for oxidation. The “end-to-end” $\Delta M_{\text{T}}F/Q_{\text{T}}$ values can be calculated for the five recorded cycles and are shown in Table 4.1 to give an overall picture of the species entering/leaving WO_3 . It can be seen that all the measured values are greater than 7 g mol^{-1} (the value expected for Li^+ insertion), which indicates that there is a second species being inserted into the WO_3 film parallel to Li^+ . This second species may be either propylene carbonate or the existence of ion pairs both in the solution and in the WO_3 film.

Table 4.1 : Table showing calculated “end to end” $\Delta M_T F/Q_T$ values for reduction and oxidation of a WO_3 film in 0.1M $LiClO_4$ /propylene carbonate. Five scans recorded at a scan rate 10 mV s^{-1} . Data obtained from Figure 4.7a

Cycle Total number	$\Delta M_T F/Q_T / \text{g mol}^{-1}$		
	Li^+	reduction	oxidation
1	-7	-8.2	-8.7
2	-7	-8.3	-8.6
3	-7	-8.3	-8.4
4	-7	-8.4	-8.4
5	-7	-8.4	-8.5
	average	-8.3 ± 0.1	-8.5 ± 0.1

It can be seen from the cyclic voltammogram for Li^+ insertion (4.6a) that the mass still increases as the current changes sign (i.e., $\Delta M \neq 0$ when $i = 0$). Electroneutrality dictates that if the current is equal to zero, then there must be no charged species moving either in or out of the film. Therefore, it appears that there may be a neutral species moving alongside Li^+ .

The absence of hysteresis on a mass change versus charge plot is a requirement for single ion movement. If hysteresis is seen on the plot, then this is an indication that there must be more than one species entering and leaving the film. However, it may be the case though that there is more than one species being inserted into the film but the speed of the species are comparable and hysteresis is not seen. Therefore, if there were only one species being inserted/expelled, then the plot seen would track on both reduction and oxidation with the correct $\Delta M_T F/Q_T$ value for single cation insertion. The mass versus charge response using 0.1M $LiClO_4$ /propylene carbonate (Figure 4.7a) shows slight hysteresis and the $\Delta M_T F/Q_T$ values do not equal 7 g mol^{-1} . Therefore this be considered as evidence for insertion of neutral species.

Work carried out by D'Aprano and co-workers^[25] give a value for K_a , the ion pair association constant for $LiClO_4$ in propylene carbonate. Two values are given, the first, $5.1 \pm 0.1 \text{ dm}^3 \text{ mol}^{-1}$ is suggested to be for solvent separated ion pairs, whilst a value of 1.0

$\pm 0.3 \text{ dm}^3 \text{ mol}^{-1}$ is quoted for contact ion pairs. If there are ion pairs in the LiClO_4 /propylene carbonate solution seen here, then they may enter the WO_3 film alongside Li^+ in the form of a neutral species. This may be why the $\Delta M_{\text{T}}F/Q_{\text{T}}$ values do not equal zero and indicate that there may be either ion pairs entering the WO_3 film, propylene carbonate entering or a combination of the two. Work carried out by Salomon and Plichta^[27] suggests that for Li^+ salts in pure propylene carbonate, then only contact ion pairs are formed, with the presence of solvent separated ion pairs seen with the addition of dimethoxymethane.

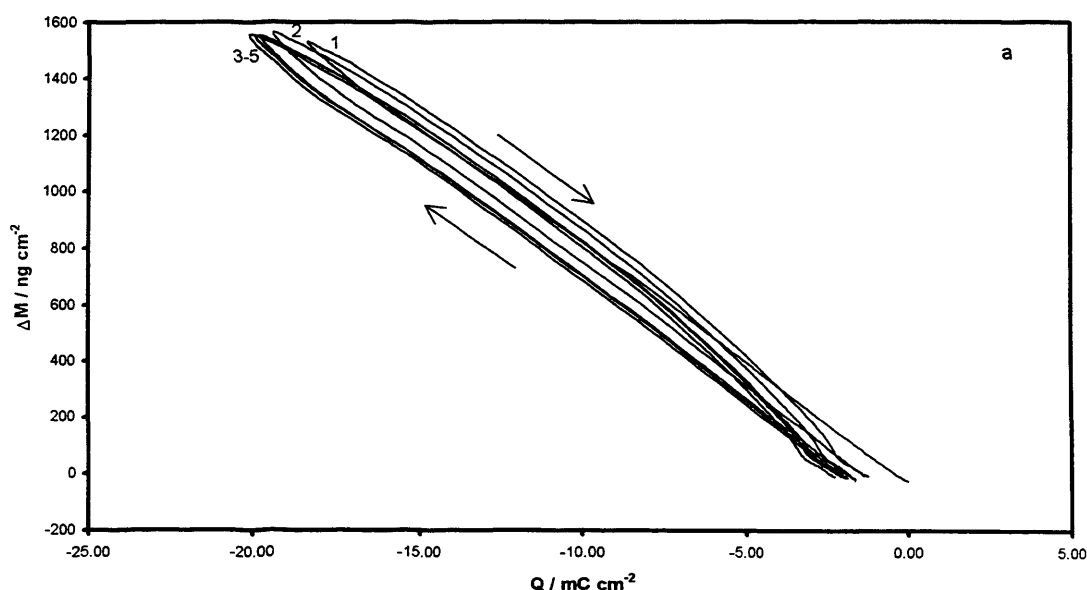
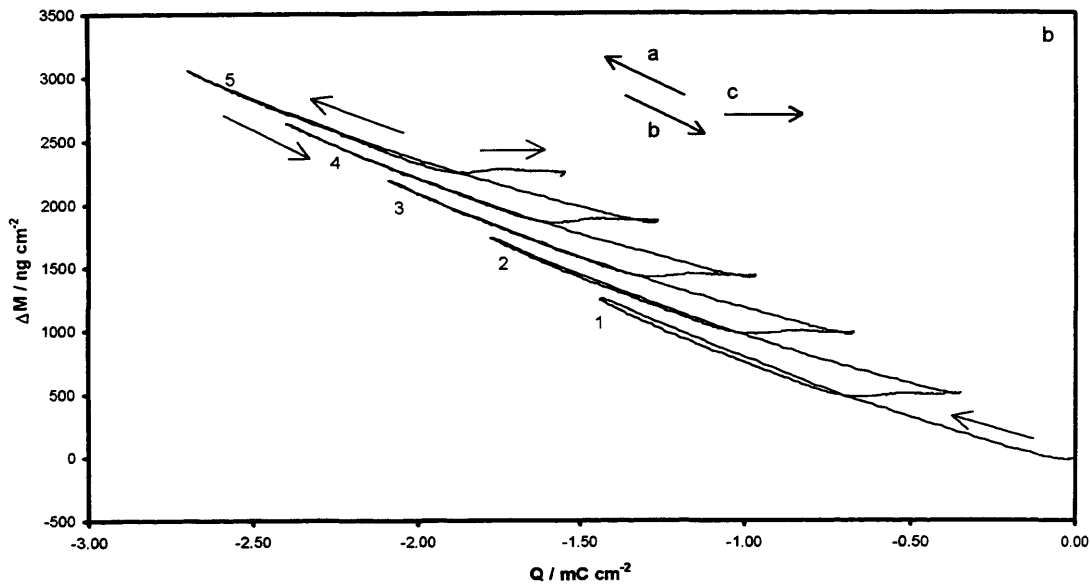


Figure 4.7 : Mass changes versus charge responses for voltammetric experiments to show the effect of using two different electrolytes to study cation insertion into 2700\AA thick WO_3 films. Electrolytes : 0.1M LiClO_4 /propylene carbonate (4.7a) and 0.1M NaClO_4 /propylene carbonate (4.7b). Total number of cycles recorded : 5 (marked on plot). Scan rate 10 mV s^{-1} . $\Gamma \cong 640 \text{ nmol cm}^{-2}$.



It is possible to calculate the amount of ion (x) being inserted into the WO_3 film from the charge values obtained from the voltammetric experiments using^[28]

$$x = \frac{QM}{FdlA} \quad [4.6]$$

where Q is the injected charge (C), M is the molecular weight of WO_3 (232 g mole^{-1}), F is the Faraday constant, d is the density of WO_3 (5.5 g cm^{-3}), l is defined as the thickness of the film (cm) and A is the electrode area (cm^2). Table 4.2 shows the x values calculated for the reduction and oxidation of WO_3 when cycled in 0.1M LiClO_4 /propylene carbonate.

Table 4.2 : Table showing calculated x values for insertion of Li^+ into a WO_3 film using 0.1M LiClO_4 /propylene carbonate as the electrolyte. Values obtained from experimental data shown in Figure 4.7a.

Cycle number	x	
	reduction	oxidation
1	0.297	0.278
2	0.294	0.288
3	0.293	0.289
4	0.292	0.289
5	0.292	0.289
average	0.294 ± 0.002	0.289 ± 0.004

It is seen that 0.294 Li^+ are inserted for every mole of WO_3 during the five recorded cycles and almost all of the Li^+ is expelled on oxidation. Since the total coverage of WO_3 on the electrode is known, (Γ_{WO_3}) then it is possible to calculate the absolute value for x by calculating the total amount of charge which can be inserted into the WO_3 film (Γ_{e^-}) and dividing Γ_{e^-} by Γ_{WO_3} . The equations are found in the Theory chapter. The total amount of x which can be inserted into the WO_3 film when being cycled in 0.1M LiClO_4 /propylene carbonate is 0.356. Therefore, the amount of x calculated for a WO_3 film cycled in 0.1M LiClO_4 /propylene carbonate at 10 mV s^{-1} shows a 17% difference to the total amount of x able to be inserted. The experiment during which these x values were calculated was initially cycled at a scan rate of 5 mVs^{-1} . Those x values are not discussed here, since the first cycle of an unused WO_3 film gives slightly different results. This difference will be discussed in Chapter 5.

The plot for the experiment carried out in 0.1M NaClO_4 /propylene carbonate (figure 4.7b) looks slightly different to that for 0.1M LiClO_4 /propylene carbonate. Again, a single slope is seen for reduction of the WO_3 film, but for the oxidation, there are two distinct slopes seen. The “end-to-end” $\Delta M_{\text{T}}F/Q_{\text{T}}$ values are given in Table 4.3, where the gradients are labelled “a”, “b” and “c” (as seen on Figure 4.7b). It is seen that the values for reduction of WO_3 by Na^+ are much larger than the expected value of 23 g mol^{-1} . This indicates a gradual accumulation of Na^+ in the WO_3 film, as mass changes and charge values do not return to zero so complete re-oxidation of the film does not occur. For the work carried out here, it may be that, at the concentrations studied here, it is possible to relate NaClO_4 to the referenced results for NaCF_3SO_3 mentioned above. In NaCF_3SO_3 there are more “free” ions seen in NaCF_3SO_3 than in LiCF_3SO_3 ^[26]. If it is considered that the same effect may also be seen in NaClO_4 , then the large amount of “free” ions seen in NaClO_4 may be the reason why the $\Delta M_{\text{T}}F/Q_{\text{T}}$ values are larger than expected.

The K_a values have also been given for NaClO₄/propylene carbonate by D'Aprano^[25]. They give $4.6 \pm 0.4 \text{ dm}^3 \text{ mol}^{-1}$ for solvent separated ion pairs and $1.7 \pm 0.2 \text{ dm}^3 \text{ mol}^{-1}$ for contact ion pairs. These values are close to those quoted for LiClO₄ in propylene carbonate, which indicates that there also may be contact ion pairs entering/leaving alongside Na⁺. It may be that the third distinct linear slope (“c”) may be related to the movement of ion pairs.

Table 4.3 : Table showing calculated “end to end” $\Delta M_T F / Q_T$ values for reduction and oxidation of a WO₃ film using 0.1M NaClO₄/propylene carbonate. Five scans recorded at a scan rate 10 mV s⁻¹. Data obtained from Figure 4.7b.

Cycle number	$\Delta M_T F / Q_T / \text{g mol}^{-1}$			
	Na ⁺	reduction (a)	oxidation (b)	oxidation (c)
1	-23	-84.7	-98.3	6.7
2	-23	-83.6	-95.1	2.3
3	-23	-82.5	-93.8	2.3
4	-23	-81.9	-92.0	2.4
5	-23	-80.4	-95.2	0.0
	average	-82.6 ± 1.5	-94.9 ± 2.1	3.4 ± 1.9

The linearity of the plot as seen by “a” and “b” indicate that any second species entering alongside Na⁺ is also leaving at the same time, ie, there is no “lag” seen. This is not the case for Li⁺ insertion, when the $\Delta M_T F / Q_T$ plot indicates that there is “lagging” behind the insertion/expulsion of Li⁺. On oxidation, the third calculated gradient is very small. This third gradient “c” gives an “end to end” $\Delta M_T F / Q_T$ value very close to zero and it can be seen in Figure 4.7b that very little change in mass is seen although the charge appears to change. Since ions, in this case Na⁺ have a specific mass, then it is suggested that some neutral species, is moving into the WO₃ film as Na⁺ leaves on oxidation of the tungsten bronze. As this neutral species is moving in the opposite direction then this would lead to a compensation in the mass changes seen.

Again, as for Li⁺ insertion, the x values for insertion and expulsion of Na⁺ into WO₃ can be calculated. Table 4.4 shows the x values for both reduction (“a”) and oxidation (“b”)

and “c”) of the WO₃ film. The x values are much smaller ($\approx 90\%$ smaller) than for the corresponding experiment in 0.1M LiClO₄/propylene carbonate. This indicates that there is much less Na⁺ inserted into WO₃. The absolute amount of Na⁺ able to be inserted into the WO₃ film has been calculated to be 0.029 and there is much less Na⁺ being inserted into the film than expected (21% of the x value for Li⁺). The x values for the reduction of WO₃ in 0.1M NaClO₄/propylene carbonate are all equal. This indicates that although it appears that there is an accumulation of both mass and ionic charge in the WO₃ film, there is still the same amount of Na⁺ inserted during each of the five reduction half cycles recorded here.

Table 4.4 : Table showing calculated x values for insertion of Na⁺ into a WO₃ film using 0.1M NaClO₄/propylene carbonate as the electrolyte. Values obtained from experimental data shown in Figure 4.7b.

Cycle number	x		
	reduction (a)	oxidation (b)	(c)
1	0.023	0.012	0.005
2	0.023	0.013	0.005
3	0.023	0.013	0.005
4	0.023	0.013	0.005
5	0.023	0.013	0.005
average	0.023 \pm 0	0.013 \pm 0	0.289 \pm 0.004

4.3.4 Variations from the $\Delta M_T F/Q_T$ data

As mentioned in Section 4.1.4, it is possible use Equation [4.5] to investigate whether there is more than one species being inserted into the WO₃ film. For the experiments described above, Equation [4.5] was used with the values for m_{ion} entered as 7 g mol⁻¹(Li⁺) and 23 g mol⁻¹(Na⁺) for the respective experiments and z_{ion} equal to +1 for both calculations. The mass changes versus charge response and Φ changes versus charge responses for the first recorded scans are shown in Figure 4.8.

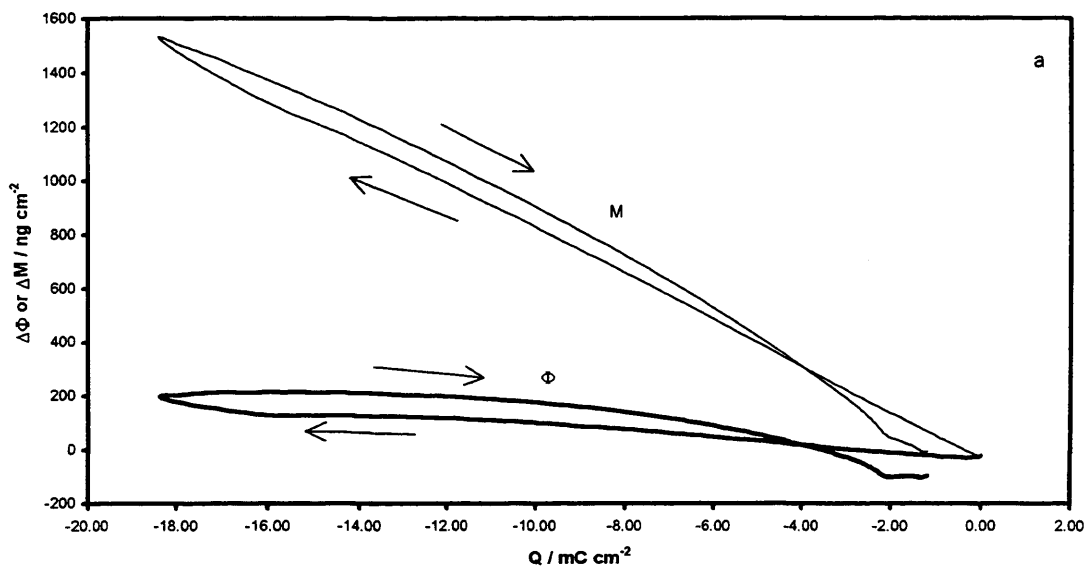
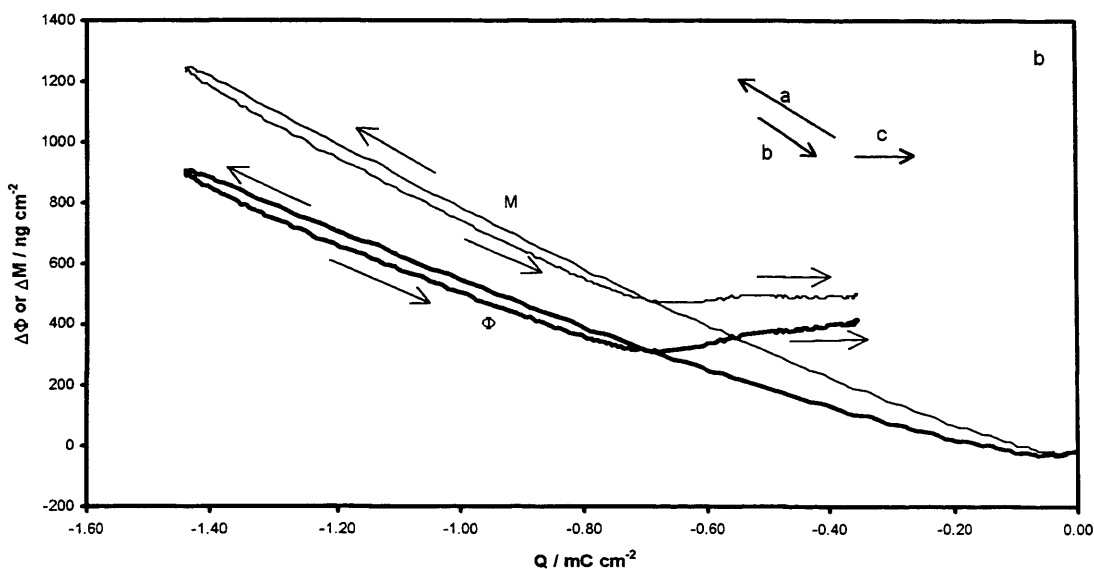


Figure 4.8 : Mass changes versus charge and Φ changes versus charge responses (marked on plot) for voltammetric experiments carried out to show the effect of using two different electrolytes to study cation insertion into 2700Å thick WO_3 films. Electrolytes : 0.1M LiClO_4 /propylene carbonate (4.8a) and 0.1M NaClO_4 /propylene carbonate (4.8b). Total number of cycles recorded : 5 (1st cycle from each experiment shown for ease of comparison between ΔM and Φ plots). Scan rate 10 mV s^{-1} . $\Gamma \cong 640 \text{ nmoles cm}^{-2}$.



It is seen that for the insertion of Li^+ into WO_3 using 0.1M LiClO_4 /propylene carbonate, the response where the values for Li^+ have been inserted ($\Delta\Phi_{\text{Li}^+}$) when plotted

against the charge passed are smaller than the corresponding response for mass changes against charge (difference of 87%). As the values substituted into Equation [4.5] do not equal zero then it implies that there may be neutral species entering and leaving the WO₃ film. If it believed that only solvent enters and leaves the WO₃ film, then it is possible to calculate the amount of propylene carbonate entering and leaving the WO₃ film by

$$\left[\left(\frac{\Delta\Phi_T F}{Q_T} \right) / MW_{PC} \right] = A \quad [4.7]$$

where $\Delta\Phi_T F/Q_T$ is the calculated value from $\Delta\Phi$ versus charge plots (g mol⁻¹), MW_{PC} is the molecular weight of propylene carbonate (104 g mol⁻¹), and the answer (A) is given in the number of moles of propylene carbonate per mole of C⁺/e⁻ where C⁺ is the cation being studied. For ion insertion using 0.1M LiClO₄/propylene carbonate, the amount of propylene carbonate entering and leaving WO₃ has been calculated to be one molecule of propylene carbonate for every 100 molecules of Li⁺.

In comparison, when the values for Na⁺ are inserted into Equation [4.5], the plotted response is much larger. Using Equation [4.7], the value for propylene carbonate entering and leaving the WO₃ film when using 0.1M NaClO₄/propylene carbonate has been calculated as being 0.6 molecules of propylene carbonate for every 1 molecule of Na⁺. This large value suggests that there is more solvent entering the WO₃ film with Na⁺. This is unexpected due to the fact that, as for the mass changes versus charge response for ion insertion into WO₃ using 0.1M NaClO₄/propylene carbonate (Figure 4.7b), three distinct gradients are seen (these are marked “a”, “b” and “c” in Figure 4.8b) which are much larger than their corresponding Li⁺ values. The “end to end” $\Delta\Phi_T F/Q_T$ values for Li⁺ and Na⁺ are shown in Tables 4.5 and 4.6.

Table 4.5 : Table showing calculated “end to end” $\Delta\Phi_{TF}/Q_T$ values for reduction and oxidation of a WO_3 film in 0.1M $LiClO_4$ /propylene carbonate. Five scans recorded at a scan rate 10 mV s^{-1} . Data obtained from Figure 4.8a. Value for $m_{ion} = 7\text{ g mol}^{-1}$ and $z_{ion} = +1$ substituted into equation [4.5] to equal Li^+ insertion.

Cycle number	$\Delta\Phi_{TF}/Q_T / \text{g mol}^{-1}$		
	Li^+	reduction	oxidation
1	-7	-1.2	-1.7
2	-7	-1.3	-1.6
3	-7	-1.3	-1.4
4	-7	-1.4	-1.4
5	-7	-1.4	-1.5
	average	-1.3 ± 0.1	-1.5 ± 0.1

Table 4.6 : Table showing calculated “end to end” $\Delta\Phi_{TF}/Q_T$ values for reduction (“a”) and oxidation (“b”) and (“c”) of a WO_3 film in 0.1M $NaClO_4$ /propylene carbonate. Five scans recorded at a scan rate 10 mV s^{-1} . Data obtained from Figure 4.8b. Value for $m_{ion} = 23\text{ g mol}^{-1}$ and $z_{ion} = +1$ substituted into equation [4.5] to equal Na^+ insertion.

Cycle number	$\Delta\Phi_{TF}/Q_T / \text{g mol}^{-1}$			
	Na^+	reduction (a)	oxidation (b)	oxidation (c)
1	-23	-61.7	-75.3	29.7
2	-23	-60.6	-72.1	25.3
3	-23	-59.5	-70.80	25.3
4	-23	-58.9	-69.0	25.4
5	-23	-57.4	-72.2	23
	average	-59.6 ± 1.5	-71.9 ± 2.1	25.7 ± 2.2

4.4 EFFECT OF CHANGING ANION

4.4.1 Introduction

It was shown in the previous section that changing the cation can give information regarding the ability of various cations to insert into WO_3 . It is also possible to investigate different anions, to see whether they are involved in the insertion process alongside the cation. Anion intercalation has been deemed unfavourable under most conditions due to both steric and energetic reasons^{[5][29]}. For this study, the cation (Li^+) was held fixed, and the anions studied were ClO_4^- and $CF_3SO_3^-$ (triflate). The experiments were carried out on two WO_3 coated quartz crystals in solutions of 0.1M $LiClO_4$ /propylene carbonate and 0.1M $LiCF_3SO_3$ /propylene carbonate. To compare the effects of using two different electrolytes, a scan rate of 10 mV s^{-1} was chosen. The two WO_3 coated crystals which were used for

this study were of different thickness. The crystal chosen to study ion insertion into WO_3 using 0.1M LiClO_4 /propylene carbonate as the electrolyte was coated with a 2700Å thick WO_3 film. This is compared to the crystal which used 0.1M LiCF_3SO_3 /propylene carbonate as the electrolyte which was 2400Å thick. Since the thicknesses are similar there should be no dramatic structural changes, but the two films cannot be compared directly and all experimental information obtained from EQCM experiments must be “normalised”. The “normalisation” involves dividing the experimental values obtained by the film thickness to give a fair representation of the results. By “normalising” the results it is possible to overcome any differences caused purely by the thickness of the WO_3 film. As in the previous section, the current and mass responses during a cyclic voltammogram are compared.

4.4.2 Current responses recorded for ion insertion into WO_3 using 0.1M LiClO_4 /propylene carbonate and 0.1M LiCF_3SO_3 /propylene carbonate

Figure 4.9, shows a comparison between the normalised cyclic voltammograms obtained when two 2700Å and 2400Å thick WO_3 films were cycled in 0.1M LiClO_4 /propylene carbonate and 0.1M LiCF_3SO_3 /propylene carbonate respectively. It can be seen that even after normalisation of the current response, there is less current passed when LiCF_3SO_3 /propylene carbonate is the chosen electrolyte ($\approx 30\%$ difference when WO_3 is cycled in 0.1M LiCF_3SO_3 /propylene carbonate). This suggests that, since the problem of film thickness has been overcome by normalising the responses, then the effect must be electrochemical. Both cyclic voltammograms show the same shape and oxidation is seen to begin at $-0.847 (\pm 0.004)\text{V}$ for LiClO_4 and $-0.816 (\pm 0.004)\text{V}$ for LiCF_3SO_3 . This suggests that the choice of anion here does not appear to affect the electrochemical characteristics of ion insertion. As the sizes of the two anions are very similar then it is expected that the two

cyclic voltammograms are of similar proportion.

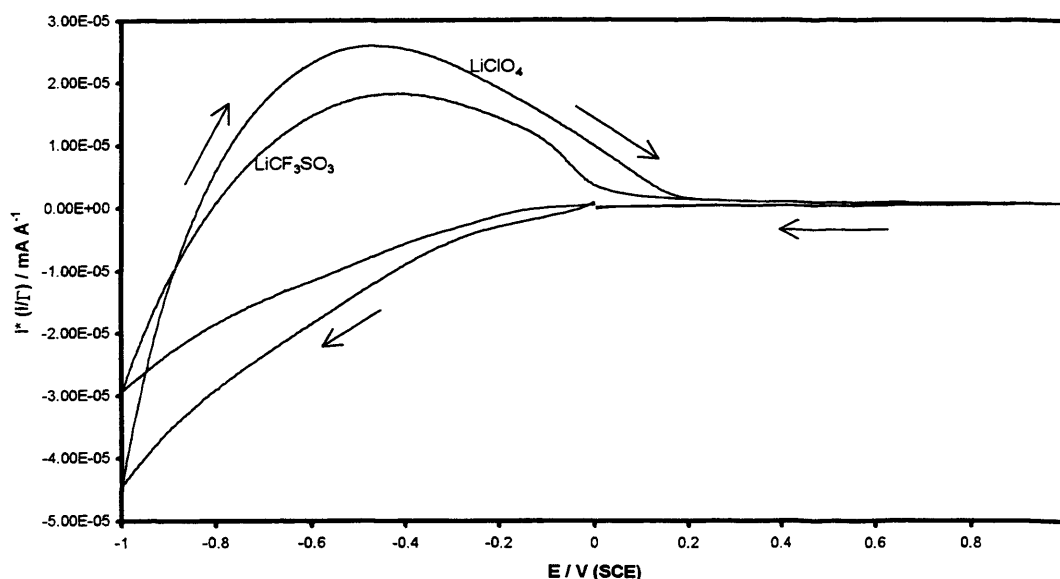


Figure 4.9 : Normalised cyclic voltammograms showing the effect of using two different electrolytes to study anion insertion into WO_3 films. Electrolytes : 0.1M LiClO_4 /propylene carbonate and 0.1M LiCF_3SO_3 /propylene carbonate (marked on plot). Total number of cycles recorded : 5 (1st cycle from each experiment shown for ease of comparison). Scan rate 10 mV s^{-1} . Thickness of WO_3 film cycled in 0.1M LiClO_4 /propylene carbonate : 2700 \AA ($\Gamma \cong 640 \text{ nmol cm}^{-2}$). Thickness of WO_3 film cycled in 0.1M LiCF_3SO_3 /propylene carbonate : 2400 \AA ($\Gamma \cong 569 \text{ nmol cm}^{-2}$).

The integrated current values will give charge values, which can then be normalised with respect to the film thickness. The two experiments recorded in 0.1M LiClO_4 /propylene carbonate and 0.1M LiCF_3SO_3 /propylene carbonate show very few differences in the normalised responses. Again, as for the cyclic voltammogram, the normalised charge values calculated for the experiment using 0.1M LiCF_3SO_3 /propylene carbonate show a 33% difference in values when compared to the corresponding experiment in 0.1M LiClO_4 /propylene carbonate and both plots, show that there is slightly less charge passed on the first recorded cycle, compared to the following cycles.

As for the experiments described in the previous section regarding the insertion of ions using 0.1M NaClO_4 /propylene carbonate and 0.1M LiClO_4 /propylene carbonate, there appears to be a slight drift of charge seen for both experiments, which may indicate a small

accumulation of charge in both films. The minimum charge is recorded at $-0.848 (\pm 0.045)V$ for $0.1M LiClO_4/propylene carbonate$ and $-0.815 (\pm 0.004)V$ for $0.1M LiCF_3SO_3/propylene carbonate$ which is expected as the onset of oxidation in both electrolytes studied and lies within the experimental error. Table 4.7 shows the normalised values of charge calculated for both electrolytes studied.

Table 4.7 : Table showing information regarding potential responses and normalised charge (Q^*) values for ion insertion into WO_3 films using different electrolytes. Electrolytes used : $0.1M LiClO_4/propylene carbonate$ and $0.1M LiCF_3SO_3/propylene carbonate$. Experiments carried out at $10 mV s^{-1}$. Charge values obtained from integration of current responses. Normalisation required due to two different thickness of WO_3 films used. Thickness of WO_3 film cycled in $0.1M LiClO_4/propylene carbonate$: 2700\AA . Thickness of WO_3 film cycled in $0.1M LiCF_3SO_3/propylene carbonate$: 2400\AA .

Cycle number	Potential where oxidation begins / V	Potential where recorded / V	Potential where recorded / V		$Q^* / C cm^{-3}$	
	0.1M $LiClO_4/propylene carbonate$	0.1M $LiCF_3SO_3/propylene carbonate$	0.1M $LiClO_4/propylene carbonate$	0.1M $LiCF_3SO_3/propylene carbonate$	0.1M $LiClO_4/propylene carbonate$	0.1M $LiCF_3SO_3/propylene carbonate$
1	-0.840	-0.808	-0.838	-0.808	-680.4	-448.8
2	-0.847	-0.815	-0.845	-0.815	-718.5	-478.6
3	-0.850	-0.818	-0.847	-0.818	-730.4	-492.9
4	-0.850	-0.818	-0.850	-0.818	-737.8	-505.0
5	-0.850	-0.820	-0.850	-0.818	-744.1	-513.3
average	-0.847 ± 0.003	-0.816 ± 0.004	-0.846 ± 0.005	-0.815 ± 0.004	-722.2 ± 22.6	-487.7 ± 22.7

4.4.3 Mass responses

As for the cyclic voltammogram responses, the simultaneous mass changes recorded have been normalised for the ease of comparison and to exclude any effects seen due to film thickness. Figure 4.10 shows the normalised mass changes versus potential plot for ion insertion into WO_3 using $0.1M LiClO_4/propylene carbonate$ and $0.1M LiCF_3SO_3/propylene carbonate$ electrolytes. As for all experiments shown, the shapes of the plots are very similar.

Even after the mass changes have been normalised, it appears that there is smaller mass change recorded for LiCF_3SO_3 than for LiClO_4 ($\approx 32\%$ difference) which shows that there appears to be less Li^+ entering the WO_3 film.

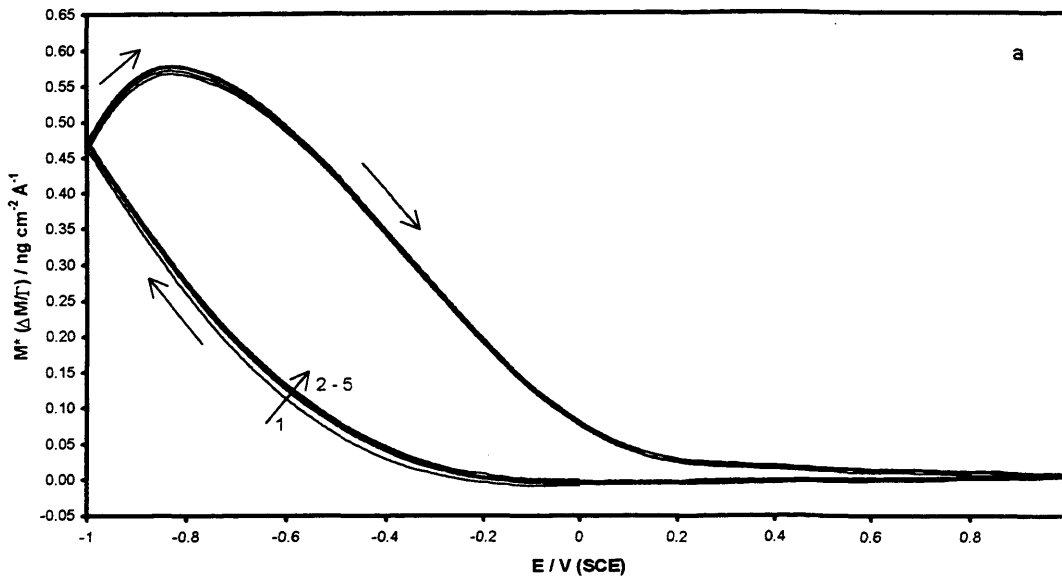
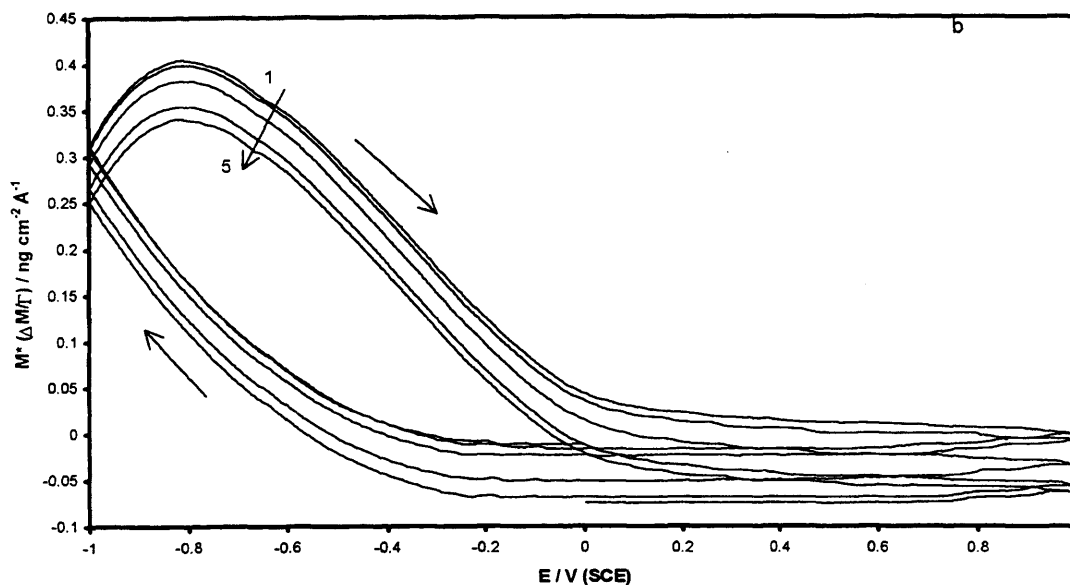


Figure 4.10 : Normalised mass changes versus potential response for a voltammetric experiment showing the effect of using two different electrolytes to study anion insertion into WO_3 films. Electrolytes : 0.1M LiClO_4 /propylene carbonate (4.10a) and 0.1M LiCF_3SO_3 /propylene carbonate (4.10b). Total number of cycles recorded : 5 (marked on plot). Scan rate 10 mV s^{-1} . Thickness of WO_3 film cycled in 0.1M LiClO_4 /propylene carbonate : 2700 \AA ($\Gamma \cong 640 \text{ nmoles cm}^{-2}$). Thickness of WO_3 film cycled in 0.1M LiCF_3SO_3 /propylene carbonate : 2400 \AA ($\Gamma \cong 569 \text{ nmoles cm}^{-2}$).



It is possible to measure the potential at which the normalised maximum mass value is recorded; the data is shown in Table 4.8. For the experiment carried out in 0.1M LiClO₄/propylene carbonate, the maximum mass value is recorded at -0.827 (± 0.007)V, shortly after scan reversal. This is slightly more positive than the recorded potential at which oxidation begins. This increase in mass that is seen during the early stages of oxidation may be due to inhomogeneous distribution of Li⁺ through the WO₃ film.

For the experiment carried out in 0.1M LiCF₃SO₃/propylene carbonate, the mass changes versus potential response shows a decrease in mass as the WO₃ film is cycled. This decrease in mass may indicate small solvent changes. The potential where the maximum mass is recorded is at -0.833 (± 0.002)V which is at a more negative potential than the potential recorded for the beginning of oxidation. This may be because no more Li⁺ can be inserted into the tungsten bronze and hence the film is considered to be saturated.

If the normalised values at which the maximum mass values are recorded are studied, then, the two mass values are different by 0.02 g cm⁻³. If only Li⁺ was being inserted into the WO₃ film, then, regardless of the electrolyte chosen for study, the recorded

mass changes would be equal. Therefore, it appears that this effect may be either due to the choice of electrolyte in this study or the film composition.

Table 4.8 : Table showing information regarding potential responses and normalised mass changes (M^*) values for ion insertion into a WO_3 film using different electrolytes. Electrolytes used : 0.1M $LiClO_4$ /propylene carbonate and 0.1M $LiCF_3SO_3$ /propylene carbonate. Experiments carried out at 10 mV s^{-1} . Mass values obtained from mass changes versus potential responses shown in Figure 4.10. Normalisation required due to two different thickness of WO_3 films used. Thickness of WO_3 film cycled in 0.1M $LiClO_4$ /propylene carbonate : 2700 \AA . Thickness of WO_3 film cycled in 0.1M $LiCF_3SO_3$ /propylene carbonate : 2400 \AA .

Cycle number	Potential where oxidation begins / V		Potential where recorded / V		M^* / g cm^{-3} ($\Delta M/T$)	
	0.1M $LiClO_4$ /propylene carbonate	0.1M $LiCF_3SO_3$ /propylene carbonate	0.1M $LiClO_4$ /propylene carbonate	0.1M $LiCF_3SO_3$ /propylene carbonate	0.1M $LiClO_4$ /propylene carbonate	0.1M $LiCF_3SO_3$ /propylene carbonate
1	-0.840	-0.808	-0.825	-0.808	0.057	0.040
2	-0.847	-0.815	-0.818	-0.798	0.058	0.040
3	-0.850	-0.818	-0.830	-0.798	0.057	0.038
4	-0.850	-0.818	-0.830	-0.798	0.057	0.035
5	-0.850	-0.820	-0.837	-0.811	0.057	0.034
average	-0.847 ± 0.003	-0.816 ± 0.004	-0.828 ± 0.006	-0.803 ± 0.005	0.057 ± 0.0004	0.037 ± 0.002

At more positive potentials ($> +0.200\text{V}$), it appears that there is very little mass change recorded for both electrolytes, which indicates that all the cation inserted into the WO_3 film has been expelled.

As potentials above $\approx -0.800\text{V}$ indicate that oxidation of the WO_3 film is occurring, it would be expected that if any anions were being inserted, then there would be a change in mass at the oxidation potentials. As there is no significant difference in either electrolyte, it appears that the anion chosen does not contribute to colouration of the WO_3 film.

4.4.3. Correlation of mass and charge responses

Figure 4.11 shows the mass changes versus charge responses for ion insertion into WO_3 using 0.1M $LiClO_4$ /propylene carbonate and 0.1M $LiCF_3SO_3$ /propylene carbonate. It can be seen that there is a single measurable slope for both reduction and oxidation of the

WO₃ film when the film is cycled in either 0.1M LiClO₄/propylene carbonate or 0.1M LiCF₃SO₃/propylene carbonate. Both responses show slight hysteresis which indicates that more than one species is entering and leaving the film.

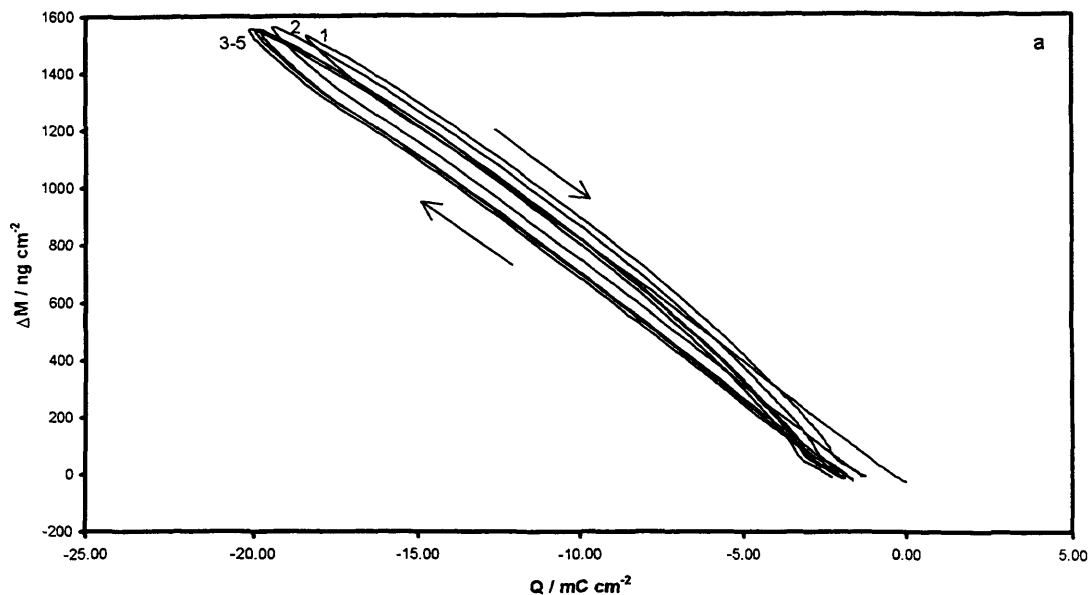
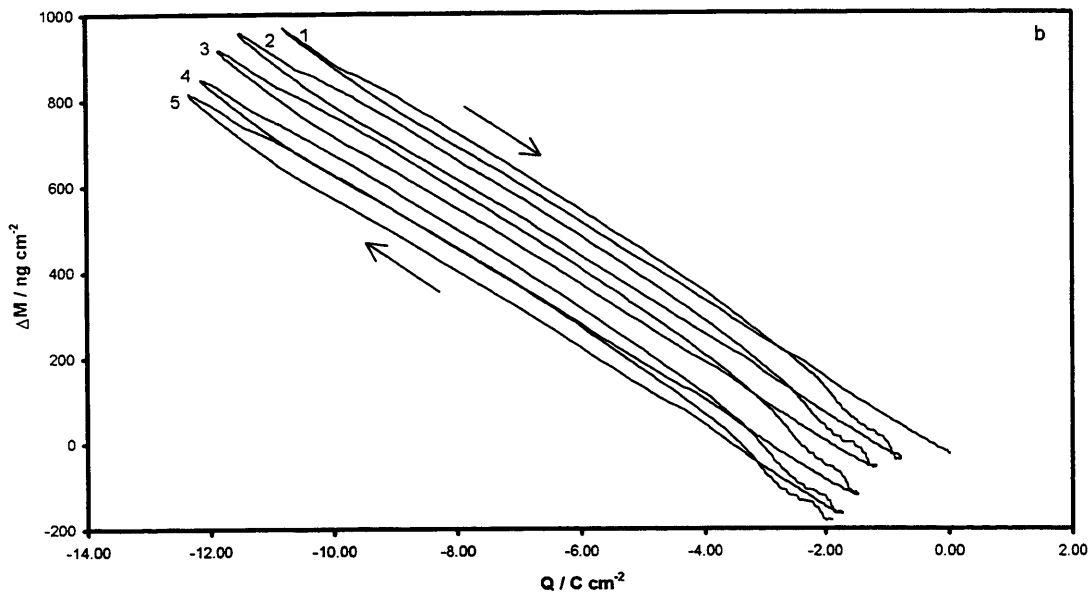


Figure 4.11 : Mass changes versus charge response for voltammetric experiments to show the effect of using two different electrolytes to study anion insertion into WO₃ films. Electrolytes : 0.1M LiClO₄/propylene carbonate (4.11a) and 0.1M LiCF₃SO₃/propylene carbonate (4.11b). Total number of cycles recorded : 5 (marked on plot). Scan rate 10 mV s⁻¹. Thickness of WO₃ film cycled in 0.1M LiClO₄/propylene carbonate : 2700 Å ($\Gamma \cong 640 \text{ nmoles cm}^{-2}$). Thickness of WO₃ film cycled in 0.1M LiCF₃SO₃/propylene carbonate : 2400 Å ($\Gamma \cong 569 \text{ nmoles cm}^{-2}$).



The “end to end” $\Delta M_{TF}/Q_T$ ratios calculated for both experiments shown in Figure 4.11 are given in Table 4.9. As the $\Delta M_{TF}/Q_T$ values are given as ratios, then it is not necessary to normalise the plots. The calculated values for ion insertion into WO_3 using both 0.1M $LiClO_4$ /propylene carbonate and 0.1M $LiCF_3SO_3$ /propylene carbonate show values that are greater than 7 g mol^{-1} , which, as mentioned above, indicates a second species is also entering WO_3 alongside Li^+ .

Work carried out by Starkey and Frech^[30] of $LiCF_3SO_3$ in a mixture of propylene carbonate-poly(acrylonitrile) find that the $LiCF_3SO_3$ is highly associated and that there is a stronger interaction between Li^+ and propylene carbonate than between Li^+ and poly(acrylonitrile). It is suggested that the dominant species is $[Li_2CF_3SO_3]^+$ in this solution, which indicates that there is little possibility of the presence of “free” $CF_3SO_3^-$ or just simple $Li^+ - CF_3SO_3^-$ pairs. This may account for the larger $\Delta M_{TF}/Q_T$ values seen for the EQCM experiment carried out in 0.1M $LiCF_3SO_3$ /propylene carbonate than for those in

LiClO₄/propylene carbonate as along with Li⁺ there may be triple ions also being inserted into the WO₃ film.

When the mass change versus potential plot and cyclic voltammogram are studied, then for both WO₃ films cycled in either LiClO₄/propylene carbonate or LiCF₃SO₃/propylene carbonate, the mass appears to be changing when the current is equal to zero, which, as already mentioned, indicates the movement of a neutral species. Vibrational spectroscopic studies carried out by Huang *et al*^[31] suggests that for Li⁺ in a mixed solvent system, for example propylene carbonate-poly(ethylene oxide), if Li⁺ is preferentially solvated to propylene carbonate, then the cation may move through the PEO matrix into a solvent shell of small propylene carbonate molecules. It is also suggested that some of the propylene carbonate may enter cation intercalating materials such as V₆O₁₃ as the Li⁺ moves into the layered structures of these types of materials. This may also be the case for WO₃ films as therefore, in LiCF₃SO₃ there may be insertion of propylene carbonate along with Li⁺ insertion. Therefore, this neutral species may be either propylene carbonate, ion pairs or a combination of the two.

For samples of LiCF₃SO₃-propylene carbonate-diglyme solutions, it appears that, although propylene carbonate does not compete with diglyme in co-ordinating the Li⁺, molecules of propylene carbonate may decrease the amount of associated LiCF₃SO₃, as propylene carbonate reduces the concentration of associated LiCF₃SO₃ only in samples with a low salt concentration. For the LiCF₃SO₃ solution used here, the concentration may be too low to clearly see any major change due to the association of LiCF₃SO₃. It therefore, appears that we are seeing solvation in the solution and that there appears to be the presence of ion pairs in the WO₃ film. As these ion pairs carry a neutral charge then the insertion of a neutral species at $i = 0$ may be due, not only to the solvent (propylene carbonate) but also to the presence of some ion pairs.

Table 4.9 : Table showing calculated “end to end” $\Delta M_T F / Q_T$ values for reduction and oxidation of WO_3 film using two different electrolytes. Electrolytes chosen : 0.1M $LiClO_4$ /propylene carbonate and 0.1M $LiCF_3SO_3$ /propylene carbonate. Five scans recorded at a scan rate 10 mV s^{-1} . Data obtained from Figure 4.11.

Cycle number	$\Delta M_T F / Q_T \text{ / g mol}^{-1}$			
	0.1M $LiClO_4$		0.1M $LiCF_3SO_3$	
	reduction	oxidation	reduction	oxidation
1	-8.2	-8.7	-9.0	-9.8
2	-8.3	-8.6	-9.0	-9.5
3	-8.3	-8.4	-8.8	-9.7
4	-8.4	-8.4	-8.8	-9.4
5	-8.4	-8.5	-9.0	-9.2
average	-8.3 ± 0.1	-8.5 ± 0.1	-8.9 ± 0.1	-9.5 ± 0.2

As for the calculation of x values using equation [4.6] for ion insertion into a WO_3 film using 0.1M $LiClO_4$ /propylene carbonate and 0.1M $NaClO_4$ /propylene carbonate mentioned above, it is also possible to calculate the x values for the electrolytes studied here. Table 4.10 shows the x values for the ion insertion into WO_3 using 0.1M $LiClO_4$ /propylene carbonate. As for the above section, the values are comparable for both reduction and oxidation of the WO_3 film.

Table 4.10 : Table showing calculated x values for insertion of ions into a WO_3 film using 0.1M $LiClO_4$ /propylene carbonate as the electrolyte. Values obtained from experimental data shown in Figure 4.11a.

Cycle number	x	
	reduction	oxidation
1	-0.297	0.278
2	-0.294	0.288
3	-0.293	0.289
4	-0.292	0.289
5	-0.292	0.289
average	-0.294 ± 0.002	0.289 ± 0.004

For the insertion of ions into WO_3 using 0.1M $LiCF_3SO_3$ /propylene carbonate as the electrolyte, the x values are shown in Table 4.11. It can be seen that the x values are smaller than for the corresponding experiment in 0.1M $LiClO_4$ /propylene carbonate. This may be due to the nature of the electrolyte used, as all effects due to film thickness have been eliminated by normalising all experimental data.

Table 4.11 : Table showing calculated x values for insertion of ions into a WO_3 film using 0.1M LiCF_3SO_3 /propylene carbonate as the electrolyte. Values obtained from experimental data shown in Figure 4.11b.

Cycle number	x	
	reduction	oxidation
1	-0.196	0.182
2	-0.195	0.188
3	-0.194	0.189
4	-0.194	0.190
5	-0.194	0.190
average	-0.195 ± 0.001	0.188 ± 0.003

Although the mass changes versus charge responses indicate that there is a second neutral species entering the WO_3 film, the $\Delta M_T F / Q_T$ values calculated do not give detailed information regarding the species which is recorded being inserted and expelled. As previously mentioned, the equation relating Φ to the overall mass changes, Equation [4.1] can be used to separate charged and neutral species.

It is possible to insert the values for m_{ion} and z_{ion} for both cations (in this case, Li^+) and also anions (ClO_4^- and CF_3SO_3^-). Figure 4.12 shows the normalised mass changes versus normalised charge responses and also the normalised Φ changes versus normalised charge responses (for both cations and anions).

The EQCM data for WO_3 films cycled in either 0.1M LiClO_4 /propylene carbonate or 0.1M LiCF_3SO_3 /propylene carbonate show that even after normalisation of the data there are still minor structural changes which may affect the cation insertion rate. It has been shown that the different electrolytes have slightly different solvent activity/penetration which may indicate why the “end to end” $\Delta M_T F / Q_T$ and $\Delta \Phi_T F / Q_T$ values are different.

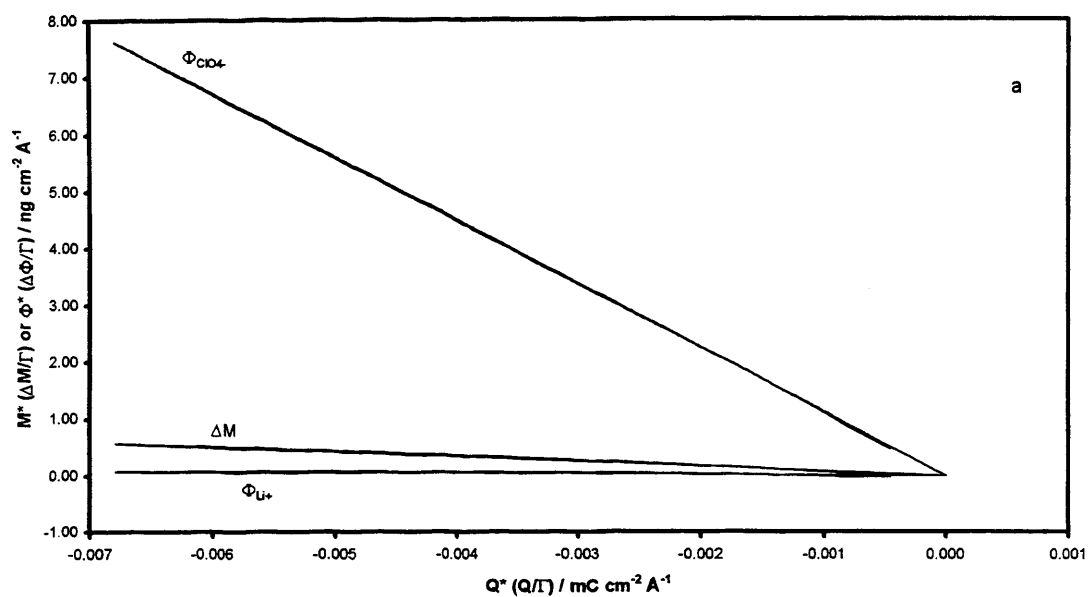
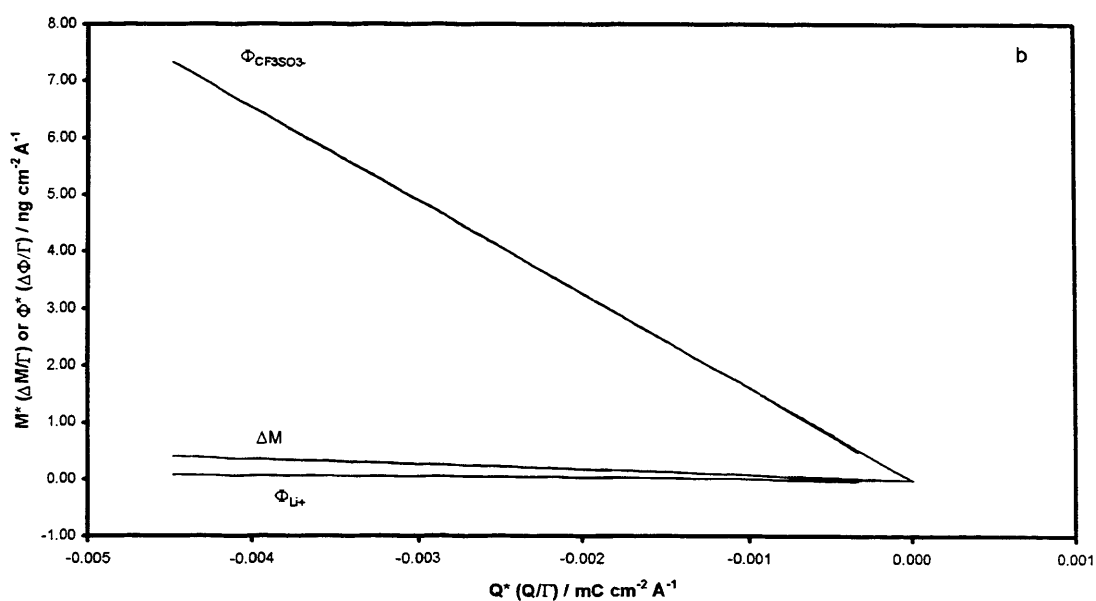


Figure 4.12 : Normalised mass changes versus charge and Φ changes versus charge responses (marked on plot) for voltammetric experiments carried out to show the effect of using two different electrolytes to study ion insertion into WO_3 films. Electrolytes - 0.1M LiClO_4 /propylene carbonate (4.12a) and 0.1M LiCF_3SO_3 /propylene carbonate (4.12b). Total number of cycles recorded - 5 (1st cycle from each experiment shown for ease of comparison). Scan rate 10 mV s^{-1} . Thickness of WO_3 film cycled in 0.1M LiClO_4 /propylene carbonate - 2700 \AA ($\Gamma \cong 640 \text{ nmol cm}^{-2}$). Thickness of WO_3 film cycled in 0.1M LiCF_3SO_3 /propylene carbonate - 2400 \AA ($\Gamma \cong 569 \text{ nmol cm}^{-2}$).



Tables 4.12 and 4.13 shows the $\Delta\Phi_{TF}/Q_T$ values for both cation (Li^+) and anion (ClO_4^- and CF_3SO_3^-) for both experiments carried out to study the ion insertion into WO_3 using 0.1M LiClO_4 /propylene carbonate and 0.1M LiCF_3SO_3 /propylene carbonate respectively. For the Φ_{Li^+} data for ion insertion using both 0.1M LiClO_4 /propylene carbonate and 0.1M LiCF_3SO_3 /propylene carbonate the calculated values are very close to zero, whereas for $\Phi_{\text{ClO}_4^-}$ and $\Phi_{\text{CF}_3\text{SO}_3^-}$, the values are much larger. The Φ_{Li^+} values indicate that it is predominantly cation insertion into the WO_3 film, and the large Φ_{A^-} values have a gradient which is virtually equal to the molar mass of the salts being studied (106 g mol^{-1} for LiClO_4 and 156 g mol^{-1} for LiCF_3SO_3). The effects seen for Φ_{A^-} indicate that there is not pure anion insertion into the WO_3 film, but as the two anions are of similar sizes, then it is very difficult to distinguish any effect due to the anions.

Table 4.12 : Table showing calculated “end to end” $\Delta\Phi_{TF}/Q_T$ values for reduction and oxidation of WO_3 film using 0.1M LiClO_4 /propylene carbonate. $\Delta\Phi_{TF}/Q_T$ values calculated for both $m_{\text{ion}} = 7 \text{ g mol}^{-1}$, $z_{\text{ion}} = +1$ (Li^+) and $m_{\text{ion}} = 99 \text{ g mol}^{-1}$, $z_{\text{ion}} = -1$ (ClO_4^-) using equation [4.5]. Five scans recorded at a scan rate 10 mV s^{-1} . Data obtained from Figure 4.12a.

Cycle number	$\Delta\Phi_{TF}/Q_T / \text{g mol}^{-1}$			
	$\Phi = \text{Li}^+$		$\Phi = \text{ClO}_4^-$	
	reduction	oxidation	reduction	oxidation
1	-1.2	-1.7	-107.2	-107.7
2	-1.3	-1.6	-107.3	-107.6
3	-1.3	-1.4	-107.3	-107.4
4	-1.4	-1.4	-107.4	-107.4
5	-1.4	-1.5	-107.4	-107.5
average	-1.3 ± 0.1	-1.4 ± 0.1	-107.3 ± 0.07	-107.4 ± 0.07

Table 4.13 : Table showing calculated “end to end” $\Delta\Phi_{TF}/Q_T$ values for reduction and oxidation of WO_3 film using 0.1M LiCF_3SO_3 /propylene carbonate. $\Delta\Phi_{TF}/Q_T$ values calculated for both $m_{\text{ion}} = 7 \text{ g mol}^{-1}$, $z_{\text{ion}} = +1$ (Li^+) and $m_{\text{ion}} = 149 \text{ g mol}^{-1}$, $z_{\text{ion}} = -1$ (CF_3SO_3^-) using equation [4.5]. Five scans recorded at a scan rate 10 mV s^{-1} . Data obtained from Figure 4.12b.

Cycle number	$\Delta\Phi_{TF}/Q_T / \text{g mol}^{-1}$			
	$\Phi = \text{Li}^+$		$\Phi = \text{CF}_3\text{SO}_3^-$	
	reduction	oxidation	reduction	oxidation
1	-2.0	-2.8	-157.9	-158.7
2	-2.0	-2.5	-158.0	-158.5
3	-1.8	-2.7	-157.8	-158.7
4	-1.8	-2.4	-157.8	-158.4
5	-2.0	-2.2	-157.9	-158.2
average	-1.9 ± 0.1	-2.5 ± 0.2	-157.9 ± 0.07	-158.5 ± 0.07

4.5 EFFECT OF CHANGING ELECTROLYTE CONCENTRATION

4.5.1 Introduction

Since the effect of changing both the cation and anion has been investigated, the final variable is the electrolyte concentration. These experiments were carried out using LiClO_4 /propylene carbonate as the electrolyte at concentrations of 0.1M, 0.5M and 0.7M. As the concentrations of the electrolytes are increased then the activity of the solutions also increases. Therefore, as increasing concentration leads to increasing activity then the two phrases can be interchanged.

An electrolyte concentration of 1.0M LiClO_4 /propylene carbonate was preferred for the experiments, but the resonant frequency was damped by a viscous medium (propylene carbonate) which indicated that the quartz crystal was not oscillating freely and therefore, a lower concentration (and hence, activity) of 0.7M LiClO_4 /propylene carbonate was chosen instead. As for the experiments carried out in 0.1M LiCF_3SO_3 /propylene carbonate, the quartz crystal chosen to study ion insertion into WO_3 at 0.5M LiClO_4 /propylene carbonate was coated with a 2400Å thick WO_3 film, compared to the two quartz crystals used in the study of ion insertion into WO_3 using 0.1M LiClO_4 /propylene carbonate and 0.7M LiClO_4 /propylene carbonate which are both 2700Å thick. Therefore, it is necessary to “normalise” the experimental data to account for the varying thickness of films.

4.5.2 Cyclic voltammetric responses for differing activities of LiClO_4 /propylene carbonate

Figure 4.13 shows comparative normalised cyclic voltammograms at all three LiClO_4 /propylene carbonate activities. All three plots for experiments carried out at different concentrations of LiClO_4 /propylene carbonate show the same cyclic

C

voltammogram. Oxidation does not commence until after reversal of the potential scan. The normalised current responses recorded in 0.5M LiClO₄/propylene carbonate are slightly larger than the cyclic voltammogram response measured in 0.7M LiClO₄/propylene carbonate. The potentials where oxidation begins for each measured LiClO₄ concentration are shown in Table 4.14.

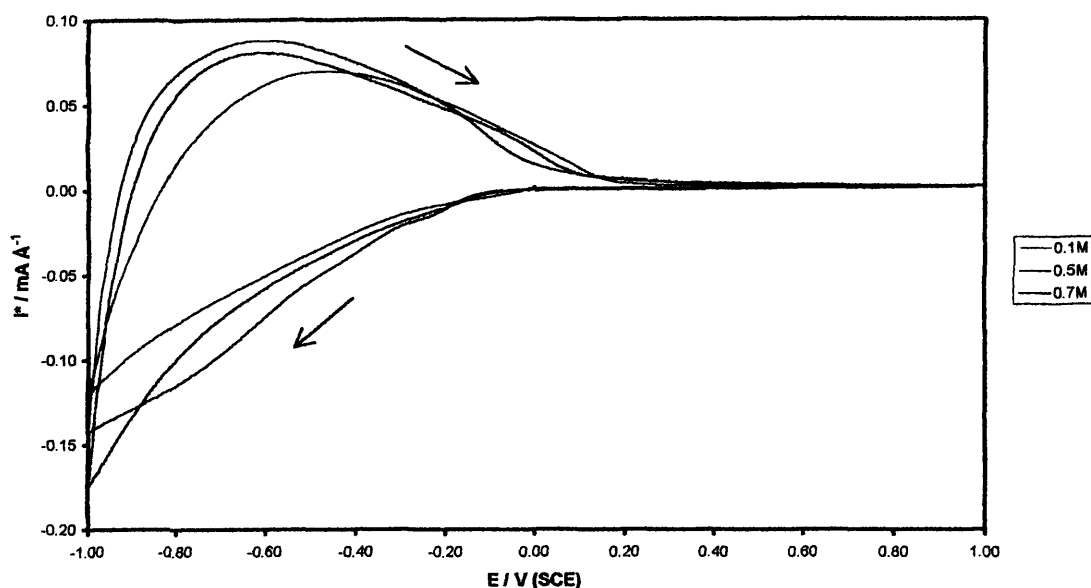


Figure 4.13 : Normalised cyclic voltammogram showing the effect of using different electrolyte activity to study ion insertion into WO₃ films. Electrolytes : 0.1M LiClO₄/propylene carbonate, 0.5M LiClO₄/propylene carbonate and 0.7M LiClO₄/propylene carbonate (marked on legend). Total number of cycles recorded : 5 (1st cycle from each experiment shown for ease of comparison). Scan rate : 10 mV s⁻¹. Thickness of WO₃ film cycled in 0.1M LiClO₄/propylene carbonate and 0.7M LiClO₄/propylene carbonate : 2700Å ($\Gamma \cong 640$ nmoles cm⁻²). Thickness of WO₃ film cycled in 0.5M LiClO₄/propylene carbonate : 2400Å ($\Gamma \cong 569$ nmoles cm⁻²).

Table 4.14 : Table showing measured potentials at which oxidation begins for a WO₃ film cycled at 10 mV s⁻¹ in various activities of LiClO₄/propylene carbonate.

[LiClO ₄]	Potential at which oxidation begins / V		
	0.1M	0.5M	0.7M
Cycle number			
1	-0.840	-0.930	-0.901
2	-0.847	-0.930	-0.906
3	-0.850	-0.933	-0.908
4	-0.850	-0.933	-0.908
5	-0.850	-0.933	-0.911
average	-0.847 ± 0.004	-0.932 ± 0.002	-0.907 ± 0.003

For all activities, there is very little current passed at more positive potentials, and more current is seen to be passed as the concentration increases. As there are no significant differences in all three activities, it appears that varying the electrolyte concentration and therefore, activity does not lead to any major changes in the cyclic voltammograms recorded.

The normalised charge data calculated for the various activities show very little changes. For the first cycle, it appears that there is less charge passed for all three activities, and as seen for experiments in 0.1M LiClO₄/propylene carbonate, 0.1M NaClO₄/propylene carbonate and 0.1M LiCF₃SO₃/propylene carbonate, it appears that there is a small drift seen during the experiment, which appears to be independent for each experiment. The normalised minimum charge value recorded for each concentration is seen at approximately the same potential at which oxidation begins as is expected, and very little charge is passed after a potential of +0.2V has been reached on the anodic scan. Table 4.15 shows this data.

Table 4.15 : Table showing information regarding potential responses and normalised charge (Q*) values for ion insertion into a WO₃ film using various activities of LiClO₄/propylene carbonate. Charge values obtained from integration of current responses. Normalisation required due to two different thickness of WO₃ films used. Thickness of WO₃ film cycled in 0.1M LiClO₄/propylene carbonate and 0.7M LiClO₄/propylene carbonate : 2700Å. Thickness of WO₃ film cycled in 0.5M LiClO₄/propylene carbonate : 2400Å.

	Potential at which Q* is recorded / V			Q* (Q/Γ) / C cm ⁻³		
	[LiClO ₄] 0.1M	0.5M	0.7M	0.1M	0.5M	0.7M
Cycle number						
1	-0.837	-0.928	-0.901	-680.4	-959.5	-814.9
2	-0.845	-0.930	-0.906	-718.5	-940.1	-796.4
3	-0.847	-0.930	-0.906	-730.4	-933.6	-789.1
4	-0.850	-0.930	-0.908	-737.8	-928.2	-784.5
5	-0.825	-0.933	-0.908	-744.1	-923.2	-778.5
average	-0.846 ± 0.005	-0.930 ± 0.002	-0.906 ± 0.002	-722.2 ± 22.6	-936.9 ± 12.6	-792.5 ± 12.7

4.5.3 Normalised mass responses

The information obtained from the normalised mass changes versus potential data can give an insight into whether the concentration (or activity) of the salt used will play a major part in the colouration of WO_3 . At very low salt concentrations, very little salt is expected to be entering the film^{[15][17]} and hence, the EQCM mass changes recorded under these permselective conditions are solely for ion and solvent transfer

$$\Delta M_{perm} = \Delta M_{solv} + \Delta M_{ion} \quad [4.8]$$

At higher salt concentrations, EQCM mass changes will include salt transfer (ΔM_{salt}), as the salt can enter the film and the conditions have become nonpermselective. The equation for ΔM will therefore become

$$\Delta M_{nonperm} = \Delta M_{solv} + \Delta M_{salt} + \Delta M_{ion} \quad [4.9]$$

ΔM_{salt} can be calculated, as it is approximately the only component which varies with respect to concentration and is considered to be a diagnostic tool. ΔM_{salt} is the difference between $\Delta M_{nonperm}$ (Equation [4.9]) and ΔM_{perm} (Equation [4.8]).

For all three concentrations, the normalised mass changes versus potential responses follows the shape seen in Figure 4.14. The mass begins to increase at approximately -0.200V on the reduction of the WO_3 film, and does not reach a maximum until after the scan has been reversed. For all three different activities, the maximum normalised mass change is recorded after oxidation has begun. It must be noticed that even after normalisation of the films used, there appears to be a greater mass change when the WO_3 film is cycled in 0.5M LiClO_4 /propylene carbonate. This effect is not due to film thickness as that problem has been overcome with normalisation. It appears to be an effect seen at 0.5M LiClO_4 /propylene carbonate in more than one experiment.

L

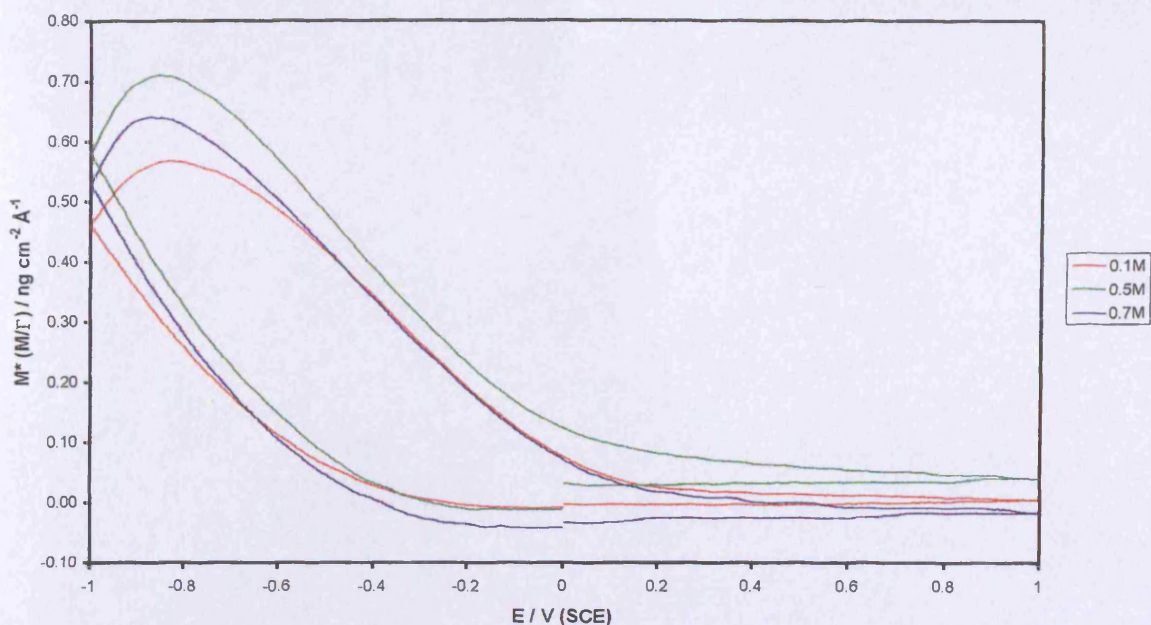


Figure 4.14 : Normalised mass changes versus potential response for a voltammetric experiment to show the effect of using different activities to study ion insertion into WO_3 films. Electrolytes : 0.1M LiClO_4 /propylene carbonate, 0.5M LiClO_4 /propylene carbonate and 0.7M LiClO_4 /propylene carbonate (marked on legend). Total number of cycles recorded : 5 (1st cycle from each experiment shown for ease of comparison with other experiments). Scan rate 10 mV s^{-1} . Thickness of WO_3 film cycled in 0.1M LiClO_4 /propylene carbonate and 0.7M LiClO_4 /propylene carbonate : 2700 \AA ($\Gamma \cong 640 \text{ nmoles cm}^{-2}$). Thickness of WO_3 film cycled in 0.5M LiClO_4 /propylene carbonate : 2400 \AA ($\Gamma \cong 569 \text{ nmoles cm}^{-2}$).

As for the normalised charge data, it is possible to tabulate the potential at which the normalised maximum mass was recorded, and also the normalised maximum mass values recorded. Table 4.16 shows these values.

Table 4.16 : Table showing information regarding potential responses and normalised mass changes (M^*) values for ion insertion into a WO_3 film using various activities of $LiClO_4$ /propylene carbonate. Mass values obtained data seen in Figure 4.14. Normalisation required due to two different thickness of WO_3 films used. Thickness of WO_3 film cycled in 0.1M $LiClO_4$ /propylene carbonate and 0.7M $LiClO_4$ /propylene carbonate : 2700Å. Thickness of WO_3 film cycled in 0.5M $LiClO_4$ /propylene carbonate : 2400Å.

	Potential at which M^* is recorded / V			M^* ($\Delta M/T$) / $g\ cm^{-3}$		
	0.1M	0.5M	0.7M	0.1M	0.5M	0.7M
[$LiClO_4$]						
Cycle number						
1	-0.825	-0.876	-0.896	0.057	0.073	0.068
2	-0.818	-0.876	-0.903	0.058	0.071	0.068
3	-0.830	-0.876	-0.901	0.057	0.071	0.068
4	-0.830	-0.872	-0.903	0.057	0.070	0.068
5	-0.837	-0.881	-0.906	0.057	0.070	0.067
average	-0.828 ± 0.006	-0.876 ± 0.003	-0.902 ± 0.003	0.057 ± 0.0004	0.071 ± 0.001	0.068 ± 0.001

It is possible, as when comparing both effect of changing the cation and anion, to calculate the x values for the different concentrations of $LiClO_4$ used. Table 4.17 shows the x values for both reduction and oxidation of the WO_3 films studied using 0.1M $LiClO_4$ /propylene carbonate, 0.5M $LiClO_4$ /propylene carbonate and 0.7M $LiClO_4$ /propylene carbonate.

Table 4.17 : Table showing calculated x values for insertion of ions into a WO_3 film using various activities of $LiClO_4$ /propylene carbonate. Values obtained from mass changes versus charge responses cycled in the chosen electrolyte at $10\ mV\ s^{-1}$.

Cycle number	x values					
	0.1M $LiClO_4$ /propylene carbonate		0.5M $LiClO_4$ /propylene carbonate		0.7M $LiClO_4$ /propylene carbonate	
	reduction	oxidation	reduction	oxidation	reduction	oxidation
1	0.297	0.278	0.419	0.407	0.357	0.338
2	0.294	0.288	0.411	0.404	0.348	0.341
3	0.293	0.289	0.406	0.399	0.345	0.339
4	0.292	0.289	0.406	0.399	0.343	0.337
5	0.292	0.289	0.404	0.398	0.340	0.335
average	0.294 ± 0.002	0.289 ± 0.004	0.409 ± 0.005	0.401 ± 0.003	0.347 ± 0.006	0.338 ± 0.002

The x values for 0.1M $LiClO_4$ /propylene carbonate, 0.5M $LiClO_4$ /propylene carbonate and 0.7M $LiClO_4$ /propylene carbonate all show that the amount of Li^+ measured entering the WO_3 film upon reduction, also leaves as the film is oxidised. Again, the

C

experiment carried out in 0.5M LiClO₄/propylene carbonate gives a greater number of Li⁺'s entering and leaving the system compared to the other two concentrations studied.

The effect of x values and scan rate has been studied. Figure 4.15 shows the plot of average x values versus the inverse square root of the scan rate for both reduction and oxidation of a WO₃ film using the three different electrolyte concentrations studied in this section.

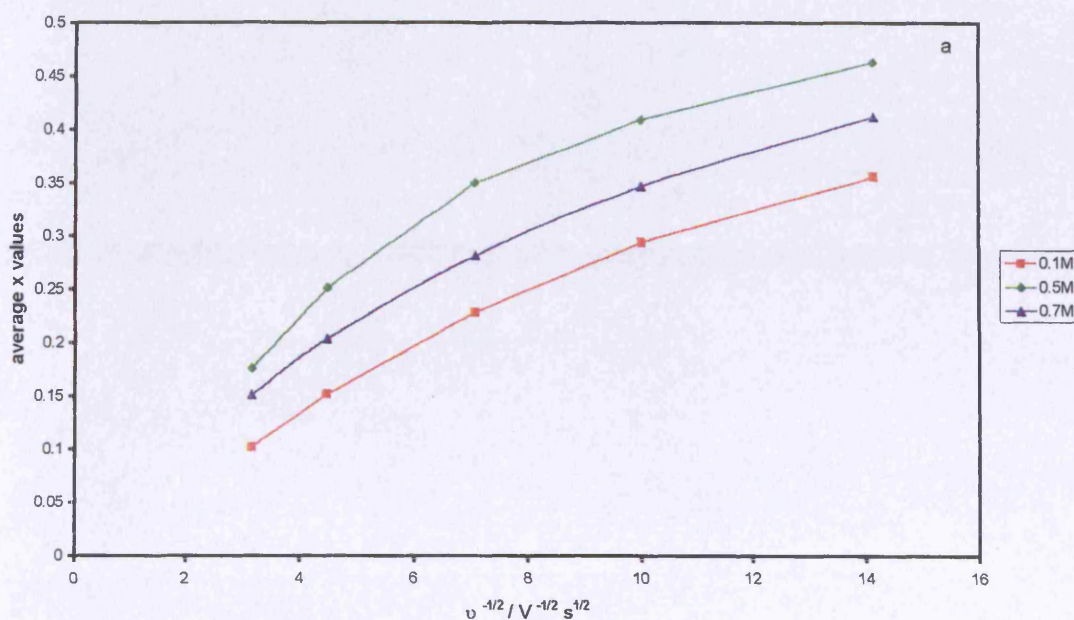
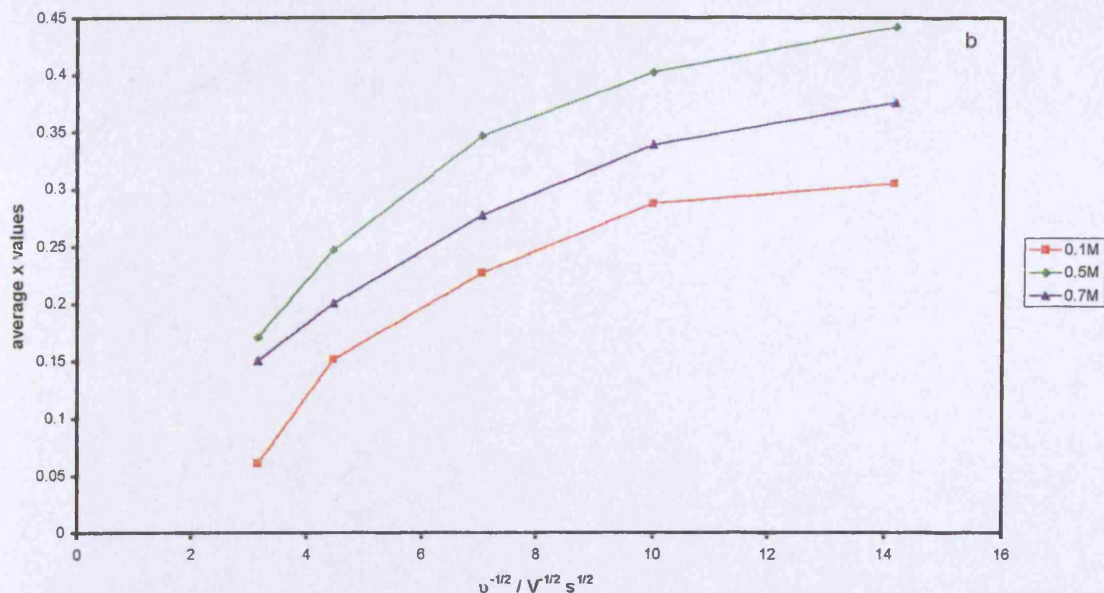


Figure 4.15 : Plot showing relationship between average x values and the inverse square root of the scan rate chosen when using different electrolyte concentration to study ion insertion into a WO₃ film for reduction (4.15a) and oxidation (4.15b) of the film. Electrolytes : 0.1M LiClO₄/propylene carbonate, 0.5M LiClO₄/propylene carbonate and 0.7M LiClO₄/propylene carbonate (marked on legend). Thickness of WO₃ film cycled in 0.1M LiClO₄/propylene carbonate and 0.7M LiClO₄/propylene carbonate : 2700Å ($\Gamma \cong 640\text{nmol cm}^{-2}$). Thickness of WO₃ film cycled in 0.5M LiClO₄/propylene carbonate : 2400Å ($\Gamma \cong 569\text{nmol cm}^{-2}$).

C



The plot showing x values for the reduction of the WO_3 film (4.15a) show that the experiment is not under full thermodynamic control, as the average x values plotted do not reach a constant value. For oxidation of the tungsten bronze, complete conversion of Li_xWO_3 back to $Li^+ + WO_3$ at the slowest scan rate measured (5 mV s^{-1}) is seen. At 100 mV s^{-1} , the experiment appears to be under purely kinetic control. For each experiment carried out at the different scan rates measured the charge value was set at zero at the beginning of each experiment. Therefore, all x values summarised in Table 4.17 and in Figure 4.15 are all taken from zero mC cm^{-2} .

4.5.3.1 Normalised mass changes versus charge responses for different electrolyte activities of $LiClO_4$

The response showing the mass changes versus charge for the three different activities studied is shown in Figure 4.16. As for the other set of experiments which required normalisation (0.1M $LiClO_4$ /propylene carbonate and 0.1M $LiCF_3SO_3$ /propylene

C

carbonate), the responses shown below have been normalised for ease of comparison. It can be seen that there are two distinct measurable slopes (one for reduction, the other for oxidation) for all three concentrations studied. It can be noted that there is hysteresis seen for all three LiClO_4 concentrations studied, which is an indication of a species other than Li^+ entering the WO_3 film.

Work carried out by Huang *et al*^[31] finds that in a mixture of LiCF_3SO_3 -propylene carbonate-diglyme, at highly concentrated solutions, there is evidence for the presence of triple ions and ion pairs in the solution. Upon decreasing the concentration, there are “free” ions which are seen only at low salt concentrations. Therefore, at the three concentrations (activities) studied here, there may be both ion pairs (which are neutral) and triple ions (charged) entering and leaving the WO_3 film alongside Li^+ . This may why the plot shown in Figure 4.16 and the results in Table 4.18 do not give “idealised” $\Delta M_T/F/Q_T$ values of 7 g mol^{-1} .

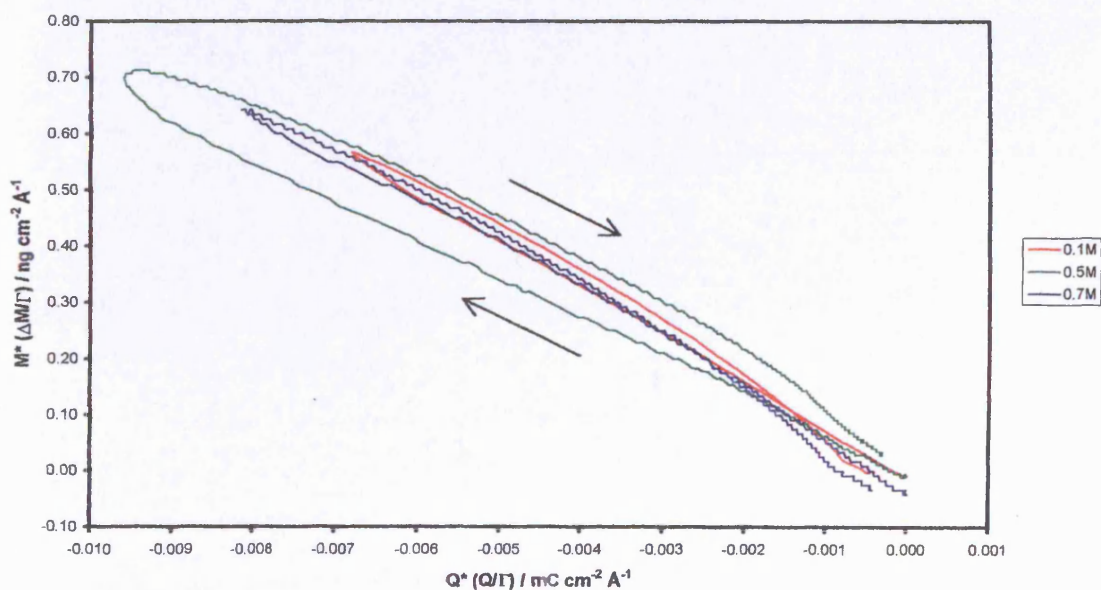


Figure 4.16 : Normalised mass changes versus charge response for voltammetric experiments to show the effect of using different electrolyte activities to study ion insertion into WO_3 films. Electrolytes : 0.1M LiClO_4 /propylene carbonate, 0.5M LiClO_4 /propylene carbonate and 0.7M LiClO_4 /propylene carbonate (marked on legend). Total number of cycles recorded : 5 (1st cycle from each experiment shown for ease of comparison). Scan rate 10 mV s^{-1} . Thickness of WO_3 film cycled in 0.1M LiClO_4 /propylene carbonate and

0.7M LiClO₄/propylene carbonate : 2700Å ($\Gamma \cong 640\text{nmoles cm}^{-2}$). Thickness of WO₃ film cycled in 0.5M LiClO₄/propylene carbonate : 2400Å ($\Gamma \cong 569\text{nmoles cm}^{-2}$).

The “end-to-end” $\Delta M_{TF}/Q_T$ values can still be calculated even if the mass and charge responses have been normalised and are shown in Table 4.18. With the exception of the oxidation of WO₃ in 0.5M LiClO₄/propylene carbonate, all the $\Delta M_{TF}/Q_T$ values are greater than 7 g mol⁻¹. This implies that there is a second, neutral, species accompanying Li⁺ into the WO₃ film. The smaller values seen for 0.5M LiClO₄/propylene carbonate may be due to the thinner film used in this experiment. However, as the values calculated are a ratio of the mass changes and charge calculated, then thickness of film should not be a factor here.

Table 4.18 : Table showing calculated “end to end” $\Delta M_{TF}/Q_T$ values for reduction and oxidation of WO₃ film using various activities of LiClO₄/propylene carbonate. Five scans recorded at a scan rate 10 mV s⁻¹. Values obtained from mass changes versus charge responses cycled in the chosen electrolyte at 10 mV s⁻¹.

Cycle number	$\Delta M_{TF}/Q_T / \text{g mol}^{-1}$					
	0.1M LiClO ₄		0.5M LiClO ₄		0.7M LiClO ₄	
	reduction	oxidation	reduction	oxidation	reduction	oxidation
1	-8.2	-8.7	-7.1	-6.9	-8.1	-8.4
2	-8.3	-8.6	-7.2	-7.0	-8.2	-8.3
3	-8.3	-8.4	-7.3	-7.1	-8.2	-8.3
4	-8.4	-8.4	-7.2	-6.9	-8.3	-8.4
5	-8.4	-8.5	-7.2	-6.9	-8.3	-8.4
average	-8.3 ± 0.1	-8.5 ± 0.1	-7.2 ± 0.1	-7.0 ± 0.1	-8.2 ± 0.1	-8.4 ± 0.1

4.5.4 Explanation of non ideal $\Delta M_{TF}/Q_T$ values

As for all the previous experiments, Φ can be used to separate out the overall mass changes recorded by the EQCM. Table 4.19 shows the calculated “end to end” $\Delta \Phi_{TF}/Q_T$ values for the three varying LiClO₄ concentrations. It can be seen that the “end to end” $\Delta \Phi_{TF}/Q_T$ values for 0.1M and 0.7M LiClO₄/propylene carbonate lie well within each others experimental error. This shows that there is very little difference between either 0.1M LiClO₄/propylene carbonate or 0.7M LiClO₄/propylene carbonate and it appears that there

is <1% salt/Li⁺ entering the WO₃ film at 0.7M LiClO₄/propylene carbonate. Therefore, it appears that salt does not play a major part in cation insertion into WO₃, although there may be ion pairs which enter the WO₃ film as neutral species.

Table 4.19 : Table showing calculated “end to end” $\Delta\Phi_{TF}/Q_T$ values for reduction and oxidation of WO₃ film using various activities of LiClO₄/propylene carbonate. $\Delta\Phi_{TF}/Q_T$ values calculated for $m_{ion} = 7 \text{ g mol}^{-1}$ and $z_{ion} = +1$ using equation [4.5]. Values obtained from mass changes versus charge responses cycled in the chosen electrolyte at 10 mV s^{-1} .

Cycle number	$\Delta\Phi_{TF}/Q_T / \text{g mol}^{-1}$					
	0.1M LiClO ₄		0.5M LiClO ₄		0.7M LiClO ₄	
	reduction	oxidation	reduction	oxidation	reduction	oxidation
1	-1.2	-1.7	-2.1	+0.1	-1.1	-1.4
2	-1.3	-1.6	-2.2	0.0	-1.2	-1.3
3	-1.3	-1.4	-2.3	-0.1	-1.2	-1.3
4	-1.4	-1.4	-2.2	+0.1	-1.3	-1.4
5	-1.4	-1.5	-2.2	+0.1	-1.3	-1.4
average	-1.3 ± 0.1	-1.5 ± 0.1	-2.2 ± 0.1	0.0 ± 0.1	-1.2 ± 0.1	-1.4 ± 0.1

4.5.5 Influence of increasing concentration of LiClO₄

As mentioned in Section 4.5.3, the effect of increasing salt concentration can be investigated to determine whether the experiment has moved from permselective to nonpermselective conditions by using Equations [4.8] and [4.9]. In these experiments, the salt concentration was increased from 0.1M LiClO₄/propylene carbonate to 0.7M LiClO₄/propylene carbonate. Although both WO₃ films used for these two experiments were of the same thickness (2700Å), it appears initially that there is a significant difference in the mass changes recorded, which would suggest that a small amount of salt does enter into the WO₃ film. However, it appears that there is a 14% difference in both the charge values calculated and the recorded mass changes for both films. Therefore, it appears that there is no salt entering during reduction and oxidation of the WO₃ film.

4.6 SUMMARY

Reduction and oxidation of WO_3 films has been examined using three different variables: cation, anion and concentration (or activity) of the electrolyte. In the first comparison, the electrolytes used to study the effect of changing the cation were 0.1M LiClO_4 /propylene carbonate and 0.1M NaClO_4 /propylene carbonate. It will be seen in Chapter 5 that at the slowest scan rate studied (5 mV s^{-1}), there is incomplete charge recovery for WO_3 films cycled in 0.1M LiClO_4 /propylene carbonate. The experiments studied here were carried out at 10 mV s^{-1} , after the initial slower scan. By studying the cyclic voltammogram at 10 mV s^{-1} for ion insertion into WO_3 using these two electrolytes, it appears that Li^+ insertion/expulsion is a successful, reproducible experiment, with complete charge recovery seen. For Na^+ insertion/expulsion, however, there is an indication that complete charge recovery does not occur upon oxidation of the WO_3 film. Also, the fact that the mass responses do not return to zero mass either, indicates that there is a gradual accumulation of Na^+ in the WO_3 film at the slow scan rate studied here (10 mV s^{-1}).

The $\Delta M_{\text{T}}/Q_{\text{T}}$ values calculated for cation insertion show that for both experiments, there is a second, neutral species entering the WO_3 film alongside the cation. This neutral species could be either the solvent (propylene carbonate) or ion pairs as these have been seen by other workers in LiCF_3SO_3 ^[30]. It has been suggested^[31] that propylene carbonate may preferentially solvate Li^+ and that some of the propylene carbonate may enter cation-intercalating materials alongside Li^+ . If the assumption is made that only propylene carbonate enters the WO_3 film alongside the cations, then calculations show that there is 1 propylene carbonate molecule entering the WO_3 film for every 100 Li^+ 's. For the insertion of Na^+ , there appear to be 0.6 molecules of propylene carbonate entering the WO_3 film for every 1 Na^+ .

The three slopes (“a”, “b” and “c”) of the mass changes versus charge plots seen in Figure 4.7b are seen for the reduction and oxidation of WO_3 in 0.1M NaClO_4 /propylene carbonate but not in 0.1M LiClO_4 /propylene carbonate. The small amount of hysteresis seen for Na^+ insertion indicates that there is a neutral species which enters and leaves the film at the same time as the cation, ie, the kinetics are almost equal. The third slope (labelled “c” in Figures 4.7b and 4.8b) may be due to neutral species such as solvent and/or ion pairs entering the WO_3 film after Na^+ leaves on re-oxidation. In the case of Li^+ insertion and expulsion, more hysteresis is seen, which indicates that the neutral species is “lagging” behind the cation and the kinetics are dominated by the cation.

Studies have been carried out^[25] where there is evidence for contact ion pairs being formed in a solution of LiClO_4 /propylene carbonate. If these contact ion pairs are formed, then this may be why the $\Delta M_{\text{T}}F/Q_{\text{T}}$ values seen are greater than expected (ie greater than 7 g mol^{-1}) as not only Li^+ may be entering the WO_3 film, but also LiClO_4 . This may also be the case for studied in NaClO_4 , as the values for the ion pair association constant for NaClO_4 is very close to LiClO_4 .

FTIR studies of NaCF_3SO_3 and LiCF_3SO_3 suggests that there may be more “free” ions present in NaCF_3SO_3 than in the corresponding Li solution^[26]. This may indicate why the $\Delta M_{\text{T}}F/Q_{\text{T}}$ and $\Delta \Phi_{\text{T}}F/Q_{\text{T}}$ values for Na^+ insertion are so large. If there are more Na^+ 's than Li^+ 's present in the electrolyte then this would lead to more “free” Na^+ being inserted and hence a larger $\Delta M_{\text{T}}F/Q_{\text{T}}$ value may be seen.

It is also possible to calculate the x values for both Li^+ and Na^+ insertion and expulsion. These values establish the colour of the tungsten bronze when viewed optically^[7]. For Li^+ insertion, there are ≈ 0.3 Li^+ 's being inserted (and expelled) for every WO_3 molecule. This leads to a blue colouration of the tungsten bronze when optical measurements are studied. x values for Na^+ insertion/expulsion are much smaller ($x =$

0.023), which indicates that the colour contrast of a reduced WO_3 film using 0.1M NaClO_4 /propylene carbonate is less intense as a similar WO_3 film cycled using LiClO_4 /propylene carbonate electrolyte. The large amount of neutral species which are seen to be entering the WO_3 film alongside Na^+ may account for the smaller x values seen.

The next variable studied was the effect of changing the anion. 0.1M LiCF_3SO_3 /propylene carbonate and 0.1M LiClO_4 /propylene carbonate were the electrolytes studied (therefore, ClO_4^- and CF_3SO_3^- were the anions chosen for these set of experiments). However, the size of both anions is very similar and so any difference between the two electrolytes will not be easily seen. The two experiments were carried out on WO_3 films of different thickness and so the experimental values had to be normalised. From the normalised current and mass change responses studied, it appears that the choice of anion indicates that there are no obvious differences between the two electrolytes studied. The $\Delta M_{\text{T}}F/Q_{\text{T}}$ values also show that there appears to be movement of a neutral species both in and out of the WO_3 film during ion insertion. For LiCF_3SO_3 , it has been seen by other workers that $[\text{Li}_2\text{CF}_3\text{SO}_3]^+$ is present in solution^[30], which may also be inserted into the WO_3 film alongside Li^+ , leading to larger $\Delta M_{\text{T}}F/Q_{\text{T}}$ values than expected. It is possible to calculate the expected mass changes if there was any anion involved in ion insertion by using equation [4.5]. Values for m_{ion} and z_{ion} were substituted into Equation [4.5] for both cations (Li^+) and anions (ClO_4^- and CF_3SO_3^-). For the $\Delta\Phi_{\text{T}}F/Q_{\text{T}}$ values calculated for Li^+ , it appears that neutral species are inserted alongside ions into the WO_3 film, but the $\Delta\Phi_{\text{T}}F/Q_{\text{T}}$ values obtained for the different anions are very close to the mass of the salt which indicates that there may not be pure anion insertion into the WO_3 film. However, the choice of the two anions here, make it difficult to distinguish clearly between the two electrolytes.

The x values calculated for both electrolytes show that for 0.1M LiClO_4 /propylene carbonate the values indicate that a blue tungsten bronze would be seen optically. For 0.1M

LiCF₃SO₃, the values are slightly lower, which indicates that the optical change would not be so intense. Since normalisation has been carried out for both films, then any effects which are due to film thickness have been eliminated. Therefore the differences seen in the two electrolytes may be due to slightly different solvent activity between the two electrolytes

The final variable was changing the concentration of LiClO₄/propylene carbonate. By increasing the concentration of the electrolytes, then the activity of the solution is also increased. 0.1M, 0.5M and 0.7M LiClO₄/propylene carbonate were the concentrations chosen to be studied. In these experiments, as for the different anions studied, the experimental values had to be normalised to eliminate any effects due to film thickness.

All three activities showed very little difference in the overall shape of the current and mass changes responses but the normalised responses obtained for experiments in 0.5M LiClO₄/propylene carbonate showed larger values than those obtained for experiments carried out in 0.7M LiClO₄/propylene carbonate. This effect was seen on other experiments carried out in 0.5M LiClO₄/propylene carbonate with WO₃ films of the same thickness (2400Å).

The $\Delta M_T F / Q_T$ values calculated for the differing activities of LiClO₄/propylene carbonate show that there is a small amount of neutral species entering and leaving the WO₃ film alongside the cation. It has been seen by other workers that the presence of ion pairs and triple ions are seen at high concentrations. Upon decreasing the concentration, there are also “free” ions seen^[31]. Therefore, at the three concentrations (activities) studied here, there may be both ion pairs (which are neutral) and triple ions (charged) entering and leaving the WO₃ film alongside Li⁺. If the two experiments using 0.1M LiClO₄/propylene carbonate and 0.7M LiClO₄/propylene carbonate are studied, it can be seen that their $\Delta M_T F / Q_T$ values are almost identical, which indicates that salt does not insert into the WO₃

film even at high concentrations. The normalised charge and mass values for these two concentrations both show a difference of 14% which accounts for the difference in maximum mass changes recorded.

The x values for the three different activities all show that for the faster scan rates (100 mV s^{-1}), the reaction is under kinetic control. At the slower scan rates (5 mV s^{-1}), it appears that reduction and oxidation of the WO_3 film occurs with the maximum x value for each concentration nearly being achieved.

Overall, it appears that lithium is the better of the two cations studied for colouration, although there may be ion pairs, or even triple ions also entering the WO_3 film as these are present in solution. Sodium, although there may be more “free” ions, does not give good x values, which are required for the intense colour changes needed for ECDs. All electrolytes show movement of neutral species, which may be either solvent (propylene carbonate) or the formation of ion pairs. The choice of anion used here does show any significant differences, although this may be due to the similar size of the two anions. The choice of concentration (or activity) in the range $0.1\text{M LiClO}_4/\text{propylene carbonate}$ to $0.7\text{M LiClO}_4/\text{propylene carbonate}$ does not appear to alter the insertion of Li^+ into the WO_3 film, although, again, the question of ion pairs must be considered when looking at the neutral species movement..

REFERENCES

1. B. Reichman and A. J. Bard, *Journal of the Electrochemical Society*, 126, 4, (1979), 583.
2. M. S. Burdis and J. R. Siddle, *Thin Solid Films*, 237, (1994), 320.
3. R. A. Batchelor, *Pilkington Group Research Report*, (1993),
4. R. A. Batchelor, M. S. Burdis, and J. R. Siddle, *Journal of the Electrochemical Society*, 143, 3, (1996), 1050.
5. C. G. Granqvist, Handbook of Inorganic Electrochromic Materials, Elsevier Science B.V., Amsterdam, 1995.
6. C. G. Granqvist, *Physics of Thin Films*, 17, (1993), 301.
7. P. M. S. Monk, R. J. Mortimer, and D. R. Rosseinsky, Electrochromism. Fundamentals and Applications, VCH Publishers, Weinheim, 1995.
8. J. P. Randin and R. Viennet, *Journal of the Electrochemical Society*, 129, 10, (1982), 2349.
9. O. Bohnke and M. Rezrazi, *Materials Science and Engineering B-Solid State Materials For Advanced Technology*, 13, 4, (1992), 323.
10. O. Bohnke and B. Vuillemin, *Materials Science and Engineering B-Solid State Materials For Advanced Technology*, 13, 3, (1992), 243.
11. T. Nishimura, K. Taira, and S. Kurita, *Applied Physics Letters*, 36, 7, (1980), 585.
12. S. K. Mohapatra, G. D. Boyd, F. G. Storz, and S. Wagner, *Journal of the Electrochemical Society*, 126, 5, (1979), 805.
13. J. P. Randin, *Journal of Electronic Materials*, 7, 1, (1978), 47.
14. S. Bruckenstein and M. P. Shay, *Electrochimica Acta*, 30, 10, (1985), 1295.

15. S. Bruckenstein and A. R. Hillman, in Surface Imaging and Visualisation (A. T. Hubbard, ed.), CRC Press, 1995, Boca Raton London, Chapter 9.
16. R. A. Batchelor and M. J. Burdis, *Pilkington group research, private communication*, 1995-1997.
17. A. R. Hillman, M. J. Swann, and S. Bruckenstein, *Journal of Physical Chemistry*, 95, (1991), 3271.
18. A. R. Hillman, N. A. Hughes, and S. Bruckenstein, *Journal of the Electrochemical Society*, 139, 1, (1992), 74.
19. A. T. Howe, S. H. Sheffield, P. E. Childs, and M. G. Shilton, *Thin Solid Films*, 67, (1980), 365.
20. R. D. Giglia and G. Haacke, *Proceedings of the SID*, 23, 1, (1982), 41.
21. K.-C. Ho, T. G. Rukavina, and C. B. Greenberg, *Journal of the Electrochemical Society*, 141, 8, (1994), 2061.
22. E. L. Tassi and M. A. De Paoli, *Electrochimica Acta*, 39, 16, (1994), 2481.
23. H. Inaba, M. Iwaku, T. Tatsuma, and N. Oyama, *Journal of Electroanalytical Chemistry*, 387, 1-2, (1995), 71.
24. D. Dini, F. Decker, and E. Masetti, *Journal of Applied Electrochemistry*, 26, 6, (1996), 647.
25. D'Aprano, M. Salomon, M. Iammarino, *Journal of Electroanalytical Chemistry*, 403, (1996), 245.
26. D.R.. MacFarlane, P. Meakin, A. Bishop, D. McNaughton, J.M. Rosalie, M. Forsyth, *Electrochimica Acta*, 40, (1995), 2333.
27. M. Salomon, E. Plichta, *Electrochimica Acta*, 28, (1983), 1681.
28. O. Bohnke, B. Vuillemin, C. Gabrielli, M. Keddam, H. Perrot, H. Takenouti, and R. Torresi, *Electrochimica Acta*, 40, 17, (1995), 2755.

29. R. Schollhorn, *Angew. Chem. Int. Ed.*, 19, (1980), 983.
30. S.R. Starkey, R. Frech, *Electrochimica Acta*, 42, (1997), 471.
31. W. Huang, R. Frech, P. Johansson, J. Lindgren, *Electrochimica Acta*, 40, (1995), 2147.

CHAPTER 5 : THE EFFECT OF ELECTRODE HISTORY

5.1 INTRODUCTION

This chapter will look at the deviation from the basic electrochemical characteristics of WO_3 , as a consequence of electrode history. In chapter 4, results were studied for WO_3 films which had been cycled initially at a slower scan rate than 10 mV s^{-1} . The effects seen at this slower scan rate are now investigated. The first cycle of an unused WO_3 film cycled at 5 mV s^{-1} is investigated, where the “break-in” effect is seen. This effect is studied and described in electrochemical, quartz crystal microbalance and spectroscopic terms. Also, the effect of long term cycling is investigated using the electrochemical quartz crystal microbalance.

5.2 ELECTROCHEMISTRY OF WO_3

5.2.1 Electrochemical features

The cyclic voltammetric response for typical cation insertion into a WO_3 film has been discussed in Chapter 4. Reduction of the WO_3 film leads to a decrease in current as cation insertion is seen. Reduction and hence colouration of the WO_3 film is associated with the increasing negative charge although ion insertion still continues even after scan reversal. Oxidation or bleaching of the tungsten bronze is not seen to occur until approx -0.80V , when deintercalation takes place. At more positive potentials the current is seen to return to 0 indicating bleaching is occurring.

5.2.2 The “break-in” effect

The “break-in” effect is more commonly associated with redox polymers^[1], where it is characterised by the fact that the electrochemical response during the first cycle in an experiment is different to that for the following scans. This can be seen from figure 5.1, where the current response during first scan of an unused WO_3 film cycled at 5 mV s^{-1} is different from the subsequent scans. It appears that there is a significant amount of current passed during the initial reduction of WO_3 which is not recovered on the oxidation of the film. The following scans follow the normal cyclic voltammogram expected from ion intercalation. The appearance of a reduction peak at $\approx -0.6 \text{ V}$ (vs SCE) on the initial cathodic half cycle is not seen on subsequent scans. This “break-in” cycle is seen for new WO_3 films when cycled at 5 mV s^{-1} regardless of electrolyte composition or concentration.

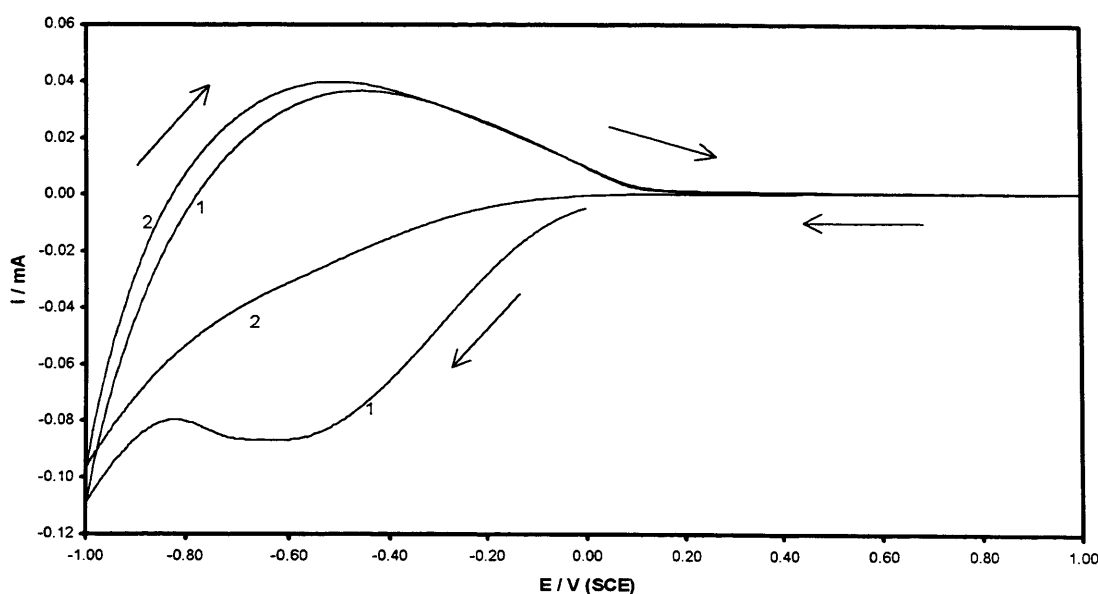


Figure 5.1 : Cyclic voltammograms showing Li^+ insertion into a 2700 \AA thick WO_3 film. Electrolyte : $0.1 \text{ M LiClO}_4/\text{propylene carbonate}$. Total number of cycles recorded : 5 (first two scans marked on plot). Scan rate 5 mV s^{-1} . First two scans shown to indicate the “break-in” effect seen on scan one.

5.2.3 Effect of potential scan rate

It will be shown in the following chapter that the cyclic voltammograms obtained at different scan rates still show the same characteristics of ion insertion/expulsion, but the peak height increases with increasing scan rate. If a faster scan rate, for example 100 mV s^{-1} is chosen as the scan rate for the initial cycle of an unused WO_3 film then there is no indication that the “break-in” effect is occurring. Figure 5.2 shows this effect, when a faster scan rate is chosen as the initial scan rate in the set of experiments. It can be seen that the first scan appears slightly different to the subsequent scans, but there is no significant reduction peak as seen in Figure 5.1.

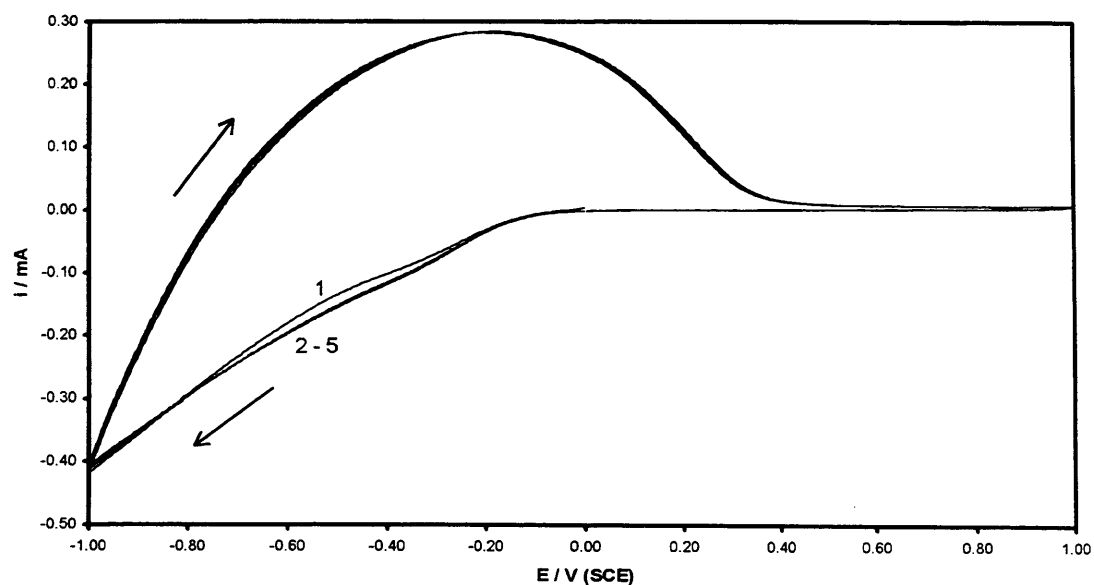


Figure 5.2 : Cyclic voltammograms showing Li^+ insertion into a 2700 \AA thick WO_3 film. Electrolyte : $0.1 \text{ M LiClO}_4/\text{propylene carbonate}$. Total number of cycles recorded : 5 (marked on plot). Scan rate 100 mV s^{-1} . Scans two to five are penwidth reproducible.

5.2.4 Cation insertion into WO₃

Lithium is known to insert quite easily into WO₃ due to its small size, high solubility and it cannot be reduced to lithium metal^[2-4]. Sodium is a larger cation than lithium, but work has been carried out on its insertion into the WO₃ lattice^[5-6] and it appears to be a suitable cation to compare against Li^[7]. Protons have also been studied by various authors^[8-11], but studies have shown that when H₂SO₄ is used as the electrolyte degradation of the WO₃ film occurs^[12].

5.3 ELECTROCHEMICAL QUARTZ CRYSTAL MICROBALANCE STUDIES OF WO₃

5.3.1 Quartz crystal microbalance experiments.

Figure 5.3 shows both the cyclic voltammogram for ion intercalation/extracalation and also the corresponding mass vs potential plot as discussed in Chapter 4. On the first cycle down to -1.0V, very little mass change is seen until approximately -0.2V, when the mass begins to increase. The mass increase continues after reversal of the scan, and as seen in figure 5.1, the current is still negative, therefore reduction of the WO₃ film is still occurring. The mass change is seen to reach a maximum value of approximately 1000 ng cm⁻² at -0.9V, and then a decrease is seen. As the potential is scanned to more positive values and oxidation of the film occurs, the mass decreases until at 0V on the reverse scan, there are very small mass changes seen. As the potential is scanned up to +1.0V, very small mass changes are seen, as complete bleaching of the WO₃ film is occurring. By observing the crystal with the naked eye, the deepest colouration is not seen to occur until scan reversal, and complete bleaching is not seen to occur until more positive potentials such as +0.3V.

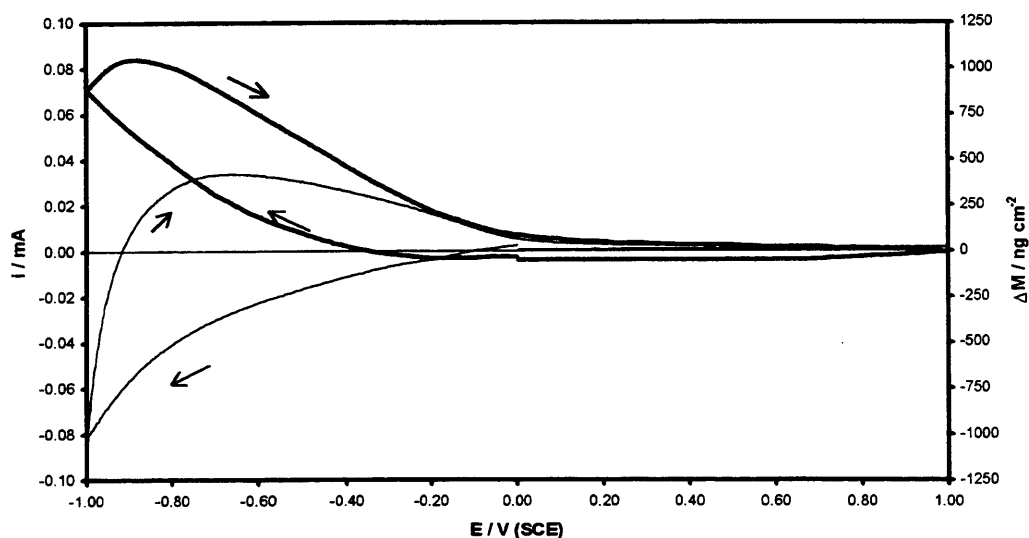


Figure 5.3 : Cyclic voltammogram and corresponding mass changes versus potential response for a voltammetric experiment on a 2700Å thick WO_3 film. Electrolyte : 0.5M LiClO_4 /propylene carbonate. Total number of cycles recorded : 5 (1st cycle (“break-in”) from each experiment only shown for ease of comparison). Scan rate : 5 mV s^{-1} . Cyclic voltammogram marked as normal line, mass changes versus potential plot marked as bold line.

Figure 5.4 shows the mass change versus potential response for a voltammetric experiment showing the “break-in” effect. As can be seen, there is an initial large increase in mass on the first reduction scan, which corresponds to the initial current trace shown in figure 5.1. When comparison is made between the first and second mass vs potential plots, then it should be noted that on completion of the first scan, approximately 3000 ng cm^{-2} of mass is found to be left in the WO_3 film. This non-recoverable mass change is not usually seen when a faster scan rate (for example 100 mV s^{-1}) is chosen for the initial experiment. When Babinec^[13] investigated H^+ insertion into WO_3 films using the EQCM, they noted that on completion of the first cycle, there was a decrease in mass. There has been no other work carried out on the initial cycle for Li^+ insertion using the EQCM.

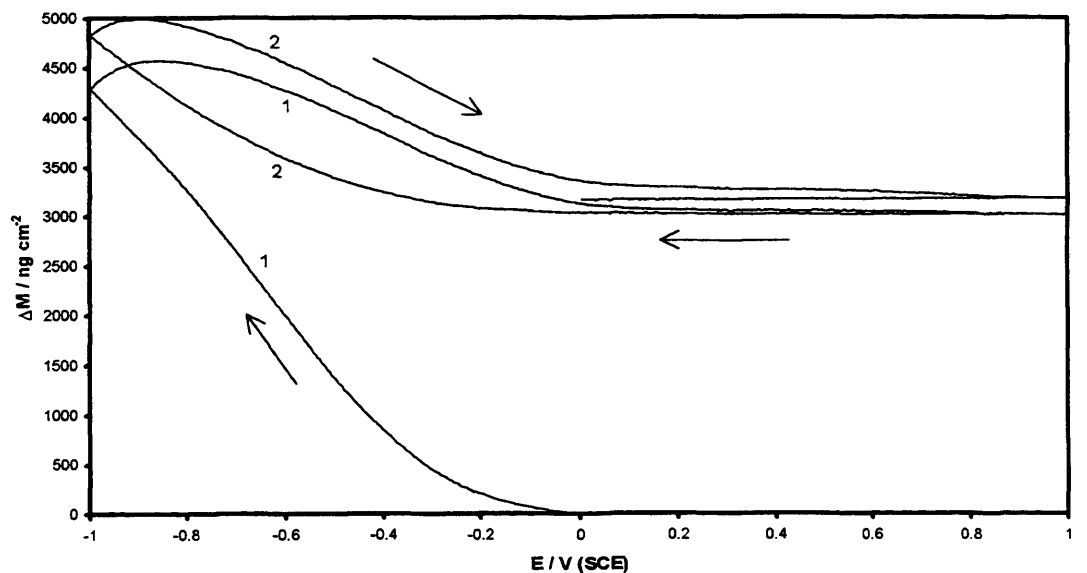


Figure 5.4 : Mass changes versus potential response for a voltammetric experiment on a 2700Å thick WO_3 film. Electrolyte : 0.1M LiClO_4 /propylene carbonate. Total number of cycles recorded : 5 (1st two cycles marked on plot for ease of comparison). Scan rate : 5 mV s^{-1} .

5.3.2 Analysis of electrochemical quartz crystal microbalance data

The EQCM experiment allows correlation between measured mass changes and charge passed. This data can be plotted together as mentioned in chapter 4., to give information about the type of species entering and leaving the WO_3 film. In the case of these experiments, zero charge is defined as being the point at which the film is fully oxidised (bleached). Therefore, a decrease in charge and hence a negative charge value indicates that the film is in its reduced (coloured) state. For the mass data, again, the point at which mass change equals zero is defined as that for a fully oxidised film, and any mass increase seen indicates ion insertion into the reduced WO_3 film. Figure 5.5 shows the mass change versus charge plots for the first two cycles of an experiment, where the “break-in” effect is seen on the corresponding cyclic voltammogram in Figure 5.1.

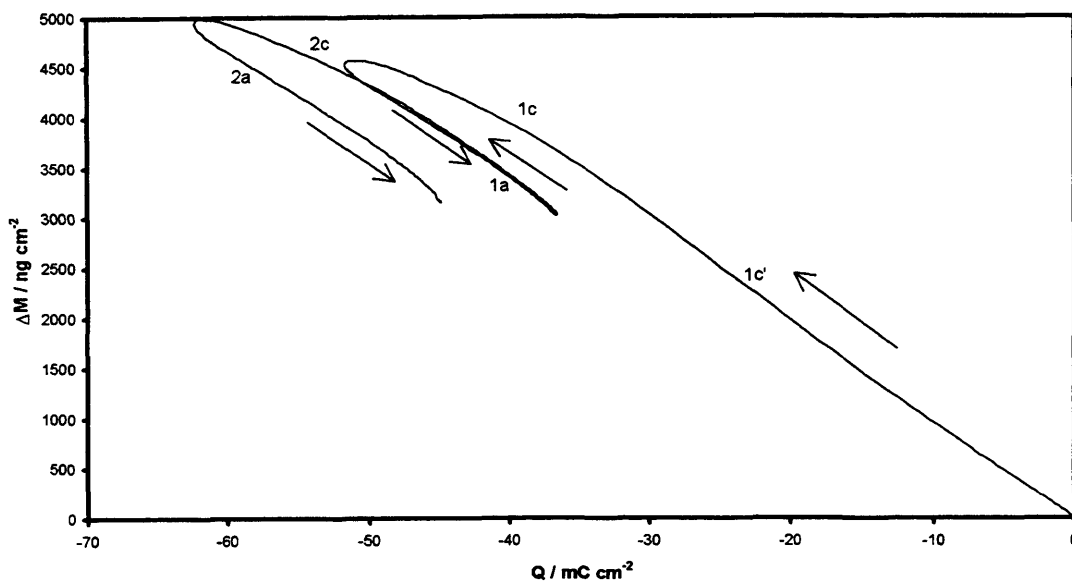


Figure 5.5 : Mass changes versus charge response for voltammetric experiments to show the “break-in” effect when looking at ion insertion into a 2700Å thick WO_3 film. Electrolyte : 0.1M LiClO_4 /propylene carbonate. Total number of cycles recorded : 5 (1st two cycles from experiment shown for ease of comparison). Scan rate 5 mV s^{-1} . c' indicates non reversible mass and charge changes during initial reduction, c indicates reversible behaviour for cathodic half cycle. a represents reversible behaviour for anodic half cycle.

Figure 5.5 shows a large decrease in charge and increase in mass as the film goes from being oxidised (W^{VI}) to the reduced state of W^{V} . The decrease in mass and increase in charge that is seen on reversal of the scan indicates that the WO_3 film is being oxidised, and it can be seen very clearly that for the first scan, neither the charge nor the mass changes return to their initial values for the fully oxidised film. Therefore, after this first “break-in” scan, there is a substantial amount of charge and mass remaining in the film. On the second scan, it appears that nearly all the mass change is recovered at the end of the cycle, but the charge is found to be at a lower value.

It is possible to calculate the “end to end” $\Delta M_{\text{T}}F/Q_{\text{T}}$ ratio to give information about the amount of ion insertion into the film. This initial $\Delta M_{\text{T}}F/Q_{\text{T}}$ ratio can be calculated and is found to be larger than 7 g mol^{-1} , which is expected for Li^+ insertion only. The initial

$\Delta M_{TF}/Q_T$ value for the first cycle is also larger than the “end to end” $\Delta M_{TF}/Q_T$ ratios calculated for the subsequent scans. This is shown in table 5.1.

Table 5.1 : $\Delta M_{TF}/Q_T$ ratios calculated from mass change versus charge responses for voltammetric experiments showing the effect of using different electrolyte concentration to study ion insertion into a WO_3 film. Electrolytes used : various concentrations of $LiClO_4$ /propylene carbonate and $NaClO_4$ /propylene carbonate. Scan rate : 5 mV s^{-1} . $1c'$ refers to $\Delta M_{TF}/Q_T$ value for “break-in” effect, c refers to cathodic half cycle, a to anodic half cycle as seen in Figure 5.5.

Salt	[salt] / M	$\Delta M_{TF}/Q_T / \text{g mol}^{-1}$					
		cation	$1c'$	$1c$	$1a$	2-5c	2-5a
$LiClO_4$	0.1	7	-9.6	-5.3	-9.6	-7.7 ± 0.2	-8.9 ± 0.6
	0.5	7	-8.0	-6.2	-5.4	-8.6 ± 0.6	-7.0 ± 0.4
	0.7	7	-10.2	-3.2	-8.5	-7.9 ± 0.4	-8.4 ± 0.3
$NaClO_4$	0.1	23	-94.4	-94.7	31.0	-90.0 ± 4.3	-46.6 ± 10
	0.5	23	-45.4	-56.2	30.8	-42.2 ± 2.2	-10.0 ± 7.6
	0.7	23	-37.6	-67.4	42.0	-50.0 ± 4.2	-23.5 ± 15

It can be seen that the initial $\Delta M_{TF}/Q_T$ value ($1c'$) is larger than the value for cation insertion into WO_3 . The $\Delta M_{TF}/Q_T$ value for the gradient labelled $1c$ is seen to be smaller than for the following reductions for Li^+ insertion, but is larger than the subsequent values for Na^+ . In the case of the varying concentrations of Li^+ , it should be noted that the $\Delta M_{TF}/Q_T$ ratios do not increase uniformly as the concentration increases. It should be noted that the film deposited on the crystal chosen for the experiment in 0.5M $LiClO_4$ /propylene carbonate is thinner ($2400 \text{ \AA} \pm 100 \text{ \AA}$) than the films deposited for the other $LiClO_4$ /propylene carbonate experiments (2700 \AA). However, this should not make any difference, as the thickness variation is very small ($\approx 12\%$) and although there will be a smaller number of redox sites on the surface of the film, if everything is fully oxidised and reduced for all films, then the ratios should not be affected. In the case of Na^+ insertion, all films are of the same thickness and the above factor does not have to be considered.

Calculations of the $\Delta M_{TF}/Q_T$ ratios show that there is a significant amount of ionic and electronic charge left inserted in the WO_3 film after the first scan at a slow scan rate.

After the initial $\Delta M_{TF}/Q_T$ ratio, then the following $\Delta M_{TF}/Q_T$ ratios are calculated “end-to-end” to give an overall picture of the ion intercalation/deintercalation occurring, as referred to in Chapter 4.

5.3.3 Insertion of neutral species

It can be seen from Table 5.1 that there is significant difference between the $\Delta M_{TF}/Q_T$ values calculated from the EQCM experiments and those expected for pure cation insertion into the WO_3 film. This is an indication that there must be a second species being inserted into the film together with the cation. It is proposed that this second species is a neutral species, such as solvent or ion pairs, discussed in Chapter 4. Although neutral species intercalation has been discounted by other authors^[14-16], we present here good evidence that some neutral species are inserted during film reduction.

Another indication that insertion of a neutral species is occurring can be seen qualitatively by looking at the combined cyclic voltammogram and mass change vs potential plot, shown in figure 5.3. If a comparison is made between the two plots, it can be seen that where the current is equal to zero ($E = -0.916V$), then there is still a mass change occurring when the current is zero. If only charged species were being inserted/expelled from WO_3 films, then electroneutrality requires that there should be no mass change when the current is zero.

5.3.4 Separation of overall mass changes into charged and neutral species.

Using equation [4.5] and the information from figure 5.5, it is possible to plot $\Delta\Phi$ versus charge, and from this plot obtain $\Delta\Phi_{TF}/Q_T$ values. Table 5.2 shows the calculated $\Delta\Phi_{TF}/Q_T$ values for various $LiClO_4$ /propylene carbonate and $NaClO_4$ /propylene carbonate concentrations at a scan rate of 5 mVs^{-1} .

Table 5.2 : $\Delta\Phi_{T}F/Q_{T}$ ratios calculated from Φ changes versus charge responses for voltammetric experiments showing the effect of using different electrolyte concentration to study ion insertion into a WO_3 film. Electrolytes used : various concentrations of $LiClO_4$ /propylene carbonate and $NaClO_4$ /propylene carbonate. Scan rate : 5 mV s^{-1} . $1c'$ refers to $\Delta\Phi_{T}F/Q_{T}$ value for “break-in” effect, c refers to cathodic half cycle, a to anodic half cycle as seen in Figure 5.5.

Salt	[salt] / M	$\Delta\Phi_{T}F/Q_{T}$ / g mol^{-1}					
		cation	$1c'$	$1c$	$1a$	2-5c	2-5a
$LiClO_4$	0.1	7	-2.6	1.7	-2.6	-0.6 ± 0.3	-1.9 ± 0.6
	0.5	7	-1.0	0.8	1.6	-1.2 ± 0.3	0.0 ± 0.4
	0.7	7	-3.8	2.1	-1.5	-0.9 ± 0.4	-1.4 ± 0.3
$NaClO_4$	0.1	23	-71.4	-71.7	54.0	-67.0 ± 4.3	-24 ± 10
	0.5	23	-22.4	-33.2	53.8	-19.2 ± 2.2	13 ± 7.6
	0.7	23	-14.6	-44.4	33.1	-27.0 ± 4.2	-0.5 ± 15.5

It can be seen from the above table that the $\Delta\Phi_{T}F/Q_{T}$ values for Na^+ are much higher than for Li^+ . In this study, the insertion of Li^+ is the cation of most interest as it has been proposed to be the most suitable cation for electrochromic displays. The $\Delta\Phi_{T}F/Q_{T}$ values for Li^+ are quite near to zero which indicates that there is only a small amount of neutral species entering the WO_3 film. When the $\Delta\Phi_{T}F/Q_{T}$ values are studied for Na^+ , it can be seen that these values are more positive, which is an indication that there is a large amount of neutral species entering the WO_3 film alongside Na^+ .

It can be seen that the $\Delta M_{T}F/Q_{T}$ values calculated for ion insertion using both $LiClO_4$ /propylene carbonate and $NaClO_4$ /propylene carbonate are much greater than the $\Delta M_{T}F/Q_{T}$ value for single cation insertion. This therefore shows that there is a second species being inserted and expelled from the WO_3 films studied. Expressed differently, the $\Delta\Phi_{T}F/Q_{T}$ values do not equal zero, indicating of movement of a neutral species which may be propylene carbonate or ion pairs.

Since a slow scan rate is being used when observing the “break-in” effect, then the question of whether the neutrals are left in the film after the first scan must be asked. As has already been seen, a significant amount of cation and charge is left inserted into the

WO₃ film. Since values of $\Delta\Phi_T F/Q_T$ for the following scans are slightly lower than the initial reduction and oxidation values, then there is a slightly smaller amount of neutral species left in the WO₃ film after the first cycle.

Experiments carried out by other workers^[16-18] have shown that the addition of solvents into WO₃ films significantly effects the performance of the electrochromic film response. If there are enough neutrals in the WO₃ film after the first cycle, then this will subsequently effect the colouration efficiency of an electrochromic device when used for display purposes.

5.3.5 Ion insertion into WO₃ films

It has been known for over twenty years^[19] that the amount of cation inserted into WO₃ and the colour of the reduced film are linked. Many authors have used the optical density and charge inserted into the film to calculate the stoichiometric constant for ion inserted into the film (x)^{[14-15][20]}. By using the change of resonant frequency (obtained by using a network analyser to obtain an overall picture of crystal impedance) between an uncoated and coated crystal, it is possible to calculate the amount of cation expected to be inserted into the WO₃ film during the “break-in” effect.

It is possible to use the amount of charge passed on the initial reduction and divide by the Faraday constant to give the number of moles per cm² of electrons (I_e). By using the change in frequency of the uncoated/coated crystal, then the mass of WO₃ can be calculated, since 1Hz \equiv 1.1 ng. This mass value can be used to determine the number of

moles per cm² of WO₃ (Γ_{WO_3}) in the film. When Γ_e is divided by Γ_{WO_3} , then x can be calculated. Relevant data for a range of electrolytes are summarised in Table 5.3.

Table 5.3 : Table giving the x values calculated using data obtained from crystal impedance data (Γ_{WO_3}) and EQCM (Γ_e) data. x values given are for initial (“break-in”) reduction of WO₃ films using different electrolytes. Electrolytes : various concentrations of LiClO₄/propylene carbonate and NaClO₄/propylene carbonate

Salt	[salt] / M	Δf / kHz	mass of WO ₃ / μg	Γ_{WO_3} / mol cm ⁻²	Charge / mC cm ⁻²	Γ_e / mol cm ⁻²	x ($\Gamma_e/\Gamma_{\text{WO}_3}$)
LiClO ₄	0.1	45.322	49.85	768	-33.8	350	0.46
	0.5	42.363	46.60	717	-48.7	505	0.58
	0.7	46.752	51.43	719	-47.5	492	0.62
NaClO ₄	0.1	44.752	49.23	757	-2.86	29.6	0.039
	0.5	47.322	52.05	802	-3.18	33.0	0.041
	0.7	48.322	53.15	819	-3.80	39.4	0.048

The values of x calculated are for the “break-in” experiments, where the charge is the amount that is passed during the initial reduction of the film not all of which is recovered after the first scan. It can be seen that the value of x for Li⁺ insertion into WO₃ films is an order of magnitude greater than for Na⁺ insertion under these identical conditions. Observations with the naked eye during insertion of Na⁺ into WO₃ films show that there is very little colouration seen at all during reduction of the film, compared to the distinctive colour change for Li⁺ insertion.

The question must be addressed about the x values for the subsequent scans, as to whether their calculated x values incorporate the “break-in” effect. It has been shown that charge and mass still remain in the film after the initial scan, and so it would be expected that there would be some reoxidised colouration of the film. A standard colouration table for the insertion of cations into WO₃ films has been long established, and is shown in table 5.4. The regular method for the calculation of x values for ion insertion is to use coulometry. Many cycles are measured before average x values are quoted^[21], therefore if

any charge and mass were left inserted in the film after the initial cycle, then the effect would not be noticed.

If the “break-in” effect was not considered, then the values of x for the following scans in this set of experiments should be lower than calculated.

Table 5.4 : Table showing values of x and their respective colours dependent on amount of x inserted. Values for both Li^+ and Na^+ insertion into WO_3 given.

$x\text{M}^+ + e^- + \text{WO}_3 \rightleftharpoons \text{M}_x\text{WO}_3$ $x =$	“Colour” produced by insertion of x	
	$\text{Li}^{+[22]}$	$\text{Na}^{+[23]}$
0	Pale yellow	Pale yellow
0.1	Grey	
0.2	Blue	Dark grey
0.4	Blue	Royal blue
0.6	Purple	Purple
0.7	Brick red	Brick red
0.8	Golden bronze	Orange
0.9	Golden bronze	Golden yellow
1.0	Golden bronze	

5.4 SPECTROSCOPY OF WO_3 FILMS

5.4.1 Spectroscopic experiments

Spectroscopic measurements for Li^+ and Na^+ insertion into WO_3 films were carried out using a Perkin Elmer Lambda 19 spectrophotometer. Measurements were made in the ultra violet, visible and near infra red regions. It was found that Na^+ insertion into WO_3 gave very little change in absorbance from the fully oxidised film to the fully reduced film ($\approx 11\%$ of absorbance values given for Li^+ insertion). If the x values calculated for the initial insertion of cations into the film are studied (Table 5.4), then it can be seen that the values for Na^+ are $\approx 90\%$ smaller than for Li^+ insertion. These small x values could explain the poor changes in absorbance seen for Na^+ , as the EQCM crystals and the F-doped ITO glass used for spectroscopy are coated at the same time and there should be a reasonable comparison between the two media. Therefore, only the Li^+ insertion will be discussed.

5.4.2 The “break-in” effect

It is possible to monitor the “break-in” effect using spectroscopy to record the differences in absorbance for the initial scan and the following scans. The spectrophotometer is only capable of measuring one fixed wavelength at a time, and so it was only possible to record the “break-in” effect at one wavelength in any given experiment. The film was cycled at 5 mV s^{-1} between the potential limits usually chosen for the voltammetric experiment. Changes in absorbance were measured every second, and, by relating the scan rate and time interval, it was possible to calculate the potential at which absorbance changes occurred. As the “break-in” effect is seen only on the initial scan, then it was only possible to record the effect at one wavelength and then measure the following scans, as in the EQCM experiments. The cyclic voltammogram was also recorded during the initial cycle and the “break-in” effect was also seen, indicating that the effect was not just seen on the quartz crystals used for the EQCM measurements, it is a real effect. Experiments were carried out where the absorbance changes for first wavelength chosen were recorded again after the initial cycle. It was seen that the absorbance changes followed the same pattern as for the subsequent scans. Also, different starting wavelengths were chosen to measure the change in absorbance for the “break-in” effect, thus proving that the effect was seen independent of wavelength.

For ease of comparison, the absorbances chosen have all been “normalised” with respect to the maximum absorbance value at each wavelength. This is shown in figure 5.7, where the wavelength chosen to record the “break-in” effect is 650nm.

U

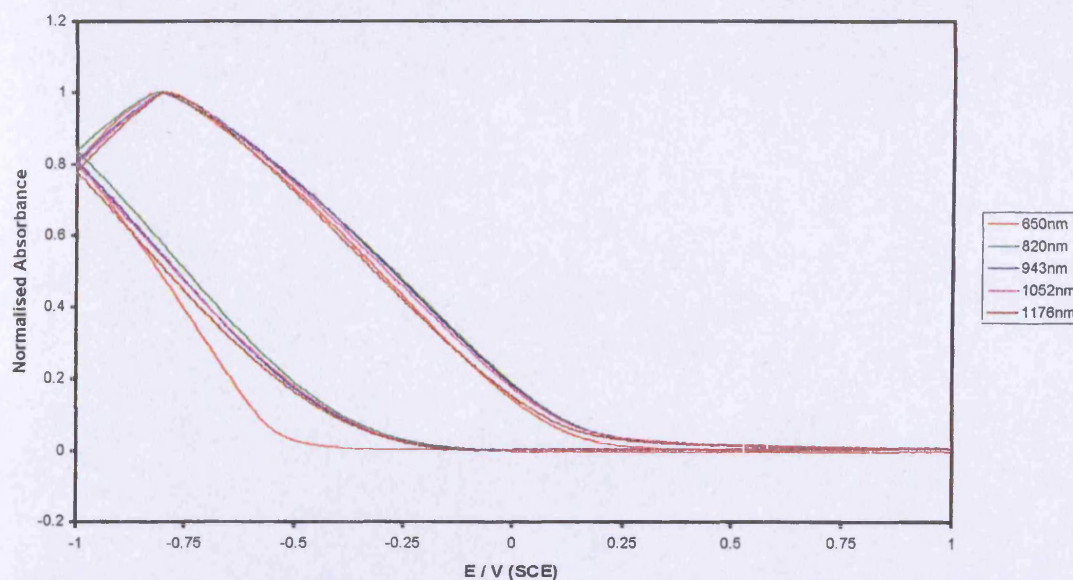


Figure 5.6 : Normalised absorbance versus potential responses for Li^+ insertion into a 2400\AA thick WO_3 film coated onto ITO glass. Electrolyte : $0.5\text{M LiClO}_4/\text{propylene carbonate}$. Total number of wavelengths recorded : 5 (marked on legend). Scan rate : 5 mV s^{-1} . First cycle (“break-in”) measured at 650nm .

It can be seen that the absorbance does not begin to change until -0.50V on initial reduction of the WO_3 film. The subsequent wavelengths measured all show that the absorbance begins to increase at a much earlier potential than for the first cycle. When the cyclic voltammogram of the initial cycle is studied, it can be seen that the “break-in” effect is recorded, as has been seen in the EQCM experiments (figure 5.3). The “break-in” effect has been recorded for all three concentrations of LiClO_4 , and the potentials where maximum absorbance is recorded can be measured. These are summarised in Table 5.5. It should be noted that the potentials where maximum absorbance was recorded were on the anodic half cycle.

Table 5.5 : Table showing potential at which the maximum absorbance is recorded for various concentrations of LiClO₄/propylene carbonate. Maximum absorbance measured at a series of different wavelengths. “break-in” wavelength : 650nm for all three experiments.

Wavelength / nm	Potential of maximum absorbance/ V		
	0.1M LiClO ₄ /propylene carbonate	0.5M LiClO ₄ /propylene carbonate	0.7M LiClO ₄ /propylene carbonate
650	-0.505	-0.815	-0.760
820	-0.725	-0.805	-0.790
943	-0.735	-0.795	-0.795
1052	-0.730	-0.795	-0.790
1176	-0.745	-0.800	-0.790
1428	-0.765	-0.800	-0.795
average	-0.744 ± 0.013	-0.799 ± 0.004	-0.792 ± 0.002

The mean potential indicates that the potential where maximum absorbance is measured is independent of the wavelength chosen. The initial scan at 650nm is not included when calculating this value as it is where the “break-in” effect is seen. Vuillemin and Bohnke^[24] has proposed a step by step insertion mechanism which relates the electrochemical reaction and the optical properties of ion insertion into a WO₃ film. This mechanism is proposed to determine which process governs the current response and colouration of the film. Vuillemin and Bohnke compared the cyclic voltammogram (which will give the rate of electrochemical reaction at the WO₃/electrolyte interface) with the rate of WO₃ colouration (dA/dt) and also the charge density measured with the optical density variation. From these comparisons, it was seen that the electrochemical reaction that occurs, leads to optical reactions and no secondary electrochemical reactions are observed in the potential range studied by Vuillemin and Bohnke. The potentials at which $i = 0$ (oxidation begins) and where $dA/dt = 0$ (the maximum absorbance measured), can be compared. It can be seen in Table 5.6, that for the wavelengths chosen to be studied (650nm and 820nm) oxidation occurs at a higher potential on the anodic half cycle than where the maximum absorbance is recorded. Therefore, the assumption made by Vuillemin and Bohnke that the kinetics of the electrochemical reaction are faster than the

corresponding colouration kinetics appears to be true for the three concentrations of LiClO₄ studied here.

Table 5.6 : Table showing recorded potentials where $i = 0$ (and hence minimum charge is recorded) and potentials at which maximum absorbance is recorded. Electrolytes : various concentrations of LiClO₄/propylene carbonate. Wavelengths measured : 650nm (1st scan) and 820nm (2nd scan).

[LiClO ₄] / M	Potential at $i=0$ and maximum charge passed / V		Potential of max Absorbance / V	
	1 st scan (650nm)	2 nd scan (820nm)	1 st scan (650nm)	2 nd scan (820nm)
0.1	-0.775	-0.824	-0.505	-0.725
0.5	-0.922	-0.946	-0.815	-0.805
0.7	-0.821	-0.897	-0.760	-0.790

5.4.3 EQCM and spectroscopic data

Since both the quartz crystals and F-doped ITO glass used for study of WO₃ films were coated at the same time, it can be assumed that the films deposited on them are of identical thickness and have the same properties. This means that it is possible to combine the EQCM and spectroscopic data to give information about the charge, mass and absorbance measured in both sets of experiments.

If the charge passed during an EQCM experiment and the absorbance measured in a “fixed wavelength” experiment are combined, it is possible to plot absorbance vs charge passed. This is shown in figure 5.7, where the “break-in” effect is shown at 650nm.

It can be seen that there are three slopes of varying gradient for each wavelength measured. They are labelled “a”, “b” and “c” in figure 5.7. It is therefore possible to calculate the extinction coefficient (ϵ), via the following relationship:

$$Abs = \epsilon cL = \epsilon \Gamma \quad [5.2]$$

$$Abs = \left(\frac{\epsilon}{FA} \right) Q \quad [5.3]$$

where c is the concentration of chromophore (mol cm⁻³), L is the optical pathlength (cm), Γ the amount of material (mol cm⁻²) deposited on an area A (cm²), and Q the charge passed

C

(C). Table 5.7 shows the values of ε calculated for WO_3 films exposed to varying concentrations of LiClO_4 .

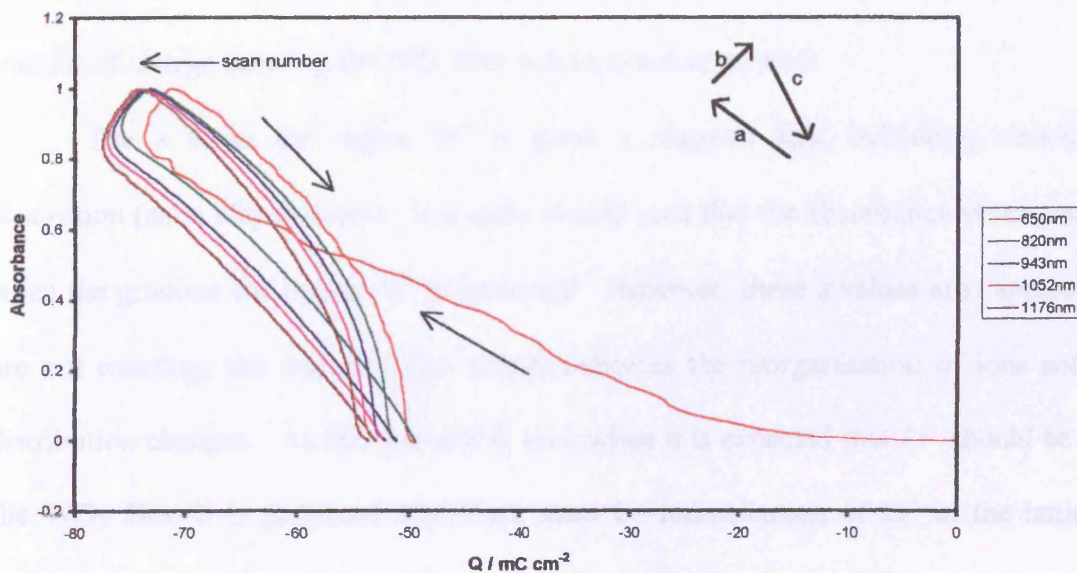


Figure 5.7 : Normalised absorbance versus charge responses from a combined spectrophotometric and EQCM experiment for the reduction and oxidation of a 2400Å thick WO_3 film coated on ITO. Electrolyte : 0.5M LiClO_4 /propylene carbonate. Total number of wavelengths recorded : 5 (marked on legend). Scan rate : 5 mV s^{-1} . “break-in” effect measured at 650nm.

Table 5.7 : Table showing the apparent extinction coefficients (ε) calculated for different wavelengths recorded at various concentrations of LiClO_4 . Data taken from Figure 5.7

[LiClO_4] / M	$\varepsilon / *10^6$ $\text{cm}^2 \text{mol}^{-1}$	Wavelength / nm				
		650	820	943	1052	1176
0.1	a	0.13	5.15	5.28	5.39	5.39
	b	-16.4	-12.4	-11.7	-10.3	-10.4
	c	13.8	8.76	8.00	7.66	7.51
0.5	a	0.23	4.95	4.88	4.94	4.92
	b	-8.18	-5.71	-6.13	-6.41	-7.60
	c	6.66	6.53	6.85	6.97	6.99
0.7	a	0.35	4.29	4.55	4.62	4.66
	b	-7.84	-9.35	-6.43	-6.97	-7.37
	c	8.17	6.92	6.69	6.84	6.95

As mentioned in the Theory Chapter, ε varies with the chosen wavelength. As ε is defined as a measure of the strength of the optical absorbance at each wavelength, it can be seen that for each wavelength measured after the “break-in” cycle, ε is approximately

constant for “a”, “b” and “c” for each concentration studied. The value of ε at 650nm for each concentration is different than the following wavelengths which may be due to the “break-in” effect. The small ε value measured at “a” for 650nm, may be due to the large amount of charge entering the WO_3 film, which is not recovered.

The ε value for region “b” is given a negative sign, indicating emission, not absorption (as in ellipsometry). It is quite clearly seen that the absorbance is still increasing when the gradient for region “b” is measured. However, these ε values are “apparent” and are not emitting; the negative sign simply indicates the reorganisation of ions and hence distribution changes. As this increase is seen when it is expected that Li^+ should be leaving the WO_3 film, it is proposed that there must be redistribution of Li^+ in the lattice until maximum absorbance has been reached, when the absorbance begins to decrease and bleaching occurs. From Table 5.7 it is seen that the potential where maximum absorbance is recorded at a later potential to that where the current changes sign.

It can be seen that during the first scan there is a large amount of charge entering the film, which is not fully recovered, as was seen in the EQCM experiments. On the following scans, as in the cyclic voltammograms there is more charge recovered on completion of the cycle although, not all charge is completely recovered. This has been seen in Chapter 4, Figure 4.3. On the first cycle, it can be seen that there is an approximately linear increase in absorbance (region “a”) during reduction of the WO_3 film. Upon the reversal of the scan, region “b” appears to be approximately linear, but region “c” shows non linearity, which indicates that there are neutral species entering and leaving the WO_3 film during the scan. For the following scans, this trend is also seen, and is common throughout the varying concentrations studied here.

C

If the relationship between the absorbance and mass changes is studied, as shown in Figure 5.8, again, it can be seen that there is a large amount of mass being inserted into the film on the first cycle, which is not recovered at the end of this cycle. This experiment is in effect a “mixed” experiment, as we are taking both EQCM and spectrophotometric data together for study. In the spectroscopic experiment, the absorbance changes only are being studied, and all the wavelengths should show identical absorption characteristics. In the case of the EQCM experiments, the increase in mass that is seen is an effect of the specific cycle for that experiment. Therefore, the hysteresis that is seen in Figure 5.8 is an effect of the ion which has been recorded from the EQCM experiment and not the recorded spectroscopic changes.

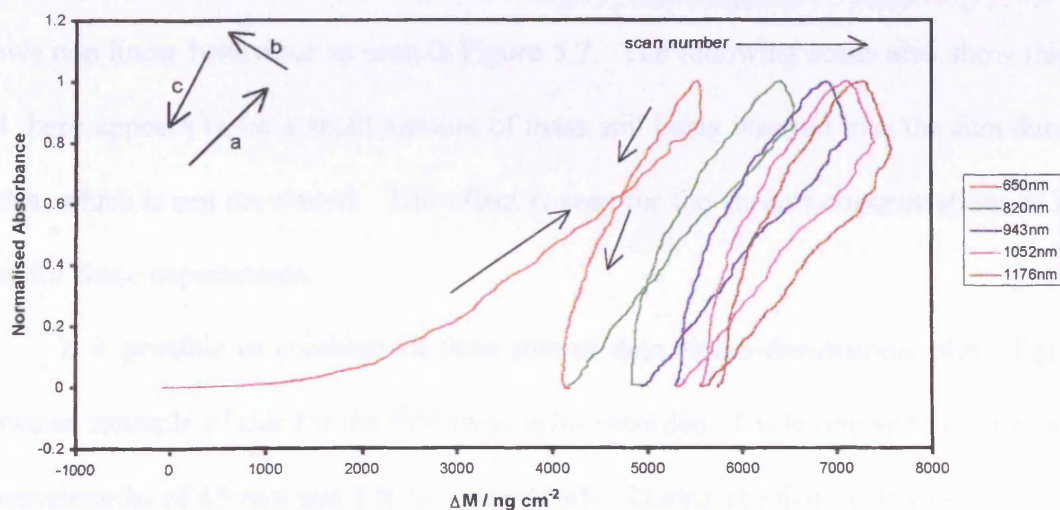


Figure 5.8 : Normalised Absorbance versus mass changes responses from a combined spectrophotometric and EQCM experiment for the reduction and oxidation of a 2400Å thick WO_3 film coated on ITO. Electrolyte : 0.5M LiClO_4 /propylene carbonate. Total number of wavelengths recorded : 5 (marked on legend). Scan rate : 5 mV s^{-1} . “break-in” effect measured at 650nm.

Hysteresis is seen during the initial cycle where the “break-in” effect is recorded, as a number of electrons are ejected. This effect is seen optically with changes in normalised absorbance and also in mass changes, which give information regarding ion and solvent properties. It is by choice that the experiment is not at equilibrium, as the overall mass

changes are studied with the EQCM experiment. Therefore, it is unclear as to whether all the WO_3 film used in the spectrophotometric experiment is coloured evenly, with the same x value across the film, or whether x varies across the coating during colouration. The hysteresis seen in the plot may indicate two effects; firstly, that neutrals (in the form of ion pairs or solvent) contribute to the mass changes, which are not seen in Figure 5.8 but are implied by the mass change progressing from left to right, and secondly, the film changes colour, which is seen by a change in absorbance.

As for the absorbance versus charge data, it is seen that for the first cycle, there is an approximate linear relationship between the normalised absorbance and mass change for the reduction (region "a"), and also for the initial oxidation (region "b") of the film. Region "c" shows non linear behaviour as seen in Figure 5.7. The following scans also show this trend and there appears to be a small amount of mass still being inserted into the film during the cycles, which is not recovered. This effect is seen for the various concentrations of LiClO_4 used for these experiments.

It is possible to combine all three sets of data as a 3-dimensional plot. Figure 5.9 shows an example of this for the first two cycles recorded. Cycle one and two are recorded at wavelengths of 650nm and 820nm respectively. During the first cycle (650nm), it can be clearly seen that both mass and charge passed are not recovered, although the absorbance does return to zero. The mass is seen to increase by approximately 4000 ng cm^{-2} , and the charge to decrease by 50 mC cm^{-2} . When the second scan is studied (820nm), the absorbance returns to zero at the completion of the cycle and there is very little change in charge seen. The mass is seen to have increased again by approximately 1000 ng cm^{-2} .

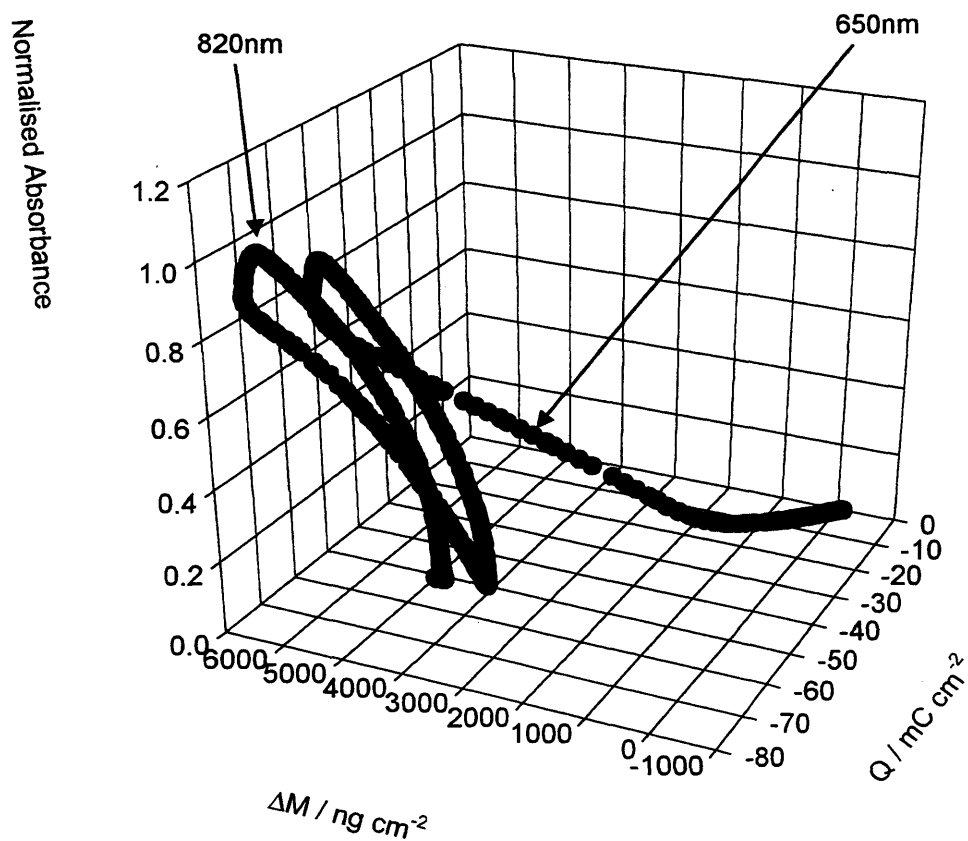


Figure 5.9 : 3-dimensional plot showing the normalised absorbance, mass changes and charge responses for a combined spectrophotometric and EQCM experiment to investigate the “break-in” effect for ion insertion into a 2400Å thick WO₃ film coated onto ITO glass. Electrolyte : 0.5M LiClO₄/propylene carbonate. Total number of cycles recorded : five (first two cycles (650nm and 820nm) plotted only). Scan rate : 5 mV s⁻¹. “break-in” effect recorded for 650nm.

5.5 EFFECTS OF LONG TERM CYCLING

5.5.1 Introduction

The effect on the film of long term cycling has been studied using the EQCM to record the first and last ten cycles of an experiment in which a film is cycled for more than 10,000 cycles at 100 mV s^{-1} . This has been studied before^[25-29] by various authors, but the effect on mass has not been studied. Two films were studied; the first was cycled in $0.1\text{M LiClO}_4/\text{propylene carbonate}$, and the second in $0.1\text{M NaClO}_4/\text{propylene carbonate}$. In both cases, the first ten cycles were recorded using the EQCM, and then the films were left to cycle. The first ten cycles recorded by the EQCM have been labelled from 1 to 10. In the case of the Li^+ electrolyte, the film was cycled for 125.5 hours (overall, 11,295 cycles). The experiment using NaClO_4 was cycled for 121 hours (overall, 10,890 cycles). After this time period, the last ten redox cycles of the film were recorded on the EQCM for comparison with the initial cycles. For the ease of comparison with the initial EQCM data recorded, these final recorded cycles have been labelled A-J.

5.5.2 Li^+ insertion

The first ten cycles in the experiment are shown in Figure 5.10. When looking at the cyclic voltammetric response for these first ten cycles, there is a difference between the first five and last five scans. The first five scans have a different response to that expected for cycling in LiClO_4 at this scan rate (compare fig 5.2), and show a “break-in” effect which is complete after cycle 5. This “break-in” effect is also seen in the mass versus potential data. For the first five cycles, a mass increase is seen, where the mass is not recovered and Li^+ remains in the film. A steady-state response is seen for both current and mass after completion of the first five cycles.

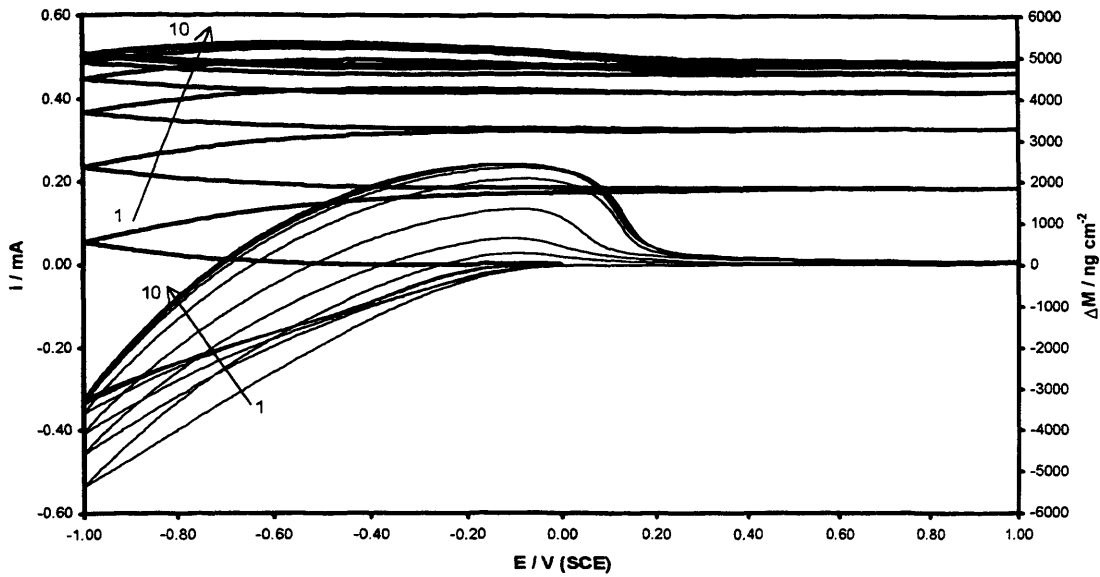


Figure 5.10 : Cyclic voltammogram and mass changes versus potential response showing the effects of extended cycling of a WO_3 film. Electrolyte : $0.1\text{M LiClO}_4/\text{propylene carbonate}$. Total number of cycles recorded : ten (marked on plot). Scan rate : 100 mV s^{-1} . Cyclic voltammetric response marked in normal line, mass change versus potential response marked as bold line.

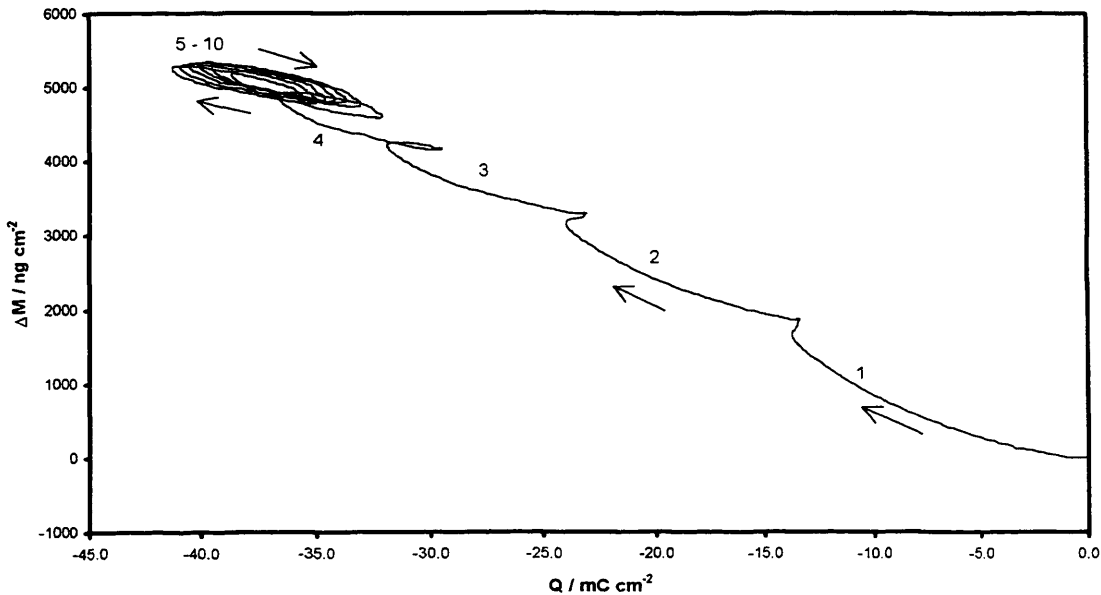


Figure 5.11 : Mass changes versus charge response for a voltammetric experiment showing the effects of extended cycling of a WO_3 film. Electrolyte : $0.1\text{M LiClO}_4/\text{propylene carbonate}$. Total number of cycles recorded : ten (marked on plot). Scan rate : 100 mV s^{-1} .

If the $\Delta M/F/Q$ plots as shown in Figure 5.11, are studied, it can also be seen that there is very little charge recovered during the first five scans. The “break-in” effect is seen clearly for the first five scans. Scans 6-10 show the evolution of steady-state populations of electrons/ ClO_4^- . Hysteresis is also seen in the plots, which signifies that there is more than one species is entering and leaving the WO_3 film.

The “end-to-end” $\Delta M_{\text{T}}F/Q_{\text{T}}$ ratios can be calculated and are shown in Table 5.8. It can be seen that for the first five cycles, as seen in figure 5.12, that the $\Delta M_{\text{T}}F/Q_{\text{T}}$ ratios for reduction of the WO_3 film are larger than the expected value for Li^+ insertion, and indicate insertion into the film by a neutral species such as propylene carbonate. By scans 6-10 however, the $\Delta M_{\text{T}}F/Q_{\text{T}}$ ratios appear to have become more reproducible. At this steady-state response the “end to end” $\Delta M_{\text{T}}F/Q_{\text{T}}$ values are more consistent with Li^+ injection/extraction, although hysteresis seen in the plots indicate the presence of a neutral species. This effect is also seen on the oxidation of the film, where the initial five scans show very variable $\Delta M_{\text{T}}F/Q_{\text{T}}$ values in comparison with the following five cycles.

Table 5.8 : Table showing “end to end” $\Delta M_{\text{T}}F/Q_{\text{T}}$ values for reduction and oxidation of a WO_3 film. Values calculated from the mass changes versus charge response (shown in Figure 5.11) for first ten recorded cycles of Li^+ insertion into a WO_3 film.

Cycle number	$(\Delta M_{\text{T}}F/Q_{\text{T}}) / \text{g mol}^{-1}$	
	reduction	oxidation
1	-11.6	55.5
2	-11.7	14.8
3	-10.1	-2.2
4	-9.8	-5.8
5	-8.3	-6.9
6	-7.6	-7.5
7	-7.2	-7.6
8	-7.1	-7.8
9	-6.9	-7.8
10	-6.7	-7.8

The current and mass change versus potential plots for the last 10 cycles of the experiment are shown in Figure 5.12. It can be seen that the cyclic voltammogram follows the expected path for Li^+ insertion into WO_3 .

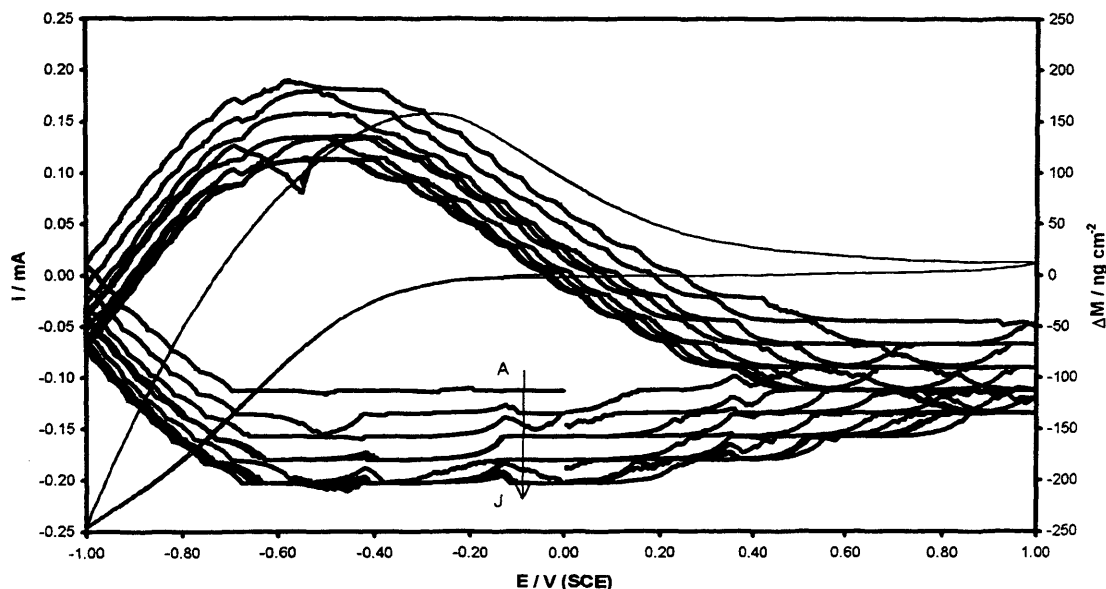


Figure 5.12 : Cyclic voltammogram and mass changes versus potential response showing the effects of extended cycling of a WO_3 film. Electrolyte : 0.1M LiClO_4 /propylene carbonate. Total number of cycles recorded : ten (last ten cycles of 11295 cycles). Scan rate : 100 mV s^{-1} . Cyclic voltammetric response marked in normal line (all ten scans are penwidth reproducible), mass change versus potential response marked as bold line (scans A - J marked on plot).

As both EQCM experiments for the long term cycling experiments required the frequency data to be zeroed before beginning any experiment, then it is not possible to compare the mass change versus potential data from Figure 5.10 and 5.12 directly. The only comparison which can be made is the amount of mass change recorded during the cycle. The final cycle (number 10) recorded initially by the EQCM has a ΔM value of $\approx 493 \text{ ng cm}^{-2}$, whereas the cycles A - J give ΔM values of $\approx 310 \text{ ng cm}^{-2}$. It can be seen that the mass has decreased by $\approx 40\%$ during long term cycling. Again the plots follow the expected

course for the experiment. The $\Delta M_T F / Q_T$ data obtained for the final ten cycles, shows the response which has been seen for many experiments carried out with a scan rate of 100 mV s^{-1} , with the “end to end” $\Delta M_T F / Q_T$ ratios shown in Table 5.9.

Table 5.9 : Table showing “end to end” $\Delta M_T F / Q_T$ values for reduction and oxidation of a WO_3 film. Values calculated from the mass change versus charge response for last ten recorded cycles (labelled A-J) of Li^+ insertion into a WO_3 film.

Cycle number	$(\Delta M_T F / Q_T) / \text{g mol}^{-1}$	
	reduction	oxidation
A	-6.3	-6.1
B	-5.6	-6.1
C	-5.7	-6.0
D	-5.6	-5.8
E	-5.7	-6.1
F	-5.7	-5.8
G	-5.6	-5.9
H	-5.8	-6.0
I	-6.0	-6.0
J	-6.0	-6.0

It can be noted that the $\Delta M_T F / Q_T$ ratios for the final ten cycles are somewhat lower than for the initial ten cycles. These lower values may be due to the amount of solvent which has irreversibly entered the WO_3 film during the experiment, which may mean that a smaller amount of Li^+ is entering the film. When comparison is made between the mass change and charge values obtained for Li^+ insertion into WO_3 for the last cycle of the initial EQCM experiment (cycle number 10) and the first cycle of the second set of EQCM experiments (cycle number A) then it can be seen that there is very little different between either set of values. This implies that the effect of long term cycling upon Li^+ insertion/extraction into a WO_3 film does not alter much after the first ten cycles.

5.5.3 Na⁺ insertion

The initial cycles for Na⁺ insertion are shown in Figure 5.13. It is noted that the first cycle of the experiment shows a larger input of charge compared to the following cycles. The current passed during this experiment is smaller than the corresponding Li⁺ experiment, but similar results have been seen in earlier experiments carried out, when the first scan rate chosen was 100 mV s⁻¹.

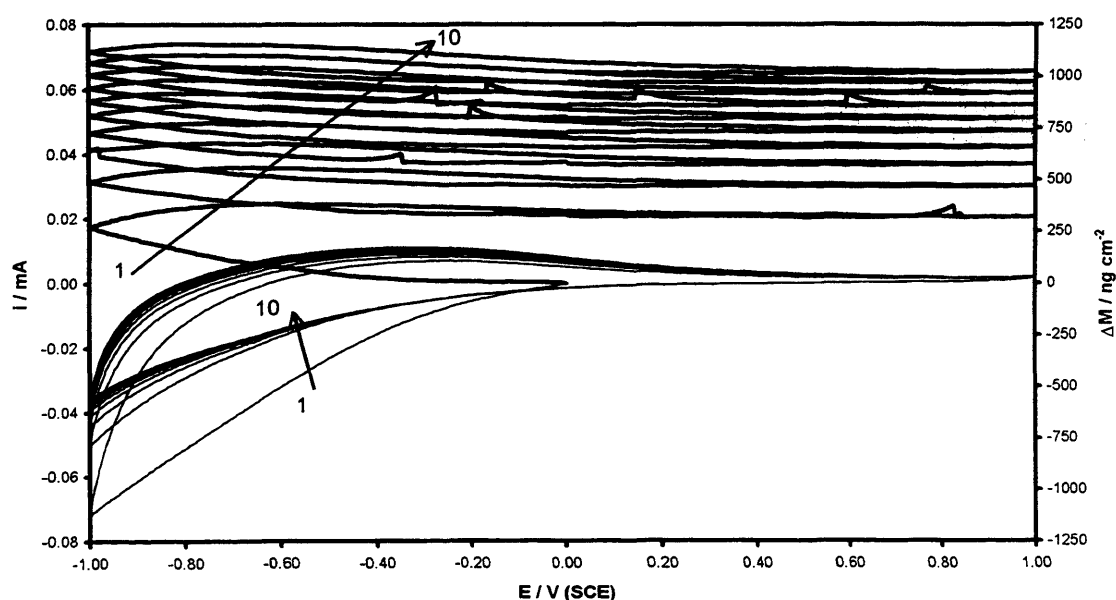


Figure 5.13 : Cyclic voltammogram and mass changes versus potential response showing the effects of extended cycling of a WO₃ film. Electrolyte : 0.1M NaClO₄/propylene carbonate. Total number of cycles recorded : ten (marked on plot). Scans 5 - 10 are penwidth reproducible. Scan rate : 100 mV s⁻¹. Cyclic voltammetric response marked in normal line, mass changes versus potential response marked as bold line.

Again, the “break-in” effect is seen during the first cycle, but when compared to Li⁺ insertion, it should be noted that the current versus potential response appears to reach a steady-state after three cycles. When the mass versus potential responses are studied, there is an increase in mass seen on the first cycle, but the mass does not reach a steady-state as seen for Li⁺.

Figure 5.14 shows the mass versus charge response for the first ten cycles. It can be seen that there is very little hysteresis for the insertion of Na^+ when compared to Li^+ , although there is still both mass and charge left in the WO_3 film.

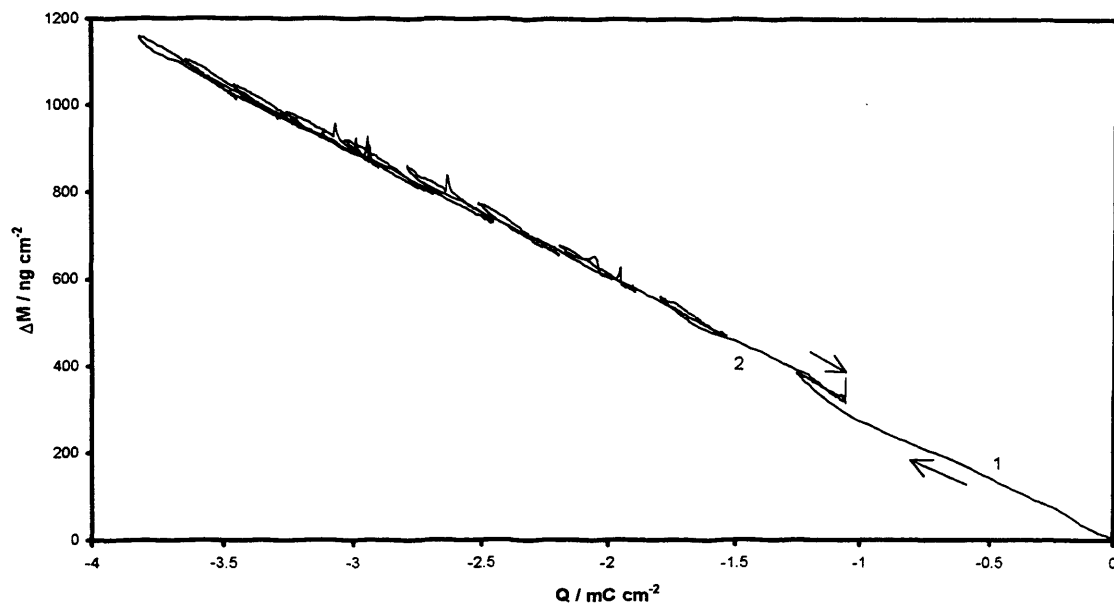


Figure 5.14 : Mass changes versus charge response for a voltammetric experiment showing the effects of extended cycling of a WO_3 film. Electrolyte : 0.1M NaClO_4 /propylene carbonate. Total number of cycles recorded : ten (1st two cycles marked on plot). Scan rate : 100 mV s^{-1} .

The $\Delta M_{\text{T}}/Q_{\text{T}}$ ratios for the insertion of Na^+ into the WO_3 film are shown in Table 5.10. It can be seen that for all ten cycles, the $\Delta M_{\text{T}}/Q_{\text{T}}$ ratios for reduction are similar to those for oxidation. Again, the ratios are larger than those expected for only Na^+ insertion, which indicates that there must be neutral species insertion/expulsion into the film. It is noted that the mass versus charge plot for Na^+ insertion shows very little hysteresis compared to Li^+ insertion. If only the single cation Na^+ was entering/leaving the film, then the $\Delta M_{\text{T}}/Q_{\text{T}}$ values would equal 23 g mol^{-1} and the mass versus charge plot would have no hysteresis. The small hysteresis indicates that the e^-/Na^+ transfer is rate limiting and that the neutral species which enters alongside the cation keeps up during insertion/expulsion.

Table 5.10 : Table showing “end to end” $\Delta M_{TF}/Q_T$ values for reduction and oxidation of a WO_3 film. Values calculated from the mass changes versus charge response (shown in Figure 5.14) for first ten recorded cycles of Na^+ insertion into a WO_3 film.

Cycle number	$(\Delta M_{TF}/Q_T) / g mol^{-1}$	
	reduction	oxidation
1	-29.3	-31.9
2	-32.1	-35.8
3	-31.5	-35.7
4	-32.5	-36.6
5	-33.5	-37.9
6	-31.6	-35.0
7	-32.1	-34.7
8	-33.1	-34.8
9	-32.8	-34.4
10	-32.7	-36.9

The film was cycled 10,890 times, then transferred back to the EQCM equipment for analysis of the final ten cycles, as for the Li^+ electrolyte experiment. However, the EQCM crystal on which the WO_3 film was sputtered would not oscillate and so only a cyclic voltammogram could be recorded. Figure 5.15 shows this cyclic voltammogram for the last ten cycles of Na^+ insertion. The first cycle (A) appears to be slightly different from the following cycles. This effect may be due to the fact that cycling of the WO_3 film was stopped, prior to trying to obtain the EQCM measurements. Therefore, it is thought that this larger input of current is not a real effect, but is due to the “stopping and starting” of the experiment.

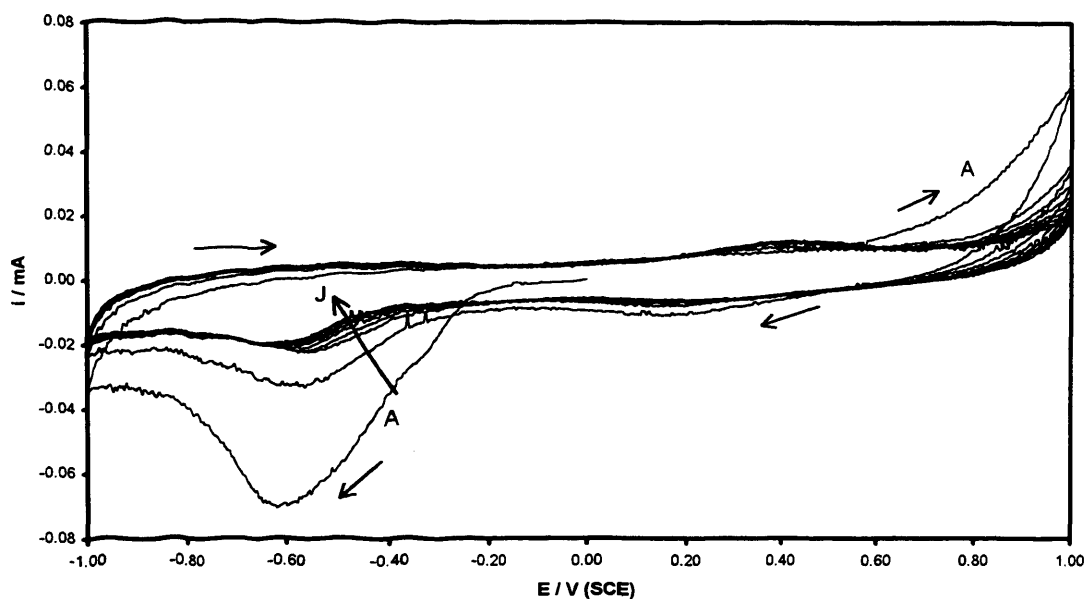


Figure 5.15 : Cyclic voltammogram response showing the effects of extended cycling of a WO_3 film. Electrolyte : 0.1M NaClO_4 /propylene carbonate. Total number of cycles recorded : ten (last ten cycles of 10890 cycles). Scan rate : 100 mV s^{-1} .

It can be seen that the response is not the same as for the first ten cycles. The reason for this may be that the WO_3 film has dissolved and only the gold is left on the crystal. When a cyclic voltammogram was recorded in 0.1M NaClO_4 /propylene carbonate on an uncoated gold quartz crystal, then a similar cyclic voltammetric response was seen. This effect shows that using Na^+ for prolonged periods of time is not suitable for an electrochromic display.

5.6 SUMMARY

At slow scan rates in LiClO_4 /propylene carbonate and NaClO_4 /propylene carbonate, the initial cyclic voltammogram is found to be different from the following ones. This is termed the “break-in” effect and can be seen for both Na^+ and Li^+ insertion using both EQCM and spectrophotometry at all concentrations studied. In all cases, there is a general, initial increase in mass during this “break-in” cycle, which is not recovered. This leads to

the conclusion that after the first cycle of a new film, there are cations left behind in the WO_3 lattice.

$\Delta M_{\text{T}}F/Q_{\text{T}}$ values are greater than expected for pure cation insertion. Φ values indicate that a neutral species (propylene carbonate and/or ion pairs) enters WO_3 , along with the cation.

Values for x calculated for the “break-in” experiment, using network analyser data, show that during this initial increase in mass, a substantial amount of Li^+ is inserted into the film. This is not the case with Na^+ however, which shows that there is a much smaller amount of Na^+ being inserted into the film. This is also seen in spectrophotometric experiments, where the changes in absorbance for Na^+ insertion are very small.

Li^+ insertion is seen to be stable for extended cycling (in this case over 10,000 cycles). This reliability is essential for electrochromic displays. In the case of Na^+ , it appears that the WO_3 film does not appear to survive the extended cycling, and leads to the conclusion that using a Na^+ salt for electrochromic displays would not be practical.

REFERENCES

1. A. R. Hillman, N. A. Hughes, and S. Bruckenstein, *Journal of the Electrochemical Society*, 139, 1, (1992), 74.
2. S. K. Mohapatra, *Journal of the Electrochemical Society*, 125, 2, (1978), 284.
3. T. Kamimori, J. Nagai, and M. Mizuhashi, *Proceedings of the Society of Photo-Optical Instrumentation Engineers*, 428, (1983), 51.
4. J. G. Zhang, C. E. Tracy, D. K. Benson, and S. K. Deb, *Journal of Materials Research*, 8, 10, (1993), 2649.
5. M. Green and A. Travlos, *Philosophical Magazine B-Structural Electronic Optical and Magnetic Properties*, 51, 5, (1985), 501.
6. M. Green and A. Travlos, *Philosophical Magazine B-Structural Electronic Optical and Magnetic Properties*, 51, 5, (1985), 521.
7. D. Dini, F. Decker, and E. Masetti, *Journal of Applied Electrochemistry*, 26, 6, (1996), 647.
8. O. Bohnke and M. Rezrazi, *Materials Science and Engineering B-Solid State Materials For Advanced Technology*, 13, 4, (1992), 323.
9. O. Bohnke and B. Vuillemin, *Materials Science and Engineering B-Solid State Materials For Advanced Technology*, 13, 3, (1992), 243.
10. S. K. Mohapatra, G. D. Boyd, F. G. Storz, and S. Wagner, *Journal of the Electrochemical Society*, 126, 5, (1979), 805.
11. T. Nishimura, K. Taira, and S. Kurita, *Applied Physics Letters*, 36, 7, (1980), 585.
12. J. P. Randin and R. Viennet, *Journal of the Electrochemical Society*, 129, 10, (1982), 2349.
13. S. J. Babinec, *Solar Energy Materials and Solar Cells*, 25, 3-4, (1992), 269.

14. O. Bohnke, B. Vuillemin, C. Gabrielli, M. Keddou, and H. Perrot, *Electrochimica Acta*, 40, 17, (1995), 2765.
15. O. Bohnke, B. Vuillemin, C. Gabrielli, M. Keddou, H. Perrot, H. Takenouti, and R. Torresi, *Electrochimica Acta*, 40, 17, (1995), 2755.
16. H. Inaba, M. Iwaku, T. Tatsuma, and N. Oyama, *Journal of Electroanalytical Chemistry*, 387, 1-2, (1995), 71.
17. H. Inaba, M. Iwaku, T. Tatsuma, and N. Oyama, *Denki Kagaku*, 61, 7, (1993), 783.
18. O. Bohnke, C. Bohnke, G. Robert, and B. Carquille, *Solid State Ionics*, 6, 2, (1982), 121.
19. S. K. Deb, *Philosophical Magazine*, 27, (1973), 801.
20. M. S. Burdis and J. R. Siddle, *Thin Solid Films*, 237, (1994), 320.
21. R. A. Batchelor and M. J. Burdis, *Pilkington Group Research, private communication*, 1995-1997.
22. P. M. S. Monk, R. J. Mortimer, and D. R. Rosseinsky, Electrochromism, Fundamentals and Applications, VCH Publishers, Weinheim, 1995.
23. F. G. K. Baucke and J. A. Duffy, *Chemistry in Britain*, July, (1985), 643.
24. B. Vuillemin and O. Bohnke, *Solid State Ionics*, 68, 3-4, (1994), 257.
25. A. Kuzmin and J. Purans, *Journal of Physics, Condensed Matter*, 5, (1993), 9423.
26. C. Bohnke and M. Rezaei, *Materials Science and Engineering B-Solid State Materials For Advanced Technology*, 10, 4, (1991), 313.
27. J. L. Paul and J. C. Lassegues, *Journal of Solid State Chemistry*, 106, 2, (1993), 357.
28. H. Akram, H. Tatsuoka, M. Kitao, and S. Yamada, *Journal of Applied Physics*, 62, 5, (1987), 2039.

29. J. Nagai, T. Kamimori, and M. Mizuhashi, *Proceedings of the Society of Photo-Optical Instrumentation Engineers*, 502, (1984), 59.

CHAPTER 6 : EFFECTS OF EXPERIMENTAL TIME SCALE ON ION INSERTION INTO WO₃ FILMS

6.1 INTRODUCTION

This chapter will deal with the effects of time scale upon ion insertion into a WO₃ film. Initially, the electrochemical results obtained from chronoamperometric experiments will be discussed, followed by the accompanying EQCM data. The effect of changing the scan rate on a cyclic voltammetric experiment will also be discussed.

6.2 GENERAL ELECTROCHEMICAL INTERPRETATION

6.2.1 Introduction

This section will describe the electrochemical features associated with chronoamperometric experiments, the current - time relationship and also the derived diffusion coefficients and x values associated with insertion of cations into a WO₃ film.

6.2.2 Chronoamperometry

As mentioned in the Theory chapter, a chronoamperometric experiment involves “stepping” from one potential to another pre-set potential and recording the current - time response. For the experiments carried out to investigate ion insertion into a WO₃ film, a double potential step was first carried out, in which the potential was stepped from 0V to a negative potential limit (to reduce the WO₃ film), held at that negative potential for 300 seconds, and then stepped back to 0V for a further 300 seconds, so as to ensure that oxidation of the WO₃ film could occur. The potentials stepped to were chosen at 0.1V intervals, beginning at -0.1V and finishing at -1.0V; a potential at which reduction of the WO₃ film was known to occur from cyclic voltammetric experiments.

The second set of chronoamperometric experiments consisted of a triple potential step. The potential was initially “stepped down” to -1.0V , and held at that potential for 300 seconds to reduce the film. After the time interval had elapsed, the potential was “stepped up” to a less negative potential, and held there for a further 300 seconds. Again, these potential limits were increased at 0.1V intervals, beginning at -0.9V and finishing at 0V . Finally, the potential was again stepped up to 0V and held for a further 300 seconds. For this set of experiments studied here, the electrolyte chosen was $0.1\text{M LiClO}_4/\text{propylene carbonate}$, although identical experiments have been carried out in $0.5\text{M LiClO}_4/\text{propylene carbonate}$ and $0.7\text{M LiClO}_4/\text{propylene carbonate}$.

Figure 6.1 shows the current versus time response for a double chronoamperometric experiment where the potential is stepped from 0V to -1.0V for a WO_3 film in $0.1\text{M LiClO}_4/\text{propylene carbonate}$. Initially, the WO_3 film is held for 20 seconds at 0V before the potential is “stepped”, so as to obtain a steady current base line.

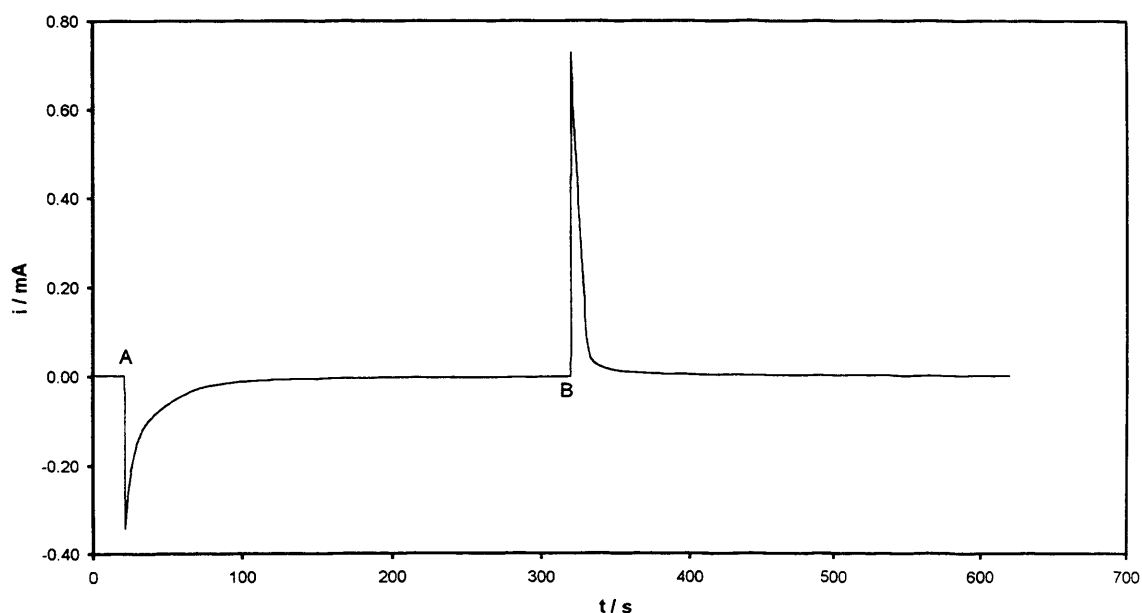


Figure 6.1 : Current versus time response for a double chronoamperometric experiment showing Li^+ insertion into a 2400\AA thick WO_3 film. Electrolyte : $0.1\text{M LiClO}_4/\text{propylene carbonate}$. Point A indicates step from $0\text{V} \rightarrow -1.0\text{V}$ for 300 seconds. Point B indicates step from $-1.0\text{V} \rightarrow 0\text{V}$ for 300 seconds.

It can be seen that upon stepping down to -1.0V, a current spike measuring -0.314 mA is seen, and the current response rises slowly towards 0 mA for the next 300 seconds. After that time has elapsed, it appears that the current has fallen to approximately zero. When the potential is stepped back to 0V, there is a sharp current spike recorded (0.726 mA), which decays back to 0mA after approximately 200 seconds. The fact that the current takes a longer time to return to zero after insertion of the lithium ion compared to the time measured for expulsion of the same ion indicates that the colouration of the WO₃ film using a 0.1M LiClO₄/propylene carbonate electrolyte occurs slower than the subsequent bleaching. This effect has been seen elsewhere by other authors^[1-3], who also indicate that the colouration current decays at a $t^{-1/2}$ dependence, whereas for bleaching the current decays at a $t^{-3/4}$ rate. By taking natural logs of the current and time data, it is possible to analyse the reduction and re-oxidation responses. This is shown in Figure 6.2.

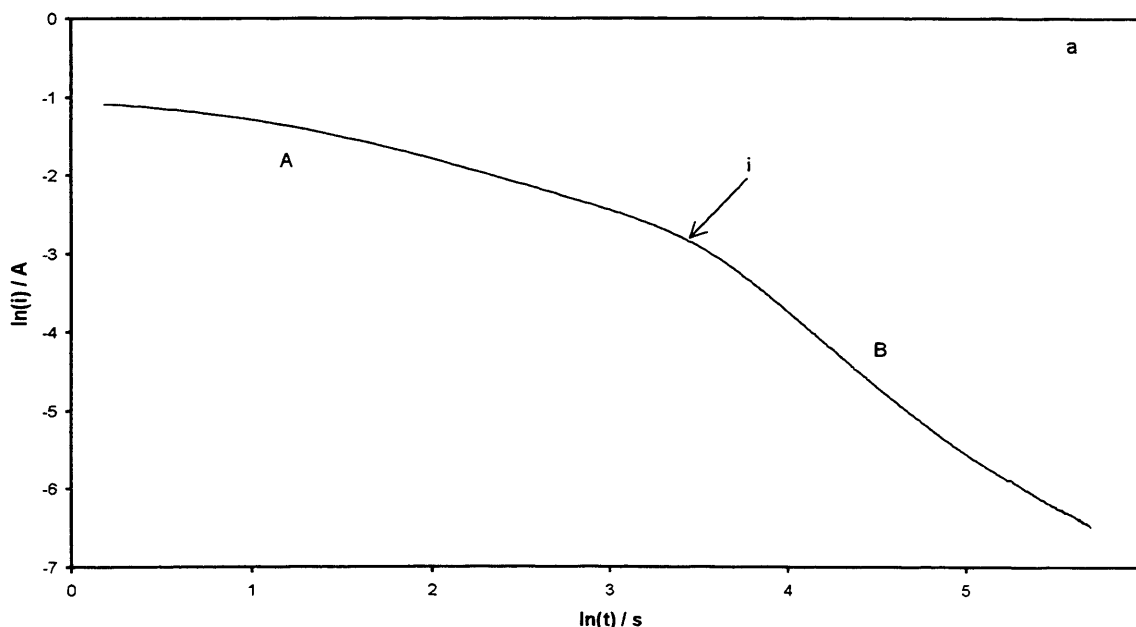
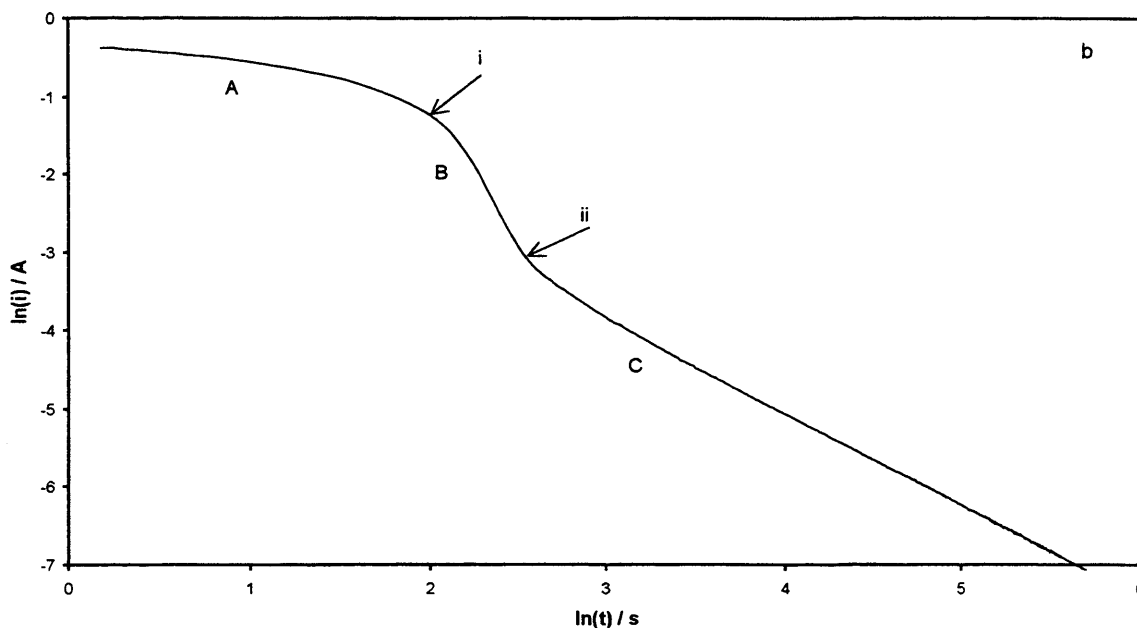


Figure 6.2 : $\ln(\text{current})$ versus $\ln(\text{time})$ plots for a double chronoamperometric experiment showing Li⁺ insertion into a 2400Å thick WO₃ film. Electrolyte : 0.1M LiClO₄/propylene carbonate. Figure 6.2a shows reduction. Figure 6.2b shows re-oxidation.



For reduction of the WO_3 film (Figure 6.2a) it is seen that there are two distinct regions “A” and “B” where gradients can be measured. Region “A” has a gradient of ≈ 0.46 and region “B” has a gradient of ≈ 1.62 . The point “i” marked on the plot is where the two regions meet. This point is measured at 30.4 seconds, where $\approx 65\%$ of the charge has already been passed. For re-oxidation of the tungsten bronze as seen in Figure 6.2b, three measurable regions are seen “A”, “B” and “C”. Region “A” has a shallow gradient of ≈ 0.01 , region “B” has a gradient of ≈ 3.87 and “C” has a gradient measured to be ≈ 1.18 . Point “i”, where “A” and “B” intersect is measured at 7.6 seconds and 58% of the charge has already been passed. Point “ii” is at 12.8 seconds and there has been 69% of charge passed by this time. The values do not follow the current decay dependence quoted by Faughnan and Crandall^[1], but are seen for all three concentrations of LiClO_4 /propylene carbonate when studied using chronoamperometric experiments.

As for the cyclic voltammetric experiments, it is also possible to plot the charge versus time response for the chronoamperometric experiment, since charge is the integral of current with respect to time. As for the previous two chapters, the fully oxidised film

defines charge as equal to zero, and reduction charge is subsequently negative. As the film is reduced, then the charge values become negative, and therefore, as the film is oxidised the charge values begin to increase and tend towards zero. Figure 6.3 shows the charge versus time response for the chronoamperometric experiment shown in Figure 6.1.

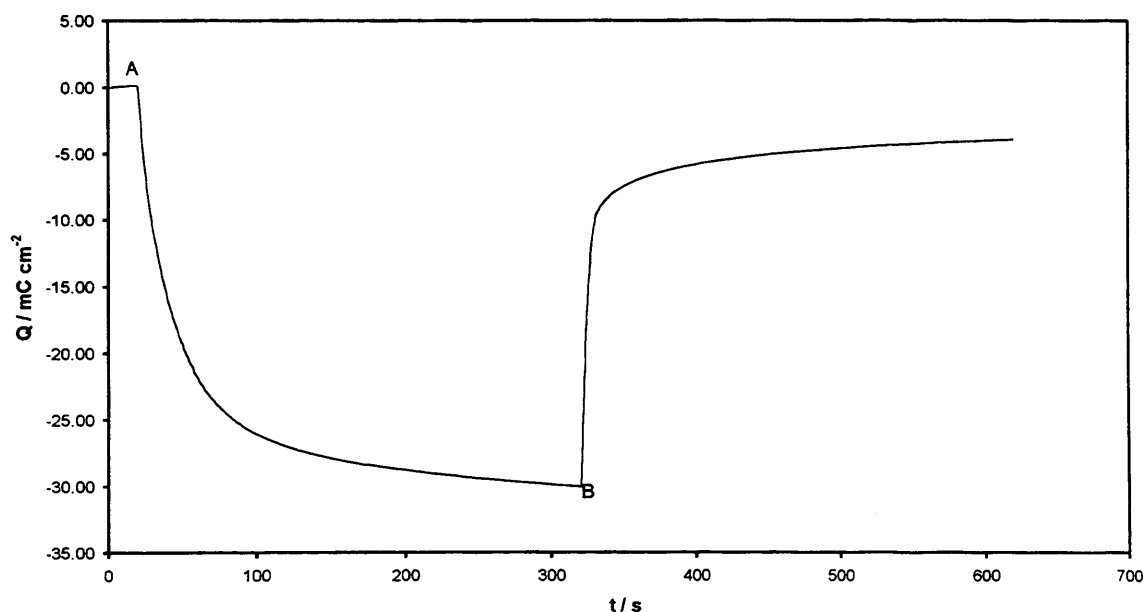


Figure 6.3 : Charge versus time response for a double chronoamperometric experiment showing Li^+ insertion into a 2400\AA thick WO_3 film. Electrolyte : $0.1\text{M LiClO}_4/\text{propylene carbonate}$. Point A indicates step from $0\text{V} \rightarrow -1.0\text{V}$ for 300 seconds. Point B indicates step from $-1.0\text{V} \rightarrow 0\text{V}$ for 300 seconds.

It can be seen that as the potential is stepped down to -1.0V the charge begins to decrease, which is expected for the reduction of the WO_3 film. As the potential is held at -1.0V for 300 seconds, the charge still decreases and does not reach a steady value. This indicates that reduction of the film is occurring throughout the initial potential step. When the film is oxidised by stepping back to 0V , the charge begins to increase at a much faster rate (as for the current - time response of figure 6.1), although it can be seen that complete charge recovery does not occur on the time scale of this experiment. This indicates that the

film is not fully reoxidised on the time scale chosen, although the oxidation of the WO_3 film appears to occur much faster than the reduction process, as seen in Figure 6.1.

Figure 6.4 shows a triple potential step, where a WO_3 film is stepped down to -1.0V initially for 300 seconds, followed by a step up to -0.4V for a further 300 seconds. Finally, the potential is again stepped back to 0V for another 300 seconds as for the double potential step to allow for re-oxidation of the WO_3 film. The potential for the second potential step was chosen to be -0.4V since, at that potential, oxidation of the reduced WO_3 film in $0.1\text{M LiClO}_4/\text{propylene carbonate}$ is known to occur.

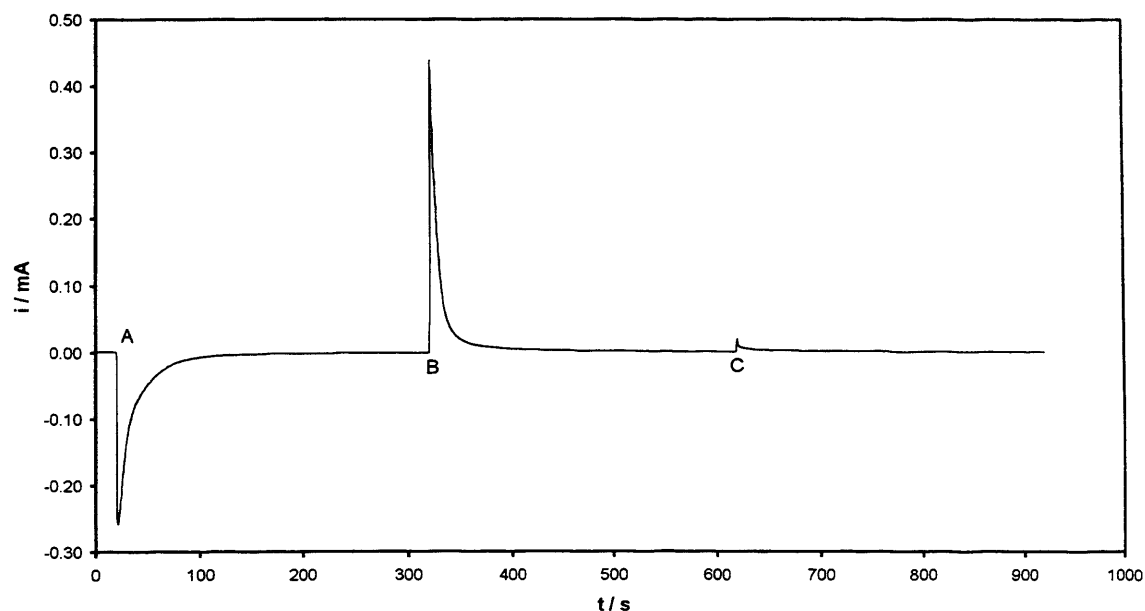


Figure 6.4 : Current versus time response for a triple chronoamperometric experiment showing Li^+ insertion into a 2400\AA thick WO_3 film. Electrolyte : $0.1\text{M LiClO}_4/\text{propylene carbonate}$. Point A indicates step from $0\text{V} \rightarrow -1.0\text{V}$ for 300 seconds. Point B indicates step from $-1.0\text{V} \rightarrow -0.4\text{V}$ for 300 seconds. Point C indicates step from $-0.4\text{V} \rightarrow 0\text{V}$ for 300 seconds.

As for the double potential step, the initial current response ($0\text{V} \rightarrow -1.0\text{V}$) appears to decay at a slower rate than the following two current versus time responses ($-1.0\text{V} \rightarrow -0.4\text{V}$ and $-0.4\text{V} \rightarrow 0\text{V}$). Again, the initial amount of charge passed for reduction is smaller than that recorded for the initial re-oxidation of the tungsten bronze.

The current recorded for the step of -0.4V back to 0V is very small (a maximum current of 0.020mA), which indicates that the WO₃ film is almost fully re-oxidised at this potential.

Again, as for the double chronoamperometric experiment, the charge response can also be plotted as a function of time. This is shown in Figure 6.5 where it is seen that for the initial step from 0V down to -1.0V, the charge does not reach a constant value, which implies that the film is still being reduced when the tungsten bronze is stepped up to the next potential of -0.4V. When the potential is finally stepped from -0.4V to 0V, there is very little difference in the charge being passed and at the end of the experiment, although the charge response has not levelled out, it appears that there is almost complete charge recovery, which indicates that the film has been fully re-oxidised.

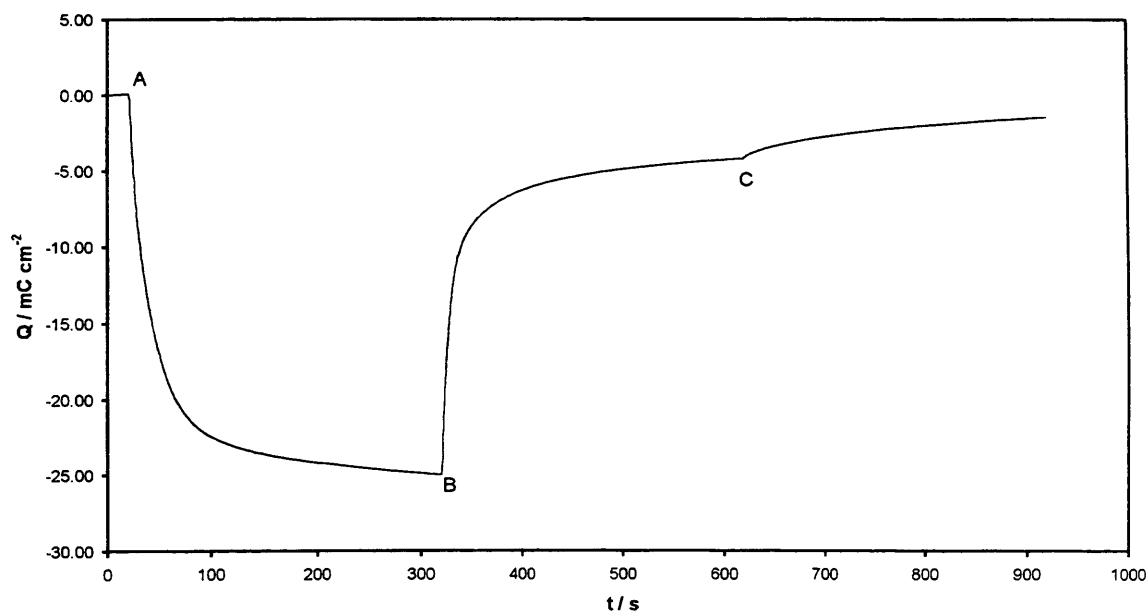


Figure 6.5 : Charge versus time response for a triple chronoamperometric experiment showing Li⁺ insertion into a 2400Å thick WO₃ film. Electrolyte : 0.1M LiClO₄/propylene carbonate. Point A indicates step from 0V → -1.0V for 300 seconds. Point B indicates step from -1.0V → -0.4V for 300 seconds. Point C indicates step from -0.4V → 0V for 300 seconds.

6.2.3 x values

As mentioned in Chapter 4, the x values can be calculated to give information about the amount of lithium being inserted into the WO_3 film under study using equation [6.1] seen below. It is possible to take the maximum charge value recorded during the chronoamperometric experiment at the end of the first step (for example, $0\text{V} \rightarrow -1.0\text{V}$) and calculate the x values for experiments carried out at different potential limits. Table 6.1 shows the potential limits and the calculated x values at the end of both the reduction (300 seconds) and re-oxidation (600 seconds) of the WO_3 film for three different concentrations of LiClO_4 /propylene carbonate.

$$x = \frac{QM}{FdIA} \quad [6.1]$$

where Q is the injected charge (C), M is the relative molar mass of WO_3 (232 g mol^{-1}), F is the Faraday constant, d is the density of WO_3 (5.5 g cm^{-3}), l the thickness of the film (cm) and A is the electrode area (cm^2)^[4]

Table 6.1 : Table showing the x values calculated from chronoamperometric experiments carried out on a WO_3 film in 0.1M LiClO_4 /propylene carbonate. x values obtained from charge data at the end of reduction and re-oxidation.

E / V 0V →	x values at reduction	the end of oxidation
-0.1	0.04	0.05
-0.2	0.13	0.17
-0.3	0.15	0.14
-0.4	0.15	0.13
-0.5	0.12	0.08
-0.6	0.16	0.09
-0.7	0.28	0.15
-0.8	0.44	0.22
-0.9	0.43	0.08
-1.0	0.55	0.07

The x values for ion insertion into a WO_3 film using 0.1M LiClO_4 /propylene carbonate show that until a cathodic potential limit of -0.6V is reached, the x values are not

large enough to produce a useful colour change (see Table 5.4), for optical applications. As the negative potential limit is decreased down to -1.0V, the x values increase and at -1.0V there appears to be a substantial amount of Li^+ entering the WO_3 film. This large amount of Li^+ should ensure a red/purple colouration for the reduced WO_3 film. The x values calculated for the re-oxidation show how much Li^+ is left in the film at the end of the experiment. It can be seen that for chronoamperometric experiments where the lower potential limits are -0.7V and -0.8V, there appears to be more Li^+ left in the WO_3 film than when the potential limits are less than -0.6V. However, when the lower potential limit is set at -0.9V or -1.0V almost all the Li^+ has left the film. Similar x values are seen for ion insertion into WO_3 films using 0.5M LiClO_4 /propylene carbonate and 0.7M LiClO_4 /propylene carbonate

6.2.4 Diffusion coefficients

The diffusion coefficient for chronoamperometric experiments can be calculated using the Cottrell equation [6.2], by plotting i versus $t^{1/2}$. The straight line will give the diffusion coefficient D_{Li^+} .

$$i = nFAc_R^{bulk} \left(\frac{D_R}{\pi t} \right)^{1/2} \quad [6.2]$$

where c is the concentration of the species being investigated (mol cm^{-3}), n is the number of electrons (in this case, the x value), A the electrode area (cm^2) and F the Faraday constant (C mol^{-1}). As seen in the Theory chapter (section 2.2.3) the concentration of Li^+ is known to be $0.0237 \text{ mol cm}^{-3}$ for the experiment being studied, then the only unknown is the diffusion coefficient which can be calculated from the gradient. Table 6.2 gives the calculated diffusion coefficients for the various potential limits studied in the double chronoamperometric experiments carried out in 0.1M LiClO_4 /propylene carbonate.

Table 6.2 : Table showing D_{Li^+} values and t^* values for chronoamperometric experiments carried out on a WO_3 film in 0.1M $LiClO_4$ /propylene carbonate.

E / V 0V →	D_{Li^+} / $\times 10^{-12} \text{ cm}^2 \text{ s}^{-1}$	t^* / s
-0.6	5.56	71.7
-0.7	4.01	99.5
-0.8	2.76	144.7
-0.9	5.38	74.2
-1.0	5.07	78.8

The D_{Li^+} values are $\approx 5.0 \times 10^{-12} \text{ cm}^2 \text{ s}^{-1}$, with literature values for D_{Li^+} being quoted between 10^{-11} and $5 \times 10^{-13} \text{ cm}^2 \text{ s}^{-1}$ [2][5]. Therefore, the calculated values lie within the literature values. Also given in Table 6.2 are the t^* values which can be used as a check on the gradient-derived value of D . These values are derived from equation [2.2.17] in the Theory chapter and are used to check the derived value of D_{Li^+} .

6.2.5 Cyclic voltammetric experiments

The effect of time can also be studied using cyclic voltammetry by looking at different scan rates. Figure 6.6 shows the different cyclic voltammograms obtained for a WO_3 film cycled in 0.1M $LiClO_4$ /propylene carbonate at five different scan rates. The cyclic voltammogram recorded at 5 mV s^{-1} is in fact the second recorded cycle, as the first cycle showed the "break-in" effect discussed in Chapter 5. As expected, the peak current increases with increasing scan rate. Also the potential at which the maximum current response is recorded gradually increases.

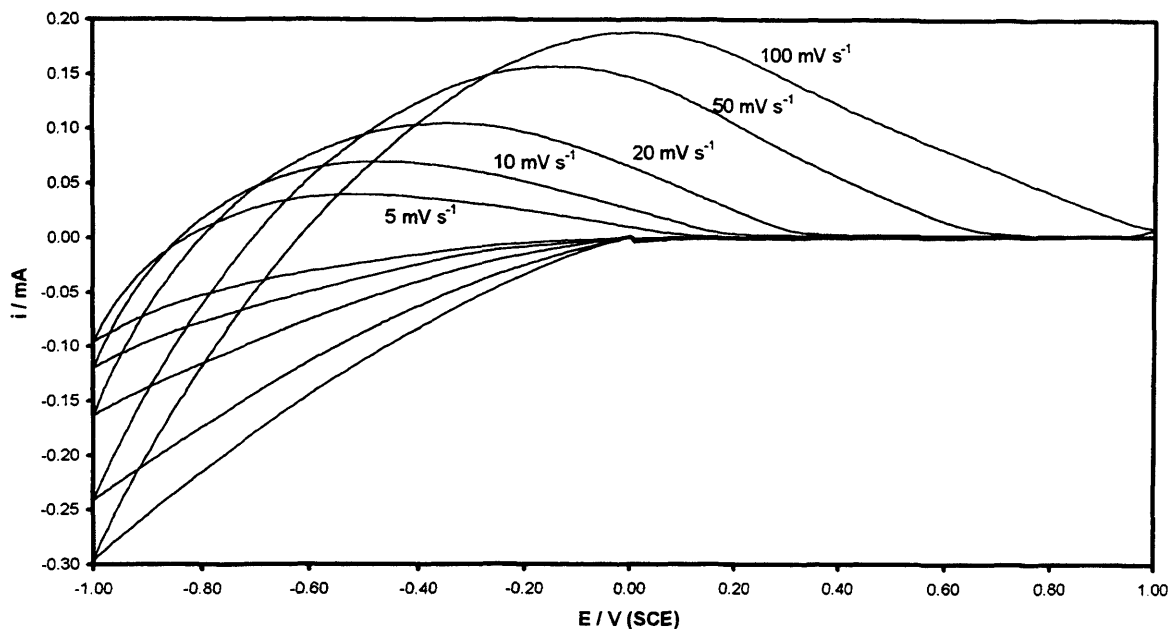


Figure 6.6 : Cyclic voltammogram showing Li^+ insertion into a 2700\AA thick WO_3 film at five different scan rates. Electrolyte : $0.1\text{M LiClO}_4/\text{propylene carbonate}$. Number of cycles recorded : 5 (1st cycle from each experiment shown for ease of comparison). Scan rates : $5\text{ mV s}^{-1} \rightarrow 100\text{ mV s}^{-1}$ (marked on plot).

All five scans have the same shape, which indicates that only Li^+ is being inserted when the WO_3 film is reduced. Reichman and Bard^[6] studied H^+ insertion into WO_3 films at different scan rates and current at a given potential was found to be proportional to $\nu^{1/2}$ at the slower scan rates studied ($1 - 50\text{ mV s}^{-1}$), with a smaller dependence at the higher scan rates of 100 and 200 mV s^{-1} . They implied that the electrochromic process studied for an amorphous WO_3 thin film is diffusion controlled at slow scan rates. This can be seen for WO_3 films cycled at scan rates between 5 and 50 mV s^{-1} in $0.1\text{M LiClO}_4/\text{propylene carbonate}$, $0.5\text{M LiClO}_4/\text{propylene carbonate}$ and $0.7\text{M LiClO}_4/\text{propylene carbonate}$.

It is not possible to use Equation [2.2.3] in the Theory chapter to calculate D_{Li^+} from the cyclic voltammetry experiments as, although the reduction of WO_3 is a reversible process, at the potential limits chosen here there is no defined reduction peak. Therefore,

the WO_3 film is not fully reduced and the oxidation peak seen upon scan reversal cannot be used to calculate D_{Li^+} .

6.3 EQCM MEASUREMENTS

6.3.1 Introduction

This section describes EQCM data obtained for the chronoamperometric experiments of the previous section. The mass response with respect to time was studied for the chronoamperometric experiments ($0\text{V} \rightarrow -1.0\text{V}$ and $0\text{V} \rightarrow -1.0\text{V} \rightarrow -0.4\text{V} \rightarrow 0\text{V}$) described in the previous section. We use this to explore the relationship between the mass change and the injected charge.

6.3.2 EQCM data

Figure 6.7 shows the mass change versus time response for the double potential step described in Section 6.2. For ease of explanation, the current versus time response has also been plotted. As in the previous two chapters, the zero of mass is defined as that for a fully oxidised WO_3 film; increases in the mass represent reduction of the film.

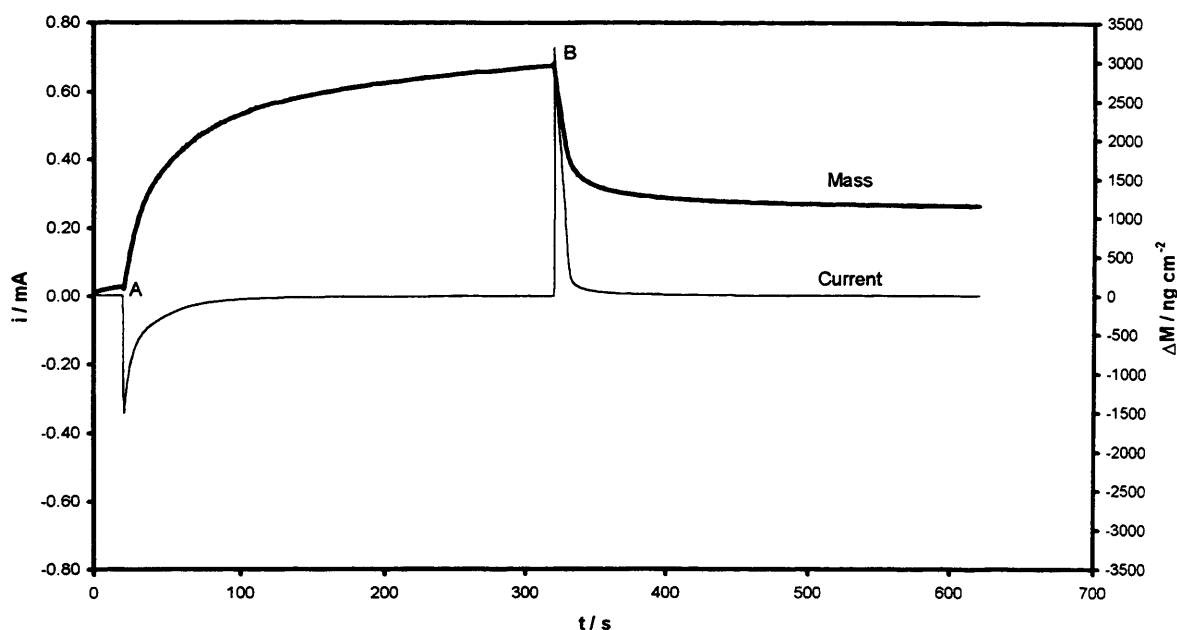


Figure 6.7 : Mass change versus time and current versus time responses for a double chronoamperometric experiment showing Li^+ insertion into a 2400\AA thick WO_3 film. Electrolyte : $0.1\text{M LiClO}_4/\text{propylene carbonate}$. Point A indicates step from $0\text{V} \rightarrow -1.0\text{V}$ for 300 seconds. Point B indicates step from $-1.0\text{V} \rightarrow 0\text{V}$ for 300 seconds. Mass and current responses marked on plot.

As the film is reduced, the mass increases, then decreases as the film is subsequently oxidised. It can be seen that there is a large increase in mass as the film is held at -1.0V where reduction of the WO_3 film is occurring. This increase does not appear to reach a steady value, even after 300 seconds have elapsed. As the current response at very long time scales (>200 seconds) appears to be very close to zero, then electroneutrality dictates that if there is no current being recorded, then there cannot be a charged species moving. Therefore, the only species which are moving are neutrals (ion pairs and/or solvent).

As the potential is stepped from 0V down to -1.0V , there is a slight decrease in mass. This effect is seen only for 0.4 seconds, and then the mass begins to increase. This effect has been seen by other authors and it has been suggested that for chronoamperometric experiments, at $t < 1$ second, anions are expelled from the electrode surface into the bulk of the electrolyte^[4]. Babinec^[7] stated that for cyclic voltammetric

experiments, an initial decrease in mass could be attributed to either the loss of WO_3 , the loss of H_2O from the WO_3 film or the expulsion of OH^- . Since the data acquisition time for the chronoamperometric experiments was 0.4 seconds, only two data points were recorded during the mass decrease outlined above. Therefore, we are unable to attribute any explanation to the results seen here and commented upon in ref^[4].

As the film is then reoxidised back to 0V, there is a sharp increase in mass, from the value recorded at the end the first step ($0\text{V} \rightarrow -1.0\text{V}$) which is seen for only 0.4 seconds. The mass then begins to decrease at a faster rate than that seen for reduction of the WO_3 film, and appears to reach a steady value after ≈ 250 seconds of oxidation, compared to the reduction of the film where no steady value was reached. At the end of the experiment, it can be seen that not all the mass is recovered from the WO_3 film. Calculations show that there is 1160ng cm^{-2} of mass remaining in the re-oxidised film at the end of the experiment.. This difference implies that incomplete oxidation of the WO_3 film has occurred and that there is a substantial amount of mass left in the WO_3 film in the form of Li^+ . This was also seen in the charge versus time responses in the previous section, where there is incomplete recovery of charge, implying that there is electronic charge left in the partially re-oxidised WO_3 film.

6.3.3 Mass change versus charge responses

As for cyclic voltammetry experiments, it is possible to plot the mass change against charge responses and measure the “end to end” $\Delta M_{\text{T}}F/Q_{\text{T}}$ values. Figure 6.8 shows the mass changes versus charge response for the double chronoamperometric experiment $0\text{V} \rightarrow -1.0\text{V} \rightarrow 0\text{V}$. Also shown on the plot is the ideal gradient of “ $7/F$ ” which is the slope expected to be seen if only Li^+ insertion was occurring during reduction of the WO_3 film.

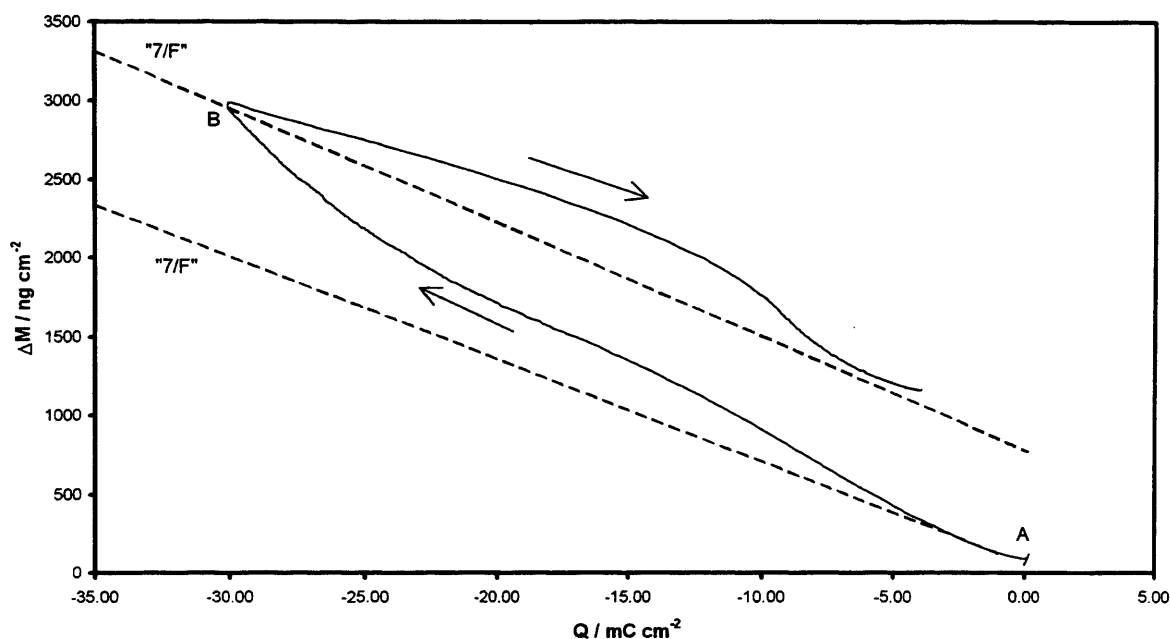


Figure 6.8 : Mass changes versus charge response for a double chronoamperometric experiment showing Li^+ insertion into a 2400\AA thick WO_3 film. Electrolyte : $0.1\text{M LiClO}_4/\text{propylene carbonate}$. Point A indicates step from $0\text{V} \rightarrow -1.0\text{V}$ for 300 seconds. Point B indicates step from $-1.0\text{V} \rightarrow 0\text{V}$ for 300 seconds. Ideal gradient of “7/F” marked as dotted line on plot.

This plot clearly shows that neither the mass changes, nor the calculated charge are totally recovered at the end of the experiment. It can also be seen very clearly that the plot is not linear and deviates from the ideal gradient of “7/F”, which implies a neutral species (ion pairs and/or propylene carbonate) entering and leaving the WO_3 film. Table 6.3 shows the “end to end” $\Delta M_{\text{T}}F/Q_{\text{T}}$ values for both the step down to -1.0V and the subsequent step back to 0V for the three various concentrations of $\text{LiClO}_4/\text{propylene carbonate}$ used. The “end to end” values are calculated from the times at which the potential was stepped ie, at 20 seconds and 320 seconds.

Table 6.3 : Table showing calculated “end to end” $\Delta M_T F / Q_T$ ratios reduction and re-oxidation for double chronoamperometric experiments (0V \rightarrow -1.0V \rightarrow 0V) carried out on WO₃ films .

[LiClO ₄] / M	$\Delta M_T F / Q_T$ / g mol ⁻¹	
	reduction	oxidation
0.1	-9.2	-6.8
0.5	-4.8	-5.3
0.7	-5.9	-5.8

If the mass change versus time and the corresponding current versus time response is plotted for the triple chronoamperometric experiment of 0V \rightarrow -1.0V \rightarrow -0.4V \rightarrow 0V, as seen in Figure 6.9, then it can be seen that as for the double chronoamperometric experiment there is a large increase in mass upon reduction of the WO₃ film. Again, the mass changes do not appear to reach a steady maximum after the WO₃ film is held at -1.0V for 300 seconds, although the current appears fallen to approximately zero. There is a small decrease in mass seen initially (for 0.4 seconds) as for the previous chronoamperometric experiment discussed above. When the reduced WO₃ film is then stepped from -1.0V up to -0.4V, there is a small increase in the mass changes seen for 0.4 seconds after the film is stepped. This mass change is very small (≈ 15 ng cm⁻²), but is seen for both the double and triple chronoamperometric experiments. The mass changes for oxidation decrease much quicker than the corresponding mass changes for reduction of the WO₃ film, which is seen also in the current versus time response.

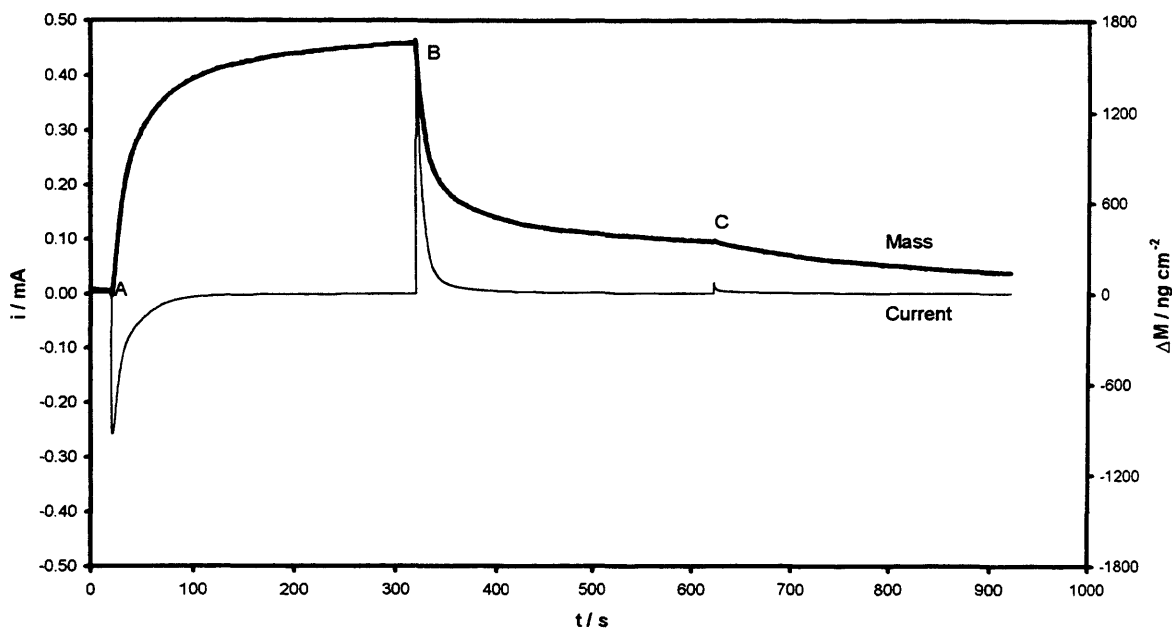


Figure 6.9 : Mass change versus time and current versus time responses for a triple chronoamperometric experiment showing Li^+ insertion into a 2400\AA thick WO_3 film. Electrolyte : $0.1\text{M LiClO}_4/\text{propylene carbonate}$. Point A indicates step from $0\text{V} \rightarrow -1.0\text{V}$ for 300 seconds. Point B indicates step from $-1.0\text{V} \rightarrow -0.4\text{V}$ for 300 seconds. Point C indicates step from $-0.4\text{V} \rightarrow 0\text{V}$ for 300 seconds. Mass changes and current responses marked on plot.

When the WO_3 film is finally stepped from -0.4V up to 0V again, there is only a slight change in the mass changes versus time response. At the end of the experiment, there is still a small amount of mass which appears to be left in the film ($\approx 206\text{ ng cm}^{-2}$), but it seems that the WO_3 film is almost fully re-oxidised at the end of the triple chronoamperometric experiment compared to that for the double chronoamperometric experiment. Although the WO_3 film is given twice as long to be reoxidised in the triple chronoamperometric experiment, it appears from the mass changes versus time response for the double chronoamperometric experiment that the mass would not return to zero.

Figure 6.10 shows the mass change versus charge response for the triple chronoamperometric experiment described above. It can be seen that both the mass change and charge responses almost return to zero upon oxidation of the WO_3 film. The ideal

gradient of “ γ/F ” is also plotted and the response again deviates from the ideal gradient, which implies that a neutral species is being inserted and expelled from the WO_3 film alongside Li^+ . From Chapter 4, it is suggested that the neutral species may be ion pairs or solvent, which may be entering the WO_3 film alongside Li^+ .

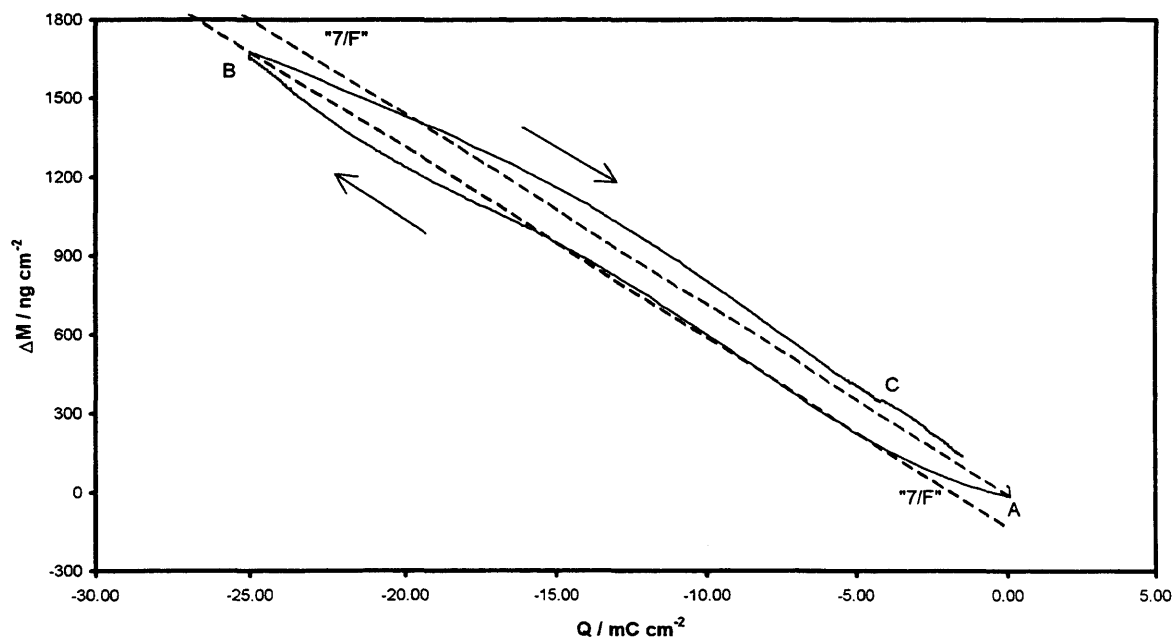


Figure 6.10 : Mass changes versus charge response for a triple chronoamperometric experiment showing Li^+ insertion into a 2400\AA thick WO_3 film. Electrolyte : $0.1\text{M LiClO}_4/\text{propylene carbonate}$. Point A indicates step from $0\text{V} \rightarrow -1.0\text{V}$ for 300 seconds. Point B indicates step from $-1.0\text{V} \rightarrow -0.4\text{V}$ for 300 seconds. Point C indicates step from $-0.4\text{V} \rightarrow 0\text{V}$ for 300 seconds. Ideal gradient of “ γ/F ” marked as dotted line on plot.

The “end to end” $\Delta M_{\text{T}}F/Q_{\text{T}}$ values can also be calculated for this experiment. The “end to end” values are taken as being the mass and charge responses at the moment that the WO_3 potential is “stepped” (20 seconds, 320 seconds and 620 seconds). Table 6.4 shows the $\Delta M_{\text{T}}F/Q_{\text{T}}$ values for the triple chronoamperometric experiment carried out in three concentrations of $\text{LiClO}_4/\text{propylene carbonate}$.

Table 6.4 : Table showing calculated “end to end” $\Delta M_T F / Q_T$ ratios reduction and re-oxidation for triple chronoamperometric experiments (0V \rightarrow -1.0V \rightarrow -0.4V \rightarrow 0V) carried out on WO₃ films .

[LiClO ₄] / M	$\Delta M_T F / Q_T$ / g mol ⁻¹		
	0V \rightarrow -1.0V	-1.0V \rightarrow -0.4V	-0.4V \rightarrow 0V
0.1	-6.4	-6.2	-0.01
0.5	-4.9	-5.0	-6.3
0.7	-5.3	-5.4	-6.6

It can be seen that for all three concentrations of LiClO₄/propylene carbonate the $\Delta M_T F / Q_T$ values are less than 7 g mol⁻¹, which may be due to an underestimation in the values as the “end to end” values do not take into account the curvature of the plots. For 0.5M LiClO₄/propylene carbonate and 0.7M LiClO₄/propylene carbonate, the $\Delta M_T F / Q_T$ values are all very similar, which implies that at the step -0.4V \rightarrow 0V, there is still a substantial amount of Li⁺ leaving the film.

6.3.4 Three-dimensional data analysis

As for the combined EQCM and spectroelectrochemical experiments shown in Chapter 5., it is possible to construct a 3-D plot of time, mass changes and charge for both the double and triple chronoamperometric experiment. Figure 6.11 shows the 3-D plot for the double chronoamperometric experiment carried out on a WO₃ film in 0.1M LiClO₄/propylene carbonate. As the WO₃ film is reduced by “stepping” down to -1.0V for 300 seconds, it can be seen that the charge response decreases, whilst the mass changes increase, as seen on the corresponding mass versus charge responses. The 3-D plot clearly shows that the relationship for the reduction of the WO₃ film in 0.1M LiClO₄/propylene carbonate is not linear, and that there is hysteresis. When the film is reoxidised by stepping back to 0V, again, the relationship is again not linear, and it can be seen clearly that there is

incomplete charge and mass recovery. This indicates that there is a substantial amount of Li^+ left in the WO_3 film after oxidation has taken place.

Figure 6.12 shows the 3-D plot for the triple chronoamperometric experiment carried out on a WO_3 film immersed in 0.1M LiClO_4 /propylene carbonate. Again, as for the double chronoamperometric experiment, on reduction of the WO_3 film, the relationship is not linear and does not have a $\Delta M_{\text{T}}F/Q_{\text{T}}$ value of 7 g mol^{-1} , indicating that there is more than one species entering and leaving the WO_3 film. As the film is stepped from -1.0V to -0.4V, the mass begins to decrease, and the charge response increases. Again, this relationship is not linear, which implies that there is a second species leaving the reduced tungsten bronze in parallel to Li^+ . The final part of the experiment (-0.4V to 0V) shows very little change in either the mass or charge responses.

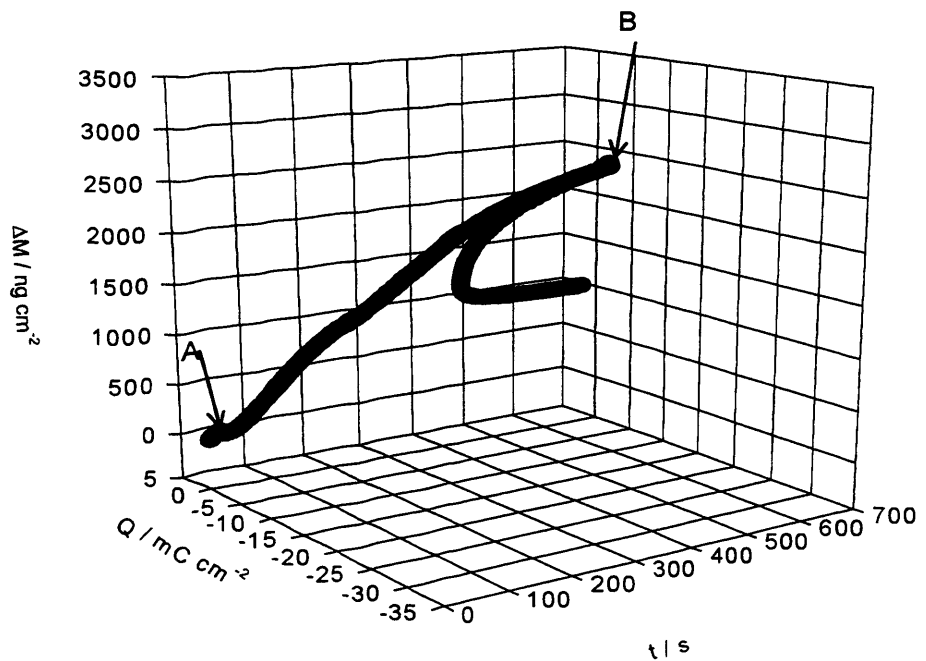


Figure 6.11 : 3-Dimensional plot showing the mass change, charge and time responses for a double chronoamperometric experiment showing Li^+ insertion into a 2400\AA thick WO_3 film. Electrolyte : 0.1M $\text{LiClO}_4/\text{propylene carbonate}$. Point A indicates step from $0\text{V} \rightarrow -1.0\text{V}$ for 300 seconds. Point B indicates step from $1.0\text{V} \rightarrow 0\text{V}$ for 300 seconds.

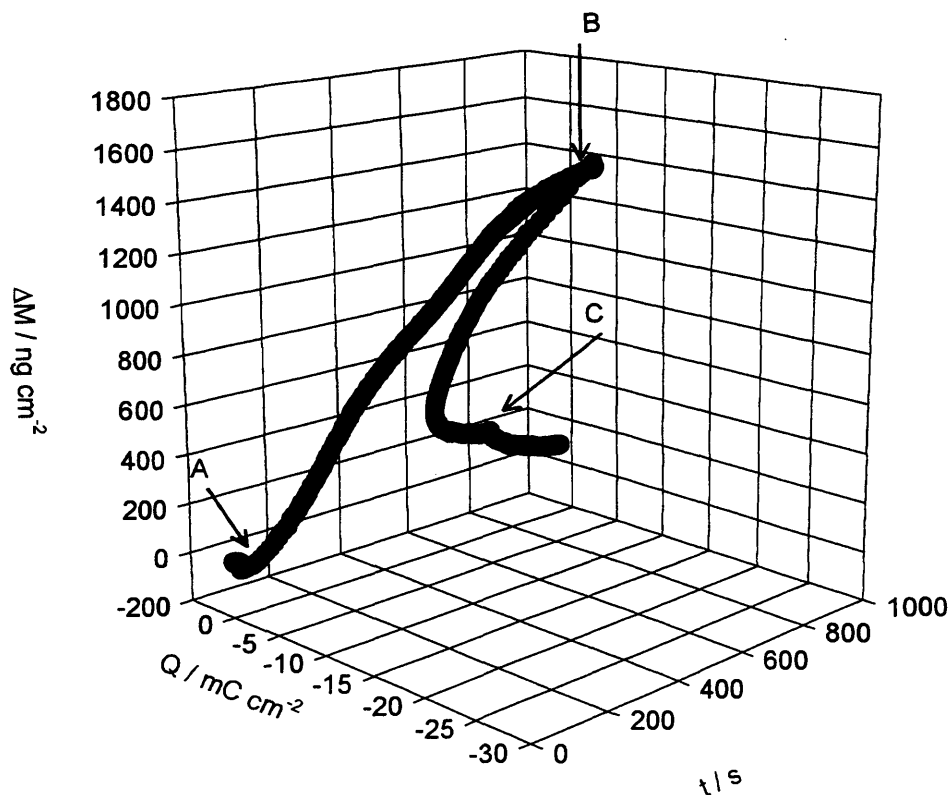


Figure 6.12 : 3-Dimensional plot showing the mass change, charge and time responses for a triple chronoamperometric experiment showing Li^+ insertion into a 2400\AA thick WO_3 film. Electrolyte : 0.1M $\text{LiClO}_4/\text{propylene carbonate}$. Point A indicates step from $0\text{V} \rightarrow -1.0\text{V}$ for 300 seconds. Point B indicates step from $1.0\text{V} \rightarrow -0.4\text{V}$ for 300 seconds. Point C indicates step from $-0.4\text{V} \rightarrow 0\text{V}$ for 300 seconds.

6.3.5 The “break-in” effect

As discussed in Chapter 5, the initial, slow (5 mV s^{-1}) scan of a new WO_3 film shows different current and mass responses. This effect has been termed the “break-in” effect by previous authors^[8], and has been seen for the reduction of WO_3 films during these sets of experiments. The chronoamperometric experiments were also carried out on new WO_3 films, i.e. films that had not been cycled prior to any chronoamperometric experiment, and to probe the “break-in”. As the films were gradually “stepped” down to more negative potentials, it has been seen that there is incomplete recovery of both the mass changes and the charge. Therefore, it appears that the “break-in” effect is being seen as the WO_3 films are being reduced further during each experiment. This would explain the fact that for the double chronoamperometric experiment described above ($0\text{V} \rightarrow -1.0\text{V}$) neither the mass nor the charge response returns back to zero.

In addition to the triple chronoamperometric experiments, at the end of each set of experiments, the WO_3 film was again stepped down to -1.0V for 300 seconds before being stepped back to 0V for a further 300 seconds (a second double chronoamperometric experiment). Therefore, it is possible to compare the current versus time and mass versus time responses for the same WO_3 film, but for experiments carried out both before and after “break-in”. For ease of comparison, the first experiment (pre-“break-in”) where the potential was stepped from $0\text{V} \rightarrow -1.0\text{V}$ has been labelled experiment I and the second chronoamperometric experiment (post-“break-in”) under identical conditions has been labelled experiment II.

Figure 6.13 shows the current versus time responses for experiments I and II. It can be seen that in experiment I there appears to be more current passed as the WO_3 film is reduced compared to that for experiment II. On reduction of the WO_3 film, both plots show that the current does not appear fall to zero until ≈ 130 seconds. When the tungsten

bronze is reoxidised by stepping back to 0V, the current responses are very similar. Both plots clearly show that oxidation of the WO_3 film occurs at a faster rate than reduction. The current versus time responses for experiment I and experiment II are superimposable, which shows that there is very little difference between either experiment. Therefore, the “break-in” effect cannot be easily seen using current versus time responses.

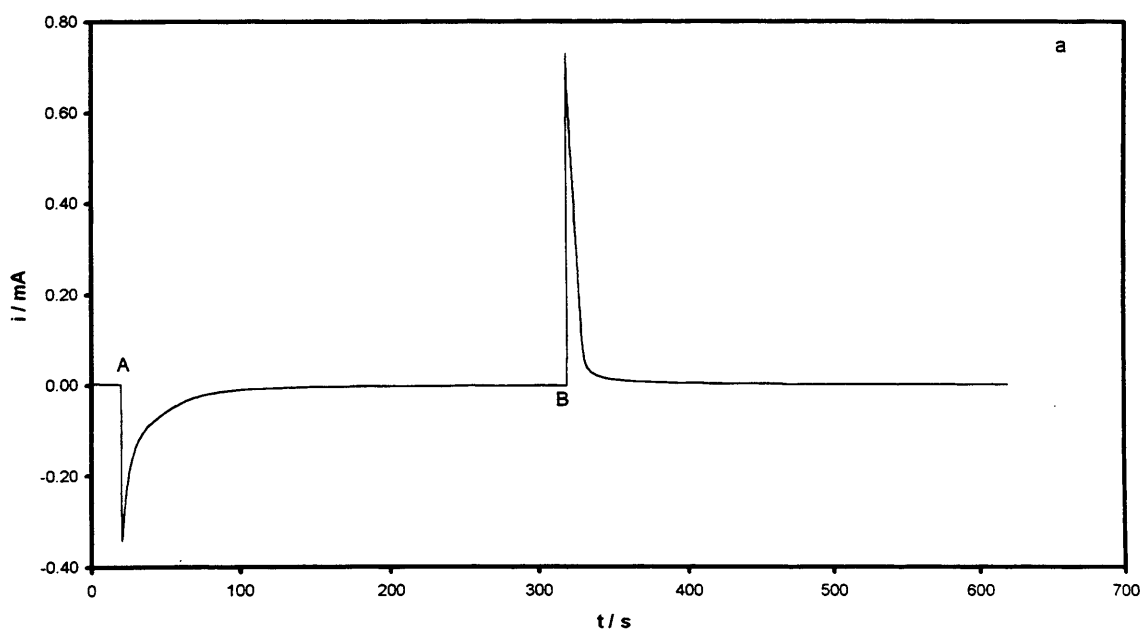
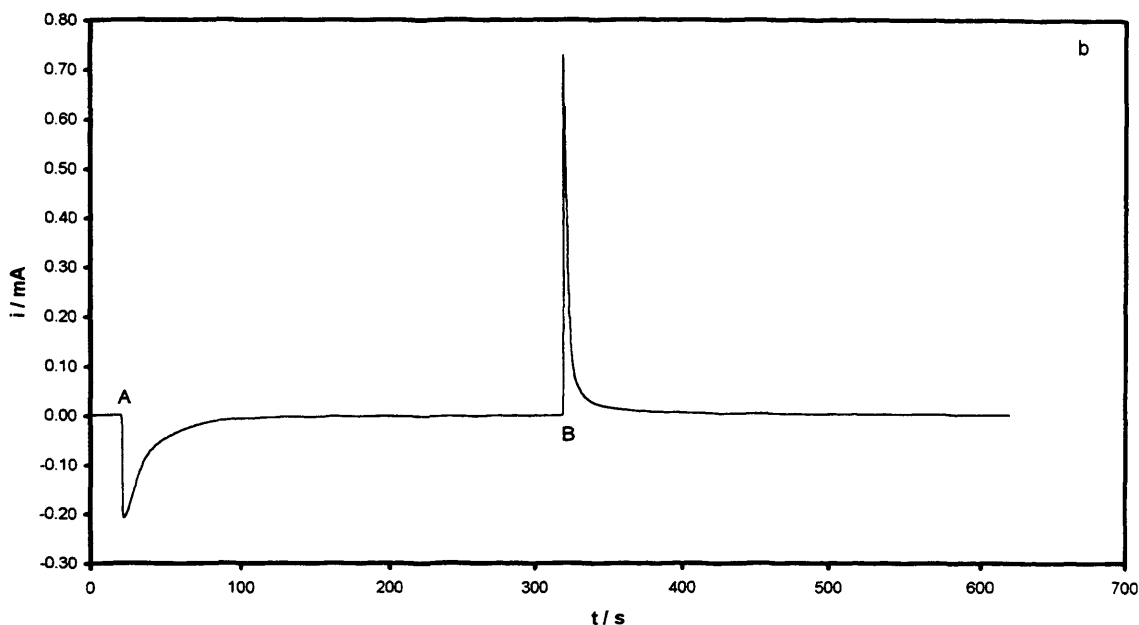


Figure 6.13 : Current versus time response for a double chronoamperometric experiment showing Li^+ insertion into a 2400\AA thick WO_3 film. Electrolyte : $0.1\text{M LiClO}_4/\text{propylene carbonate}$. Point A indicates step from $0\text{V} \rightarrow -1.0\text{V}$ for 300 seconds. Point B indicates step from $-1.0\text{V} \rightarrow 0\text{V}$ for 300 seconds. Experiment I shown in figure 6.13a. Experiment II shown in figure 6.13b.



Since the current versus time responses do not show much difference in the two experiments, then by integrating the current with respect to time, it is possible to compare the charge versus time plots for experiments I and II as shown in Figure 6.14. It can be clearly seen that there is a difference between the two experiments. During experiment I there is more charge passed upon reduction of the WO_3 film, and this charge is not completely recovered at the end of the experiment. In experiment II less charge is passed (77% of the total charge passed in experiment I), but upon re-oxidation, there appears to be almost the same amount of charge recovered as in experiment I. It is not possible to establish whether the charge recorded at the end of experiment I equals the initial amount of charge passed at the beginning of experiment II. This is because at the beginning of each experiment the initial charge value is defined at being 0 mC cm^{-2} . Therefore, a comparison between the two experiments in this way is not possible.

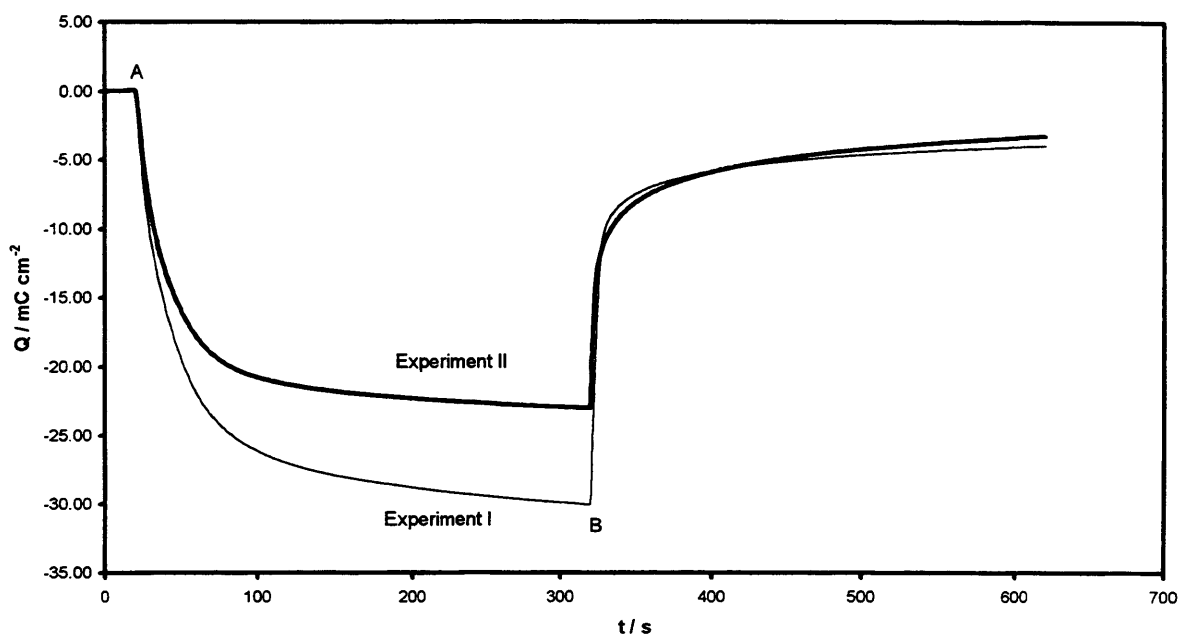


Figure 6.15 : Charge versus time responses for a double chronoamperometric experiment showing Li^+ insertion into a 2400\AA thick WO_3 film for experiment I and experiment II. Electrolyte : 0.1M $\text{LiClO}_4/\text{propylene carbonate}$. Point A indicates step from $0\text{V} \rightarrow -1.0\text{V}$ for 300 seconds. Point B indicates step from $-1.0\text{V} \rightarrow 0\text{V}$ for 300 seconds. Charge responses for experiment I and experiment II marked on plot.

The response showing mass changes versus time for experiments I and II is shown in Figure 6.16. It can be seen that both mass responses do not reach a steady value on reduction of the WO_3 film, even though the current versus time responses show that there is very little current being passed after ≈ 130 seconds. The mass values recorded after the film has been held at -1.0V for 300 seconds show that the mass changes for experiment I are over twice as big as those mass changes recorded at the same time for experiment II. When the film is reoxidised back to 0V , it appears that less mass is not recovered in experiment II than I, which implies that there is still a small amount of Li^+ inside the WO_3 film after oxidation, but the amount is not as much as seen in experiment I. Again, as for the charge versus time data, it is not possible to directly compare the two experiments as the mass values at the beginning of each experiment are set effectively to zero.

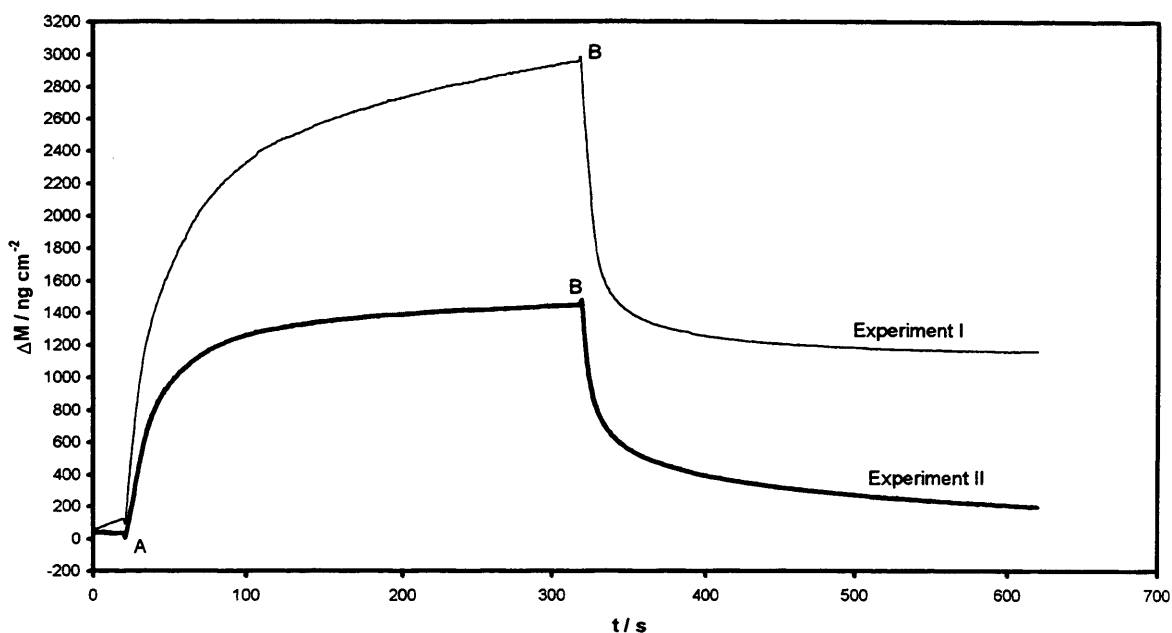


Figure 6.15 : Mass changes versus time responses for a double chronoamperometric experiment showing Li^+ insertion into a 2400\AA thick WO_3 film for experiment I and experiment II. Electrolyte : $0.1\text{M LiClO}_4/\text{propylene carbonate}$. Point A indicates step from $0\text{V} \rightarrow -1.0\text{V}$ for 300 seconds. Point B indicates step from $-1.0\text{V} \rightarrow 0\text{V}$ for 300 seconds. Mass responses for experiment I and experiment II marked on plot.

It is possible to compare the mass changes versus charge response for experiments I and II, and from this data obtain “end to end” $\Delta M_{\text{T}}F/Q_{\text{T}}$ values for both the reduction and oxidation of the WO_3 film being investigated. Figure 6.16 shows the plots obtained from experiments I and II. Both plots are non linear and do not have a calculated “end to end” $\Delta M_{\text{T}}F/Q_{\text{T}}$ value of exactly 7 g mol^{-1} . This data indicates that there is a second, neutral species entering and leaving the WO_3 film alongside Li^+ . It can be seen that at the completion of experiment II, there is less charge not recovered than at the end of experiment I. As has been mentioned above, the mass changes recorded for experiment II are also nearer to zero at the end of the experiment. This indicates that there is still a small amount of Li^+ left in the film at the end of experiment II, but not as much as seen at the end

of experiment I. As seen above, a direct comparison between the two experiments is not possible.

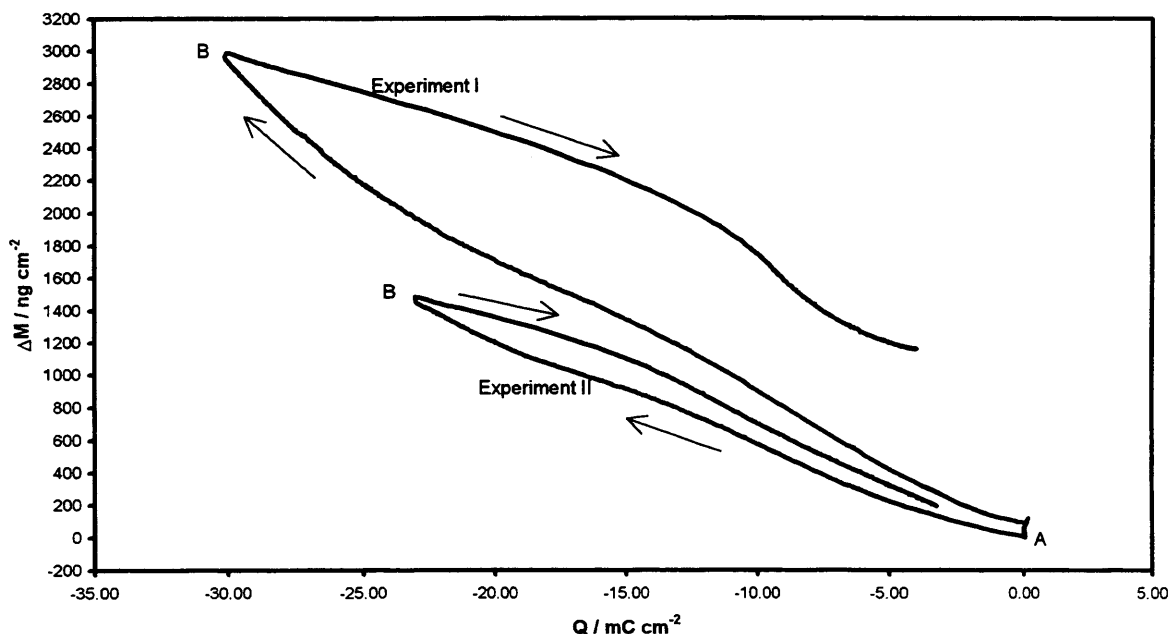


Figure 6.16 : Mass changes versus charge responses for a double chronoamperometric experiment showing Li^+ insertion into a 2400\AA thick WO_3 film for experiment I and experiment II. Electrolyte : 0.1M $\text{LiClO}_4/\text{propylene carbonate}$. Point A indicates step from $0\text{V} \rightarrow -1.0\text{V}$ for 300 seconds. Point B indicates step from $-1.0\text{V} \rightarrow 0\text{V}$ for 300 seconds. Responses for experiment I and experiment II marked on plot.

The “end to end” $\Delta M_{\text{T}}F/Q_{\text{T}}$ values can be calculated and are shown in Table 6.5 for the three various concentrations of $\text{LiClO}_4/\text{propylene carbonate}$ used to study the effect of chronoamperometric experiments on WO_3 films.

Table 6.5 : Table showing calculated “end to end” $\Delta M_{\text{T}}F/Q_{\text{T}}$ values for the double chronoamperometric experiment ($0\text{V} \rightarrow -1.0\text{V} \rightarrow 0\text{V}$) for a WO_3 film. Reduction and re-oxidation values shown for experiments I and II at three different concentrations of LiClO_4 .

Experiment	$\Delta M_{\text{T}}F/Q_{\text{T}} / \text{g mol}^{-1}$			
	I		II	
$[\text{LiClO}_4] / \text{M}$	reduction	oxidation	reduction	oxidation
0.1	-9.2	-6.8	-6.1	-6.3
0.5	-4.8	-5.3	-4.9	-5.7
0.7	-5.9	-5.8	-5.2	-6.7

For the experiment carried out in 0.1M LiClO₄/propylene carbonate, the $\Delta M_{TF}/Q_T$ values obtained for the reduction of the WO₃ film in experiment I are larger than those for experiment II, indicating that here may be more Li⁺ entering the WO₃ film during the “break-in” experiment, which is not fully extracted and therefore is still in the WO₃ film when experiment II is carried out. For the experiments carried out in 0.5M LiClO₄/propylene carbonate and 0.7M LiClO₄/propylene carbonate, the “end to end” $\Delta M_{TF}/Q_T$ values are smaller than 7 g mol⁻¹, as seen in table 6.3, and there may be more neutral species entering the WO₃ film than in 0.1M LiClO₄/propylene carbonate.

6.3.6 Mass responses from cyclic voltammetric data shown with respect to time

As seen in the previous section, the effect of time scale can also be investigated using cyclic voltammetric experiments by changing the scan rate. As the two previous chapters have shown, the EQCM can measure mass changes which can then be plotted as a function of potential to investigate the species entering and leaving a WO₃ film. Figure 6.17 shows mass change versus potential response for five different scan rates for a WO₃ film cycled in 0.1M LiClO₄/propylene carbonate. As for the current responses shown in Figure 6.6 the second cycle at 5 mV s⁻¹ is shown as the initial cycle showed the “break-in” effect as discussed in Chapter 5.

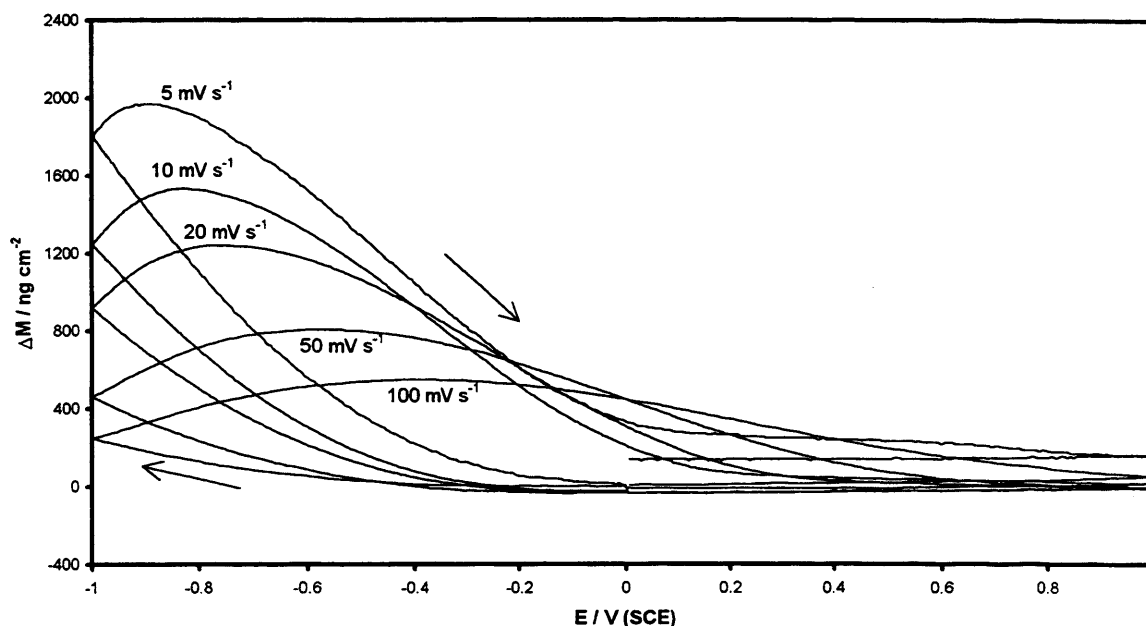


Figure 6.17 : Mass change versus potential responses for cyclic voltammetric experiments showing Li^+ insertion into a 2700\AA thick WO_3 film at five different scan rates. Electrolyte : $0.1\text{M LiClO}_4/\text{propylene carbonate}$. Total number of cycles recorded : 5 (one cycle from each experiment shown for ease of comparison). Scan rates : $5\text{ mV s}^{-1} \rightarrow 100\text{ mV s}^{-1}$ (marked on plot).

It can be seen that for all scan rates studied, the responses have a similar shape. At the slowest scan rate measured, there is more time for Li^+ to enter the WO_3 film than at the faster scan rates, and therefore the mass changes are larger. Although the five responses shown all have a similar shape, at the faster scan rates (50 mV s^{-1} and 100 mV s^{-1}), there are still substantial mass changes being recorded at relatively positive potentials, whereas for the slower scan rates there appears to be very little mass change for potentials positive of $+0.4\text{V}$ on the anodic half cycle. This effect is expected, as the Li^+ entering at WO_3 film at the faster scan rates has less time to leave as oxidation of the film begins. With the exception of the mass change versus potential response at 5 mV s^{-1} , the recorded mass change at 0V at completion of the recorded cycle appears to be very close to its original value. This indicates that there is only a small amount of Li^+ trapped inside the WO_3 film

after completion of the cycle at scan rates faster than 10 mV s^{-1} , but there is an accumulation of Li^+ seen at 5 mV s^{-1} .

Figure 6.18 shows the mass change versus charge response for cyclic voltammetric experiments carried out on a WO_3 film cycled in $0.1\text{M LiClO}_4/\text{propylene carbonate}$ at 10 mV s^{-1} and 100 mV s^{-1} .

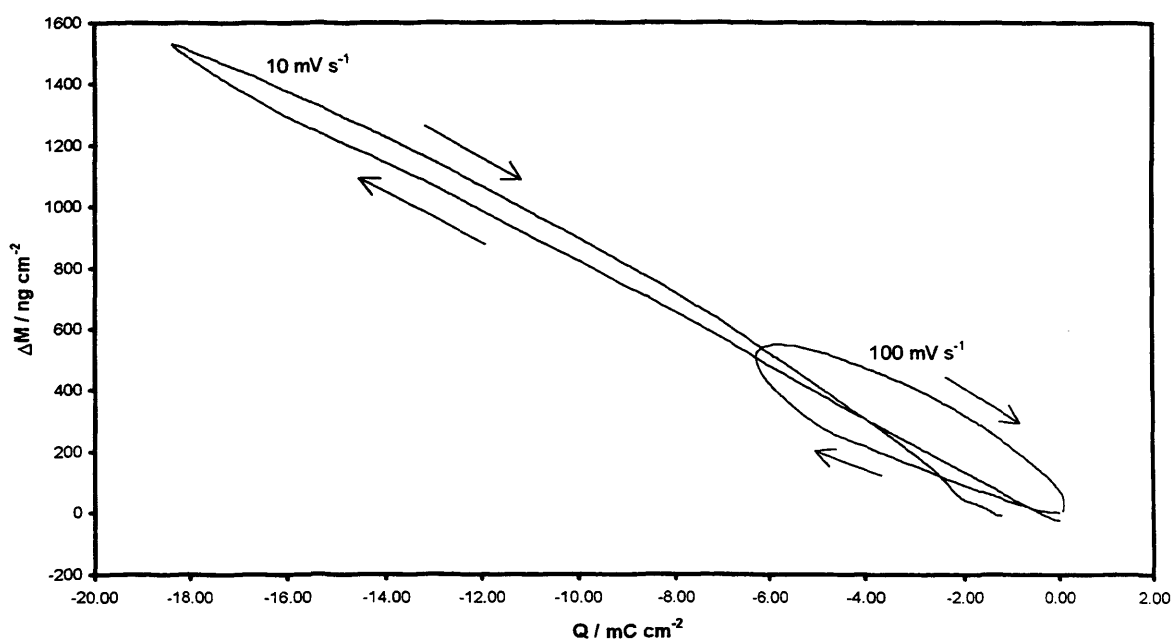


Figure 6.18 : Mass changes versus charge responses for cyclic voltammetric experiments showing Li^+ insertion into a 2700\AA thick WO_3 film at two different scan rates. Electrolyte : $0.1\text{M LiClO}_4/\text{propylene carbonate}$. Total number of cycles recorded : 5 (one cycle from each experiment shown for ease of comparison). Scan rates : 10 mV s^{-1} and 100 mV s^{-1} .

If the plot at 10 mV s^{-1} is studied, it can be seen that there is a small amount of hysteresis seen, which indicates the presence of a second, neutral species (propylene carbonate and/or ion pairs) entering and leaving the WO_3 film. The response for the experiment carried out at 100 mV s^{-1} shows much more hysteresis and there is only approximately a third of the charge entering the WO_3 film compared to the experiment at 10 mV s^{-1} . The film when cycled at 10 mV s^{-1} does not show complete charge or mass

recovery. This indicates that at this scan rate there is a small amount of Li^+ left in the film, whereas at 100 mV s^{-1} , both the mass change and charge response have returned to approximately zero, which shows that whatever entered the film also left it by the end of the cycle. Tables 6.6 and 6.7 show the “end to end” $\Delta M_{\text{T}}F/Q_{\text{T}}$ values calculated for both reduction and oxidation of a WO_3 film cycled at five different scan rates; carried out in three different concentrations of LiClO_4 /propylene carbonate.

Table 6.6 : Table showing calculated “end to end” $\Delta M_{\text{T}}F/Q_{\text{T}}$ values for reduction of WO_3 films cycled in three different concentrations of LiClO_4 at five different scan rates.

[LiClO_4] / M	$\Delta M_{\text{T}}F/Q_{\text{T}} / \text{g mol}^{-1}$				
	$\nu / \text{mV s}^{-1}$				
	5	10	20	50	100
0.1	-7.2 ± 1.0	-8.3 ± 0.1	-8.6 ± 0.0	-8.4 ± 0.0	-7.4 ± 0.2
0.5	-7.8 ± 0.9	-7.2 ± 0.1	-6.6 ± 0.0	-6.1 ± 0.0	-5.4 ± 0.0
0.7	-7.3 ± 1.3	-8.2 ± 0.1	-8.3 ± 0.1	-7.9 ± 0.1	-6.9 ± 0.1

Table 6.7 : Table showing calculated “end to end” $\Delta M_{\text{T}}F/Q_{\text{T}}$ values for oxidation of WO_3 films cycled in three different concentrations of LiClO_4 at five different scan rates.

[LiClO_4] / M	$\Delta M_{\text{T}}F/Q_{\text{T}} / \text{g mol}^{-1}$				
	$\nu / \text{mV s}^{-1}$				
	5	10	20	50	100
0.1	-9.1 ± 0.6	-8.5 ± 0.1	-8.7 ± 0.0	-8.4 ± 0.0	-7.3 ± 0.0
0.5	-6.7 ± 0.7	-7.0 ± 0.1	-6.5 ± 0.0	-6.1 ± 0.0	-5.5 ± 0.1
0.7	-8.4 ± 0.3	-8.4 ± 0.1	-8.4 ± 0.1	-8.0 ± 0.1	-6.8 ± 0.1

It can be seen that with changing both variables (time scale and concentration) the $\Delta M_{\text{T}}F/Q_{\text{T}}$ values calculated appear mostly to be greater than the expected 7 g mol^{-1} for pure Li^+ insertion. As the scan rate increases (time scale shortens), then the “end to end” $\Delta M_{\text{T}}F/Q_{\text{T}}$ values decrease for both reduction and oxidation of the WO_3 film. This implies that there appears to be a smaller amount of Li^+ entering the film, and also less neutral species, as the mass change versus charge responses show more hysteresis at the faster scan

rates. Therefore, it appears that at slow scan rates there is a more favourable amount of Li^+ being inserted into the WO_3 film. On oxidation of the film, the mass change and charge responses do not return to their original values at the slow scan rates studied. This indicates that there is some Li^+ left in the film. At the faster scan rates however, it appears that the mass change and charge responses return a value close to their original starting value, which indicates that nearly all the Li^+ which entered the film also left on oxidation. The lower $\Delta M_{\text{T}}/Q_{\text{T}}$ values and hysteresis seen on the mass versus charge responses indicate that any propylene carbonate which enters the WO_3 film upon reduction is expelled later than the corresponding Li^+ . Therefore at faster scan rates it is clearly seen that Li^+ transfer dominates the overall insertion process.

6.4 EFFECT OF CATION

6.4.1 Introduction

This section describes chronoamperometric experiments using a different electrolyte, namely NaClO_4 /propylene carbonate. As for experiments carried out using LiClO_4 /propylene carbonate as the electrolyte, three different concentrations of NaClO_4 /propylene carbonate were studied, although in this section, only 0.1M NaClO_4 /propylene carbonate will be discussed. As for the previous sections, the effect of varying timescale in both chronoamperometric experiments and cyclic voltammetry will be discussed.

6.4.2 Chronoamperometric experiments

As in Section 6.2.2 where Li^+ insertion into a WO_3 film was studied, the two chronoamperometric experiments discussed here will have identical potential limits

(0V → -1.0V → 0V and 0V → -1.0V → -0.4V → 0V). Figure 6.19 shows the mass change versus time and current versus time responses for the double chronoamperometric experiment. The current response for reduction of the WO₃ film is smaller than for the corresponding chronoamperometric experiment carried out using 0.1M LiClO₄/propylene carbonate as the electrolyte, but as Chapter 4 showed for cyclic voltammetric experiments, there is usually less current recorded for reduction of a WO₃ film using 0.1M NaClO₄/propylene carbonate. When the potential is stepped back to 0V, there is more current passed, but this is still smaller than for the corresponding experiment described in Section 6.2.2. The current changes more rapidly after the initial potential step to -1.0V compared to the identical experiment carried out in 0.1M LiClO₄/propylene carbonate. On oxidation of the tungsten bronze, again the current response decays quickly and a steady response is seen after ≈150 seconds.

Calculated D_{Na^+} values are shown in Table 6.8. The i versus $t^{1/2}$ plots for Na⁺ insertion into WO₃ films are linear and so calculation of D_{Na^+} is possible. It can be seen that the values are smaller than those for D_{Li^+} but it has been shown by other authors that $D_{Li^+} \gg D_{Na^+}$ ^{[2][9]}, indicating that Li⁺ diffuses faster into a WO₃ film than Na⁺.

Table 6.8 : Table showing D_{Na^+} values for chronoamperometric experiments carried out on a WO₃ film in 0.1M NaClO₄/propylene carbonate.

E / V 0V →	D_{Na^+} / x 10 ⁻¹³ cm ² s ⁻¹
-0.6	4.92
-0.7	4.96
-0.8	6.18
-0.9	9.19
-1.0	12.3

The x values for Na⁺ insertion can also be calculated. These are given in Table 6.9.

As for the cyclic voltammogram experiments discussed in Chapter 4, these values are lower

than those for Li^+ insertion, indicating that colouration of a WO_3 film by Na^+ is not as optically favourable as with Li^+ .

Table 6.9 : Table showing the x values calculated from chronoamperometric experiments carried out on a WO_3 film in 0.1M NaClO_4 /propylene carbonate. x values obtained from charge data at the end of reduction and re-oxidation.

E / V 0V →	x values at reduction	the end of oxidation
-0.1	0.01	0.01
-0.2	0.01	0.01
-0.3	0.02	0.02
-0.4	0.02	0.02
-0.5	0.02	0.02
-0.6	0.03	0.03
-0.7	0.05	0.03
-0.8	0.07	0.05
-0.9	0.10	0.06
-1.0	0.13	0.07

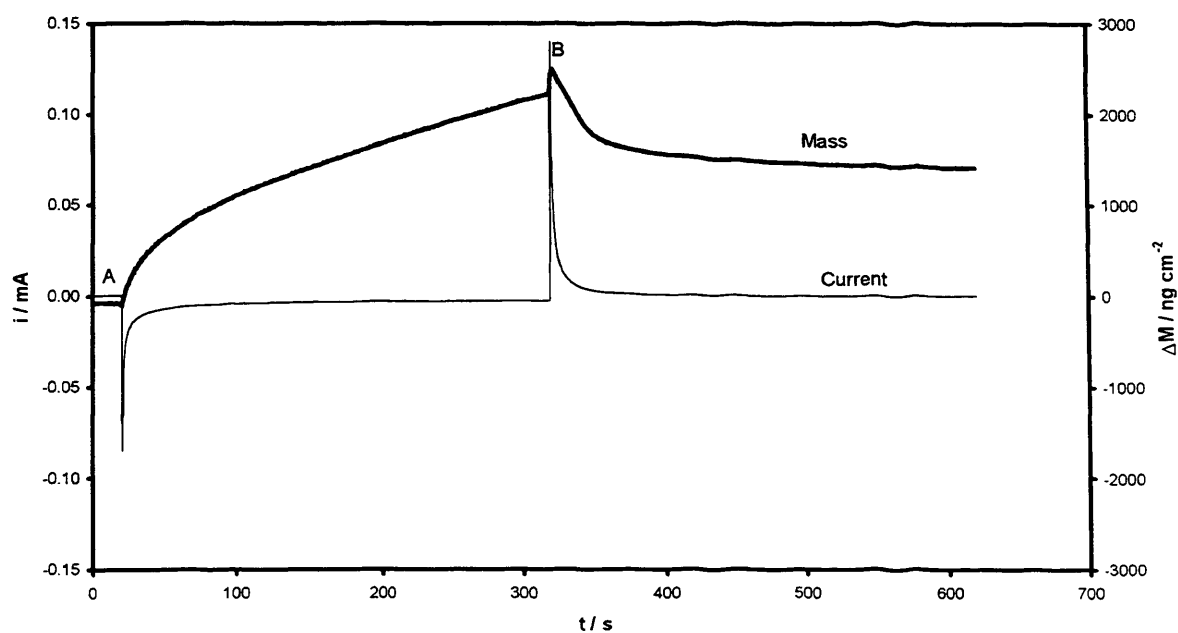


Figure 6.19 : Mass change versus time and current versus time responses for a double chronoamperometric experiment showing Na^+ insertion into a 2400\AA thick WO_3 film. Electrolyte : 0.1M NaClO_4 /propylene carbonate. Point A indicates step from 0V → -1.0V for 300 seconds. Point B indicates step from -1.0V → 0V for 300 seconds. Mass change and current responses marked on plot.

On the step down to -1.0V , the mass initially decreases for 0.4 seconds, as seen at the same point in the experiment described in Section 6.2.2. On holding the WO_3 film at -1.0V for 300 seconds, the mass steadily increases and does not reach a constant value, indicating that after 300 seconds, ions are still being inserted into the film. On re-oxidation at 0V , the mass increases sharply for ≈ 2.0 seconds, as seen for the same experiment in $0.1\text{M LiClO}_4/\text{propylene carbonate}$. As for Section 6.2.2, there are not enough data points recorded to make a reasonable assumption regarding these mass changes. The mass response does not return to the original value of 0 ng cm^{-2} after the experiment has finished, but remains at $\approx 1412\text{ ng cm}^{-2}$. The response reaches this value after 280 seconds of re-oxidation and 36% of the injected Na^+ and propylene carbonate appears to be left in the WO_3 film after the end of the experiment.

The mass change versus time and current versus time responses for the triple chronoamperometric experiment are shown in Figure 6.20. As the WO_3 film is reduced by stepping down to -1.0V , there is a large current spike of -1.519mA initially and the current response gradually increases and appears to reach a steady value of zero ≈ 200 seconds. On stepping from $-1.0\text{V} \rightarrow -0.4\text{V}$, again, there appears to be a steady value of zero seen after ≈ 150 seconds. On the final step ($-0.4\text{V} \rightarrow 0\text{V}$), the current versus time response appears more defined than for the identical experiment carried out in $0.1\text{M LiClO}_4/\text{propylene carbonate}$. again, this response decays and a value of zero is reached after ≈ 100 seconds. This final current response may be due to the fact that there is still a significant amount of Na^+ remaining in the WO_3 film after the film is stepped to -0.4V , compared to that seen for a WO_3 film in $0.1\text{M LiClO}_4/\text{propylene carbonate}$.

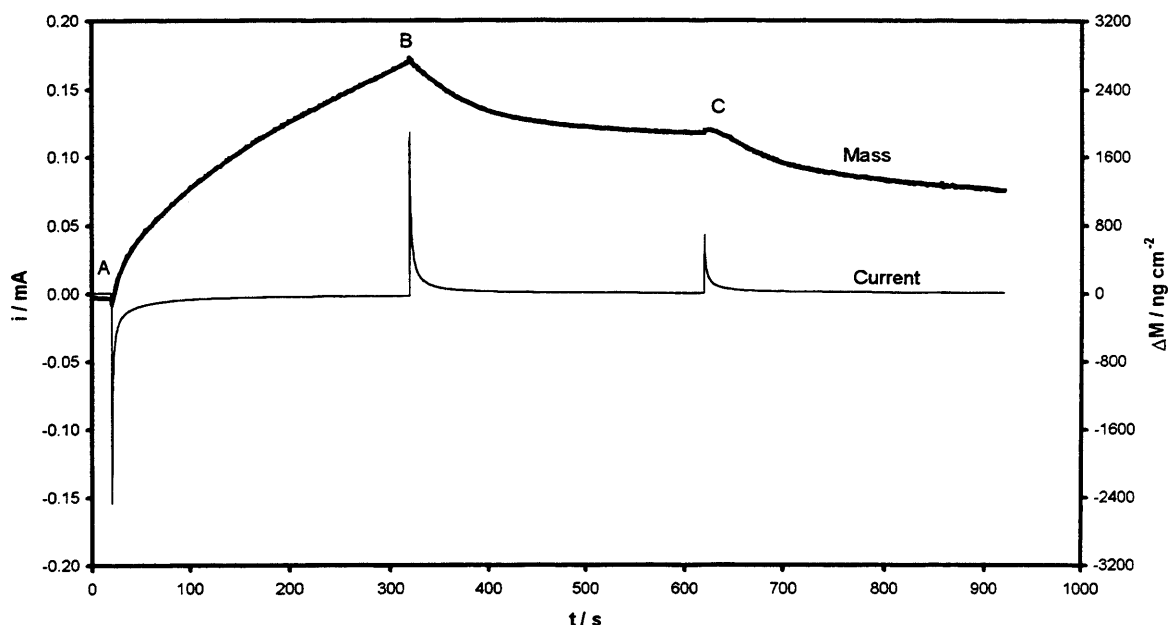


Figure 6.20 : Mass change versus time and current versus time responses for a triple chronoamperometric experiment showing Na^+ insertion into a 2400\AA thick WO_3 film. Electrolyte : $0.1\text{M NaClO}_4/\text{propylene carbonate}$. Point A indicates step from $0\text{V} \rightarrow -1.0\text{V}$ for 300 seconds. Point B indicates step from $-1.0\text{V} \rightarrow -0.4\text{V}$ for 300 seconds. Point C indicates step from $-0.4\text{V} \rightarrow 0\text{V}$ for 300 seconds. Mass change and current responses marked on plot.

The mass versus time response shows a small decrease in the mass for 0.4 seconds when the film is stepped down from $0\text{V} \rightarrow -1.0\text{V}$. The mass response again rises during reduction of the WO_3 film as seen for the double chronoamperometric experiment and reaches a maximum value of 2721 ng cm^{-2} . On the first oxidation ($-1.0\text{V} \rightarrow -0.4\text{V}$), a slight mass increase is seen for 0.8 seconds, but as the film is held at -0.4V , the mass decreases and reaches a steady value of $\approx 1880\text{ ng cm}^{-2}$ at the end of this second step. On the final step from $-0.4\text{V} \rightarrow 0\text{V}$, a mass increase is recorded for 4.0 seconds until the response begins to decrease. At the end of the experiment, the mass does not returned to zero; and the final mass change is 1205 ng cm^{-2} . This value is 56% of the mass change recorded at the end of the first potential step. Therefore, it can be seen that there is a significant amount of Na^+ and neutral species left in the WO_3 film. This is an interesting comparison to the

identical set of experiments carried out in 0.1M LiClO₄/propylene carbonate, where at the end of the triple chronoamperometric experiment, the mass change appears to have left returned to approximately zero, indicating expulsion of a majority of Li⁺ and propylene carbonate. It was seen in Chapter 4. that there is the suggestion that there is a larger amount of neutral species (as ions pairs and/or propylene carbonate) entering and leaving the WO₃ film alongside Na⁺ compared to the amount entering alongside Li⁺.

As for the sets of experiments carried out in 0.1M LiClO₄/propylene carbonate, the mass change versus charge responses can also be plotted. Figure 6.21 shows the response for the double chronoamperometric experiment, together with the ideal gradient of “23/F” expected for pure Na⁺ insertion. It can be seen that on the first step (0V → -1.0V), the response is almost linear, although it is seen to deviate from the ideal gradient and gives an “end to end” $\Delta M_{TF}/Q_T$ value of -32.0 g mol⁻¹. This value is greater than the value of 23 g mol⁻¹ expected for pure Na⁺ insertion and therefore it appears that there is a second species entering the WO₃ film alongside Na⁺. It appears that regardless of electrochemical experiment carried out, neutral species are seen to enter the WO₃ film upon cation insertion.

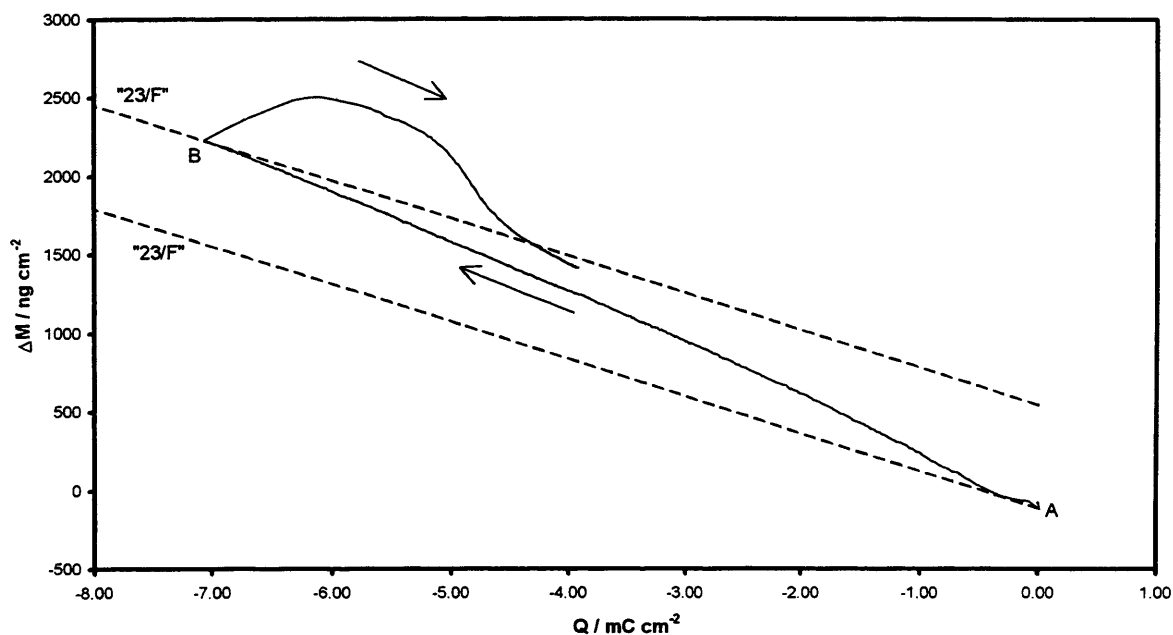


Figure 6.21 : Mass change versus charge response for a double chronoamperometric experiment showing Na^+ insertion into a 2400\AA thick WO_3 film. Electrolyte : $0.1\text{M NaClO}_4/\text{propylene carbonate}$. Point A indicates step from $0\text{V} \rightarrow -1.0\text{V}$ for 300 seconds. Point B indicates step from $-1.0\text{V} \rightarrow 0\text{V}$ for 300 seconds. Ideal gradient of “23/F” marked as dotted line on plot.

When the reduced WO_3 film is re-oxidised at 0V , the mass change versus charge response is not linear, and again there is deviation seen from the ideal gradient. It therefore appears that both Na^+ and propylene carbonate are leaving the WO_3 film upon re-oxidation. Again the “end to end” $\Delta M_{\text{T}}F/Q_{\text{T}}$ value can be calculated, although due to the curvature of the response, it will be a poor guide to the underlying process. The “end to end” $\Delta M_{\text{T}}F/Q_{\text{T}}$ value is -27.0 g mol^{-1} , ie, greater than 23 g mol^{-1} , implying that there are two species leaving the film. At the end of the experiment, it can be seen that there is a large amount of both mass and charge remaining in the re-oxidised film, which indicates that some inserted species remain in the film.

The mass versus charge response for the triple chronoamperometric experiment is shown in Figure 6.22, together with the ideal gradient of “23/F”. The response for the first

step (0V → -1.0V) is not as linear as for the double chronoamperometric experiment shown above, and gives an “end to end” $\Delta M_T F / Q_T$ value of -34.5 g mol^{-1} . The response for the second step of $-1.0\text{V} \rightarrow -0.4\text{V}$ is curved as seen for the step $-1.0\text{V} \rightarrow 0\text{V}$ in Figure 6.20, and has an “end to end” $\Delta M_T F / Q_T$ value of -25.5 g mol^{-1} . For the final step ($-0.4\text{V} \rightarrow 0\text{V}$), again the same shape is seen as for the previous step and the “end to end” $\Delta M_T F / Q_T$ value here is -31.7 g mol^{-1} .

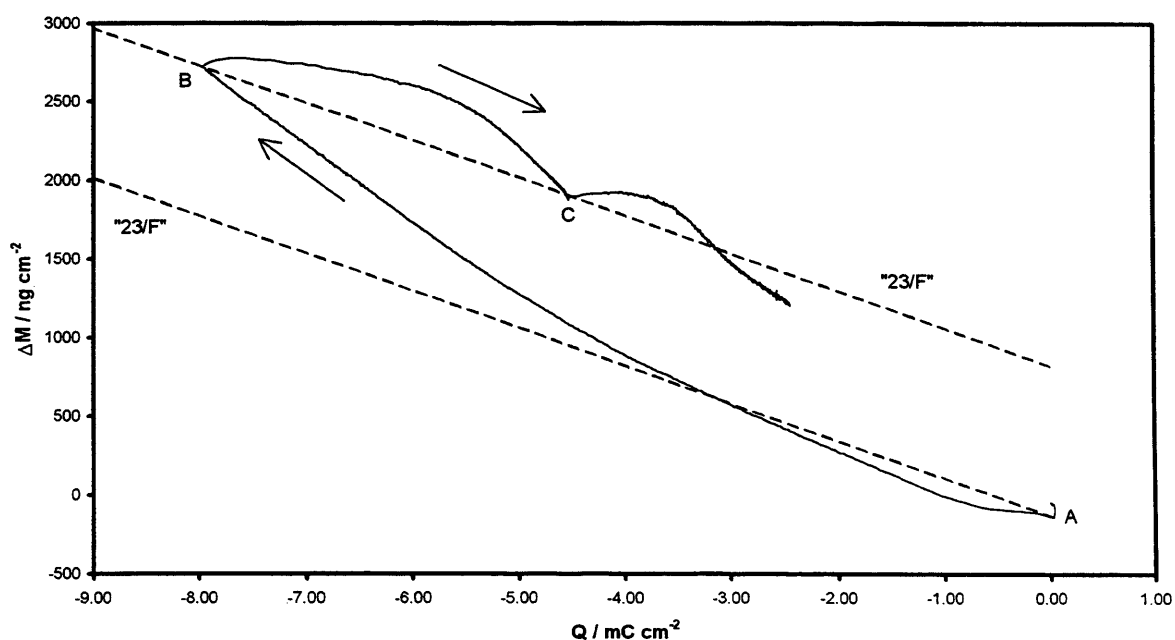


Figure 6.22 : Mass change versus charge response for a triple chronoamperometric experiment showing Na^+ insertion into a 2400\AA thick WO_3 film. Electrolyte : $0.1\text{M NaClO}_4/\text{propylene carbonate}$. Point A indicates step from $0\text{V} \rightarrow -1.0\text{V}$ for 300 seconds. Point B indicates step from $-1.0\text{V} \rightarrow -0.4\text{V}$ for 300 seconds. Point C indicates step from $-0.4\text{V} \rightarrow 0\text{V}$ for 300 seconds. Ideal gradient of “ $23/F$ ” marked as dotted line on plot.

The fact that the “end to end” $\Delta M_T F / Q_T$ values are greater than 23 g mol^{-1} indicates non-monotonic changes are being seen, with the presence of a second (neutral) species being observed. As for the double chronoamperometric experiment seen in Figure 6.21, it can be seen that neither the mass nor the charge response returns to zero after completion of the experiment. This again indicates that there is Na^+ being accumulated in the WO_3 film.

6.4.3 The “break-in” effect

As seen in Section 6.3.5, comparison of two identical chronoamperometric experiments carried out on a WO_3 film in 0.1M LiClO_4 /propylene carbonate showed that the “break-in” effect could be seen for chronoamperometric experiments as well as cyclic voltammetric experiments. It is also possible to investigate the “break-in” effect for experiments carried out in 0.1M NaClO_4 /propylene carbonate. Figure 6.23 shows the current versus time responses for a double chronoamperometric experiment ($0\text{V} \rightarrow -1.0\text{V} \rightarrow 0\text{V}$) as described in Section 6.3.5 (labelled experiments I and II). Both responses appear to be identical, although for experiment II, there is a larger current spike seen on the initial potential step ($0\text{V} \rightarrow -1.0\text{V}$). On reduction of the WO_3 film, both responses quickly return to zero after ≈ 150 seconds. On re-oxidation of the tungsten bronze, the responses both decay back to zero after ≈ 150 seconds, and there is very little difference between either experiment.

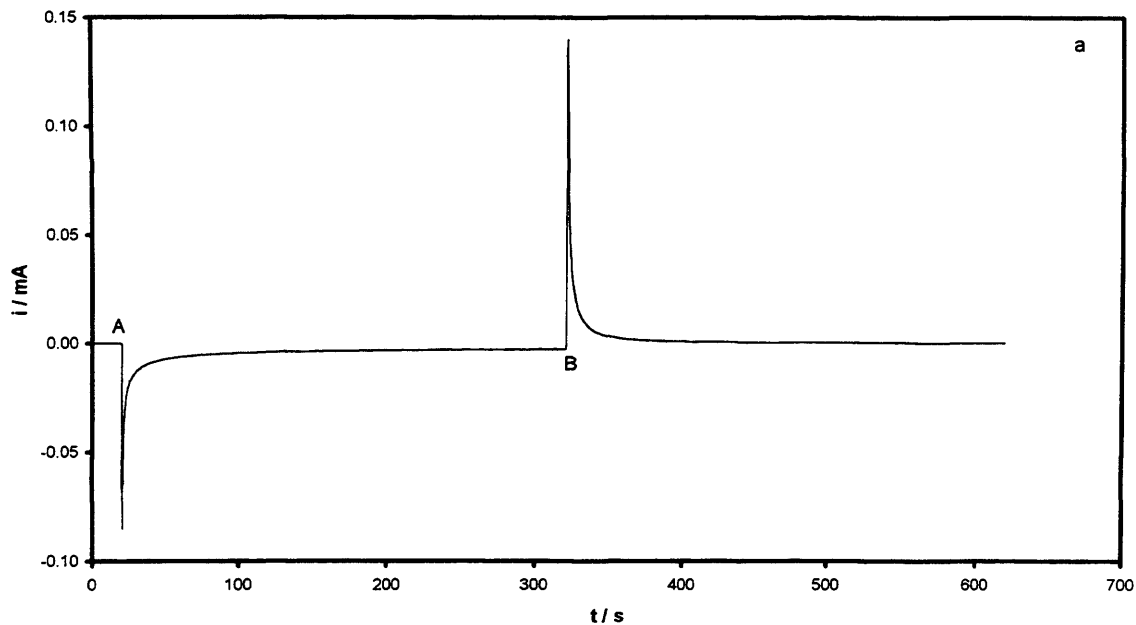
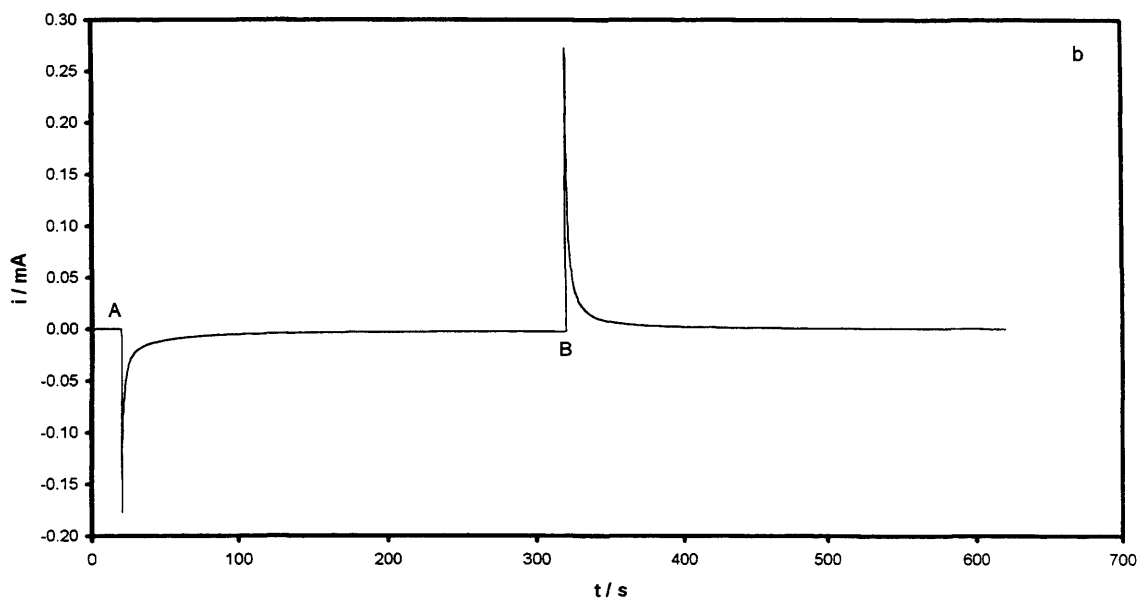


Figure 6.23 : Current versus time response for a double chronoamperometric experiment showing Na^+ insertion into a 2400\AA thick WO_3 film. Electrolyte : $0.1\text{M NaClO}_4/\text{propylene carbonate}$. Point A indicates step from $0\text{V} \rightarrow -1.0\text{V}$ for 300 seconds. Point B indicates step from $-1.0\text{V} \rightarrow 0\text{V}$ for 300 seconds. Experiment I shown in figure 6.23a. Experiment II shown in figure 6.23b.



As for the comparison of experiments I and II carried out in $0.1\text{M LiClO}_4/\text{propylene carbonate}$, it is difficult to note any major difference between experiment I and II by studying the current versus time responses alone. Therefore, as in Section 6.3.5 the charge

versus time responses are plotted in Figure 6.24 in order to see any changes between the two experiments. It can be seen that, unlike the experiments carried out in 0.1M LiClO₄/propylene carbonate, there is more charge recorded during experiment II compared to experiment I (25% more). This effect may be due to the amount of Na⁺ and propylene carbonate entering and leaving the WO₃ film. There also appears to be more charge recovered at the end of experiment II which is also different to the experiment carried out in 0.1M LiClO₄/propylene carbonate as the amount of charge recovered at the end of both experiments is approximately equal. As for the analogous experiments carried out in LiClO₄/propylene carbonate, it is not possible to compare the two experiments due to the fact that at the beginning of both experiments the charge is effectively zeroed.

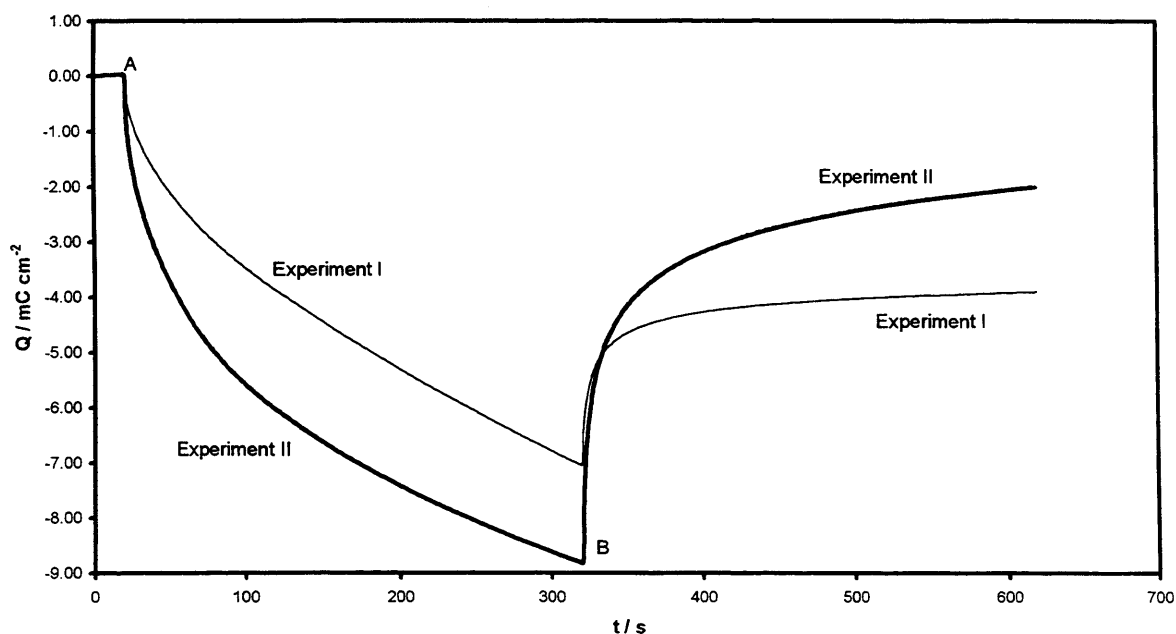


Figure 6.24 : Charge versus time responses for a double chronoamperometric experiment showing Na⁺ insertion into a 2400Å thick WO₃ film for experiment I and experiment II. Electrolyte : 0.1M NaClO₄/propylene carbonate. Point A indicates step from 0V → -1.0V for 300 seconds. Point B indicates step from -1.0V → 0V for 300 seconds. Charge responses for experiment I and experiment II marked on plot.

The mass change versus time responses are shown in Figure 6.25. Both responses show that initially, the mass change decreases for a small amount of time as reduction of the WO_3 film occurs. This decrease lasts for 0.4 seconds for experiment I and 0.4 seconds for experiment II. As previously mentioned, these mass changes are too small to be measured due to the long data acquisition time used. As the reduced WO_3 film is held at -1.0V for 300 seconds, the mass change increases. It can be seen that there is not a steady value reached after this time has elapsed. The mass change at the end of the first potential step for experiment II is larger than that seen for experiment I. This is in contrast to the comparison made using $0.1\text{M LiClO}_4/\text{propylene carbonate}$, where the mass change is smaller for experiment II than I (Figure 6.15). This larger value of mass appears to be an effect seen when using $\text{NaClO}_4/\text{propylene carbonate}$ as an electrolyte and may be due to the large amount of propylene carbonate in the reduced film.

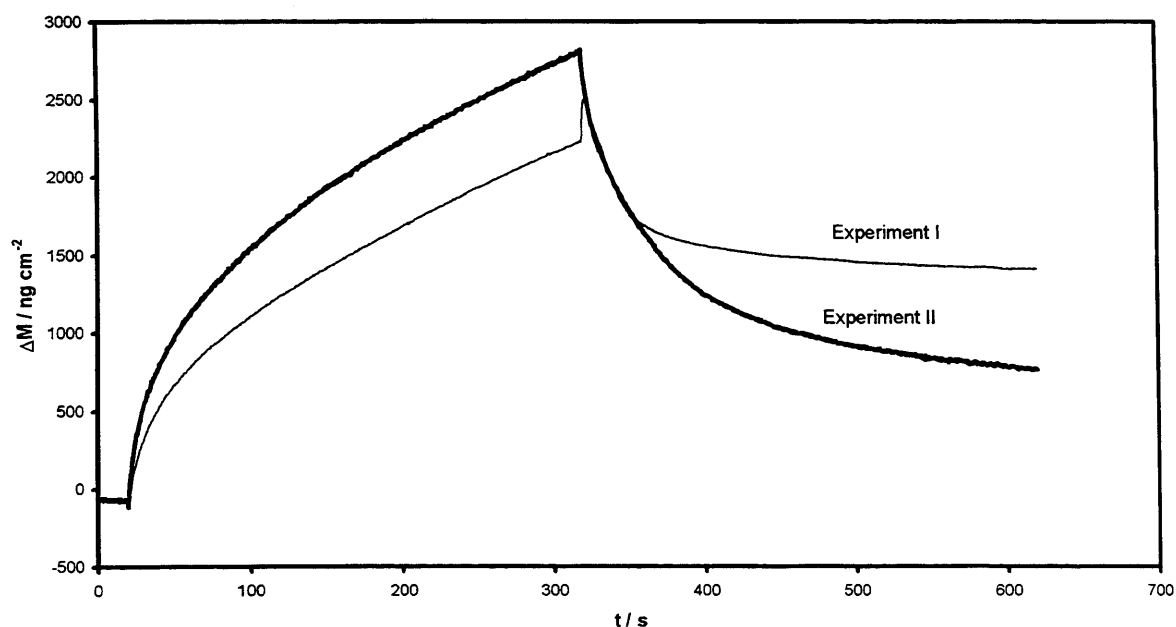


Figure 6.25 : Mass change versus time responses for a double chronoamperometric experiment showing Na^+ insertion into a 2400\AA thick WO_3 film for experiment I and experiment II. Electrolyte : $0.1\text{M NaClO}_4/\text{propylene carbonate}$. Point A indicates step from $0\text{V} \rightarrow -1.0\text{V}$ for 300 seconds. Point B indicates step from $-1.0\text{V} \rightarrow 0\text{V}$ for 300 seconds. Mass responses for experiment I and experiment II marked on plot.

As the film is re-oxidised at 0V, the mass at first increases slightly. This mass rise is seen for 0.4 seconds for experiment I, and experiment II (0.8 seconds). Neither experiment returns to its original value at the end of the experiment, and there appears to be a large mass response for both experiments I and II. As expressed above, the mass change recorded for both experiments cannot be compared as the experiments are effectively zeroed prior to the start of each experiment.

The mass change versus charge responses for experiment I and II can also be plotted together for comparison. Figure 6.26 shows these responses. Both plots show hysteresis, which is an indication of a second species (propylene carbonate) entering/leaving the WO_3 film alongside Na^+ . At the end of Experiment II, it can be seen that there is more charge and mass recovered in comparison to experiment I. The “end to end” $\Delta M_{\text{T}}F/Q_{\text{T}}$ values can be calculated and both experiments give “end to end” $\Delta M_{\text{T}}F/Q_{\text{T}}$ values greater than 23 g mol^{-1} , which shows the insertion and expulsion of both charged and neutral species. The values are not as similar than those obtained for the identical comparison carried out in $0.1\text{M LiClO}_4/\text{propylene carbonate}$, which may suggest that there is a larger accumulation of solvent and/or ion pairs in the WO_3 films reduced in $0.1\text{M NaClO}_4/\text{propylene carbonate}$, and that the “break-in” effect is more pronounced.

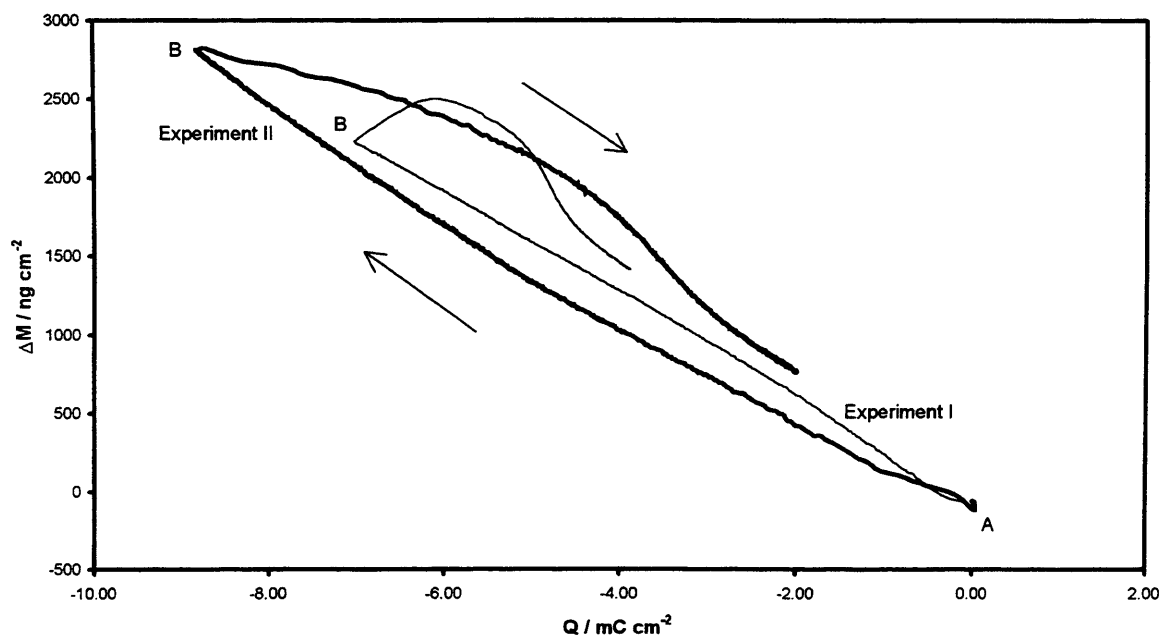


Figure 6.26 : : Mass change versus charge responses for a double chronoamperometric experiment showing Na^+ insertion into a 2400\AA thick WO_3 film for experiment I and experiment II. Electrolyte : $0.1\text{M NaClO}_4/\text{propylene carbonate}$. Point A indicates step from $0\text{V} \rightarrow -1.0\text{V}$ for 300 seconds. Point B indicates step from $-1.0\text{V} \rightarrow 0\text{V}$ for 300 seconds. Responses for experiment I and experiment II marked on plot.

6.4.4 Cyclic voltammetric data

The effect of timescale as seen in cyclic voltammetric experiments via the scan rate, can also be studied for WO_3 films cycled in $0.1\text{M NaClO}_4/\text{propylene carbonate}$. Figure 6.27 shows combined cyclic voltammograms for five different scan rates studied in $0.1\text{M NaClO}_4/\text{propylene carbonate}$. The voltammogram obtained at 5 mV s^{-1} is the second cycle in that set of experiments, as the first cycle, as for experiments carried out in $\text{LiClO}_4/\text{propylene carbonate}$ shows the “break-in” effect. As for the analogous experiments carried out in $0.1\text{M LiClO}_4/\text{propylene carbonate}$, there is more current passed as the scan rate increases. Unlike similar experiments carried out in $0.1\text{M LiClO}_4/\text{propylene carbonate}$, there is still current being recorded on the anodic half cycle, whereas for the experiment discussed in Section 6.2.5, the current response at positive potentials is almost zero. All cyclic voltammograms shown return to zero current at the termination of each experiment.

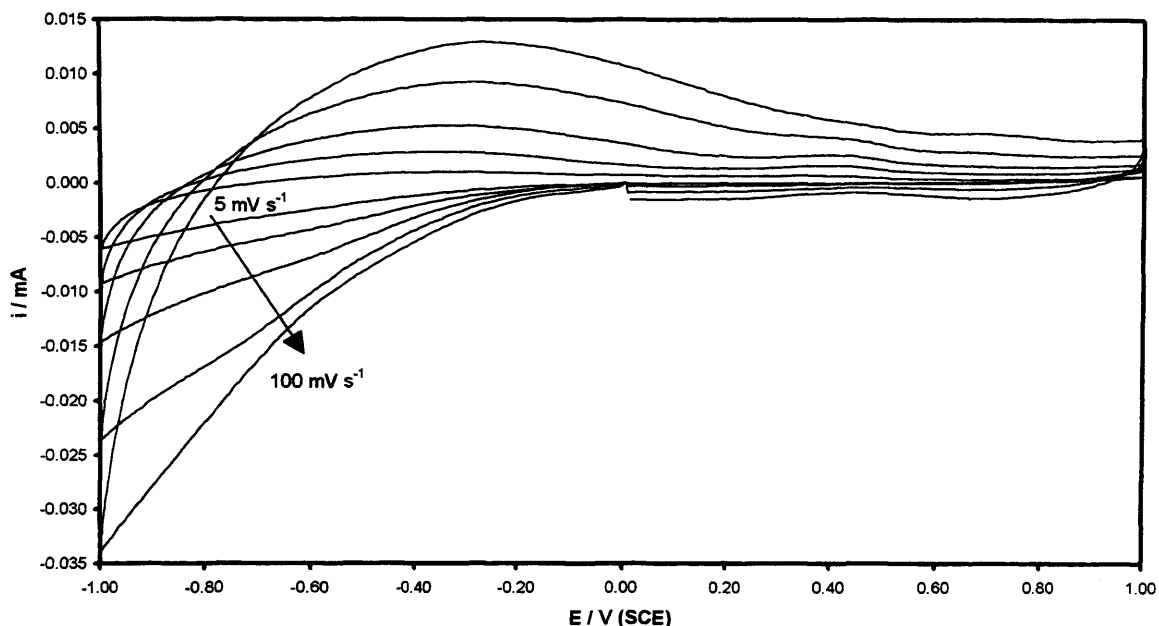


Figure 6.27 : Cyclic voltammogram showing Na^+ insertion into a 2700\AA thick WO_3 film at five different scan rates. Electrolyte : $0.1\text{M NaClO}_4/\text{propylene carbonate}$. Total number of cycles recorded : 5 (one cycle from each experiment shown for ease of comparison). Scan rates : $5\text{ mV s}^{-1} \rightarrow 100\text{ mV s}^{-1}$ (marked on plot).

The mass change versus potential response can also be plotted for the five different scan rates measured. Figure 6.28 shows these responses. Again, the second cycle from the experiment at 5 mV s^{-1} is plotted, and it can be seen that there is evidence of the “break-in” effect as at the completion of the cycle the mass changes do not return to zero, indicating that there is a large amount of mass left in the WO_3 film even on the second cycle at 5 mV s^{-1} . All mass change versus potential responses show incomplete mass recovery upon completion of the scan, which indicates that there is an accumulation of Na^+ even at fast scan rates such as 50 mV s^{-1} . This unrecovered mass was not seen for the corresponding experiments carried out using $\text{LiClO}_4/\text{propylene carbonate}$. The amount of Na^+ entering and leaving the WO_3 film decreases with increasing scan rate, which shows that at fast times less Na^+ enters the film.

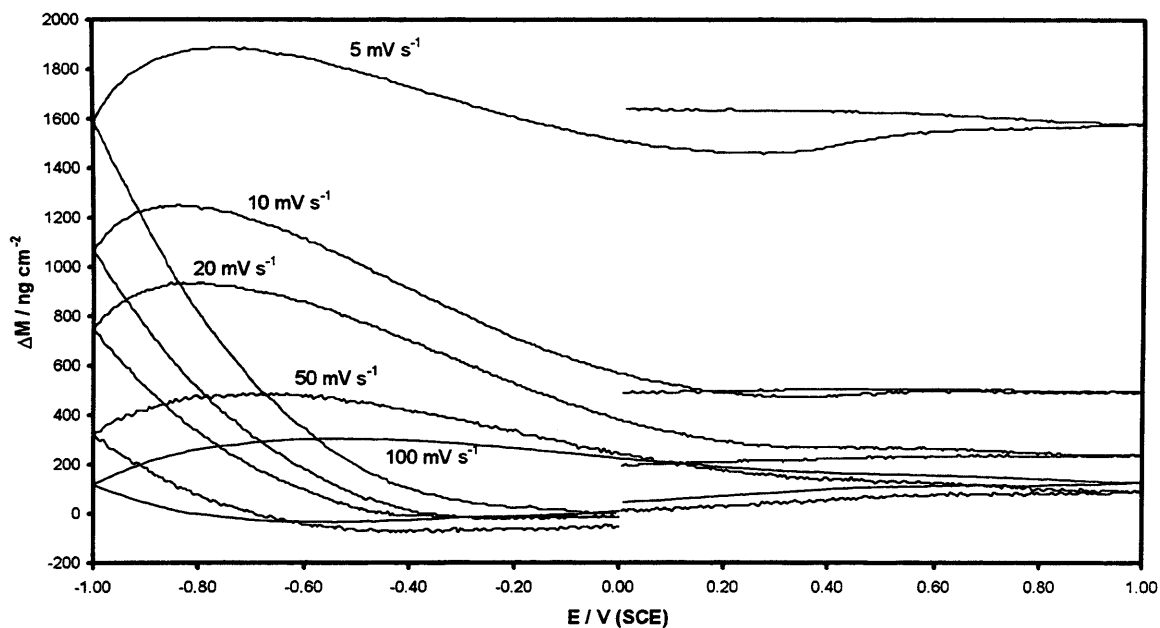


Figure 6.28 : Mass change versus potential responses for cyclic voltammetric experiments showing Na^+ insertion into a 2700\AA thick WO_3 film at five different scan rates. Electrolyte : $0.1\text{M NaClO}_4/\text{propylene carbonate}$. Total number of cycles recorded : 5 (one cycle from each experiment shown for ease of comparison). Scan rates : $5\text{ mV s}^{-1} \rightarrow 100\text{ mV s}^{-1}$ (marked on plot).

The mass change versus charge response for experiments carried out at 10 mV s^{-1} and 100 mV s^{-1} are shown in Figure 6.29. The response at 10 mV s^{-1} shows a straight line upon reduction of the WO_3 film with an “end to end” $\Delta M_{\text{T}}F/Q_{\text{T}}$ value of -82.6 g mol^{-1} . Upon re-oxidation of the tungsten bronze, there are two distinct measurable gradients seen as in Chapter 4. (Section 4.3.3).

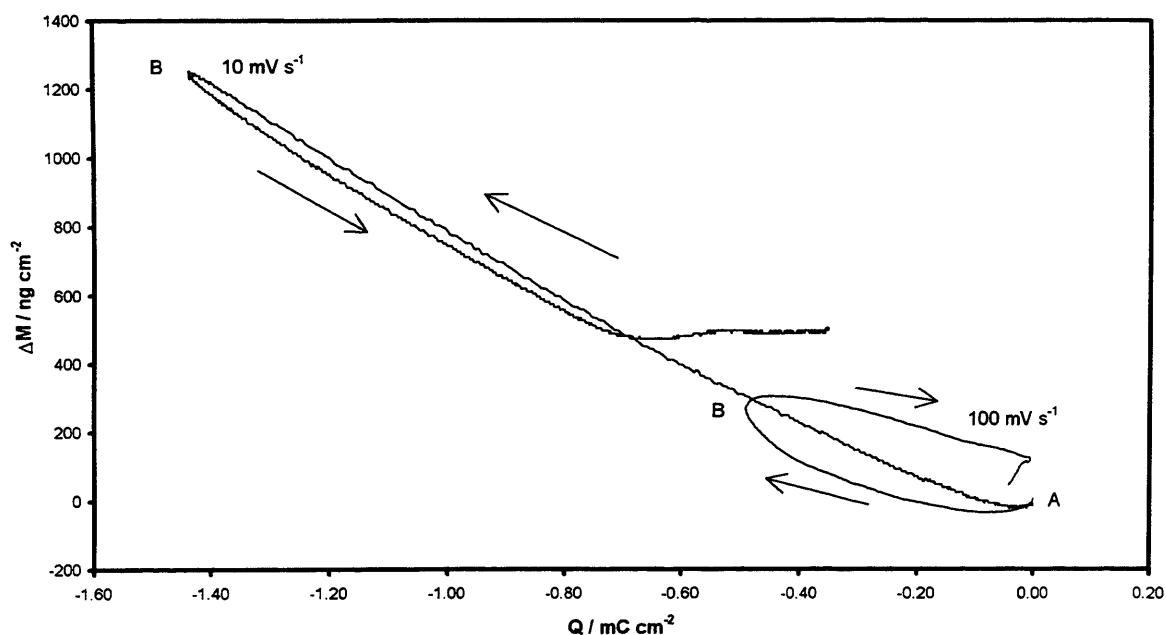


Figure 6.29 : Mass change versus charge responses for cyclic voltammetric experiments showing Na^+ insertion into a 2700\AA thick WO_3 film at two different scan rates. Electrolyte : $0.1\text{M NaClO}_4/\text{propylene carbonate}$. Number of cycles recorded : 5 (1st cycle from each experiment shown for ease of comparison). Scan rates : 10 mV s^{-1} and 100 mV s^{-1} (marked on plot).

The experiment carried out at 10 mV s^{-1} , yields two “end to end” $\Delta M_{\text{T}}/Q_{\text{T}}$ values for oxidation. These values are -94.9 g mol^{-1} and 3.4 g mol^{-1} . It can also be seen that upon completion of the experiment, neither the mass change nor the charge values return to their original values, indicating that there is still Na^+ left inside the WO_3 film after re-oxidation. As the $\Delta M_{\text{T}}/Q_{\text{T}}$ values do not equal 23 g mol^{-1} , then as discussed in Chapter 4, there may be triple ions also entering and leaving the WO_3 film. It appears that neutral species are entering and leaving the WO_3 film alongside Na^+ as seen for the chronoamperometric experiments. The plot obtained for the experiment at 100 mV s^{-1} shows more hysteresis, but at the end of the experiment, there is almost complete mass and charge recovery. The “end to end” $\Delta M_{\text{T}}/Q_{\text{T}}$ values are -36.3 g mol^{-1} for reduction and -29.4 g mol^{-1} for re-oxidation. Therefore it can be seen that at the faster scan rate there is both charged and neutral species entering the WO_3 film and also leaving the film at a comparable rate.

6.5 SUMMARY

The effect of ion insertion into WO_3 films has been studied as a function of time by both chronoamperometric experiments and cyclic voltammetric experiments. Experiments were carried out using three different concentrations of LiClO_4 /propylene carbonate and NaClO_4 /propylene carbonate. A double chronoamperometric experiment ($0\text{V} \rightarrow -1.0\text{V} \rightarrow 0\text{V}$) and a triple chronoamperometric experiment ($0\text{V} \rightarrow -1.0\text{V} \rightarrow -0.4\text{V} \rightarrow 0\text{V}$) were investigated.

For the experiments carried out in 0.1M LiClO_4 /propylene carbonate the double chronoamperometric experiment showed that the reduction process was slower than the re-oxidation process and the charge versus time response showed that at the end of the reduction step ($0\text{V} \rightarrow -1.0\text{V}$), there is still charge being inserted in to the WO_3 film, and hence the film is still being reduced. Upon re-oxidation, there is incomplete charge recovery. Incomplete mass recovery is also seen when the mass change versus time response is studied for the double chronoamperometric experiment. The mass change versus charge plot shows that the response deviates from the ideal gradient of “ $7/F$ ”, which may indicate the presence of triple ions as well as Li^+ as discussed in Chapter 4. The deviation from “ $7/F$ ” shows that neutral species are entering and leaving the WO_3 film alongside Li^+ as seen for cyclic voltammetric experiments discussed previously. These neutrals may be either the solvent (propylene carbonate) or ion-pairs present in solution. Triple chronoamperometric experiments show that at the end of the experiment there is more mass and charge recovered, but again neutral species are entering and leaving the WO_3 film alongside Li^+ .

The “break-in” effect can also be seen using chronoamperometric experiments. If two identical experiments are compared, but carried out before and after complete

reduction of the WO_3 film has been seen, then there are significant changes in mass and also the mass versus charge responses between the two experiments. It appears that after the “break-in” experiment has occurred, there is a small amount of ionic charge and also mass left in the re-oxidised WO_3 film, which does not allow as much Li^+ to enter the film on subsequent experiments.

By changing the scan rate in a cyclic voltammetric experiment, the effect of timescale can also be studied. The experiments carried out in 0.1M LiClO_4 /propylene carbonate showed that as the scan rate increased then the mass changes decreased. This is expected, as the amount of time at potentials negative enough to reduce the WO_3 film is shortened. Comparison of mass versus charge plots for experiments carried out at 10 mV s^{-1} and 100 mV s^{-1} shows that there is evidence for neutrals entering and leaving the WO_3 film alongside Li^+ since the “end to end” $\Delta M_{\text{T}}F/Q_{\text{T}}$ values, are all greater than 7 g mol^{-1} . There may also be triple ions entering alongside the Li^+ at both scan rates studied. At the faster scan rate studied, more hysteresis is seen, indicating that there is less time for the charged and neutral species to enter the WO_3 film, but also leave it, therefore kinetics appear to be dominated by Li^+ transfer.

Experiments were also carried out in NaClO_4 /propylene carbonate. The double and triple chronoamperometric experiments showed similar characteristics to LiClO_4 /propylene carbonate, with incomplete mass and charge recovery and also “end to end” $\Delta M_{\text{T}}F/Q_{\text{T}}$ values which were larger than the value expected for pure Na^+ transfer (23 g mol^{-1}), indicating the movement of neutrals. The experiment carried out to investigate the “break-in” effect showed that the effect is not as pronounced in NaClO_4 /propylene carbonate. Cyclic voltammetric experiments showed the same characteristics as for Li^+ insertion, with more hysteresis seen on the mass change versus charge plots at the faster scan rates than on the slower ones.

Therefore, it appears that chronoamperometric experiments using LiClO_4 /propylene carbonate as the electrolyte leads to incomplete charge and mass recovery initially, but that experiments carried out where a triple chronoamperometric experiment is undertaken there is more recovery at the end of the experiment. The mass versus charge plots also show that for both types of experiment there are neutrals entering and leaving the WO_3 film alongside Li^+ . The “break-in” effect is also seen on chronoamperometric experiments although the effect is not as large as at the slow scan rate of 5 mV s^{-1} discussed in Chapter 5. Cyclic voltammetric experiments where the scan rate is altered also show that less mass is inserted into the film at faster scan rates, and at fast scan rates there is more complete mass and charge recovery. These effects appear to be the same regardless of electrolyte concentration.

Chronoamperometric experiments carried out using NaClO_4 /propylene carbonate show very similar characteristics, although the current responses are smaller than for LiClO_4 /propylene carbonate. The presence of triple ions in LiClO_4 /propylene carbonate and NaClO_4 /propylene carbonate may be the reason why both electrolytes give $\Delta M_{\text{T}}F/Q_{\text{T}}$ values greater than expected and there is deviation from the ideal gradients as both “free” ions and triple ions may be moving in and out of the film. neutral species may be either solvent (propylene carbonate) or ion pairs and will lead to a $\Delta\Phi_{\text{T}}F/Q_{\text{T}}$ value greater than 0. Therefore, it appears that LiClO_4 /propylene carbonate is better than NaClO_4 /propylene carbonate as an electrolyte for chronoamperometric experiments, as there is more complete charge and mass recovery on re-oxidation.

REFERENCES

1. B. W. Faughnan and R. S. Crandall, in "Display Devices" (J. I. Pankove, ed.), Springer-Verlag, Berlin, 1980.
2. C. G. Granqvist, Handbook of Inorganic Electrochromic Materials, Elsevier Science B.V., Amsterdam, 1995.
3. S. K. Mohapatra, *Journal of the Electrochemical Society*, 125, 2, (1978), 284.
4. O. Bohnke, B. Vuillemin, C. Gabrielli, M. Keddou, and H. Perrot, *Electrochimica Acta*, 40, 17, (1995), 2765.
5. P. M. S. Monk, R. J. Mortimer, and D. R. Rosseinsky, Electrochromism, Fundamentals and Applications, VCH Publishers, Weinheim, 1995.
6. B. Reichman and A. J. Bard, *Journal of the Electrochemical Society*, 126, 4, (1979), 583.
7. S. J. Babinec, *Solar Energy Materials and Solar Cells*, 25, 3-4, (1992), 269.
8. A. R. Hillman, N. A. Hughes, and S. Bruckenstein, *Journal of the Electrochemical Society*, 139, 1, (1992), 74.
9. D. Dini, F. Decker, and E. Masetti, *Journal of Applied Electrochemistry*, 26, 6, (1996), 647.

CHAPTER 7 : CONCLUSIONS

The role of redox-driven ion insertion into WO_3 films was investigated using a combination of electrochemical, gravimetric and spectroscopic techniques. Three variables were explored: electrolyte composition, film history and time scale. Initially, the influence of these variables were studied using slow scan cyclic voltammetry and the EQCM, to investigate the effect of anion and cation identity, and electrolyte concentration on the WO_3 film upon reduction and re-oxidation. Cations chosen for study were Li^+ and Na^+ , due to their ease of insertion into WO_3 films. Li^+ was inserted more readily into the WO_3 lattice than Na^+ . Li^+ insertion/extraction proved to be a successful, reproducible effect, with mass and charge being recovered at completion of each redox cycle. For similar experiments carried out using Na^+ , the mass and charge recovery were not complete: there was a gradual accumulation of mass as the experiment proceeded.

“End to end” $\Delta M_{\text{T}}F/Q_{\text{T}}$ ratios for both cations showed values greater than those expected for pure cation insertion. There is the suggestion that triple ions may be formed, leading to larger $\Delta M_{\text{T}}F/Q_{\text{T}}$ values as these species will be inserted alongside the cation. The use of Φ , an algebraic tool used to deconvolute the overall mass change seen during the EQCM experiment, showed that there is a second, neutral species entering and leaving the WO_3 film in parallel with the cation. This species may be the solvent, propylene carbonate or the presence of ion pairs in the solution, which may then be inserted into the WO_3 film. We deduce its transfer on the basis of observed mass changes at zero current, when electroneutrality conditions dictate there must be no ion transfer. If purely propylene carbonate enters and leaves the WO_3 film, then for ion insertion using Li^+ it was calculated that there is 0.01 propylene carbonate/ Li^+ entering and leaving the film, and for Na^+ , 0.6

propylene carbonate/ Na^+ enters and leaves the tungsten bronze. The mass change versus charge plots for Na^+ insertion show three distinct slopes, indicating that upon re-oxidation of the tungsten bronze there may be some neutral species entering the film as Na^+ leaves.

The amount of cation entering and leaving the film can be calculated to give a value of x , the insertion coefficient. For Li^+ , the x value calculated here is ≈ 0.3 Li^+ entering for each WO_3 , whereas for Na^+ the x value is much smaller, 0.023. This implies that there is a greater optical contrast necessary for display purposes between the reduced and oxidised state seen for Li^+ than Na^+ insertion.

The choice of anion used does not appear to play a major role in the mechanism of ion insertion. Experiments were carried out using LiClO_4 /propylene carbonate and LiCF_3SO_3 /propylene carbonate. The choice of anion was such that distinctions between the two species were difficult as the two anions are of similar size. The presence of triple ions as $[\text{Li}_2\text{CF}_3\text{SO}_3]^+$ in solution has been suggested as again, $\Delta M_{\text{T}}/Q_{\text{T}}$ values are greater than expected for single cation insertion. The presence of neutral species as either ion pairs and/or propylene carbonate is seen when using Φ as the $\Delta\Phi_{\text{T}}/Q_{\text{T}}$ values do not equal zero. The calculated x values are slightly higher for WO_3 films cycled in 0.1M LiClO_4 /propylene carbonate than 0.1M LiCF_3SO_3 /propylene carbonate, which may be due to the presence of triple ions in LiCF_3SO_3 .

The third variable studied was the electrolyte concentration, or activity. The three concentrations chosen were 0.1M LiClO_4 /propylene carbonate, 0.5M LiClO_4 /propylene carbonate and 0.7M LiClO_4 /propylene carbonate. These results had to be normalised with respect to film thickness to allow comparison. The normalised results for 0.5M LiClO_4 /propylene carbonate are greater than expected, and have been seen for other experiments carried out at this concentration. The x values for the three different

experiments show that the thermodynamic x value is almost achieved at slow scan rates whereas insertion appears to be under kinetic control at faster scan rates. Comparison between reactions in 0.1M and 0.7M LiClO₄/propylene carbonate show that there is very little difference between the two experiments: the “end to end” $\Delta M_{TF}/Q_T$ values are similar, indicating that LiClO₄ concentration in the range 0.1M and 0.7M, does not affect cation insertion, although the influence of ion pair involvement in insertion may be influenced by increasing activities.

The second effect studied was film history. When “new” WO₃ films are cycled at a slow scan rate (5 mV s⁻¹) the initial cycle is different to the following cycles. This is termed the “break-in” effect and is seen regardless of electrolyte used. The effect is seen in both the electrochemical and gravimetric responses using the EQCM. The EQCM data recorded for the initial cycle shows that at the end of the first cycle there is some mass and charge left in the WO₃ film. This indicates that there is some cation left in the WO₃ film after the “break-in” scan. The calculated “end to end” $\Delta M_{TF}/Q_T$ and $\Delta\Phi_{TF}/Q_T$ values for this first scan show values greater than those for pure cation insertion, indicating that neutrals enter the film alongside the ion. Calculated x values for the first scan are also larger than the following scans, all of which indicate that by initial cycling of a WO₃ film at a slow scan rate, cations are left in the film after re-oxidation. This effect is not seen when “new” WO₃ films are initially cycled at faster scan rates (100 mV s⁻¹) and so this effect is an effect of timescale. The “break-in” effect has also been seen spectroscopically, when absorbance changes for the first cycle studied on a “new” piece of WO₃ coated F-doped ITO glass is slightly different to those in subsequent cycles.

The effect of long term cycling on film stability has also been investigated. WO₃ films in 0.1M LiClO₄/propylene carbonate or 0.1M NaClO₄/propylene carbonate were

cycled at 100 mV s^{-1} for over 10,000 cycles. For WO_3 films cycled in $\text{LiClO}_4/\text{propylene carbonate}$, the results showed that, even after 10,000 cycles the films were still being reduced and re-oxidised successfully. EQCM data taken at the beginning and end of the experiment showed that there was not a significant decrease in mass change during the cycling. This indicates that Li^+ is a reliable cation to be used for long term cycling. In the case of $\text{NaClO}_4/\text{propylene carbonate}$, breakdown in film stability was seen much earlier. EQCM data was collected at the beginning of the experiment but at completion of over 10,000 cycles there did not appear to be any Na^+ entering and leaving the film as it was not possible to collect any more EQCM data. This lead to the conclusion that Na^+ is not a practical cation for extended cycling experiments.

The final investigation involved the effect of experimental time scale. Electrochemical techniques employed in this area were both chronoamperometry and cyclic voltammetry, together with EQCM measurements. For experiments carried out in $0.1\text{M LiClO}_4/\text{propylene carbonate}$ and $0.1\text{M NaClO}_4/\text{propylene carbonate}$, both double ($0\text{V} \rightarrow -1.0\text{V} \rightarrow 0\text{V}$) and triple ($0\text{V} \rightarrow -0.1\text{V} \rightarrow -0.4\text{V} \rightarrow 0\text{V}$) potential steps were investigated. For the double chronoamperometric experiment, reduction was slower than oxidation and incomplete charge and mass recovery was seen for both electrolytes. Diffusion coefficients of $\approx 5 \times 10^{-12} \text{ cm}^2 \text{ s}^{-1}$ for Li^+ were calculated. EQCM data shows deviation from the “ideal” gradient, which represents single cation insertion, indicating the movement of neutrals species both in and out of the WO_3 film. The triple chronoamperometric experiments show more, but still incomplete charge and mass recovered at the end of the experiment compared to the double chronoamperometric experiments. Propylene carbonate enters the film during this experiment also.

The “break-in” effect was also seen in chronoamperometric experiments. For experiments carried out in 0.1M LiClO₄/propylene carbonate, this effect is seen to be larger than for identical experiments carried out in 0.1M NaClO₄/propylene carbonate.

By changing the scan rate used in cyclic voltammetric experiments, it is possible to study the role of kinetics. The scan rates chosen were 10 mV s⁻¹ and 100 mV s⁻¹. At faster scan rates (100 mV s⁻¹), there is more hysteresis in mass change versus charge plots, indicating that the kinetics are controlled by Li⁺ transfer. This effect is also seen in cyclic voltammetric experiments carried out in 0.1M NaClO₄/propylene carbonate.

From the two cations studied here, Li⁺ inserts more readily, and more reversibly than Na⁺ into the WO₃ film. The anions chosen here do not appear to play a major role, neither does an increase in electrolyte activity (concentration). The EQCM is a powerful technique for the study of ion insertion into WO₃ films and it can be seen clearly that there is a second, neutral species entering and leaving the film. Upon cycling at slow scan rates initially, there is a build up of both mass and charge seen, indicating that the cation, and possibly some neutrals remain in the WO₃ film after the initial cycle. This “break-in” effect is also seen in chronoamperometric experiments and so is not characteristic of cyclic voltammetry only. Therefore, from the point of view of using WO₃ as a counter electrode in an ECD a Li⁺ salt is preferential to Na⁺.

FUTURE WORK

The role of cation insertion into WO₃ films has been shown to be more complex than simple ion insertion and the experiments carried out using the EQCM have shown that further work is required to better understand the mechanism of insertion. The EQCM is a powerful technique to study electrochemical systems, but for WO₃ films it may be best used

in conjunction with more conventional analytical techniques. The use of an analytical technique such as atomic absorption spectroscopy could be used on a dissolved WO_3 film to investigate how much cation (Li^+ or Na^+) remains in the WO_3 film after the first “break-in” cycle. It would also be possible to use this technique to try and establish the amount of Li^+ which may remain in the WO_3 film after long term cycling. This would be a useful accompaniment to the results seen for insertion of Li^+ using the EQCM as it is seen that Li^+ is still inserted into WO_3 after more than 10,000 cycles. Atomic absorption spectroscopy could also be used to study the effect of the amount of cation which may remain in the WO_3 film when different scan rates are used for the initial cycle. This technique would produce definite values which could then be used to fortify existing EQCM results.

The use of neutron reflectivity to investigate the “break-in” effect is an experiment which would also verify this effect seen by the EQCM and spectrophotometric experiments. Reflectivity profiles can be obtained for the “break-in” cycle and the following cycle with changes to the film structure noted. It is intended to probe a quartz block onto which an F-doped ITO electrode has been deposited, followed by a sputtered coating of WO_3 . Preliminary reflectivity data has led to the conclusion that the “break-in” effect can be studied by this method, although an alternative to propylene carbonate is required. It may be possible to use neutron reflectivity as an accompaniment to long term cycling experiments to establish the structure of the WO_3 film after many colour/bleach cycles. This experiment would need careful planning due to the beam time allocation for neutron reflectivity experiments, but may give an insight into WO_3 film degradation over a set time period.

To firmly establish whether there is any solvent being inserted into the WO_3 film during reduction and re-oxidation, then the use of infra-red spectroscopy to see whether the C=O stretch at $\approx 1700 \text{ cm}^{-1}$ is seen on a reduced WO_3 film is a likely experiment. The use of

the EQCM, but using a different solvent (such as ethylene carbonate) to propylene carbonate would also verify solvent insertion into the WO_3 film. If all other conditions were kept identical (for example, film deposition and choice of electrolyte), then by using a different solvent, then the two sets of data could be compared and contrasted. This would be a simple diagnostic test for solvent involvement.

The use of liquid electrolytes is not considered viable when considering the construction of ECDs and “smart windows”. However, care must be taken not to use a purely solid electrolyte as the EQCM requires a liquid media in which to operate. If a gel could be found where EQCM measurements were possible then it may be possible to see difference in ion insertion into the WO_3 film, when compared to propylene carbonate.

The choice of the two anions (ClO_4^- and CF_3SO_3^-) does not, if any, really give much information regarding the role of anion insertion into WO_3 films due to their similar size. The use of a larger anion, for example para-toluene sulphonate would give a clearer indication of anion participation. By choosing a larger anion and carrying out EQCM measurements for both “break-in” experiments and standard cyclic voltammetry experiments over a range of scan rates, then the question of anion insertion may be more clearly resolved.

The controlled addition of water to a non-aqueous solvent such as propylene carbonate has been found to aid colouration. The effect of this addition with respect to the “break-in” effect using the EQCM technique may lead to a limitation for water addition being found before the contrast ratio decreases. It would also be an interesting exercise to carry out long term cycling experiments in LiClO_4 /propylene carbonate using the EQCM to see whether the amount of water would lead to faster film degradation and also if a marked change in mass could be seen. Combination of the EQCM measurements with more

analytical techniques, such as atomic absorption spectroscopy or infra red spectroscopy (in order to detect the broad O-H stretch) would also give information about the presence of water in the WO_3 film.

Ion pairs are thought to exist in the electrolytes at the concentrations studied here. There is a limitation on the concentrations used due to the sensitive nature of the EQCM, as a steady oscillation is required prior to data acquisition. The viscous nature of propylene carbonate has not made it possible to increase electrolyte concentration, although the choice of a different, less viscous solvent may allow this effect to be studied using the EQCM. The combination of cations with larger anions may also lead to the ion pair formation being seen more clearly using EQCM measurements. The use of spectroscopic techniques, such as FTIR may also aid in the further understanding of ion pairs in propylene carbonate.

The films studied here are all produced by the sputtering method. It may be a useful exercise to explore any differences seen between these films and WO_3 films produced by a different technique. However, care must be taken to produce WO_3 films by the second technique which are almost identical to each other as the properties of WO_3 films have been found to be slightly different from one film to another for individually produced films. Therefore, mass production of WO_3 appears to be a reliable way to produce films with very similar properties. The sputtering deposition method carried out on the EQCM crystals means that all the crystals are coated under the same conditions and therefore can be considered as being almost identical to each other. The "break-in" effect may be investigated to see whether it is an effect of the sputtering technique or is a universal result seen regardless of film preparation. If the "break-in" is seen only for sputtering, then it may be that this technique is not a viable method of deposition for WO_3 . The sol gel process is considered to be a rapidly growing method of WO_3 film production. The use of the EQCM

to investigate changes between films produced by this method and the more conventional method of sputtering may lead to the production of better WO_3 films for “smart windows” and ECDs.

By using “BT-” cut crystals, which have been deposited in an identical method to the conventional “AT-” cut for EQCM measurements, it would be possible to investigate any effects caused by stress. Since the comparison between “AT-” and “BT-” cut quartz crystals has already been used to investigate internal stresses then it would be useful to carry out EQCM measurements using these two cuts of crystals to probe the effect of “break-in”, the use of two different electrolytes with anions of varying sizes, the use of different solvents to investigate any effects caused by solvent insertion and the effect of the controlled addition of water to the electrolyte.

The time taken for colouring and bleaching a WO_3 film, may be of great importance for the use of WO_3 as an ECD. For windows, a rapid switching time would not be necessary, although for ECDs switching time is more crucial. Investigation into the kinetics of coloration may be able to be carried out using the EQCM, once the role of cations, anions, ion pairs, triple ions and solvent are better understood.

It appears that the many different analytical techniques available, when used in conjunction to the EQCM, may lead to a greater understanding of the ion insertion procedure, which leads to the formation of tungsten bronzes.